



THE INTERACTION OF 9-AMINOACRIDINE WITH
NATIVE AND DENATURED DNA

DAVID RICHARD TURNER B.Sc. (ADELAIDE)

Department of Physical and Inorganic Chemistry,
The University of Adelaide,
South Australia

A thesis submitted for the degree of
Doctor of Philosophy.

October, 1975.

"The Helix of Life"

by courtesy of the artist and
the Adelaide Children's Hospital Inc.



CONTENTS.

	page	
CHAPTER I	Introduction.	1
CHAPTER II	Characterization of native and denatured DNA.	9
CHAPTER III	The interaction of aminoacridines with nucleic acids.	27
CHAPTER IV	The interaction of 9-aminoacridine with native DNA.	64
CHAPTER V	The interaction of 9-aminoacridine with denatured DNA.	89
CHAPTER VI	A temperature-jump study of the interaction of 9-aminoacridine with native and denatured DNA.	110
CHAPTER VII	General discussion and conclusions.	160
CHAPTER VIII	Materials and methods.	172
APPENDIX		183

SUMMARY

The interaction of the 9-aminoacridine (9AA) cation with native DNA in neutral salt to form a complex is believed to be typical of the interactions of a wide variety of compounds important in chemotherapy which are said to intercalate between adjacent bases along the DNA double helix. The influence of the secondary structure of DNA on this intercalated complex is important to a full understanding of the interaction. In this work equilibrium and perturbation techniques have been used to investigate the interaction of 9AA with both native and denatured DNA.

The solution state of both native and denatured DNA in 0.1M NaCl has been examined. Below its melting transition the native structure is that of a stable, double helical conformation. Denatured DNA has a structure which is more disordered than the native form although interactions between the bases occur. Denatured DNA in solution can be considered to be composed of three coexisting structures:

(i) "folded" or short range helical ordered regions,
(ii) single strand, base-stacked regions and (iii) random coil regions. The denatured DNA structure is very sensitive to temperature with progressive formation of the random coil with increasing temperature. At elevated temperatures denatured DNA can undergo partial renaturation.

The spectra and binding isotherms of 9AA with each of native and denatured DNA have been measured at various temperatures. The product of the interaction of 9AA with native DNA at low extents of binding (r) produces spectra which are internally linear. Internal linearity is

associated with the existence of only two species of 9AA in a single equilibrium: viz. free 9AA and bound 9AA. In contrast to this 9AA and denatured DNA give rise to spectra which are not internally linear at room temperature but which become so at elevated temperatures. These observations have been interpreted in terms of changes with temperature in denatured DNA described by the proposed model. The association constants (equilibrium constants) for the binding sites on the two forms of DNA have been evaluated from Scatchard plots determined by spectrophotometry. Proposed safeguards must be used in the spectrophotometric determination of these plots to ensure a high degree of reproducibility. Curvature of Scatchard plots has been assigned to anti-cooperativity and evaluation of association constants for these systems is discussed. The variation of the limiting extent of binding (n) with temperature is discussed with respect to the models of native and denatured DNA in solution.

Thermodynamic parameters for the interactions have been obtained from the variation of the association constants with temperature. These are discussed in terms of the intercalation model. The free energy change for the interaction is large and favourable ($\Delta G^\circ = -25$ to -40 kJ/mole). The bonding forces are shown to be of importance whereas entropy changes for the interaction are small and unfavourable for 9AA and native DNA and large and unfavourable for 9AA and denatured DNA. This latter observation is interpreted as arising from constraint of the thermal motion of the DNA bases by the intercalation of 9AA between them thereby producing a degree of base-stacking in the denatured DNA complex.

The 9AA and native and denatured DNA systems have also been investigated by the temperature-jump, rapid perturbation technique. A single relaxation process with an inverse relaxation time linearly dependent on the concentration of reactant at equilibrium is observed for perturbations of 9AA and native DNA equilibria. The relaxation has been assigned to a rapid, bimolecular, single step process for intercalation. This result is at variance with existing literature on similar systems. The thermodynamic parameters determined by this technique are in good agreement with the equilibrium measurements.

Perturbations of 9AA and denatured DNA equilibria exhibit two distinct relaxation times. The concentration dependence of these has led to the proposition of a mechanism in which intercalation of 9AA between the bases on one strand of denatured DNA occurs in a rapid, bimolecular process. However, the potential binding sites on denatured DNA (single strand, base-stacked regions of the macromolecule) are themselves in equilibrium with a non binding form of DNA (random coil regions). This equilibrium is probably established through an intermediate in rapid equilibrium with the single strand, base-stacked form of denatured DNA.

To the best of my knowledge and belief, this thesis contains no material previously published or written by another person, nor any material previously submitted for a degree or diploma in any University, except when due reference is made in the text.

D.R. TURNER

ACKNOWLEDGEMENTS

The author wishes to express his sincere gratitude to Prof. D.O. Jordan for his supervision, interest and encouragement during the course of this work. He is also indebted to Dr. J.H. Coates for valuable discussions on the temperature-jump studies carried out. Early in this work Dr. L.N. Sansom provided many interesting discussions. The author is indebted to Mr. G. Boehm, his close colleague and friend for innumerable discussions, critical proof-reading of the text and valuable assistance with computing.

The late Dr. M.J. Barrett of the Department of Restorative Dentistry, the University of Adelaide, kindly permitted use of the OSCAR F/DCF Strip Chart and Film Digitizing System. Prof. C.A. Angel of Purdue University first drew the author's attention to the diagnostic importance of internal linearity of spectra.

The author wishes to acknowledge the capable and cheerful help of the electronics, mechanical and glassblowing workshop staff of this Department. Mr. K. Staiff of this Department prepared the diagrams.

Finally, the author is personally indebted to his wife, Linnett, and to his parents, for their continual interest and encouragement.

CHAPTER I



INTRODUCTION

Nucleic acids have been known since their discovery by Miescher in 1869¹. Their fundamental role in the continuity of life, however, is a much more recently established fact. Nucleic acids are the data bank of genetic information and the template for gene duplication by which genetic information is passed from parent to progeny. They are also the template for gene expression which permits the translation of gene structure into polypeptide structure. They are indeed the molecules of life.

Two types of nucleic acid are involved in these processes. Deoxyribonucleic acid (DNA) is the template for both gene replication and gene expression, while ribonucleic acid (RNA) is the means by which information stored in DNA is translated into proteins (see footnote).

The structure and function of nucleic acids have been elucidated, for the most part, in the last twenty years or so. DNA and RNA both consist of chains of alternating sugar and phosphate moieties joined together by C₃-C₅ phospho-diester linkages, with heterocyclic purine and pyrimidine bases attached to the C₁ atom of the sugar group. The combined unit of sugar with attached phosphate and base is called a nucleotide². The principal distinction between RNA and DNA lies in the sugar residue and the heterocyclic bases. In RNA the sugar is D-ribose and in DNA, 2'-deoxyribose. The bases usually found in RNA are adenine, guanine, cytosine and uracil. In DNA thymine replaces uracil. Careful analyses now exist of the base composition of the DNA of a large number of organisms. In some organisms bases other than those mentioned above

Footnote: In some viruses RNA can carry out both functions.

exist, usually comprising only a small percentage of the base complement.

Although elucidation of the primary structure of nucleic acids provided a significant contribution to the knowledge of nucleic acids it did^{not} contribute directly to the understanding of the relationship between their structure and their biological function, the importance of which had become recognised by 1950. The important key to this relationship lies in the secondary structure of DNA first proposed by Watson and Crick in 1953^{3,4}. This elegant proposal states that the DNA molecule is composed of two ribose-phosphate chains coiled around a common axis. The chains are anti-parallel, right hand helices on the outside of the structure with the planes of the bases arranged perpendicular to the major helix axis and directed inwards. In this manner the bases pair in a specific way by hydrogen bonding so that adenine (A) on one strand is hydrogen bonded to thymine (T) on the other, and similarly, guanine (G) is hydrogen bonded to cytosine (C). At once this proposal explained what had been known as Chargaff's Rule⁵, that in DNA the ratios of adenine to thymine and guanine to cytosine were always very nearly unity. More importantly, it provided the clue to the copying mechanism for genetic material, as the arrangement of bases on one strand of the double helix uniquely determines the bases on the other. Thus from the separation of strands of the duplex and synthesis of the opposing strand of each, two identical representations of the parent duplex will be produced with no loss of specificity. The double helical structure of DNA has since been confirmed^{6,7} and is now generally accepted as the basic structure of DNA both in vivo and in vitro. Some exceptions to this generality exist, for example DNA extracted from some phages is single stranded (e.g. ϕ x 174).

In view of the fundamental role of DNA in all living matter studies of its interaction with other chemical compounds have become a major field

of research in a wide range of disciplines, especially in biochemistry and pharmacology. Clearly, it may be anticipated that a compound which can interact with DNA to influence in any way the macromolecule's structure or composition will have a profound effect on cellular activity. This has been demonstrated many times and the manifestations of such interactions have been shown to include mutagenic,^{8, 9} carcinogenic,¹⁰⁻¹⁴ antibacterial,¹⁵⁻¹⁷ and antiprotazoal¹⁸⁻²⁰ activity. The study of such interactions has been valuable in providing further understanding of the structure of DNA in vivo and in vitro and details of its function in vivo.

Although medical interest in acridines dates from 1888, it was Browning's discovery of the antibacterial activity of proflavine and acriflavine in 1913²¹ that first saw their introduction into medical practice. Proflavine was widely used during World War I as a topical bacteriostatic agent. Interest in aminoacridines was further encouraged by the discovery²² and widespread use of mepacrine as an anti-malarial drug. At the present time a large number of aminoacridines are used in chemotherapy¹⁷ and as histological stains²³.

That the origin of the biological activity of aminoacridines arises from the interaction of these compounds with nucleic acids has been known for many years²⁰. It has also been long known that the antibacterial activity of aminoacridines is dependent on the strength of these substances as bases²⁴. That is, there is a correlation between their biological activity and their presence in solution at physiological pH as cations. The interaction of aminoacridines with DNA has been described in terms of two binding processes²⁵⁻²⁷. Cavalieri et al^{25, 26} proposed that the two forms of binding were due to the electrostatic interaction between aminoacridine cations and primary and secondary phosphate groups of the DNA. This proposal was put forward before the Watson and Crick³ model of DNA and has been rejected because of the insufficient number of secondary phosphate groups to account for the extent of binding. Peacocke and

Skerrett²⁷ assigned the two processes to a strong interaction of aminoacridine monomer predominant up to an extent of binding (bound aminoacridine per DNA phosphorous = r) of $r = 0.2$, the observable limit of the stronger binding, followed by a weaker binding of aminoacridine aggregates up to electroneutrality, that is $r = 1.0$. The Watson and Crick model of DNA, with the bases in close van der Waals contact appeared to exclude the possibility of aminoacridines interacting directly with the bases. However, in 1961 Lerman²⁸ proposed the intercalation model. In this model the DNA molecule extends to permit the insertion of aminoacridine cations between adjacent base pairs of the double helix. Evidence of such a change in the configuration of DNA has been provided by many workers and although modifications to the Lerman model have been proposed,²⁹⁻³¹ the basic concept has been accepted as the mode of binding for the stronger interaction. A more detailed discussion of the extensive experimental literature on the interaction and proposed models is presented in Chapter III of this work.

The intercalation hypothesis provides an explanation of the mutagenic activity which aminoacridines are observed to cause. In the intercalation model the distance between base pairs is doubled at the site of the bound aminoacridine^{28, 32, 33}. This modification of the DNA structure permits insertion or deletion of a base pair during replication and the resultant gene is called a frameshift mutation of the original^{9, 15, 34}. The ability of aminoacridines to induce mutants of this kind has assisted in the discovery of the triplet nucleotide basis of the genetic code³⁵. The intercalation model has been used successfully to describe the interaction of many biologically active compounds with DNA³⁶.

The second and weaker form of binding observed in the interaction of aminoacridines with DNA is generally believed to be a principally

electrostatic interaction between the aminoacridine cations and the negatively charged phosphate groups on the DNA backbone. It may also involve the binding of aminoacridine aggregates, as for many of these compounds aggregates readily form in solution³⁷.

The binding of aminoacridines to denatured DNA, in which the specificity of the double helical conformation is absent, has also been observed by a number of workers³⁸⁻⁴¹. Rather surprisingly, at room temperature, the binding is at least as strong as the binding to native DNA. Comparatively few temperature dependent studies of the comparative binding of aminoacridines to native and denatured DNA have been carried out^{41,42} and only one of these in a quantitative sense⁴². No studies have been made of the kinetics of the binding of aminoacridines to denatured DNA. Accordingly, in this work, the influence of DNA structure on the binding of 9-aminoacridine (9AA) has been investigated. 9-aminoacridine has been chosen as it is one of the structurally simplest aminoacridines which is known to intercalate with a high association constant⁴¹. An ionic strength of 0.1 μ (0.1M NaCl) neutral salt has been used throughout, as at this ionic strength the weaker binding is suppressed⁴¹. Furthermore this allows for a ready comparison with much of the existing literature on the subject.

In Chapter II the solution state of native and denatured DNA has been examined for the experimental conditions used throughout this work. Chapter III provides, as mentioned earlier, a detailed review of relevant research.

In Chapters IV and V the binding of 9-aminoacridine to native and denatured DNA, respectively, has been investigated as a function of temperature. The thermodynamic parameters for the interaction are evaluated and discussed with respect to the intercalation model.

The kinetics of the interaction have been studied by the

temperature-jump technique. The results of this study are presented in Chapter VI. Mechanisms are proposed for the interaction and these are shown to be consistent with the equilibrium measurements described in earlier chapters.

Finally, a brief general discussion of the conclusions is presented and details are provided of the materials and methods used in this work.

REFERENCES

1. Miescher, F., *Med. Chem. Unters.*, 4, 441 (1871).
2. See for example: Jordan, D.O., "The Chemistry of Nucleic Acids",
Butterworth & Co. (Publishers) Ltd., 1960.
3. Watson, J.D. and Crick, F.H.C., *Nature*, 171, 737 (1953).
4. Watson, J.D. and Crick, F.H.C., *Cold Spring Harbour Symp.*
Quant. Biol., 18, 123 (1953).
5. Chargaff, E. *et al*, *Biochim. Biophys. Acta*, 9, 402 (1952).
6. Arnott, S. *et al*, *J. Mol. Biol.*, 11, 391 (1965).
7. Luzzati, V., Nicoldieff, A. and Masson, F., *J. Mol. Biol.*,
3, 185 (1961).
8. Lerman, L.S. *J. Cell. and Comp. Physiol.*, 64, Sup. 1,1 (1964).
9. See for example: Hayes, W., "The Genetics of Bacteria and their
Viruses", 2nd edition, Blackwell Scientific Publications,
(Oxford). 1968.
10. Brookes, P. and Lawley, P.D., *Nature*, 202, 781 (1964).
11. Dingman, C.W. and Sporn, M.B., *Cancer Res.*, 27, 938 (1967).
12. Matsushima, D.T. and Lofberg, R.T., *Anal. Biochem.*, 16, 500 (1966).
13. Brookes, P. and Lawley, P.D., *Brit. Med. Bull.*, 20, 91 (1964).
14. Fuchs, R. and Daune, M., *FEBS. Lett.*, 14, 206 (1971).
15. Waring, M.J., *Nature*, 219, 1320 (1968).
16. Müller, W. and Crothers, D.M., *J. Mol. Biol.*, 35, 251 (1968).
17. See for example: Albert, A., "The Acridines", 2nd edition,
Arnold (Publishers) Ltd., (London). 1966.
18. Waring, M.J., *Mol. Pharmacol.*, 1,1 (1965).
19. O'Brien, R.L., Olenick, J.G. and Hahn, F.E.,
Proc. Nat. Acad. Sci. U.S.A., 55, 1511 (1966).
20. See for example: Albert, A., "Selective Toxicity", 4th edition,
Methuen & Co. Ltd., (Publishers), 1968.
21. Browning, C. and Gilmour, G., *J. Path. Bact.*, 18, 144 (1913).

22. Mauss and Mietzsch (I.G. Farben) (1930). quoted in ref. 17.
23. See for example: Frankel, S. et al "Clinical Laboratory Methods and Diagnosis", Vol. 1 and 2, C.V. Mosby Co., (Saint Louis).
1970.
24. Albert, A., Rubbo, S.D. and Goldacre, R., Nature, 147, 332 (1941).
25. Cavalieri, L.F. and Angelos, A., J. Amer. Chem. Soc., 72, 4686 (1950).
26. Cavalieri, L.F., Angelos, A. and Balis, M.E., J. Amer. Chem. Soc.,
73, 4902 (1951).
27. Peacocke, A.R. and Skerrett, J.N.H., Trans. Faraday Soc., 52, 261 (1956).
28. Lerman, L.S., J. Mol. Biol., 3, 18 (1961).
29. Pritchard, N.J., Blake, A. and Peacocke, A.R., Nature. 212, 1360 (1966).
30. Armstrong, R.W., Kurucsev, T. and Strauss, U.P., J. Amer. Chem. Soc.,
92, 3174 (1970).
31. Ramstein, J., Dourlent, M. and Leng, M., Biochem. Biophys. Res. Comm.,
47, 874 (1972).
- 32.. Gersch, N., Ph.D. Thesis, University of Adelaide, 1966.
33. Luzzati, V., Masson, F. and Lerman, L.S., J. Mol. Biol., 3, 634 (1961).
34. Lerman, L.S., Proc. Nat. Acad. Sci. Wash., 49, 94 (1963).
35. Crick, F.H.C. et al, Nature, 192, 1227 (1961).
36. See for example: Waring, M.J., M. and B. Lab. Bull., 10, 34 (1972).
37. Peacocke, A.R., Chem. Heterocycl. Comp., 9, 723 (1973).
38. Drummond, D.S., Simpson-Gildemeister, V.F.W. and Peacocke, A.R.,
Biopolymers, 3, 135 (1965).
39. Lloyd, P.H., Prutton, R.N. and Peacocke, A.R., Biochem. J., 107, 353
(1968).
40. Dalgleish, D.G., Fujita, H. and Peacocke, A.R., Biopolymers, 8, 633
(1969).
41. Sansom, L.N., Ph.D. Thesis, University of Adelaide, 1972.
42. Ichimura, S. et al, Biochem. Biophys. Acta., 190, 116 (1969).

CHAPTER II

Characterization of Native and Denatured DNA

<u>CONTENTS</u>	<u>Page</u>
1. Introduction	10
2. Native DNA	10
3. Denatured DNA	15
4. Renaturation	20
5. Concluding remarks	23
References	25

1. Introduction

The history of the determination of the structure of DNA is well known and has been widely described^{1, 2}. The picture of DNA proposed by Watson and Crick^{3, 4} has already been described briefly in Chapter I of this work.

In vivo DNA may exist in a variety of forms determined by the nature of its environment. In some virus particles the nucleic acid may exist as a single stranded polynucleotide chain. In other environments DNA may have the familiar double helical form of complementary strands and in still other situations this form itself may be constrained in an ordered structure. The interconversion of some or all of these structures is a necessary requirement of life. The complexity of the relationships between environmental factors and the structure of DNA in vivo is very great.

Stripped of cellular constituents, particularly nucleoproteins, DNA in vitro presents a less complex system for study. It is a system which is, none the less, very dependent on the environment of the macromolecule. It is therefore very important in all work on DNA in vitro that the solution environment should be well defined and the structure of DNA be understood in terms of its environment.

In this Chapter the properties of DNA in aqueous solution will be examined with particular reference to the neutral salt solutions used throughout this work.

2. Native DNA

In general, DNA extracted from bacteria or higher organisms undergoes moderate degradation during the extraction process. This degradation is a shearing of the DNA complement of the organism and results in particles of reduced molecular weight.

Provided that this reduced molecular weight is not too low then a solution of the DNA can be expected to behave in an homogeneous manner with respect to its interaction with small molecules. That is, end effects are a negligible contribution to observed phenomena. Throughout the course of this work a sample of DNA extracted from E.coli K-12 has been used (see Chapter VIII sections 1(a) and 1 (b) for preparation of samples and solutions). Analysis by ultracentrifugation has shown that the amount of low molecular weight material in a solution of the sample is very small and thus end effects will be insignificant.

In native DNA the principal characteristic of the macromolecule which is of interest is that through a wide range of ionic strengths of neutral salt the macromolecule exists in aqueous solution as a solvated double helix. In neutral solutions the polynucleotide chains act as a negatively charged polyelectrolyte, one negative charge residing on each phosphate of the ribose-phosphate backbone of the DNA. Clearly the effective charge on each phosphate group will depend on the concentration of the counterion in the solution⁵. Any small segment of double helical DNA may be considered as being rod-like⁶. This is a consequence of the conformation of the DNA with its planar purine and pyrimidine bases hydrogen bonded together and stacked with the plane of the bases perpendicular to the helix axis. A contribution to the rigidity of this rod-like structure arises from the mutual repulsion of the negative phosphate charges. Clearly the concentration of counterion in a solution of the polyelectrolyte will influence the interphosphate interaction and thereby the adjacent base-base distance and overall end-to-end distance of the macromolecule. That this is so has been demonstrated by viscometry⁶.

If the concentration of counterion is reduced below a certain critical level then an abrupt reduction in viscosity of DNA solutions⁷ and increase in UV absorption^{8,9} is observed. This is due to a loss of ordered double helical (secondary) structure which is only partially reversible by the subsequent addition of salt^{8,9,10}. In this disordered state the DNA is said to be dilution denatured: there is a degree of strand separation and in the absence of the conformational constraint provided by base pairing the structure collapses into a random coil which provides the minimum free energy state. The critical counterion concentration at which this occurs depends on the DNA concentration^{11,12} as the DNA itself, usually obtained as a salt, will make a contribution to the cationic counterion concentration in solution. DNA above a certain concentration will not spontaneously denature in water^{11,12}. In general, loss of long range secondary structure of DNA is termed denaturation.

Destabilization of the secondary structure of DNA can also be induced by very high concentrations of some neutral salts. This lyotropic or Hofmeister effect¹³ is not fully understood and is associated with concentrations of salts well outside the range used in this work and it will not be discussed further. In general an increase in neutral salt stabilizes the secondary structure with respect to denaturation⁵.

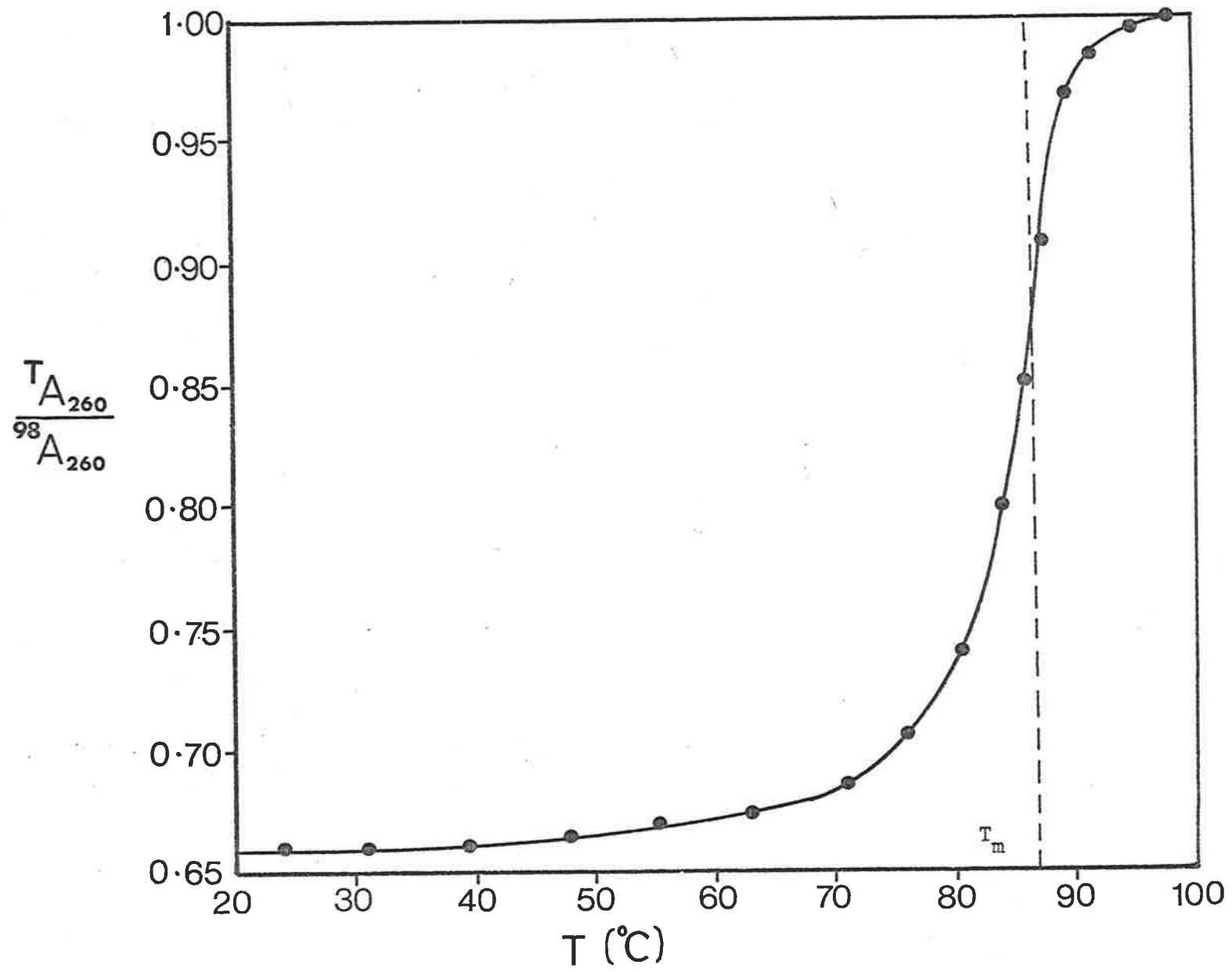
Denaturation can be induced in a number of ways in neutral salt solutions where the double helical structure is normally the most stable form of the polynucleotide. Two such methods are by alteration of the solution pH and by an increase in the solution temperature. In the former of these the hydrogen bonds between the complementary strands of DNA undergo proton

exchange, with the base or acid added, as the pH is raised or lowered. With the loss of hydrogen bonding the polynucleotide chains are free to take up the random coil conformation. Not all hydrogen bonds need be broken for a significant change in structure¹⁴. In general, the greater the stabilization of the secondary structure towards denaturation by an increase in the neutral salt concentration then the greater the pH change necessary from neutrality to cause denaturation¹⁰. In the course of this work, at a neutral salt concentration of 0.1M NaCl, the DNA double helical structure is stable through a sufficient range of pH to render buffering unnecessary.

The thermally induced transition from native to denatured forms can be observed most readily by UV spectrophotometry. The nucleic acid bases have well defined spectra in the UV¹⁵. The absorption band of native DNA, which has a maximum absorbance at about 260 nm (the precise maximum is dependent on the source of the DNA) has an extinction coefficient approximately 40% less than that which would be expected from the sum of the contributing constituents. This decrease in extinction coefficient, called hypochromicity, is a consequence of interactions between the bases when they are in a stacked conformation^{16, 17}. On denaturation, when the stacked conformation is destroyed, the resulting decrease in base-base interactions produces an increase in the UV absorption (hyperchromicity). Thus the change in absorbance of a DNA solution, observed conveniently at 260 nm, is a sensitive relative measure of base-base stacking.

In Fig. 2-1 the absorbance of a solution of native DNA in 0.1M NaCl is plotted as a function of temperature. The absorbance measurements are normalized to the absorbance at 98°C when the DNA is fully denatured. The absorbance measurements have been

Fig. 2-1. The melting curve of native DNA
in 0.1M NaCl. $T_m = 86.2^\circ\text{C}$.



corrected for volume expansion to an equivalent absorbance at 25°C,
thus:

$${}^T A_{\lambda} = {}^T A_{\lambda} \text{ (observed)} \frac{\rho_{25}}{\rho_T} \quad \text{eqn. 2-1.}$$

where ${}^T A_{\lambda}$ = volume corrected absorbance at temperature T and wavelength λ .

${}^T A_{\lambda}$ (observed) = observed absorbance at temperature T and wavelength λ .

ρ_{25} = density of pure water at 25°C.

ρ_T = density of pure water at temperature T¹⁸.

The ratio of densities of pure water at two temperatures differs insignificantly for these experiments from the ratio of densities of 0.1M NaCl for the same temperatures¹⁹. The correction described by equation 2-1. has been applied throughout this work. The reason for normalizing absorbance measurements to those of DNA at 98°C is because, as will be shown in the next section of this Chapter, difficulties arise in defining the solution state of denatured DNA at low temperatures. However, both native DNA and DNA which has been previously denatured behave identically at 98°C, thus a comparison of the UV absorbance of the two states (native and denatured) is possible at any temperature. Figure 2-1 is an example of a "melting curve" of a DNA solution. The sigmoidal shape of the curve is due to a cooperative loss of double helical secondary structure - called melting - when a temperature is reached such that the free energy change associated with a helix to coil transition becomes favourable. The temperature at which the midpoint of the transition occurs is called the melting temperature (T_m). The T_m of a given DNA

is dependent on the base composition of that DNA²⁰ and on the ionic strength of the neutral salt solution⁵. The hyperchromic change in the sample of DNA used throughout this work has been monitored with each solution of the DNA prepared in 0.1M NaCl and has been found to be:

$$\frac{A_{260}^{25}}{A_{260}^{98}} = 0.67 \pm 0.01 \quad \text{eqn. 2-2.}$$

The T_m of the DNA sample is $86.2 \pm 0.2^\circ\text{C}$.

Both the hyperchromicity and the T_m are independent of the concentration of the DNA solution throughout the range of experimental concentrations used in this work. The concentration of DNA solutions is usually defined as the concentration of DNA phosphate in solution (PO_4^-). In this work the range of concentrations used has been from approx. 10^{-6}M PO_4^- to $2 \times 10^{-3}\text{M PO}_4^-$. The concentration determination of DNA solutions is described in Chapter VIII section 1(c).

In carrying out melting curves it has been found that equilibration of solutions for approximately ten minutes is necessary before stable absorbance measurements are obtained. A heating rate of 1°C per minute through the melting range shifted the apparent T_m 3.5°C higher than the true T_m .

3. Denatured DNA

Above the thermal transition of DNA the macromolecule exists as a solvated random coil and is said to be denatured. Reduced to room temperature, the extent of reversibility of denaturation is a function of a number of variables, in particular the neutral

salt concentration and the rate of cooling^{2 1/2 2}. In general, the higher the neutral salt concentration the greater the hypochromic change on cooling. A slow rate of cooling also enhances the hypochromic change. Rapid ("shock") cooling by immersion of a sample of denatured DNA above its T_m into iced water produces a small hypochromic change once again dependent on the neutral salt concentration^{2 2}. Thus denatured DNA taken to room temperature may have a significant loss of double helical secondary structure. A variety of structures are available depending on the experimental method used. All such structures should be considered as metastable forms of DNA as their true free energy minimum is that pertaining in the native form. However, the mechanism to obtain the ordered state may not be available.

In this work DNA which has an extensive loss of secondary, double helical structure at room temperature has been prepared in the following way.

- (i) DNA has been dissolved in pure water at a concentration below the critical concentration for dilution denaturation. The concentration used has been 1 mgm/20 mls.
- (ii) After dissolution at 4°C for a minimum period of 24 hours aliquots are freeze dried. These solid samples are then stored in a desiccated atmosphere until required.
- (iii) Solutions are prepared by dissolution of the solid sample in pure water to half the required volume. The neutral salt concentration is then obtained by the addition of an equal volume of twice the salt concentration required.
- (iv) This solution is then heated for 10 minutes at 100°C and shock cooled in an ice/water mixture.

- (v) The concentration of the final solution is determined as described before.

The above procedure is followed as it has been found that resulting solutions have the maximum disruption of the double helical structure, as measured by hypochromicity, while still providing a high degree of reproducibility. This is shown by the observation that:

$$\frac{A_{260}^{20}}{A_{260}^{98}} = 0.78 \bar{0} + 0.01 \quad \text{eqn. 2-3.}$$

in 0.1M NaCl neutral salt, throughout the range of concentrations used in this work. This ratio is independent of the time of heating at 100°C if this is greater than 10 minutes.

The fact that the ratio above shows significant hypochromic change from unity indicates that even after shock cooling a significant amount of base-base interaction must be occurring. The interaction is strongly ionic strength dependent. This dependence probably arises from the variation in repulsion between the negatively charged phosphate moieties on the polynucleotide backbone with a variation in ionic strength. With an increase in neutral salt ionic strength the mutual repulsion between phosphates is reduced⁵ and with it the end to end distance of the molecule thus allowing more base-base interaction. This effect is shown in the following table:

TABLE 2-1

μ	0.001	0.01	0.10
$\frac{{}^3\text{O}_A}{260}$ $\frac{{}^9\text{B}_A}{260}$	0.917	0.882	0.804
σ	0.016	0.012	0.009

The table represents the average absorbance ratio for a number of solutions of denatured DNA with concentrations varying from $5 \times 10^{-5} \text{ M PO}_4^-$ to $2 \times 10^{-3} \text{ M PO}_4^-$. The value at ionic strength 0.001 is probably low as the ionic strength in the table refers only to the introduced neutral salt: the contribution from the polyelectrolyte cation has not been taken into account. In pure water at low DNA concentration a negligible hypochromic change was observed for a DNA sample prepared, as before, by shock cooling.

It has been suggested^{20, 23, 24} that three types of structure coexist in denatured DNA at room temperature. Base-base interactions occurring in these structures give rise to the hypochromicity observed. The three structures are:

- (i) short hair-pin loops or "folding" stabilized by short range helical order. Presumably of conventional A-T, G-C base pairs²¹
- (ii) single strand, base-stacked structures^{21, 24}
- (iii) random coils which will contribute very little to hypochromicity²⁴.

The regions in (i) above would be expected to have a spectrum of stabilities with respect to temperature. In (ii) above the stacking would decrease as the kinetic energy imparted to the bases increases with temperature. The former of these is considered by Studier²⁴ to contribute predominantly to the hypochromicity of denatured DNA.

An attempt to measure the rapidity of the random reformation of hydrogen bonding and base-stacking in (i) and (ii) above was made by using a stopped flow apparatus to follow the mixing of a shock cooled sample of denatured DNA in water with an equal aliquot of 0.2M NaCl. The mixing was followed at 275 nm where the percentage change in hypochromicity is greatest. However the process was too fast to be resolved by the instrument which had a resolution time of 5 msec. for complete mixing. Thus the formation of short hair-pin loops and single strand, base-stacking must be faster than this. These results are in agreement with the relaxation studies of Walz²⁵. The rapidity of these processes makes it unlikely that the folding, which is the principal cause of hypochromism in denatured DNA, can have any long range helical order.

The buoyant density of denatured DNA was measured by ultracentrifugation in an isopycnic density gradient of neutral CsCl. Denatured DNA had a broad distribution about a density of 1.724 skewed, with a greater component at lower densities. Native DNA had a buoyant density centred at 1.709 with a narrower, even distribution. The results for denatured DNA are consistent with a sample of E.coli K-12 DNA, of G-C content 50%, which has been denatured and in which some degradation has occurred. The reformation of an extended structure as well as the pure, collapsed, random coil is indicated by the component at low densities.

4. Renaturation

The temperature dependent properties of denatured DNA in 0.1M NaCl have been studied as this system has been used at elevated temperatures in experiments described later in this work. In particular the melting profiles, studied by UV spectrophotometry, have been investigated.

Figure 2-2 shows a comparison of the melting profiles of a native DNA solution (for which the melting profile, measured as absorbance relative to DNA at 98°C, is concentration independent) with three denatured DNA solutions of varying concentrations. In each instance an equilibration time of twenty minutes was permitted between temperature increments. As will be discussed shortly, the period of twenty minutes is an arbitrary interval. The denatured DNA absorption curves exhibit the following characteristics.

- (i) An initial sigmoidal shaped hyperchromic change in absorbance.
- (ii) A progressive increase in absorbance plateauing to a level which is inversely proportional to the DNA phosphate concentration.
- (iii) A final sigmoidal increase in absorbance with temperature occurring at a temperature which, within experimental error, is indistinguishable from that associated with the helix to coil transition of native DNA.

The following explanation is proposed for these observations.

It has already been pointed out in the previous section of this Chapter that shock cooled denatured DNA prepared as described has an absorbance, relative to denatured DNA at 98°C, which is independent

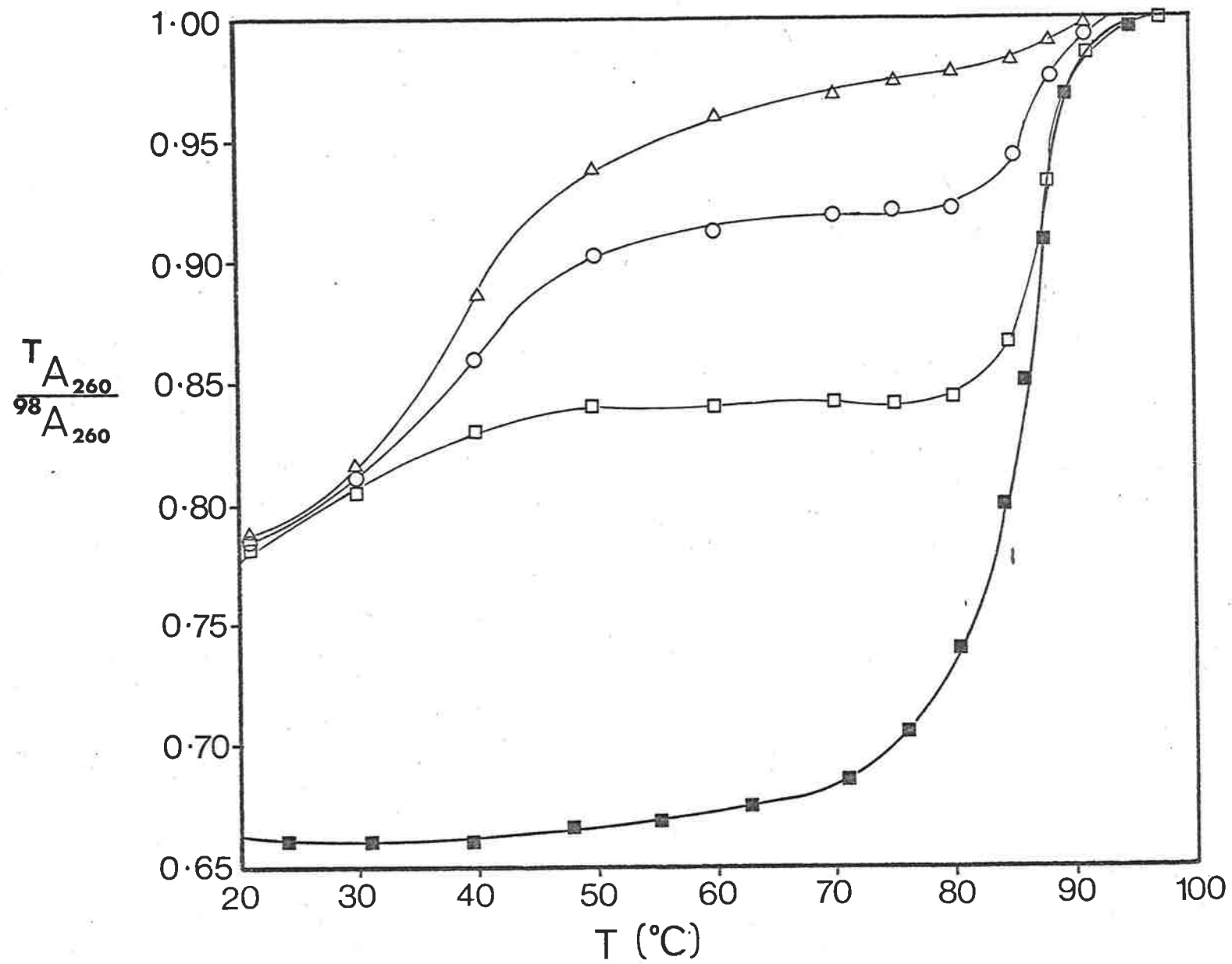
Fig. 2-2. A comparison of the melting profiles of:

(■) native DNA in 0.1 M NaCl,

(□) denatured DNA: 1.95×10^{-3} M PO_4^- , in 0.1 M NaCl,

(○) denatured DNA: 3.12×10^{-4} M PO_4^- , in 0.1 M NaCl,

(△) denatured DNA: 6.54×10^{-5} M PO_4^- , in 0.1 M NaCl.



of concentration (vide Fig. 2-2 at 20°C). This is taken to indicate the presence of a substantial amount of intramolecular base-base interaction as described in section 3 of this Chapter. An increase in temperature progressively destroys short range, helical ordered, base-pairing in what may be a broad cooperative transition at low temperatures (20°C-50°C). The steady increase in relative absorbance over this temperature range is due to this progressive loss of short range helical order and concurrent decrease in single strand stacking of bases. Throughout this loss of short range order, longer range order in the form of renaturation becomes increasingly important as the temperature increases to about 20°C below the melting temperature, $(T_m - 20)^\circ\text{C}^{26}$. Furthermore since renaturation has been shown to be a second order process²⁶⁻²⁹ over a significant range of concentration and ionic strength, the extent of renaturation per unit time increases with increasing concentration of DNA. The final sigmoidal curve is due to melting of the renatured fraction of DNA. The renatured material is indistinguishable in its melting temperature from native DNA. The observation of a plateau in the middle of the curve does bring into question the effect on hyperchromicity of the loss of single strand, base-stacking with increasing temperature as concurrent with the progressive loss of single strand, base-stacking is the increasing effect of renaturation which will tend to reduce absorbance. It may be that the observation by Studier²⁴ that loss of single strand, base-stacking does not contribute greatly to hyperchromicity is not valid. In Fig. 2-2 the curves 1, 2 and 3 are not equilibrium curves but do represent a family of curves, that is their position with respect to each other is fixed but their position relative to the absorbance axis is a function of the equilibration time between temperature increments. For the limiting case at short times, denatured DNA

which is rapidly heated to above its T_m displays a melting profile like that shown for curve 1 in Fig. 2-2, irrespective of the DNA concentration.

Figure 2-3 shows the change in absorbance with time for a denatured DNA solution heated rapidly to 70°C and maintained at that temperature. Renaturation proceeds to a point for which the absorbance is within a few per cent. of that expected for native DNA at that concentration. The loss of complete renaturation may be due to base pairing with not strictly complementary partners producing a significant extent of helix formation but with mismatched regions within the macromolecule or mismatched ends. These may be stable at the renaturing temperature (T_R). This suggestion is qualitatively in agreement with the observations of Thrower and Peacocke²⁸ who observed a decrease in extent of renaturation with increasing temperature difference between the temperature at which renaturation was measured and the melting temperature ($T_m - T_R$). This paper²⁸ also discusses the difficulties in measuring the value of absorbance at the completion of the reaction ("infinite time").

In Fig. 2-3 the infinite time value of absorbance has been determined from a plot of absorbance versus $(\text{time})^{-1}$ extrapolated to $(\text{time})^{-1} = 0$. Figure 2-4 is a second order reaction plot of the data presented in Fig. 2-3. For a second order reaction the rate law is:

$$\frac{x}{a(a-x)} = kt \quad \text{eqn. 2-4.}$$

where the quantities x , a , t , and k are defined below.

In Fig. 2-4 only relative quantities have been used: it being assumed that the extent of renaturation is proportional to the hypochromic

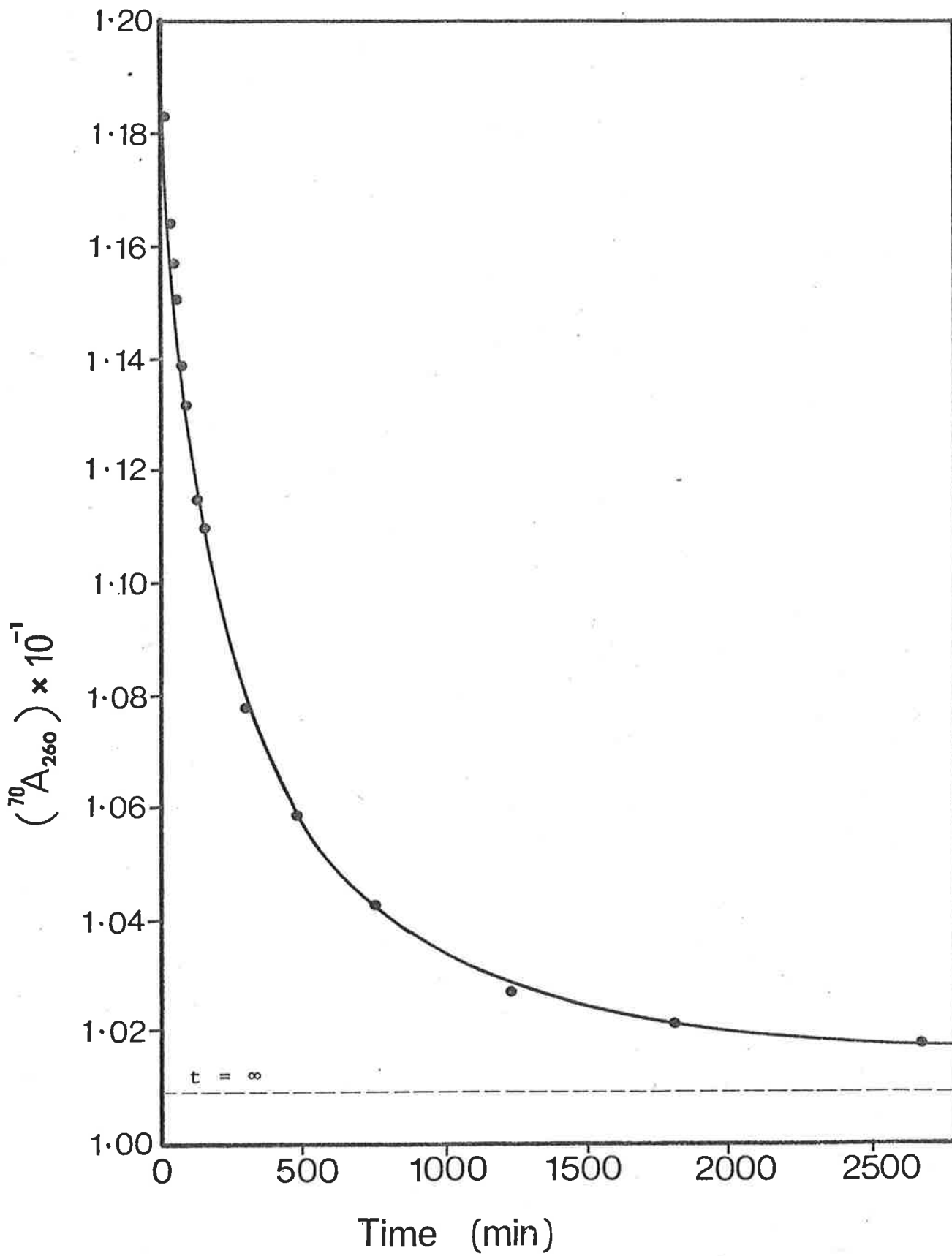


Fig. 2-3. The renaturation of denatured DNA in 0.1M NaCl heated rapidly to 70°C, studied by the change in absorbance at 260 nm with time.

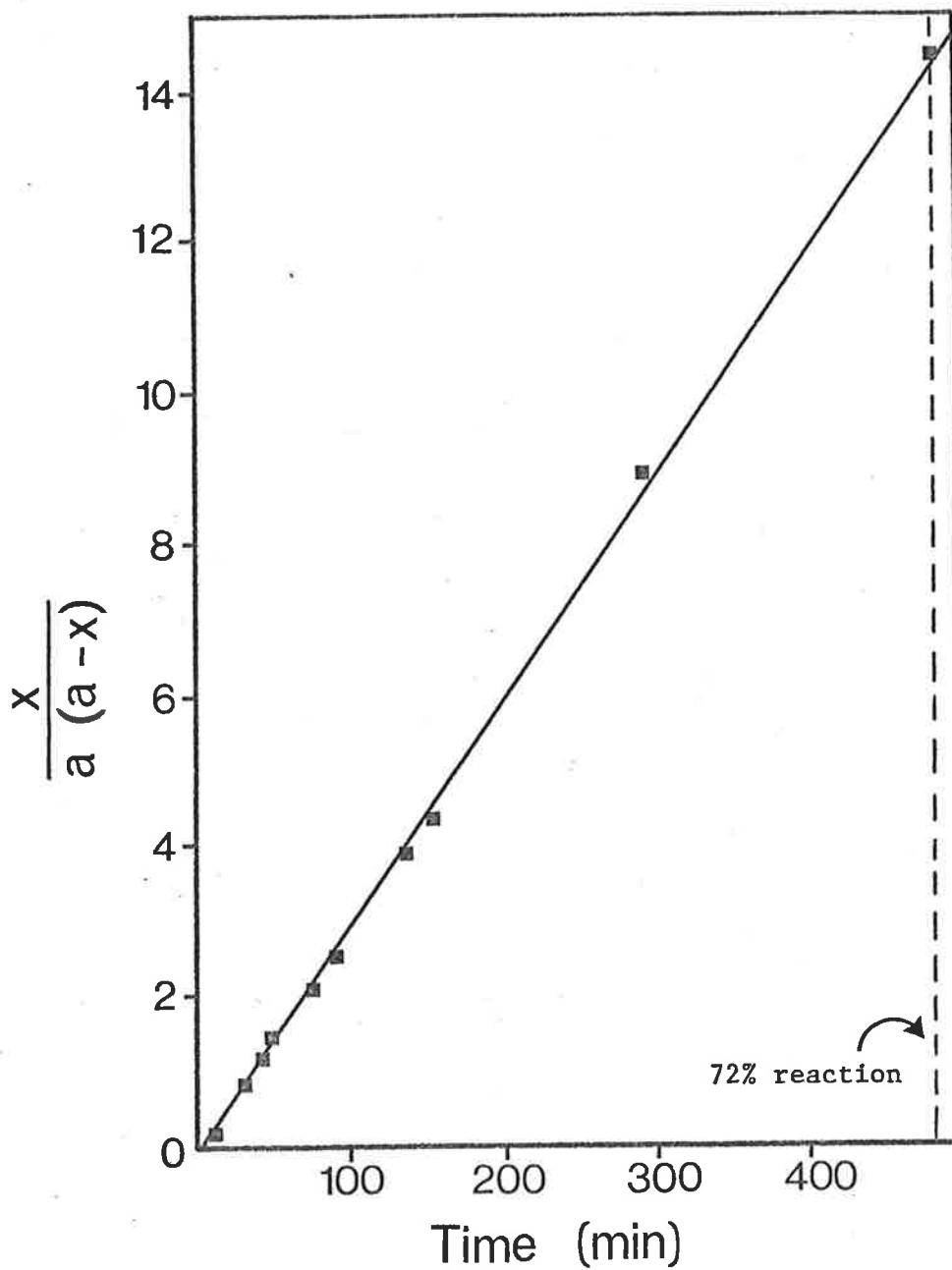


Fig. 2-4. The results of measurement recorded in Fig. 2-3. plotted according to equation 2-4. for the first 72% of reaction.

change. Thus x , the extent of renaturation at time t and a , the total extent of reaction are given by:

$$x = (A_{t=0} - A_{t=t})$$

eqns. 2-5.

$$a = (A_{t=0} - A_{t=x})$$

where A_t is the absorbance at time, t , corrected for volume expansion. It can be seen from Fig. 2-4 that renaturation obeys second order kinetics over a significant extent of reaction. From this plot alone it is not possible to determine a quantitative value for the rate constant, k . These results verify that renaturation is a second order process.

These observations have been included to show that denatured DNA in 0.1M NaCl is a system of some complexity. However, as will be discussed in relevant sections of this work, the renaturation of DNA in denatured DNA samples does not provide a significant contribution to observations in the experiments carried out, except where reference is made in the text. In general, experiments have been designed to keep the degree of renaturation a minimum.

5. Concluding remarks

Native DNA used in the experiments to be described in this work has been shown to be consistent with the double helical form of the polynucleotide throughout the range of temperatures used in studies on the interaction of 9-aminoacridine with native DNA (20°C-65°C).

Denatured DNA has been shown to be a more complex material than native DNA. In 0.1M NaCl, at room temperature, there is a significant degree of base-base interaction in the macromolecule. These interactions are believed to be A-T and G-C base pairing with short range helical order. Single strand, base-stacked regions

and random coil regions also exist. At elevated temperatures the short range helical order is lost and single strand, base-stacking is reduced. Elevated temperatures also promote renaturation of single stranded DNA.

Renaturation has been confirmed as a second order process. The rate constants are dependent, in a complex manner, on the temperature difference $(T_m - T_R)^{2\theta}$. In general, temperatures, concentrations of denatured DNA and experimental conditions can be chosen so that renatured DNA does not contribute to the effects being assigned to denatured DNA. Where this is not the case, in experiments described later in this work, specific mention is made in the text.

REFERENCES

1. Watson, J.D., "The Double Helix" W. H. Freeman & Co., 1968.
2. Crick, F.H.C., *Nature*, 248, 766 (1974).
3. Watson, J.D. and Crick, F.H.C., *Cold Spring Harbour Symp. Quant. Biol.*, 18, 123 (1953).
4. Watson, J.D. and Crick, F.H.C., *Nature*, 171, 737 (1953).
5. Schildkraut, C. and Lifson, S., *Biopolymers*, 3, 195 (1965).
6. Eigner, J. and Doty, P., *J. Mol. Biol.*, 12, 549 (1965).
7. Jordan, D.O. and Porter, M.R., *Trans. Faraday Soc.*, 50, 301 (1954).
8. Thomas, R., *Biochim. Biophys. Acta.*, 14, 231 (1954).
9. Thomas, R., *Trans. Faraday Soc.*, 50, 304 (1954).
10. Cavalieri, L.F., Rosoff, M. and Rosenberg, B.H., *J. Amer. Chem. Soc.*, 78, 5239 (1956).
11. Inman, R.B. and Jordan, D.O., *Biochim. Biophys. Acta.*, 42, 421 (1960).
12. Inman, R.B. and Jordan, D.O., *Biochim. Biophys. Acta.*, 42, 427 (1960).
13. von Hippel, P.H. and Schleich, T., in "The Structure and Stability of Biological Macromolecules" Vol. 2, Ch. 6, (1969).
14. Reichmann, M.E., Bunce, B.H. and Doty, P., *J. Polym. Sci.*, 10, 109 (1953).
15. Beaven, G.H., et al in "The Nucleic Acids" Vol. 1, (1955).
Eds. Chargaff, E. and Davidson, J.N.
16. Tinoco, I., *J. Amer. Chem. Soc.*, 82, 4785 (1960).
17. De Vries, H. and Tinoco, I., *J. Mol. Biol.*, 4, 518 (1962).
18. C.R.C. Handbook of Chemistry and Physics. Ed. Weast, R.C.,
The Chemical Rubber Co., Ohio, U.S.A. 1969-70.
19. Dunlop, P.J., personal communication.
20. Marmur, J. and Doty, P., *Nature*, 183, 1427 (1959).
21. Doty, P., et al, *Proc. Nat. Acad. Sci., Wash.*, 45, 482 (1959).

22. Marmur, J., Rownd, R. and Schildkraut, C.L., "Progress in Nucleic Acid Research" Vol. 1, 231. Eds. Davidson, J.N. and Cohn, W.E. (1963).
23. Josse, J. and Eigner, J., Ann. Rev. Biochem., 35, 789 (1966).
24. Studier, F.W., J. Mol. Biol., 41, 189 (1969).
25. Walz, F.G., Biopolymers, 11, 2365 (1972).
26. Wetmur, J.G. and Davidson, N., J. Mol. Biol., 31, 349 (1968).
27. Subirana, J.A. and Doty, P., Biopolymers, 4, 171 (1966).
28. Thrower, K.J. and Peacocke, A.R., Biochem. J., 109, 543 (1968).
29. Day, P., personal communication.

CHAPTER III

The Interaction of Aminoacridines with Nucleic Acids

<u>CONTENTS</u>	<u>Page</u>
1. Introduction	28
2. Binding sites	
(a) Calculation of the number of binding sites	29
(b) The number of binding sites and the effect of ionic strength	32
(c) Heterogeneity of binding sites	35
3. Structural factors	
(a) Effects of nucleic acid structure	37
(b) Effects of aminoacridine structure	40
4. Effects of the interaction	
(a) Effects on nucleic acids	43
(b) Effects on aminoacridines	46
5. Models for the complexes	
(a) Strong binding - complex I	49
(b) Weak binding - complex II	53
(c) Conclusions	54
6. Kinetics and mechanisms of the interaction	55
References	59

1. Introduction

The interaction of acridine derivatives with nucleic acids has been the subject of a large amount of research in the last twenty years. By far the most widely studied acridine derivatives have been the aminoacridines. The purpose of much of the research undertaken has been to elucidate the precise nature of the complexes formed in the interaction; partly in the hope that the knowledge so gained may be useful in a better understanding of their mode of action in chemotherapy, and partly in order to more fully understand the class of interactions which occurs between small ligands and biological macromolecules. Such interactions have become of burgeoning importance in recent years throughout the biological sciences.

It is a salutary comment on the complexity of the interaction that so much endeavour should have been expended without a precise definition of the interaction emerging so far. Researchers are increasingly inclined to define an interaction as specifically due to the particular constituents, and less likely to attempt to explain phenomena in a general way. In spite of individual differences a wide range of phenomena are found to be common to the interaction between different aminoacridines and nucleic acids. It is important that these aspects should be stressed as they may lead to an understanding of the interaction which is almost as complete if rather less specific.

In this Chapter a review has been made of the current models of the complexes arising from the interaction of aminoacridines (and some aminoacridine-like compounds) and their interaction with DNA. (The chemical structures of the compounds mentioned in the text are to be found in the Appendix). The experimental evidence which has led to the postulation of these models is also reviewed. A

comprehensive review of the literature would be a large undertaking; in this review only the principal contributions to the chemistry of the interaction, as seen at this time, and the most recent literature are summarized. A more complete survey of the biological role of the interaction has been given by Albert¹ and Peacocke².

2. Binding sites

(a) Calculation of the number of binding sites

In order to understand the interaction, or binding, of a small molecule onto a large one it is clearly necessary to obtain a measure of the strength of the binding and to determine the number of binding sites per identifiable unit on the macromolecule (n). In nucleic acids the most convenient unit is the nucleotide phosphorus, as this is the unit used to describe the concentration of DNA in solution. The strength of binding is obtained from a measure of the equilibrium constant for the binding. If the amount of ligand (aminoacridine) bound per nucleotide phosphorus is r and the concentration of unbound aminoacridine in equilibrium with it is c then the variation of r with c describes a Langmuir Isotherm³. The characteristic equation of the Langmuir Isotherm for a single type of binding site at which bound ligands do not interact with each other is:

$$r = \frac{nkc}{1 + kc} \quad \text{eqn. 3-1.}$$

where the variables r, n and c are defined as above and k is called the association constant and is the equilibrium constant associated with the ligand interacting with a binding site.

That is:

$$k = \frac{[\text{occupied site}]}{[\text{unoccupied site}] [\text{free ligand}]} \quad \text{eqn. 3-2.}$$

If there are j types of independent, non-interacting sites then equation 3-1 may be generalized to:

$$r = \sum_{i=1}^{i=j} \frac{n_i k_i c}{1 + k_i c} \quad \text{eqn. 3-3.}$$

From equation 3-1 the following expression can be obtained:

$$\frac{r}{c} = kn - kr \quad \text{eqn. 3-4.}$$

Thus for a single type of binding site a plot of $\frac{r}{c}$ versus r will be linear with an intercept at $r = n$ on the r axis and with a slope of $-k$. Such a plot is described as a Scatchard Plot⁴.

Scatchard Plots for the interactions of aminoacridines with nucleic acids are rarely linear. Curvature can occur for a number of reasons,⁴⁻⁶ principally from the presence of one or more of the following factors:

- (i) an electrostatic free energy dependence on r such that: $k = k' \exp (\Delta G_r^0 / RT)$.
- (ii) The existence of more than one type of binding site - as in equation 3-3.
- (iii) Interaction, direct or induced, between bound ligands.

The electrostatic dependence in (i) on page 30 can be suppressed if experimental work is carried out at a sufficiently high neutral salt concentration⁷. In case (ii) on page 30, if only two or three types of binding site are present with association constants which are well separated in magnitude it is usually possible to distinguish linear segments in the plot of $\frac{r}{c}$ versus r from which the contributing n_i and k_i may be calculated². A representation of the Scatchard Plots for one and two types of binding sites is given in Fig. 3-1. Care must be exercised in attributing curvature, as shown in Fig. 3-1 (b), to distinguishable binding sites as anticooperativity, caused by the direct or indirect interaction between the ligands bound to one type of site, may give rise to this effect, as mentioned in (iii) above. Anticooperativity will be discussed more fully in Chapter IV. Cooperative binding is rather more easily detected: this phenomenon is manifest as a curve convex to the c axis in the Langmuir Isotherm of r plotted against c . In the non-cooperative case the isotherm plateaus to a constant (limiting) r .

The analysis of cooperative and anticooperative binding curves is considerably more difficult than for binding curves arising from non-interacting sites. Some detailed statistical mechanical treatment of data has been attempted⁸. More recently, Schellman⁹ has demonstrated that even with a high degree of experimental accuracy a definitive interpretation of the type of interactions which may give rise to anticooperativity may not be unambiguously available. Nonetheless, these avenues are beginning to provide a better understanding, at the theoretical level, of empirical binding curves.

Although the detailed analysis of binding curves for aminoacridines and nucleic acids requires further attention, the curves do exhibit a number of characteristics which can be used, notwithstanding

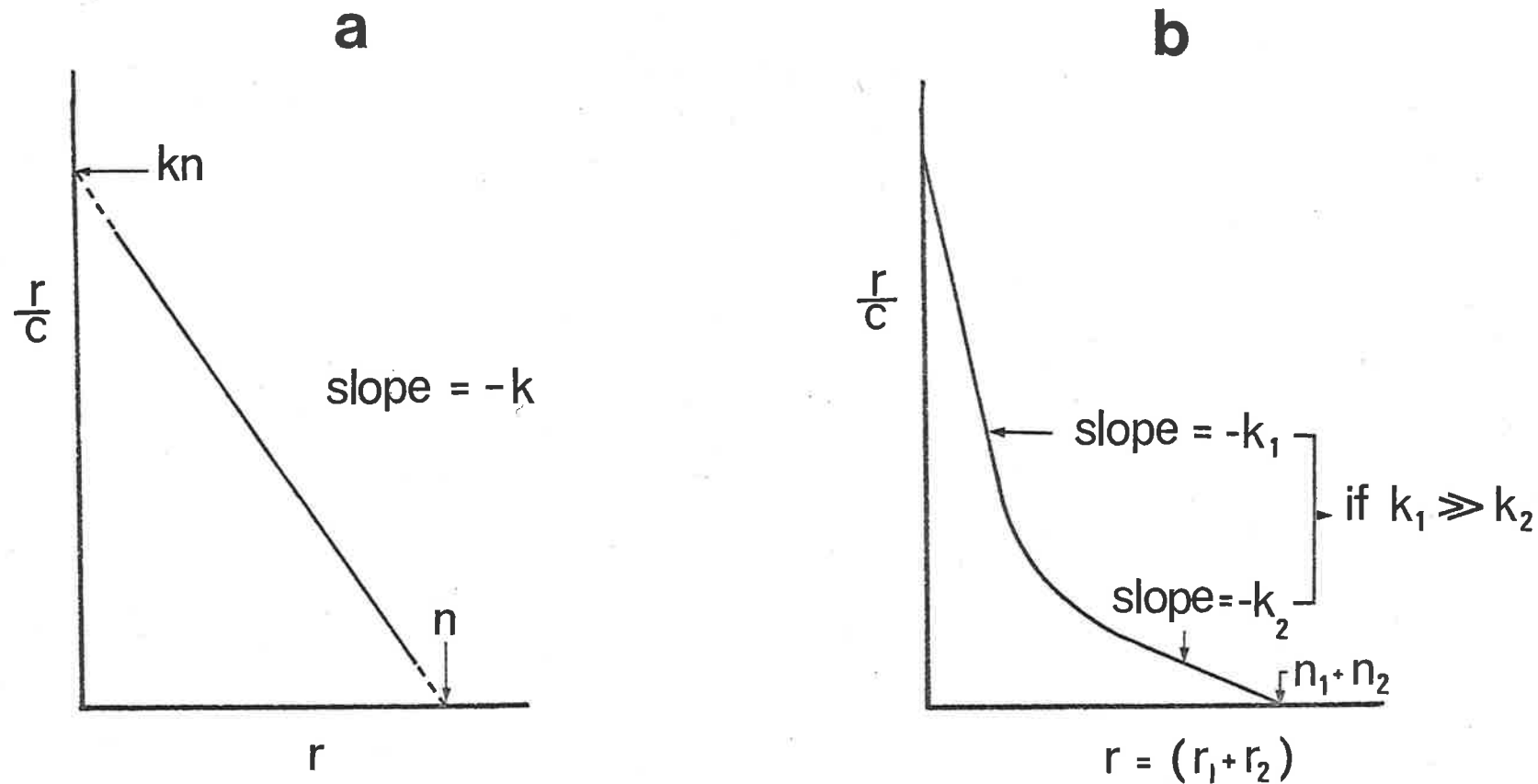


Fig. 3-1. Schematic representation of Scatchard plots
 (a) one type of binding site
 (b) two types of binding site with significantly different intrinsic association constants.

the opinions given in the previous paragraph, to quantitatively analyse them.

The methods for determining binding curves of aminoacridines on nucleic acids are numerous. They include, UV/visible spectrophotometry,^{7,10-14} equilibrium dialysis,^{7,12,13,15} sedimentation dialysis,¹⁶ partition analysis¹⁷ and fluorescence quenching¹⁷⁻²². These methods have been reviewed elsewhere and their limitations examined^{23,24}.

(b) The number of binding sites and the effect of ionic strength

Throughout the literature on the interaction of aminoacridines with nucleic acids there appears, frequently, compelling evidence of two distinct types of binding sites on the macromolecule. The earliest paper on the binding of proflavine to native DNA is typical⁷. As outlined in Chapter I these types of binding site are associated with two complexes: complex I in which the aminoacridine is strongly bound to the nucleic acid (ΔG° for the reaction ≈ -25 to -40 kJ/mole bound aminoacridine) and which binds up to about $r = 0.2$: complex II is the result of a weaker binding process (i.e. lower association constant) which prevails up to electroneutrality, that is $r = 1.0$. These observations were made initially on the basis of the shape of the Scatchard Plot which can be partitioned into two portions with the above mentioned characteristics. The binding curve r versus c shows a portion at higher r values convex to the c axis and this suggests that the formation of complex II may be a cooperative process.

At this stage it is necessary to introduce rudimentary models for the two complexes in order to be able to discuss refinements proposed in the literature. In 1961 Lerman²⁵ proposed, on the basis of his measurements of the change in contour length of DNA on its interaction with aminoacridines, that the aminoacridine

cation intercalates between the bases of the intact double helix. This occurs in such a way that the plane of the aminoacridine moiety is parallel to the plane of the purine and pyrimidine heterocyclic rings in the Watson and Crick double helix. In this way the adjacent bases on the same strand of the helix are forced apart giving rise to the observation mentioned²⁵. Subsequent research detailed in publications by Lerman supported this model of the interaction^{26,27}. This intercalation process is associated with the stronger interaction, the formation of complex I. The second and weaker complex is then associated with the electrostatic interaction between the negative polyphosphate backbone of the nucleic acid and the aminoacridine cation. In this state the aminoacridine is bound on the "outside" of the helix. The cooperative nature of the weaker interaction arises from the aggregation of aminoacridines to those already bound on the outside of the macromolecule. Aggregation of molecules in solution is a common feature of aminoacridine solutions.

The effect of the ionic strength of solutions on the binding of aminoacridines to nucleic acids is as may be expected from the above models. High ionic strengths markedly reduce the maximum extent of binding of aminoacridines to form complex II^{7,11,12,24}. This is to be expected as the effective negative charge of the polyphosphate is reduced by the large, shielding, counterion concentration, thereby suppressing the electrostatic interaction. Less expected is the observation that an increase in ionic strength also reduces the extent of binding in complex I form^{7,11,12,24}. It is not immediately apparent why the intercalated aminoacridine, in a hydrophobic environment, should be influenced by the ionic strength of solutions. Gilbert and Claverie²⁸ explained this phenomenon by demonstrating that purely electrostatic

interactions between the charges of the intercalated cation and the DNA polyphosphate occurring within a model of the intercalation system and electrostatic interactions between the bulk solution ions with the polyphosphate and aminoacridine cations could explain both the stability of the complex and its ionic strength dependence. However, in view of the extensive literature on stacking energies between heterocyclic systems arising from the interaction of permanent dipoles, induced dipoles and van der Waals forces - some of which have been specifically applied to aminoacridine - nucleic acid systems²⁹ - it seems fallacious to explain intercalation, or its ionic strength dependence only in terms of, (i) attraction between the cations and the polyphosphate, (ii) the repulsion between the cations and (iii) the reaction of the solution to the electric field of the polyphosphate and the cations. The observed dependence of the extent of complex I binding on ionic strength can be qualitatively explained by the following two proposals.

- (i) That this dependence, as measured from Scatchard Plots, is in part due to the contribution of complex II binding in the region dominated by complex I².
(At any stage in the equilibrium binding process there will be a finite contribution to r from complex II). This contribution, as mentioned before is very ionic strength dependent.
- (ii) That the base-pair separation distance in nucleic acids is reduced with increasing ionic strength as repulsion between nucleotide phosphates is reduced by counterion shielding⁸⁸. This will presumably reduce the probability of a favourable interaction occurring as well as lowering the association constant for the interaction when it does

occur, as has been observed^{2,4}.

(c) Heterogeneity of binding sites

As well as the marked heterogeneity between the binding sites marked by the existence of complex I and complex II, there exists the possibility of heterogeneity arising within the complexes. Studies on both proflavine and acridine orange binding to DNA led Armstrong et al¹³ to suggest that in the strong binding region these aminoacridines may bind as dimers onto already intercalated aminoacridines. This requires some of the intercalated aminoacridine to protrude from the helix to allow overlap between the heterocyclic ring structures. This suggestion is based on the observation of an isosbestic point occurring in the spectra, due only to the bound dye, as the value of r is changed. Unfortunately estimates of accuracy are not given for either the determination of the binding curve (measured by equilibrium dialysis) or in determining the contribution to the observed spectra due to free aminoacridine as monomer or dimer in solution. Hence the reliability of the isosbestic point cannot be judged. Furthermore the existence of the two bound species has been inferred from the presence of an isosbestic point in a series of spectra. These spectra have not been tested for internal linearity and the existence of only two species is therefore not unambiguous. The same observation could be obtained by a small but constant change in binding producing a monotone change in extinction coefficient for the bound species. The isosbestic point would then occur when:

$$\frac{\partial E_{\lambda}}{\partial \lambda} = 0 \quad \text{eqn. 3-5.}$$

where E_{λ} is the extinction coefficient of the bound species at wavelength λ ³⁰. Nonetheless the proposed model of Armstrong et al¹³ satisfactorily explains the results as presented.

At very low values of r the only bound species of aminoacridine present in detectable quantities is the intercalated, complex I, aminoacridine. In this situation the possibility of base specific heterogeneity arises. At these low values of r , fluorescence spectrophotometry has been used to determine the binding curves. Early reports suggested that adenine-thymine (A-T) bases bind aminoacridines preferentially^{19,20}. It has also been maintained that because the quantum yield of bound acridines varies with r these conclusions, based on fluorescence quenching of the aminoacridine-nucleic acid interaction, are invalid^{21,22}. However, this criticism of the earlier work has itself been questioned³¹ on the grounds that, at the low r values used, bound aminoacridines are too distant from each other for preferential energy transfer, from higher-quantum-yield sites (A-T) to lower-quantum-yield sites (G-C), to be an explanation of the variable quantum yield observed in references 19 and 22. The matter is clearly not fully resolved. The most recent publication³² on quinacrine binding to DNAs of varying G-C contents has led to the following conclusions which favour no base-specific heterogeneity.

- (1) Quinacrine has one type of binding site on differing G-C content DNAs.
- (2) Each bound molecule occupies a sequence of two pairs of DNA nucleotides.

- (3) The bound molecules are distributed randomly over all the binding sites without any G-C dependence.

The association constants quoted in this work³² are the same for the three different DNAs studied. The quinacrine-DNA complex is found to fluoresce with a high quantum yield when bound to a site with a sequence of at least three A-T base pairs, unlike proflavine and acriflavine which fluoresce with a high quantum yield on only two or more A-T base pairs³³.

3. Structural factors

(a) Effects of nucleic acid structure

For most in vitro work the two extreme structures of DNA in neutral salt solutions can be considered as being the ordered double helix, as found in native DNA at room temperature, and the disordered, single strand, random coil which is the conformation taken by DNA above its melting transition. Aminoacridines are quantitatively released from DNA when it takes up the latter structure^{24, 34}. Clearly, the structure of DNA plays an important role in the extent of binding as is to be expected from the basic model described in section 2 (b) of this Chapter. The first question to be asked is whether or not the intact double helix is required for binding to occur? The answer appears to be that this is not so. DNA which has been heat denatured and shock-cooled appears, at room temperature, to bind aminoacridines approximately as strongly as native DNA³⁴⁻³⁶. The temperature dependence of the binding, however, is much greater in denatured DNA than in the native structure, resulting in a cooperative loss of aminoacridines from denatured DNA at elevated temperatures below the melting temperature^{12, 13, 34}. Using equilibrium dialysis, Ichimura et al³⁴, have measured the thermodynamic parameters which

determine the binding of acridine orange to both native and denatured DNA. At low r values the strong binding (complex I) can be associated with a single association constant for both forms of the DNA. The free energy of reaction (ΔG°) shows a marked change with temperature in the case of denatured DNA but a small change with native DNA. This arises from a larger entropy term associated with the denatured DNA-acridine orange complex formation. The similar values for the binding constants at room temperature occur because of the larger favourable value of the enthalpy of reaction (ΔH°) for the formation of the denatured DNA-acridine orange complex as compared with the native DNA complex. Ichimura *et al*³⁴ have quoted values for the entropy of reaction (ΔS°) which are significantly more accurate than the experimental results allow since the appropriate relationship that should be used for results obtained from ΔG° values only, with no independent estimate of ΔH° , is:

$$\Delta S^\circ = \frac{-\partial \Delta G^\circ}{\partial T} \quad \text{eqn. 3-6.}$$

and not, as has been used,

$$\Delta S^\circ = \frac{\Delta H^\circ - \Delta G^\circ}{T} \quad \text{eqn. 3-7.}$$

This is discussed more fully in Chapter IV. Nonetheless, the differences between the ΔS° values for the binding of acridine orange to native and denatured DNA is significant and, as will be discussed in Chapter V, is related to a change in the conformation of denatured DNA.

DNA denatured other than by heat has been studied in its interaction with aminoacridines. Blake et al³⁵ quoted in reference 2 have observed that proflavine binds to DNA at pH 2.8 with a spectrum like that of proflavine bound to heat denatured DNA at low ionic strength. At low r the spectrum is indistinguishable from that due to complex I, however, as r increases the spectral contribution from complex II is greater than in the native DNA-proflavine material. This has been observed also in heat denatured DNA-acridine orange complexes³⁷. Similarities between the spectral shifts due to aggregation in solution free of DNA and in the presence of DNA led these authors³⁷ to propose that complex II binding is the stacking of aggregates of the aminoacridine on the outside surface of the macromolecule.

In the strong binding region the number of binding sites appears to approximately double on denaturation of the macromolecule^{24, 34}. Although this effect has been studied as a function of ionic strength²⁴, it has not been explicitly studied as a function of temperature.

The isosbestic points in acridine orange-denatured DNA complexes disappear with increasing r at low ionic strength³⁸; however with proflavine and denatured DNA a clear isosbestic point is observed²⁴. Clearly the structural requirement of nucleic acids for the binding of aminoacridines is still somewhat confused. A similarly confusing picture arises from research into the interaction of aminoacridines with synthetic polynucleotides, for which the structures of the macromolecule are often better characterized than in denatured DNA. These are competently reviewed elsewhere².

In summary, it can be said that both complex I and complex II type interactions occur for aminoacridines and both native and denatured DNAs. The number of binding sites appears to increase on denaturation. The effect of temperature is more marked on complexes with denatured DNA than with native DNA. Spectrophotometric measurements suggest that attention should be paid to the possibility of heterogeneity in denatured DNA-aminoacridine systems. This will be discussed more fully in Chapter V of this work.

(b) Effect of aminoacridine structure

It has already been pointed out earlier in this Chapter that different aminoacridines exhibit differing binding behaviours with DNA. This is to be expected as the nature and position of groups attached to the acridine nucleus will determine the electronic distribution within the molecule and will thus influence the interaction between the aminoacridines and the bases of the DNA. Steric factors also can be expected to influence the location of a bound moiety.

As pointed out in Chapter I, in parallel with their antibacterial activity only those aminoacridines which are in their cationic form interact strongly with DNA. This indicates that electrostatic forces play some part in the interaction. Löber and Achtert³⁹ have shown that amino-substitution in the 3 or 3 and 6 positions in the acridine nucleus decreases the charge located on both the C₉ and ring nitrogen positions in favour of the amino substituents. Thus interaction of the amino groups, as well as the ring nitrogen, with the negatively charged phosphate groups on the polynucleotide is possible. Substitution with electron donating groups at the 3 or 3 and 6 positions increases

the basicity of acridines¹ with a resulting enhancement in their ability to bind to DNA³⁹. In earlier work Löber⁴⁰ has shown that the association constants for the binding to DNA of a series of acridine derivatives increases with increasing pK_a of the compounds. Corresponding to this increase in basicity there is a decrease in the net positive charge on the ring nitrogen, thus the enhanced binding cannot be explained entirely by the electrostatic interaction between the ring nitrogen and the negative phosphate group.

Alkylation of the ring nitrogen of proflavine and acridine orange with methyl, ethyl, propyl, butyl and amyl groups results in a significant increase in their binding to DNA relative to the parent compound. However this increase is not sensitive to the length of the alkyl chain³⁹. On the other hand, when the ring nitrogen of acridine is alkylated its interaction with DNA does decrease as the length of the aliphatic chain increases³⁹. These observations suggest that the ring nitrogen is not very important in the interaction of aminoacridines with DNA but is critical for the interaction with DNA of the acridine base itself.

The attachment of long bulky side chains to the amino group of 9-aminoacridine, as in atebirin, does not hinder the interaction with DNA^{11,15,41}. This indicates that long chains attached to the 9-position do not sterically interfere with the interaction.

The requirements of a planar ring structure for the interaction of aminoacridines with DNA has been demonstrated by the significant reduction in binding when one ring of the 9-aminoacridine cation is saturated¹¹. Nonetheless, binding characteristics of complex I do occur and presumably complete insertion of the 3 aromatic rings is unnecessary for intercalation.

Müller and Crothers⁴² have suggested that the preferred orientation for the intercalation of 3,6-diaminoacridine (proflavine) derivatives is one in which the planes of the aminoacridine and the nucleotide bases are parallel and the semi-major axis of the compound is parallel to the line joining the phosphate groups on complementary strands of the double helix in the plane of the nucleotide bases. This conclusion arises from the observation that 2,7-tertiary butyl proflavine does not intercalate^{42,43}. If the semi-major axis of the aminoacridine and the interphosphate line, described above, were perpendicular, intercalation might occur. The same orientation is favoured for 4- and 9- substituted 9-aminoacridines studied by circular dichroism^{44,45}. Notwithstanding these observations, the proflavine and ethidium cations probably lie in some position intermediate to the parallel and perpendicular orientations mentioned above⁴⁴. Circular dichroism is potentially very useful in the examination of DNA-aminoacridine interactions. The complexity of the systems are such, however, that not a great deal has been achieved by this technique, so far, in unambiguously assigning orientations.

Recently, dichroic spectra of stretched films of ethidium bromide-DNA⁴⁶ and various dye-stuffs with DNA⁴⁷ have been measured. These have given explicit orientations for the dye stuffs with respect to the helix axis. In particular the work of Kelly⁴⁷ has demonstrated a similarity existing between proflavine and acriflavine, which both have the same substructure (7-aminoquinoline). In this work it was also demonstrated that proflavine and acriflavine each differ from 9-aminoacridine in their orientations relative to the helix axis, although no conclusive comments can be made about the similarity between proflavine and acriflavine themselves. This observation is in agreement with a postulate mentioned earlier⁴⁴.

Both Houssier⁴⁶ and Kelly⁴⁷ report that the plane of the ligands bound in complex I is not entirely parallel to the plane of the nucleotide bases. These results add significantly to the previous observations by polarized fluorescence²⁷ and flow dichroism^{27,48} which were unable to estimate the planarity of the aminoacridine-nucleotide base complex to better than $\pm 30^\circ$. It should, however, be borne in mind that in studies on films the structure of DNA is very sensitive to humidity⁴⁷ and care must be taken in extrapolating these observations to the solution state.

It will be readily appreciated from the foregoing comments that a wide variety of orientations appear available for aminoacridines intercalating into the DNA structure. At this time the conclusion of Löber and Achtert³⁹ that no single intercalation model exists for all aminoacridine derivatives seems the prudent one.

4. Effects of the interaction

(a) Effects on nucleic acids

Aminoacridines bound to nucleic acids have a marked effect on the structure of the macromolecule. These very significant changes, particularly the increase in intrinsic viscosity^{13,25,89} and the decrease in sedimentation coefficient,^{16,25,49} have presented some of the most direct evidence for the intercalation model for complex I binding. The variation of intrinsic viscosity and sedimentation coefficient measured as a function of r has been interpreted in terms of a configurational change in the DNA. The increase in viscosity, which occurs only up to an r value of about 0.2^{13,89} (that is with the aminoacridine predominantly in the complex I form) is associated with an increase in contour length of the macromolecule¹³. Drummond et al⁸⁹ have estimated that the increase in contour length is

approximately 3.4\AA° per bound aminoacridine: that is the equivalent of the normal van der Waals distance between stacked, planar heterocyclic rings. However their work carried out on DNA of principally large molecular weight fractions can only be described as tentative. A more recent study has been carried out on sonicated DNA of less than 2000 nucleotides per macromolecule⁴⁹. These results showed that the extension of the DNA molecule per bound proflavine was about 84% of the characteristic interbase spacing. The smaller molecular weight fractions provide an easier hydrodynamic system to analyse than the large macromolecules as they behave in a more rod-like fashion. These authors⁴⁹ noted that the increase in contour length was associated with some increase in flexibility of the macromolecule: an observation which was simultaneously noted by Armstrong et al¹³. The ability to increase the viscosity of DNA on interaction is by no means a property solely of aminoacridines. A wide range of compounds have been shown to have a similar effect including antibiotics, benzacridines and reporter molecules^{26,47,50,51}. The observation that the intrinsic viscosity does not match entirely the expected increase in viscosity on the Lerman model has led some workers to recently propose a variation in the binding model for proflavine and DNA⁵². In this variation the proflavine, or at least some of it, is not fully intercalated. This form may have some equivalence with the recently proposed "wedge" model of Kapicak and Gabbay⁵³ for the binding of a series of diamino substituted reporter molecules. However this model should not be confused with that proposed by Pritchard et al⁷⁵ (to be discussed later) which is itself a modification of the Lerman model.

In contrast to native DNA there is no increase in the viscosity of heat denatured DNA when proflavine or 9-aminoacridine

is bound to it at an ionic strength of $\mu = 0.1$ in the complex I binding region⁸⁹. More recently these studies have been confirmed, again by viscosity and also by the observation that there is no dependence of the sedimentation coefficient of denatured DNA on the extent of binding²⁴. These results indicate that the increase in contour length on strong binding to DNA is specific for the double helix.

The increase in contour length on the binding of proflavine to native DNA has been observed by autoradiography⁵⁴ and light scattering⁵⁵. These latter measurements reveal a corresponding increase in the radius of gyration⁵⁵. The increase in contour length is accompanied by a decrease in mass per unit length as determined by low angle x-ray measurements⁵⁶. The ultracentrifugation work of Sansom²⁴ showing a decrease in the sedimentation coefficient with increasing r for the binding of 9-aminoacridine with native DNA is in agreement with this observation. The decrease in mass per unit length is greater than that predicted by Lerman²⁵ but this can be accounted for by an increase in flexibility of DNA when intercalation occurs^{13,16,24,49}.

The extension of the helix is consistent with an unwinding of the bases relative to each other. X-ray diffraction patterns were originally shown to be consistent with an unwinding of between 12° and 45° . This result has been confirmed and refined for aminoacridines and other molecules, particularly the ethidium cation, which are believed to intercalate. On more stereochemical considerations Fuller and Waring⁵⁷ calculated an unwinding of 12° . A later study has confirmed this⁵⁸. A suggestion by Paoletti and Le Pecq⁵⁹ that intercalation may wind the helix rather than unwind it has been severely criticised by Pigram *et al*⁶⁰ who have also confirmed that unwinding occurs to the extent of about 12° in the

intercalation of ethidium bromide with DNA.

The binding of aminoacridines to nucleic acids stabilizes the double helical structure against thermal denaturation. The enhanced stability is indicated by an increase in the melting temperature of the complex^{12,24,29,61}. The increase in T_m is a linear function of r and reaches a maximum at the limit of complex I formation^{29,90}. Dye bound by complex II does not seem to increase the T_m and is dissociated at temperatures below the T_m ^{29,61}.

The increase in T_m on the binding of aminoacridines indicates that a large decrease has occurred in the free energy of the native DNA-aminoacridine system over that of the DNA alone. This decrease must be greater than the difference in free energy between denatured DNA-aminoacridine systems and denatured DNA²⁴. The free energy calculations of Gersch and Jordan²⁹ support this postulate.

(b) Effects on aminoacridines

The displacement of the electronic absorption spectrum of an aminoacridine when bound to DNA is the most characteristic, experimentally observed, feature of the interaction. In general, when the aminoacridine is bound as the monomer, the absorption maximum of the aminoacridine shifts to longer wavelengths and there is a decrease in the extinction coefficient^{7,11,62}. When the aminoacridine is bound in complex II the spectrum shifts to shorter wavelengths⁶³. This shift in the spectrum towards the blue is very similar to that obtained with solutions of aminoacridines where self association occurs and has thus been assigned to the formation of bound aggregates. The red shift in the visible spectrum is attributed to the interaction between aminoacridine cations and the planar bases of the DNA^{11,64,65}. The spectral changes associated with the

interaction of proflavine, at low r , with heat or acid denatured DNA are similar to those observed with native DNA and have been attributed to the interaction of the heterocyclic aminoacridine cations with the bases of the denatured DNA⁶⁴.

Optical rotatory dispersion (ORD) and circular dichroism (CD) are potentially more useful than absorption spectrophotometry in the study of aminoacridine-DNA interactions because of their greater sensitivity to environmental and structural factors. Aminoacridines bound to DNA exhibit extrinsic or induced Cotton effects in the regions of the absorption bands^{66,67,68}. The observed rotation in the extrinsic Cotton effect of acridine orange bound to DNA⁶⁶ has been attributed to an asymmetric perturbation of the aminoacridine chromophore by the DNA, as acridine orange is, itself, optically inactive. Such induced optical activity implies that a definite spatial relationship exists between the aminoacridine and its binding site. A number of explanations have been proposed for this optical anisotropy.

- (i) If the aminoacridine moieties are orientated in a helical array then this will produce the required asymmetry in the electronic transitions necessary for optical activity. The arrangement could result from external binding (complex II) or from intercalation (complex I)^{69,70}. However, denatured DNA with both proflavine and acridine orange each produces complexes which are optically active: indicating that long segments of double helix are not necessary for optical activity⁷¹.

- (ii) An asymmetry may be induced by the aminoacridine chromophore being bound within an asymmetric environment of the DNA^{68,72}.
- (iii) Nearest neighbour interactions can give rise to optical activity if the polynucleotide is able to hold two or more molecules in register so that their electric dipole moments may interact^{69,71}. However in 1, 2 and 9-aminoacridines acquired optical activity is independent of the extent of binding, r ⁷³. This observation is not expected from the nearest neighbour model. Aminoacridines with a 3-amino group and ethidium bromide do display, as a function of r , a steeply cooperative induced circular dichroism⁴⁴.

At the present time no single theory has been proposed which can relate the CD spectra of aminoacridine-DNA complexes to their structure and, thus far, any inference based on such observations is therefore indirect. Future development of these techniques can be expected to yield a great deal of information on the interaction of aminoacridines with DNA.

Lerman has shown⁷⁴ that the chemical reactivity of the amino groups of proflavine and other aminoacridines, as measured by diazotization rates, is markedly decreased when the compounds are bound to DNA. The reduction in rate is greater than that observed when these compounds are complexed with synthetic polymers such as polyphosphates and polystyrene sulphonate. Lerman concluded that the reduced reactivity was a consequence of the inaccessibility of the amino groups to the electrophilic reagent; this in turn was the result of the aminoacridine cation being completely enclosed within the DNA double helix.

5. Models for the complexes

In the previous sections of this Chapter an attempt has been made to summarize the experimental details of a large volume of research carried out, for the most part, over the last twenty years. Throughout this review continuous mention has been made of two complexes associated with the interaction of aminoacridines with DNA. The observation of two modes of binding was one of the first observations of the interaction and has been one of the most enduring. In this section the work reviewed will be summarized in terms of the current models for the interaction. Similar summaries have appeared elsewhere^{2,23,24}.

(a) Strong binding - complex I

The formation of complex I is associated with the following experimental characteristics.

- (1) It is a strong interaction; the free energy change for the interaction is of the order of $\Delta G^{\circ} \approx -25$ to -40 kJ/mole bound aminoacridine.
- (2) It is more favourable for aminoacridines with three aromatic rings. This is however, not an exclusive rule. The presence of one saturated ring does not preclude intercalation.
- (3) Only cations bind strongly; this may be a mechanistic requirement, although the interaction may be in part electrostatic for the interaction decreases with increasing ionic strength.
- (4) The contour length of double helical DNA is increased and its mass per unit length is decreased on binding of aminoacridines to form complex I.

- (5) The contour length of denatured DNA is not increased on binding if the ionic strength is such that the added cation has a negligible effect on the interphosphate repulsion of the phosphate groups of the macromolecule.
- (6) The plane of the bound aminoacridine cation is approximately parallel to the plane of the nucleotide bases and hence perpendicular to the axis of the double helix.
- (7) The reactivity of the amino groups on some aminoacridines is diminished on binding.
- (8) At room temperature complex I has a similar stability in both native and denatured DNAs but the extent of binding is greater in the latter.
- (9) Long side chains attached to the C₉ position of 9-aminoacridine derivatives do not hinder the interaction.
- (10) There is an upper limit to the extent of binding in complex I form of about $r = 0.20 - 0.25$ in aminoacridine-native DNA complexes.
- (11) The stability of native DNA is enhanced by aminoacridines bound in complex I form.

On the basis of observations (4), (6) and (7) Lerman²⁵⁻²⁷ proposed that the aminoacridine binds in such a way that the DNA molecule untwists and extends to allow the insertion of the cation between adjacent base pairs. This interaction is called intercalation. The aminoacridine is centrally located within the helix so that the ring nitrogen, which carries a partial positive charge is near the central axis of the DNA. The double helical structure of DNA is an essential requirement for this model (see Fig. 3-2). As mentioned previously, the degree of unwinding of the helix first proposed by

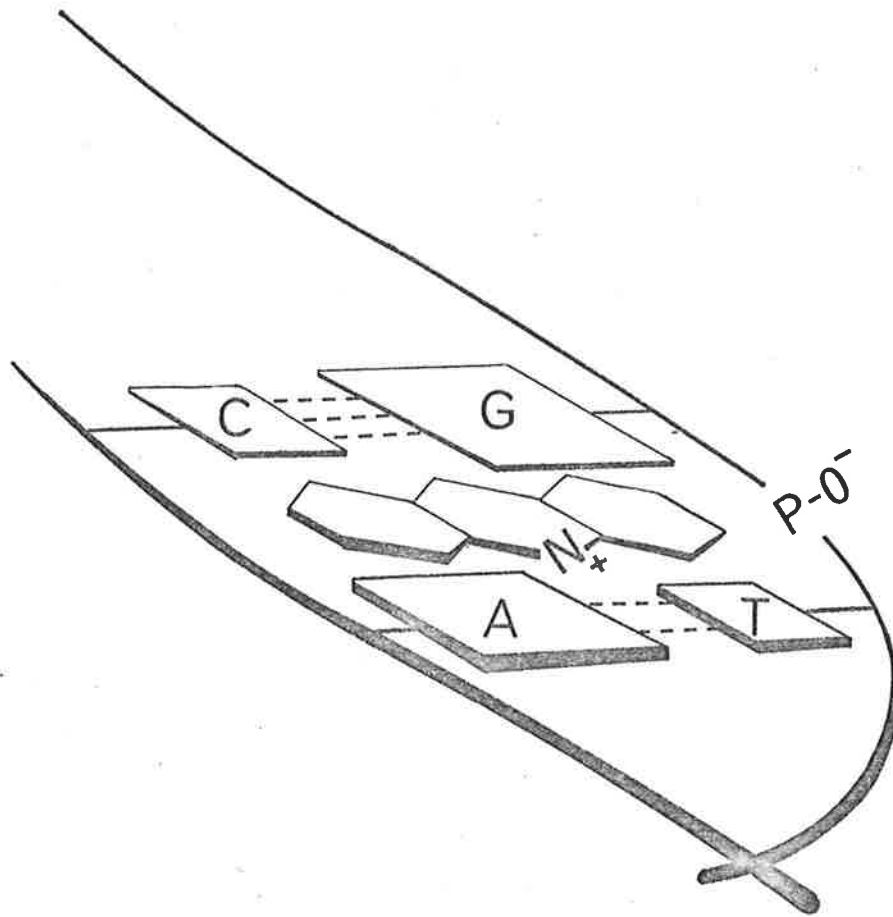


Fig. 3-2. Schematic representation of the intercalation model of Lerman for the interaction of aminoacridines with native DNA.

Lerman (45° - 12°) has been refined to the smaller angle of about 12° ^{57,60}.

Although the Lerman model satisfactorily explains a number of the observations summarized in this section it cannot account for observations (2), (5), (8) and (9). In order to explain these Pritchard et al⁷⁵ proposed a modification of the intercalation model in which the aminoacridine cation intercalates between successive bases on the same polynucleotide chain with its semi-major axis approximately perpendicular to the line joining the bases of the DNA on opposing strands (see Fig. 3-3). They further suggested that the phosphate group in the deoxyribose-phosphate backbone of the nucleic acid could deform in such a way that the negative charge may take up a position near to the positive ring nitrogen. This model can satisfactorily explain observations (2), (3), (8) and (9) as well as the observations by Lerman. Furthermore, in view of the less rigid conformation of denatured DNA, an extension of the base-base distance on interaction might be possible without the need for an increase in contour length, in accordance with observation (5). Items (1) and (11) are a direct consequence of the observably favourable interaction and need no further explanation.

Observation (10) requires some further comment.

There appears to be no immediate reason to limit the complex I binding to a number between $r = 0.20 - 0.25$. In the Lerman model it could be postulated that the limit would be $r = 0.5$; that is every pair of base pairs can have an aminoacridine cation sandwiched between them. In the Pritchard et al modification even this restriction need not apply. It is necessary, therefore, to seek some explanation for the limiting value of r . Müller and Crothers have proposed⁷⁶ for the intercalation of an antibiotic,

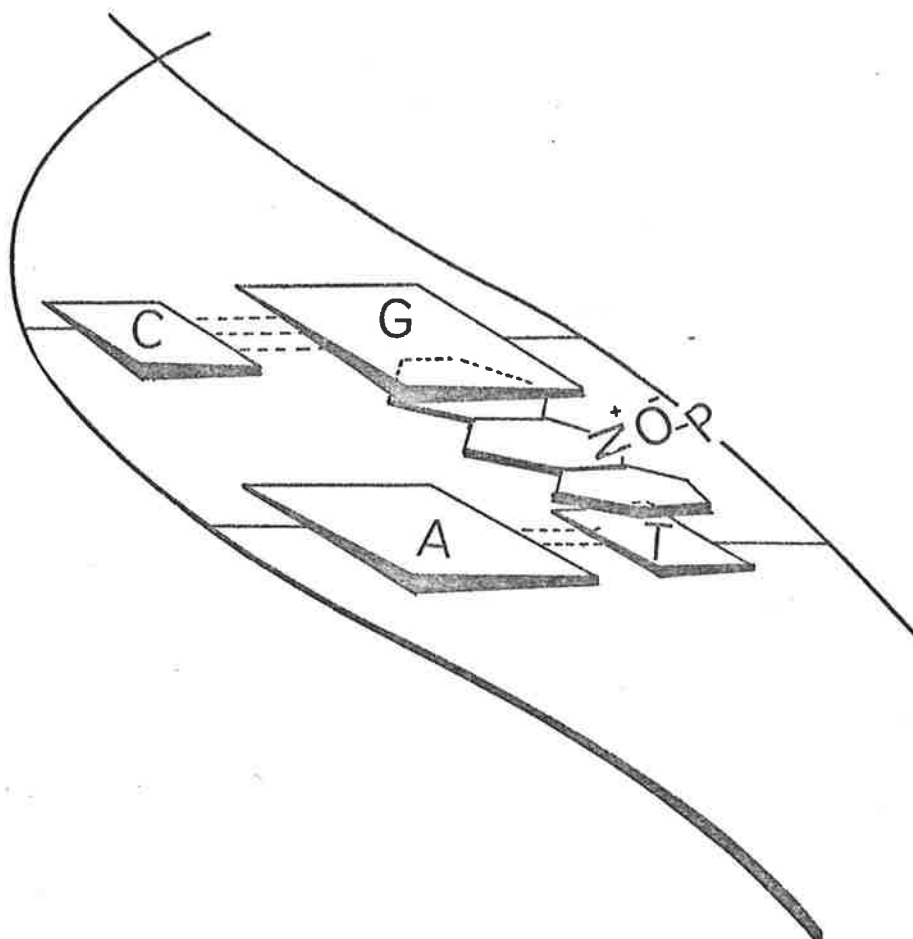


Fig. 3-3. Schematic representation of the intercalation model of Pritchard *et al* for the interaction of aminoacridines with native DNA.

that intercalation causes a distortion of the helix in the immediate vicinity of the bound antibiotic. The distortion is such that binding is prevented in a region totalling 5 base pairs surrounding the occupied site. This has been termed the site exclusion principle. It should be emphasised that this is an empirical observation only. Armstrong *et al*¹³ invoked a more rigorous proposal for the binding of aminoacridines to DNA by suggesting that:

"...every slot between two successive base pairs of the DNA helix constitutes a possible binding site for one intercalated dye (sic:aminoacridine) molecule. Intercalated dye is randomly distributed over all possible binding sites with one restriction - intercalation does not occur at sites immediately adjacent to one already occupied."

This proposal immediately introduces a limit to complex I binding at $r = 0.25$. It may be argued that the anti-cooperative nature of most binding, as demonstrated by the curvature of Scatchard plots at low r , makes the assignment of any exclusion principle redundant. Since direct evidence of neighbour exclusion is not available at the present time, the limits of r for complex I may be a consequence of aggregated distortion of the helix preventing binding to a greater extent than $r \approx 0.25$. Certainly it may be stated that binding becomes decreasingly favourable at values of r well below $r = 0.25$ as may be judged from the change in slope of the Scatchard plot in this region.

Recently Löber and co-workers⁷⁷⁻⁷⁹ have added to the understanding of the forces which stabilize the intercalation structure by demonstrating that the binding of a variety of

aminoacridines and similar compounds to DNA is reduced to below the level of detection of the complex when the complex I form is in the presence of organic solvents. This decrease in binding to DNA is attributed to increased lyophilic interactions between aminoacridine and organic solvent molecules. They suggest that the organic solvent competes with the DNA bases for hydrophobic interactions with the aminoacridines. In these experiments the DNA was believed to be in the native form. The importance of hydrophobic forces is certainly to be expected from either the Lerman or Pritchard model of the aminoacridine-DNA complex I.

Nonetheless the model of Pritchard et al⁷⁵ (Fig. 3-3) does not explain why the 2,7-di-tert-butyl proflavine molecule does not intercalate as described earlier;^{42,43,80} it would be expected to bind unless there is some mechanistic barrier influencing the rate. On the other hand the Lerman model (Fig. 3-2) would exclude binding on steric grounds. Similarly other work described earlier^{39,40} concerning alkylation of the ring nitrogen in proflavine and acridine orange favours the Lerman model. Thus it seems prudent at this time to consider the Lerman and Pritchard models as two extreme cases of essentially the same interaction. The actual configuration taken up by an aminoacridine in its interaction with native and denatured DNA to form complex I may be a blend of a number of interactions yielding for each aminoacridine in conjunction with each form of DNA a unique set of coordinates to define the interaction.

(b) Weak binding - complex II

Aminoacridine bound to nucleic acids to form complex II has the following experimental characteristics.

- (1) The binding energy is low; the free energy for the reaction is at the most a few kJoules per mole of bound aminoacridine.
- (2) It is principally electrostatic in nature and is decreased by an increase in ionic strength more markedly than aminoacridine bound in complex I form.
- (3) It can involve the interaction between bound molecules (aggregates).
- (4) Since it continues beyond the extent of binding dominated by complex I, which is an internal process, it is probably binding to the external, hydrated region of the helix.
- (5) It can occur up to electroneutrality, $r = 1.0$.

The most probable model for aminoacridines bound to form complex II is one in which the cation is bound externally to the helix with the positive ring nitrogen close to a negative phosphate group. Since the helix is extended by intercalation before it is possible to measure accurately the extent of weak binding no effect on the viscosity of DNA would be expected by increments in r above $r = 0.25$. This is found to be the case experimentally. The possibility of aggregation of aminoacridines on the outside of the helix occurs for those aminoacridines, like acridine orange, which readily self-associate.

(c) Conclusions

Other models for the binding of aminoacridines to DNA have been proposed but the concept of intercalation has now gained general acceptance. Further refinements are constantly being proposed and it is difficult to judge, in many instances, whether these are of general applicability to the interaction or are specific to the particular aminoacridine involved.

To conclude this section one recent example of modification is outlined. Armstrong et al¹³ have proposed that within the strong binding region two classes of bound dye exist for proflavine interacting with DNA. The first of these is a fully intercalated proflavine cation and the second, with a similar association constant (i.e. still strong binding), is a dimer formed by a second proflavine partially overlapping the first. Löber⁸¹ also noted, by fluorescence spectrophotometry, the presence of two forms of complex I for proflavine and DNA but gave no qualitative suggestion as to their form. More recently, Dourlent and Hélène⁸² have proposed that two forms of intercalated proflavine exist; one in which the proflavine is totally intercalated in A-T rich areas and another which is partially intercalated in G-C rich areas. (Note: Dourlent and Hélène⁸² have departed from the usual nomenclature and call complex I, as defined here, complex II and vice versa.) The questions that may be posed are:

- (i) do these three observations^{13,81,82} refer to the same states?
- (ii) Are the observations common to all aminoacridines but are not observed in some complexes because of a greater or lesser degree of self association in the aminoacridine?
- (iii) Are the observations particular to some aminoacridines which bind with a certain orientation with respect to the base pairs of DNA?

At this time too few results are available for a critical analysis.

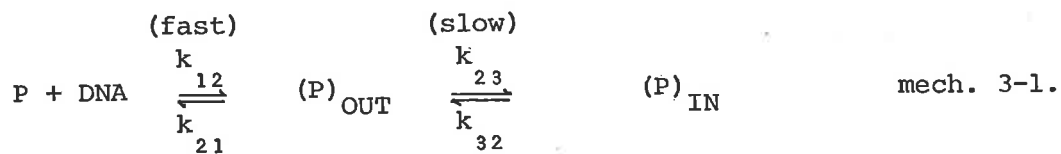
6. Kinetics and mechanisms of the interaction

The equilibrium between cationic aminoacridines and DNA is established very rapidly. In order to measure the rate processes

establishing the equilibrium it is therefore necessary to utilize perturbation or rapid mixing techniques. The latter of these has been used without conspicuous success^{83,84} except in so far as providing general support to mechanisms proposed from perturbation studies. Mixing techniques will not be discussed further. A detailed analysis of the temperature-jump perturbation technique appears in a later section of this work and so only the current results will be summarized here (see Chapter VI). In general, mechanisms deduced from perturbation techniques are not exclusive and a critical attention must be paid to equilibrium measurements and other known parameters of the system before a mechanism can be proposed.

On the basis of work using the temperature-jump technique Li and Crothers⁸⁵ have observed two well defined relaxation times for the perturbation of equilibria between proflavine and calf thymus DNA. They have proposed that two forms of the complex exist at equilibrium and that the interaction occurs by a two step mechanism. The first step is a rapid bimolecular process for which the forward rate constant approaches that for a diffusion limited process. The reverse rate constant for this bimolecular process is considerably smaller leading to a large favourable equilibrium constant. This process is assigned to the electrostatic interaction between the proflavine cations and the polyphosphate backbone of the DNA to form complex II. The dependence of the inverse relaxation time on the concentration of equilibrium reactant is linear, as expected. The second step of the interaction becomes concentration independent at high equilibrium reactant concentrations and is considerably slower than the first process. Li and Crothers⁸⁵ have proposed that the slower process arises from a conformational change in the DNA which allows intercalation to occur following external binding.

It is pointed out that no distinction can be made between this consecutive mechanism (mech. 3-1., below) and one in which the two processes are in parallel (mech. 3-2.) viz:



$$k_{12} \gg k_{21} \quad > \quad k_{23} > k_{32}$$



$$k_{12} \gg k_{21} \quad > \quad k_{23} > k_{32}$$

where P is the free proflavine at equilibrium, DNA is the concentration of free binding sites at equilibrium (see Chapter VI), and $(P)_{\text{OUT}}$ and $(P)_{\text{IN}}$ are, respectively, the concentrations of complex II and complex I at equilibrium. Li and Crothers,⁸⁵ favour mechanism 3-1. above. In a later publication Schmechel and Crothers⁸⁶ repeated the experiment with proflavine and polyA. polyU. A similar relaxation response was observed however significant variations with DNA type in the thermodynamic parameters associated with the mechanism were not explained in any qualitative sense.

It would be very fortunate if the mechanism proposed by Li and Crothers was generally applicable. However more recent publications have shown that variations may exist. Indeed, even the two relaxations in temperature perturbations of aminoacridine-DNA complexes are not always observed. In recent publications^{52,87} only a single relaxation was observed for the rapid temperature perturbation of proflavine with *M. lysodeikticus*,^{DNA} although the authors^{52,87} demonstrated that the same mechanism proposed by Li and Crothers (mech. 3-1.) could be used to explain their results by adjusting the overall kinetic parameters to agree with equilibrium measurements. The validity of this is discussed further in Chapter VI of this work.

Whether the intercalation mechanism (mech. 3-1.) requires the opening of a base pair to allow the dye to enter is not clear. However, Li and Crothers⁸⁵ favour a mechanism in which the dye can be inserted between base pairs without the necessity of base pair separation. This could be achieved by a longitudinal flexing of the DNA molecule occurring simultaneously with the insertion of the dye. In this way the rate constants for the slower reaction step may be expected to be dependent on ionic strength, as observed,⁸⁵ and also markedly dependent on temperature. However, there is little evidence to distinguish between the possibility of this mechanism and the "breathing model" of DNA⁹¹ in which interstitial unstacked regions in the macromolecule are found which would presumably facilitate intercalation.

REFERENCES

1. See for example: Albert, A., "The Acridines", 2nd edition, Arnold (Publishers) Ltd., (London). 1966.
2. Peacocke, A.R., Chem. Heterocycl. Comp., 9, 723 (1973).
3. Langmuir, I., J. Amer. Chem. Soc., 38, 2221 (1916).
4. Scatchard, G., Ann. N.Y. Acad. Sci., 51, 660 (1949).
5. Klotz, I.M., "The Proteins", Academic Press, N.Y., 1953.
6. Karush, F., J. Amer. Chem. Soc., 72, 2705 (1950).
7. Peacocke, A.R. and Skerrett, N.J.H., Trans. Faraday Soc., 52, 261 (1956).
8. Schwarz, G. et al, Eur. J. Biochem., 12, 442, 445, 461 (1970).
9. Schellman, J.A., Israel J. Chem., 12, 219 (1974).
10. Liersch, M. and Hartmann, G., Biochem. Z., 343, 16 (1961).
11. Drummond, D.S., Simpson-Gildemeister, V.F.W. and Peacocke, A.R., Biopolymers, 3, 135 (1965).
12. Chambron, J., Daune, M. and Sadron, C., Biochim. Biophys. Acta, 123, 306, 319 (1966).
13. Armstrong, R.W., Kurucsev, T. and Strauss, U.P., J. Amer. Chem. Soc., 92, 3174 (1970).
14. Jordan, D.O. and Sansom, L.N., Biopolymers, 10, 399 (1971).
15. Peacocke, A.R., Stud. Biophys. 24/25, 213 (1970).
16. Lloyd, P.H., Prutton, R.N. and Peacocke, A.R., Biochem. J. 107, 353 (1968).
17. Heilweil, H.G. and van Winkle, Q., J. Phys. Chem., 59, 939 (1955).
18. Oster, G., Trans. Faraday Soc., 47, 660 (1951).
19. Tubbs, R.K., Ditmars, W.E. and van Winkle, Q., J. Mol. Biol., 9, 545 (1964).
20. Thomas, J.C., Weill, G. and Daune, M., Biopolymers, 8, 647 (1969).

21. Ellerton, N.F. and Isenbert, I., *Biopolymers*, 8, 767 (1969).
22. Chan, L.M. and van Winkle, Q., *J. Mol. Biol.*, 40, 491 (1969).
23. Blake, A. and Peacocke, A.R., *Biopolymers*, 6, 1225 (1968).
24. Sansom, L.N., Ph.D. Thesis, University of Adelaide, 1972.
25. Lerman, L.S., *J. Mol. Biol.*, 3, 18 (1961).
26. Lerman, L.S., *J. Cell. Comp. Physiol., Suppl.* 1, 64, 1 (1964).
27. Lerman, L.S., *Proc. Nat. Acad. Sci. U.S.A.*, 49, 94 (1963).
28. Gilbert, M. and Claverie, P., *J. Theor. Biol.*, 18, 330 (1968).
29. Gersch, N.F. and Jordan, D.O., *J. Mol. Biol.*, 13, 138 (1965).
30. Brynestad, J. and Smith, G.P., *J. Phys. Chem.*, 72, 269 (1968).
31. Daune, M., quoted in reference 2.
32. Borisova, O.F. *et al*, *FEBS. Lett.*, 46, 239 (1974).
33. Chan, L.M. and McCarter, J.A., *Biochim. Biophys. Acta*, 204, 252 (1970).
34. Ichimura, S. *et al*, *Biochim. Biophys. Acta*, 190, 116 (1969).
35. Blake, A. and Peacocke, A.R., *Biopolymers*, 5, 383 (1967).
36. Jordan, D.O. and Sansom, L.N., *Stud. Biophys.*, 24/25, 225 (1970).
37. Bradley, D.F. and Wolf, M.K., *Proc. Nat. Acad. Sci. U.S.A.*, 45, 944 (1959).
38. Kharintonenkov, I.V. and Drynov, I.D., *Biofizika*, 16, 1008 (1971). Eng. trans.
39. Löber, G. and Aichert, G., *Biopolymers*, 8, 595 (1969).
40. Löber, G., *Photochem. Photobiol.* 8, 23 (1968).
41. Filipski, J., Chorazy, M. and Mendecki, J., *Stud. Biophys.*, 24/25, 249 (1970).
42. Müller, W. and Crothers, D.M., *Stud. Biophys.*, 24/25, 279 (1970).
43. Dalgleish, D.G., Feil, M.C. and Peacocke, A.R., *Biopolymers*, 11, 2415 (1972).

44. Dalglish, D.G. et al, *Biopolymers*, 10, 1853 (1971).
45. Dalglish, D.G. et al, *Biopolymers*, 11, 2387 (1972).
46. Houssier, C., Hardy, B. and Fredericq, E., *Biopolymers*, 13,
1141 (1974).
47. Kelly, G., Ph.D. Thesis, University of Adelaide, 1974.
48. Nagata, C. et al, *Biopolymers*, 4, 409 (1966).
49. Cohen, G. and Eisenberg, H., *Biopolymers*, 8, 45 (1969).
50. Waring, M.J., *M. and B. Lab. Bull.*, 10, 34 (1972).
51. Passero, F. et al, *Macromolecules*, 3, 158 (1970).
52. Ramstein, J., Dourlent, M. and Leng, M., *Biochem. Biophys.*
Res. Comm. 47, 874 (1972).
53. Kapicak, L. and Gabbay, E.J., *J. Amer. Chem. Soc.*, 97, 403 (1975).
54. Cairns, J., *Cold Spring Harbour Symp. Quant. Biol.*, 27, 311 (1962).
55. Mauss, Y. et al, *J. Mol. Biol.*, 27, 579 (1967).
56. Luzzati, V., Masson, F. and Lerman, L.S., *J. Mol. Biol.*,
3, 634 (1964).
57. Fuller, W. and Waring, M.J., *Ber. Bunsenges. Physik. Chem.*,
68, 805 (1964).
58. Neville, D.M. and Davies, D.R., *J. Mol. Biol.*, 17, 57 (1966).
59. Paoletti, J. and Le Pecq, J.P., *J. Mol. Biol.*, 59, 43 (1971).
60. Pigram, W.J., Fuller, W. and Davies, M.E., *J. Mol. Biol.*,
80, 361. (1973).
61. Kleinwachter, V., Bakarova, Z. and Bohacek, J., *Biochim. Biophys.*
Acta. 174, 188 (1969).
62. Löber, G., *Z. für Chemie.* 7, 252 (1969).
63. Michaelis, L., *Cold Spring Harbour Symp. Quant. Biol.*, 12, 131
(1947).
64. Walker, I.O., *Biochim. Biophys. Acta*, 109, 585 (1965).
65. Weill, G. and Calvin, M., *Biopolymers*, 1, 401 (1963).
66. Neville, D.M. and Bradley, D.F., *Biochim. Biophys. Acta*,
50, 397 (1961).

67. Blake, A. and Peacocke, A.R., *Nature*, 206, 1009 (1965).
68. Yamaoka, K. and Resnik, R.A., *J. Phys. Chem.*, 70, 4051 (1966).
69. Gardner, B.J. and Mason, S.F., *Biopolymers*, 5, 79 (1967).
70. Stryer, L. and Blout, E.R., *J. Amer. Chem. Soc.*, 83, 1411 (1961).
71. Blake, A. and Peacocke, A.R., *Biopolymers*, 4, 1091 (1966).
72. Aktipis, S. and Martz, W.W., *Biochem. Biophys. Res. Comm.*,
39, 307 (1970).
73. Dalgleish, D.G., Fujita, H. and Peacocke, A.R., *Biopolymers*, 8,
633 (1969).
74. Lerman, L.S., *J. Mol. Biol.*, 10, 367 (1964).
75. Pritchard, N.J., Blake, A. and Peacocke, A.R., *Nature*, 212,
1360 (1966).
76. Müller, W. and Crothers, D.M., *J. Mol. Biol.*, 35, 251 (1968).
77. Löber, G., Schuetz, H. and Kleinwachter, V., *Biopolymers*, 11,
2439 (1972).
78. Löber, G., *Stud. Biophys.*, 35, 57 (1973).
79. Löber, G. *et al*, *Stud. Biophys.*, 45, 91 (1974).
80. Müller, W., Crothers, D.M. and Waring, M.J., *Eur. J. Biochem.*,
39, 223 (1973).
81. Löber, G., *Stud. Biophys.* 24/25, 233 (1970).
82. Dourlent, M. and Hélène, C., *Eur. J. Biochem.* 23, 86 (1971).
83. Sakoda, M., Hiromi, K. and Akasaka, K., *Biopolymers*, 10,
1003 (1971).
84. Akasaka, K., Sakoda, M. and Hiromi, K., *Biochem. Biophys. Res.*
Comm., 40, 1239 (1970).
85. Li, H.J. and Crothers, D.M., *J. Mol. Biol.*, 39, 461 (1969).
86. Schmechel, D.E.V. and Crothers, D.M., *Biopolymers*, 10,
465 (1971).

87. Ramstein, J. et al, Dyn. Aspects of Conf. Changes in Biol.
Macromol. Proc. Ann. Meet. Soc. Chim. Phys., 23rd
(1972). (Published 1973) 333. Sadron, C., ed.
88. Schildkraut, C. and Lifson, S., Biopolymers, 3, 195 (1965).
89. Drummond, D.S. et al, Biopolymers, 4, 971 (1966).
90. Kleinwachter, V. and Koudelka, J., Biochim. Biophys. Acta,
91, 539 (1964).
91. von Hippel, P.H. and Wong, K.Y., J. Mol. Biol., 61, 587 (1971).

CHAPTER IV

The interaction of 9-aminoacridine with native DNA

<u>CONTENTS</u>	<u>Page</u>
1. Introduction	65
2. 9-aminoacridine	65
3. 9-aminoacridine and native DNA : spectra	66
4. 9-aminoacridine and native DNA : melting the complex	70
5. Determination of the extent of binding, r .	70
6. Extinction coefficient of bound 9-aminoacridine, ϵ_b	74
7. Determination of the intrinsic association constant, k	76
(a) - Introduction	76
(b) Anti-cooperative binding	77
(c) (i) Results	79
(ii) Thermodynamic parameters	81
8. Discussion	83
9. Concluding remarks.	85
References	87

1. Introduction

From the survey (Chapter III) of the interaction of aminoacridines with nucleic acids it is evident that a substantial number of different aminoacridines have been used in studying the interaction. 9-aminoacridine, which is to be investigated in this work, has also been studied previously^{1,2}. However, these studies^{1,2} have not provided any details of the thermodynamic parameters which govern the interaction. In this Chapter the spectral properties of the complex I form of bound aminoacridine are investigated. The results show that the spectrophotometric method for determining the binding curves³ can be used. This method has been somewhat refined and used to measure the association constant for the interaction at several temperatures. From these values the thermodynamic parameters have been calculated and are discussed in terms of the intercalation model.

2. 9-aminoacridine

9-aminoacridine (9AA) has a number of properties which makes it particularly suited to studies with DNA. The hydrochloride salt is relatively soluble in aqueous solutions, is stable and not light-sensitive, unlike widely studied proflavine⁴. As has already been pointed out, the interaction of aminoacridines with DNA is governed, in part, by their presence in solution as cations: 9AA, with a $pK_a = 10.0$,⁴ exists almost entirely as the cation in neutral salt solutions. 9AA has been found to undergo a reversible loss of one water of crystallization per molecule. Its molar extinction coefficient at 400 nm - the absorption maximum in the visible region - has been determined in this present work as $\epsilon_{400} = 10440 \pm 40$ in 0.1M NaCl. This is a higher

value than some previously reported values^{2,5} ($\epsilon_{400} = 8970$) where the water of crystallization in the molecular weight has not been taken into account. Significant deviations from Beer's Law ideality have been detected at very low concentrations; thus, as outlined in Chapter VIII section 2 all 9AA concentrations have been determined by weighed dilutions of a known stock solution.

3. 9-aminoacridine and native DNA : spectra

In the presence of DNA the maxima in the visible spectra of aminoacridine solutions undergo a red shift. This is shown in Figs. 4-1. to 4-3., each of which shows a spectrum of 9AA at a specified temperature and two other spectra of the same concentration of 9AA in differing concentrations of DNA. The concentrations are represented as:

$$T_L = (\text{ligand}) \text{ 9AA molar concentration}$$

$$T_A = \text{DNA concentration (molar phosphate)}$$

The red shift and reduction in $\epsilon_{\lambda_{\text{max}}}$ is common to many aminoacridine-DNA solutions⁶ as mentioned in Chapter III.

In each of the figures 4-1. to 4-3. a well defined isosbestic point is present. The isosbestic point is generally taken to be sufficient evidence for the presence of only two species of the chromophore (in this case 9AA) at equilibrium in the solution: viz., free 9AA and bound 9AA. Each of these species has a separate ϵ_{λ} : the isosbestic point arising when:

$$\epsilon_{\lambda}^{\text{free}} = \epsilon_{\lambda}^{\text{bound}} \quad \text{eqn. 4-1.}$$

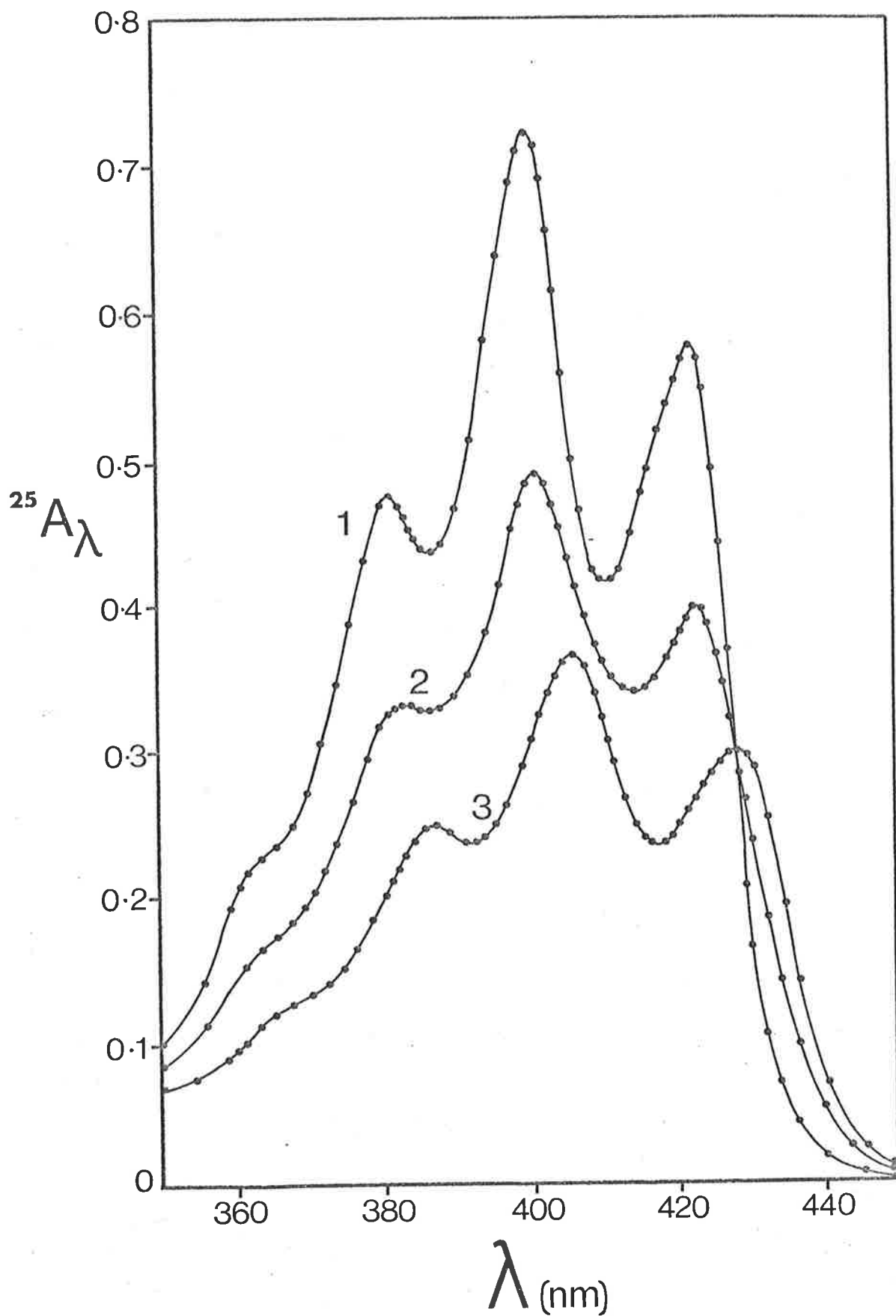


Fig. 4-1. Spectra of 9AA and native DNA in 0.1 M NaCl at 25°C: constant 9AA concentration, 7.31×10^{-5} M; curve 1: 9AA, curve 2: 9AA and native DNA: $T_L/T_A = 0.263$: $r = 0.138$, curve 3 : 9AA and native DNA: $T_L/T_A = 0.080$: $r = 0.076$.

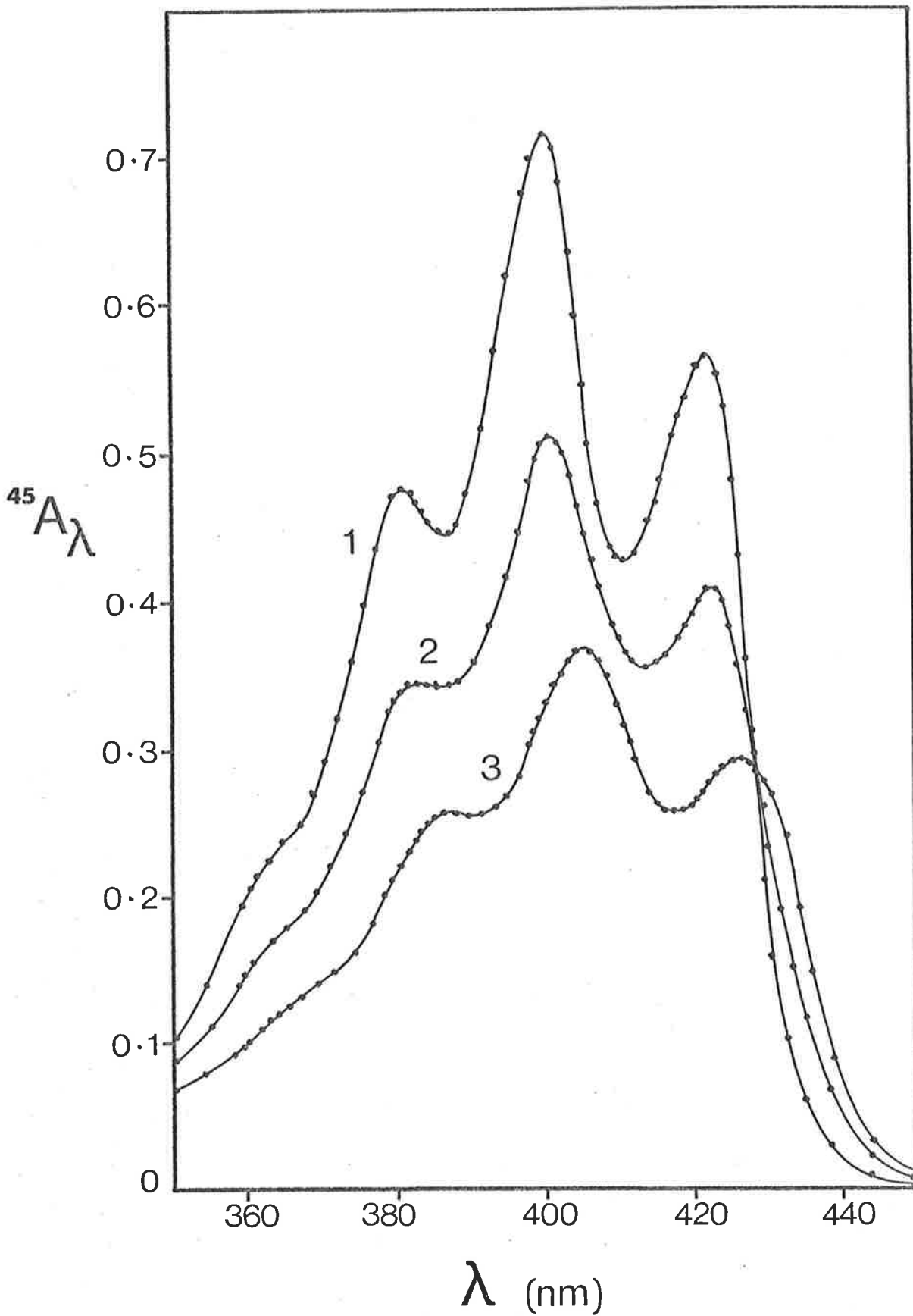


Fig. 4-2. Spectra of 9AA and native DNA in 0.1 M NaCl at 45°C: constant 9AA concentration, 7.31×10^{-5} M; curve 1: 9AA, curve 2: 9AA and native DNA: $T_L/T_A = 0.263$: $r = 0.120$, curve 3: 9AA and native DNA: $T_L/T_A = 0.080$: $r = 0.071$.

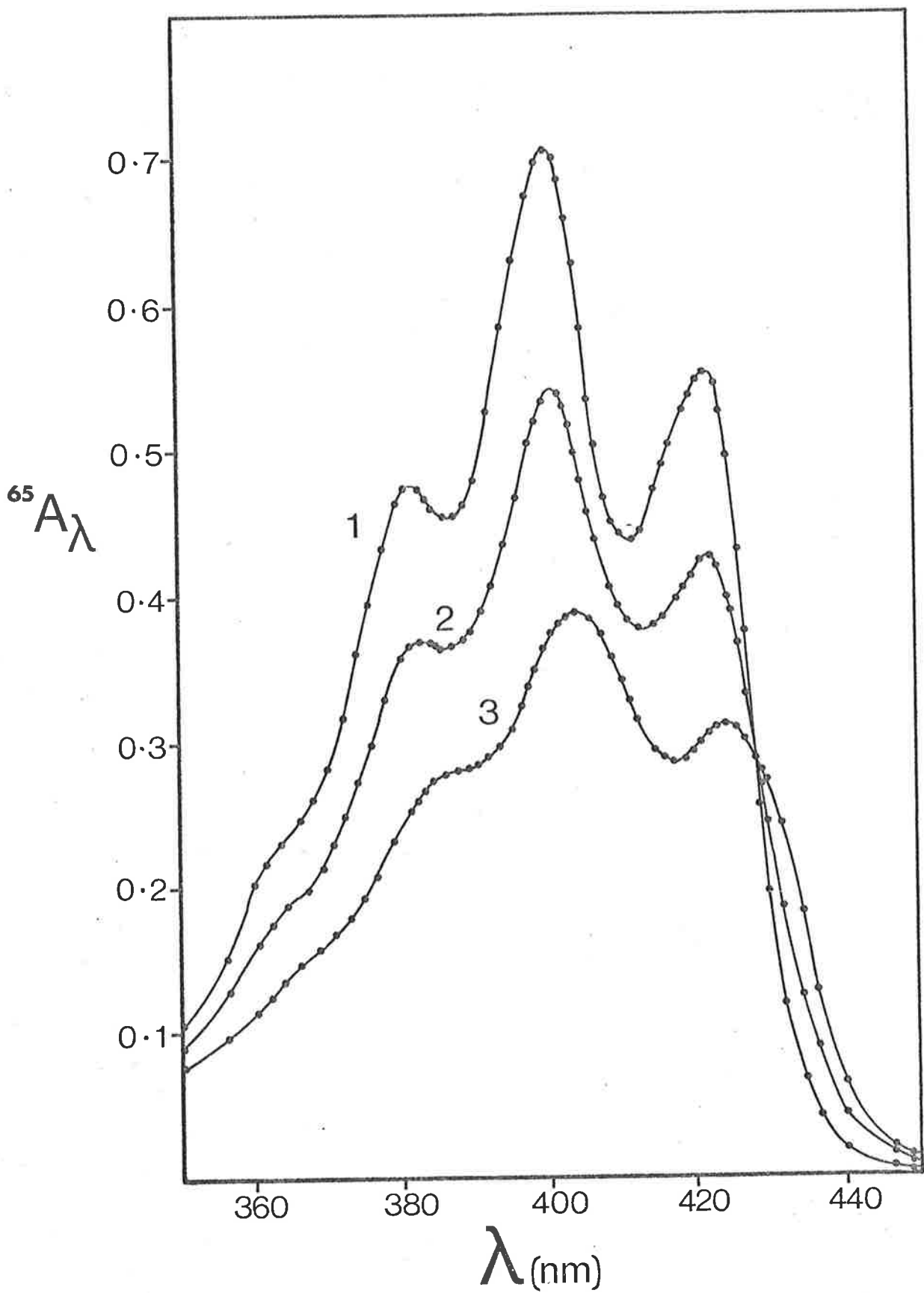


Fig. 4-3. Spectra of 9AA and native DNA in 0.1 M NaCl at 65°C: constant 9AA concentration, 7.31×10^{-5} M. Curve 1: 9AA, curve 2: 9AA and native DNA: $T_L/T_A = 0.263$: $r = 0.093$, curve 3: 9AA and native DNA: $T_L/T_A = 0.080$: $r = 0.065$.

However it has been pointed out that isosbestic points may occur under circumstances where there is not a single equilibrium between two species⁷. In particular, if the absorbance (A) is a monotonic function at all wavelengths of some non-absorbing variable, x, (this is conceivable in aminoacridine-DNA systems where x = DNA) then isosbestic points will occur at wavelengths, λ , where:

$$\frac{\partial A_{\lambda}}{\partial x} = 0 \quad \text{eqn. 4-2.}$$

It appears, therefore, that a better test for a single chemical equilibrium is to verify that a set of spectra generated, in this case by varying the DNA concentration, is internally linear⁷. That is, the i^{th} member of a set of spectra can be expressed as a linear combination of any two other members of the set. Thus:

$$\epsilon_i(\lambda) = (1 - \beta_i)\epsilon_1(\lambda) + \beta_i\epsilon_2(\lambda) \quad \text{eqn. 4-3.}$$

where: $\epsilon_i(\lambda)$ = apparent extinction coefficient of the absorbing species at wavelength, λ , in the i^{th} spectrum.

$\epsilon_1(\lambda)$ and $\epsilon_2(\lambda)$ = apparent extinction coefficient of the absorbing species at wavelength, λ , in any two nominated spectra of the set.

β_i = a number independent of λ .

If the spectra are all measured at the same concentration of absorbing species then:

$$A_i(\lambda) = (1 - \beta_i)A_1(\lambda) + \beta_i A_2(\lambda) \quad \text{eqn. 4-4.}$$

where $A_i(\lambda)$, $A_1(\lambda)$ and $A_2(\lambda)$ are the experimental absorbances at wavelength λ of the spectra defined in equation 4-3. on page 67. Internal linearity can be shown to hold true for the spectra in figures 4-1. to 4-3., for the relationship:

$$A_2(\lambda) = (1 - \beta_2)A_1(\lambda) + \beta_2 A_3(\lambda) \quad \text{eqn. 4-5.}$$

where A_1 , A_2 and A_3 are the absorbances as a function of λ for the spectra labelled 1, 2 and 3 respectively. The absorbances have been corrected for volume expansion to an equivalent absorbance at 25°C. The value for β_2 has been calculated at six wavelengths throughout the spectrum. The results are shown in Table 4-1. That the spectra are internally linear is demonstrated by the constancy of β_2 at each temperature.

TABLE 4-1.

The values of β_2^* for a set of spectra of 9AA and native DNA.

Temp. (°C)	25	45	65
λ			
380	0.558	0.531	0.504
390	0.579	0.536	0.508
400	0.571	0.534	0.496
410	0.573	0.539	0.505
420	0.576	0.543	0.506
432	0.561	0.523	0.505
average	0.570	0.534	0.504
S.D. (σ)	0.007	0.006	0.004

* as defined in the text

The presence of 9AA dimer in spectrum 1 of Figs. 4-1. to 4-3., which yields an observed absorbance $A_1(\lambda)$ lower than the true absorbance, $(A_1 + \delta)(\lambda)$, has been ignored as this term appears in both the numerator and denominator for the calculation of β_2 . That is, from equation 4-5.

$$\beta_{2 \text{ true}} = \frac{(A_1 + \delta)(\lambda) - A_2(\lambda)}{(A_1 + \delta)(\lambda) - A_3(\lambda)} \approx \frac{A_1(\lambda) - A_2(\lambda)}{A_1(\lambda) - A_3(\lambda)} = \beta_2 \quad \text{eqn. 4-6.}$$

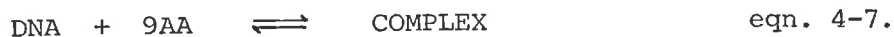
if $\delta \ll A_1$, which is experimentally the case.

There will be virtually no detectable 9AA dimer concentration in the 9AA-DNA solutions as the free 9AA concentrations in these solutions are very low.

The constant values of β_2 as a function of wavelength at each temperature satisfy the condition for the spectra to be internally linear.

To reiterate, isosbestic points are not unequivocal evidence for a single equilibrium between two species of a chromophore since although internal linearity is a sufficient condition for an isosbestic point it is by no means a necessary condition. It must be said, however, that while internal linearity is a necessary condition for a single equilibrium it may not be a sufficient condition. Nonetheless it appears that internal linearity of spectra is a better test for a single equilibrium than is an isosbestic point.

It is therefore concluded that native DNA and 9AA interact in a way which may be defined in equilibrium measurements by a single equilibrium:



The above equilibrium holds at least for the range of temperatures $25^{\circ}\text{C} - 65^{\circ}\text{C}$ and for a range of r values consistent with the spectra in Figs. 4-1. to 4-3.

4. 9-aminoacridine and native DNA : melting the complex

In common with other aminoacridines 9AA stabilizes the double helical structure of DNA with respect to denaturation. The stabilization is manifested as a shift in the melting temperature (T_m) of the complex to temperatures higher than the T_m of native DNA alone. It has been observed in common with others⁸ that this shift in T_m is a function of r and reaches its maximum when primary binding is complete. Fig. 4-4. shows a melting curve of native DNA in the presence and absence of 9AA. When observed at 260 nm. in a dilute solution of 9AA (which absorbs strongly in the U.V.), the T_m is found to coincide in temperature with the change at 400 nm. Thus 9AA is released from the complex when the secondary structure of the macromolecule is lost. Moreover there is a quantitative release of 9AA from the native DNA-9AA complex above its denaturation temperature, the 9AA chromophore then behaving as an unbound molecule.

5. Determination of the extent of binding, r

Spectra of 9AA and native DNA solutions described in section 3 of this Chapter are internally linear. This is interpreted as indicating, as has already been shown, that the interaction between the 9AA and DNA can be described by a single equilibrium in which only two forms of the chromophore exist viz. the bound 9AA with extinction coefficient ϵ_b and the free

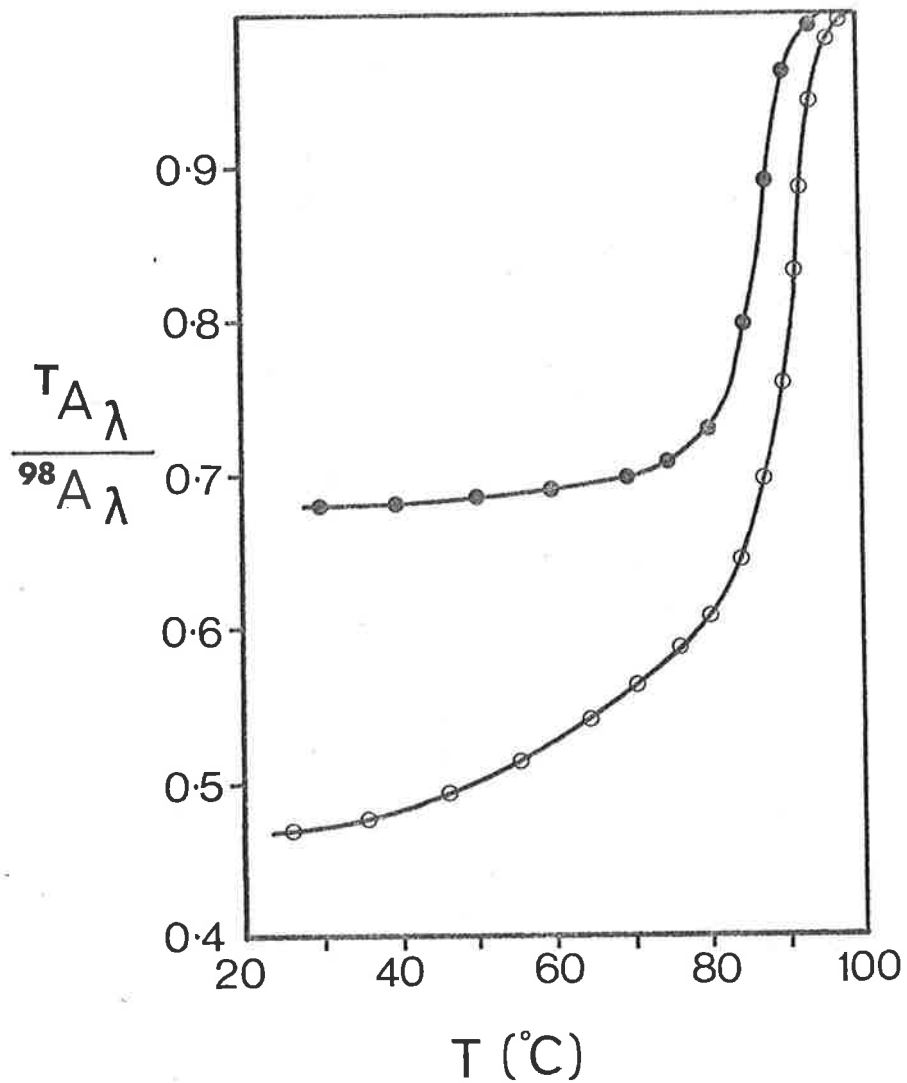


Fig. 4-4. Typical melting profiles of DNA in the presence and absence of 9AA, neutral salt concentration 0.1 M NaCl.
 (●) native DNA: $\lambda = 260 \text{ nm}$,
 (○) native DNA and 9AA: $\lambda = 400 \text{ nm}$.

9AA with extinction coefficient ϵ_b . (See footnote).

With only two forms of the chromophore in solution it is possible to determine, by spectrophotometry, the extent of binding for the interaction. The extent of binding (r) is the number of 9AA cations bound per DNA phosphate residue. This has usually been calculated from the expression:³

$$r = \frac{A_i - A}{A_i - A_{ex}} \cdot \frac{T_L}{T_A} \quad \text{eqn. 4-8}$$

where: A_i = absorbance of the 9AA solution in the absence of DNA.

A = absorbance at some point during the experiment.

r = extent of binding at that point.

T_L = total concentration of 9AA in solution at that point.

T_A = total concentration of DNA in solution at that point.

A_{ex} = the absorbance of the solution in the presence of excess DNA,

and where all the absorbance measurements are adjusted to the same T_L . Absorbance measurements are usually made at the wavelength of maximum absorbance (400 nm for 9AA). Experimental details are described in Chapter VIII, section 4. It has been pointed out that

Footnote:

Internal linearity can also occur if more than one species of bound 9AA exist and each bound species:

(i) has the same ϵ_b at all λ (trivial case).

(ii) exists such that the ratios of the two or more bound species remain the same irrespective of the extent of binding or of the free 9AA concentration. This situation could arise with spectrally distinct tautomeric forms of 9AA. However, these are not known to exist.

in measurements at temperatures other than at room temperature all absorbance measurements should be corrected for volume expansion; furthermore, $(A_i - A_{ex})$ should be determined at the appropriate temperature². Some workers appear to have assumed that $(A_i - A_{ex})$ is independent of temperature and have used $(A_i - A_{ex})_{T = 25^\circ C}$. in equation 4-8^{9,19}. Once r has been determined at some point then the free aminoacridine concentration (c) at that point is determined by the relationship:

$$c = T_L - r T_A \quad \text{eqn. 4-9.}$$

A computer program, program BINDING, has been written to calculate r and c for the experimental method used (see Appendix).

Early in this work problems arose in obtaining a high degree of reproducibility necessary for determining the association constants from Scatchard plots of binding experiments. This lack of reproducibility arises from the difficulty in establishing accurately the small changes in absorbance which occur at very low values of T_L/T_A . In this region, at low r , a small error in absorbance produces a large percentage change in c with a very small change in r since most of the aminoacridine is already bound. Thus small errors in A (equation 4-8.) at low r are manifest as large changes in the associated value of r/c . It is thus important that the value of absorbance in "excess" DNA, A_{ex} (equation 4-8.), is accurately determined and not just taken to be the absorbance of the aminoacridine chromophore in an arbitrary excess DNA concentration. As an illustration of this, Fig. 4-5. shows typical Scatchard plots for 9AA and native DNA calculated from equation 4-8. with A_{ex} determined at the T_A/T_L value shown in the diagram. Clearly, an attempt to determine

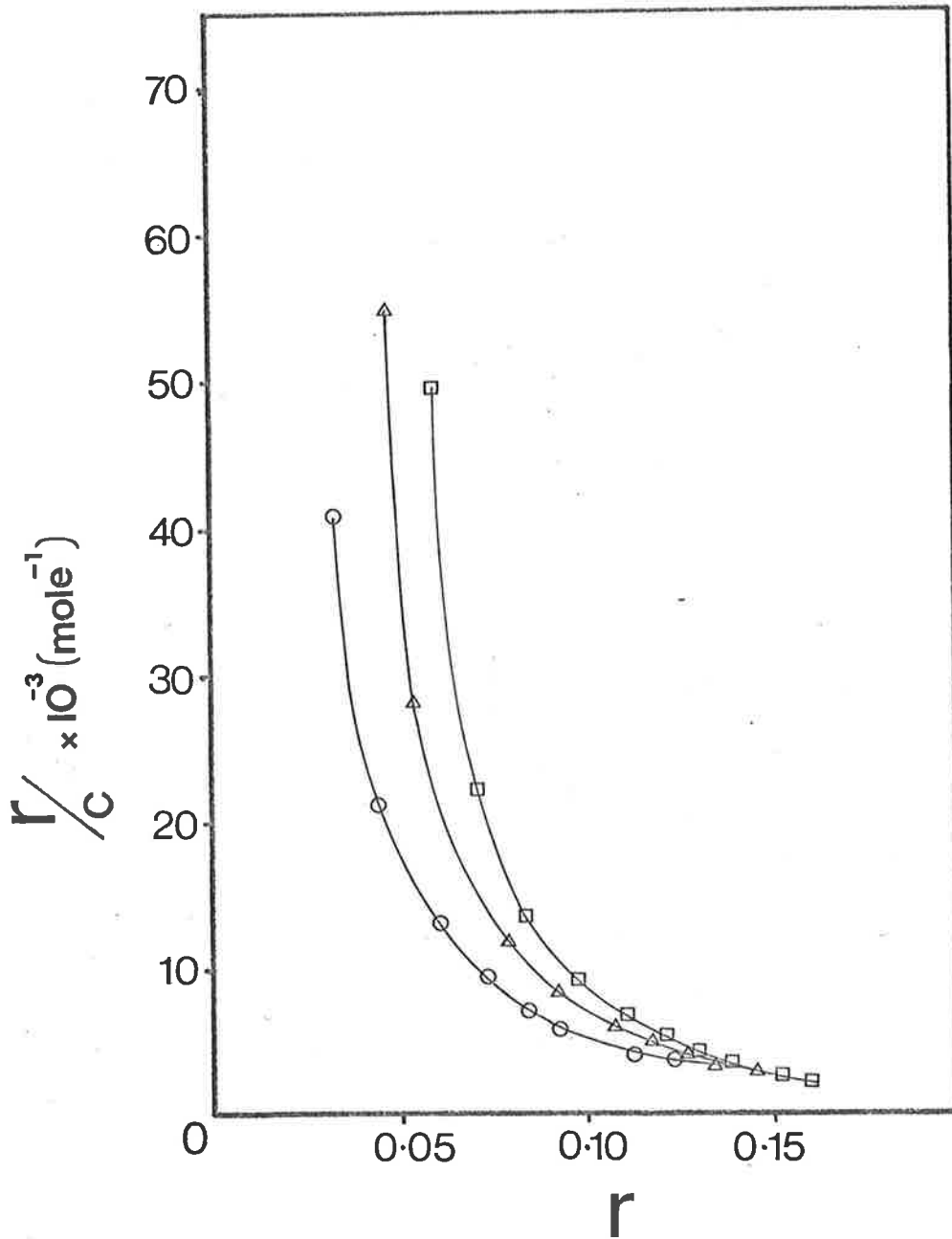


Fig. 4-5. Scatchard plots for 9AA and native DNA in 0.1 M NaCl at 45°C calculated from equation 4-8. using as A_{ex} the absorbance in varying excess DNA. Final T_A/T_L values are (□) : 20.3, (Δ) : 26.3, (○) : 44.1.

the association constant of the strong binding, the formation of complex I, will yield widely differing results for what must be a single value parameter. In order to obviate the problem associated with an arbitrary assignment of excess DNA concentration a plot of A/A_i versus T_L/T_A has been made for each set of experimental data. Fig. 4-6. shows this plot for the experimental curves in Fig. 4-5. The extrapolation of these curves to $T_L/T_A = 0$ will yield points on the A/A_i axis associated with the hypothetical state where all the aminoacridine is bound since the DNA excess is infinite. Let the intercept on the A/A_i axis be Q then:

$$A'_{ex} = A_i Q \quad \text{eqn. 4-10.}$$

where: A'_{ex} is the "true" absorbance in infinite excess DNA. If the new values, A'_{ex} are substituted in equation 4-8. then the curves in Fig. 4-5. are found to change markedly and to coalesce giving a straight line. This is demonstrated in Fig. 4-7.

The plot of A/A_i versus T_L/T_A has two further advantages.

- (i) All the values used are experimentally accessible and make no assumption about the completeness of binding, unlike the widely used Benesi-Hildebrand equation¹².
- (ii) The curve extrapolated to $T_L/T_A = 0$ yields, directly, the ratio of the extinction coefficients of the bound and free aminoacridine, i.e.,

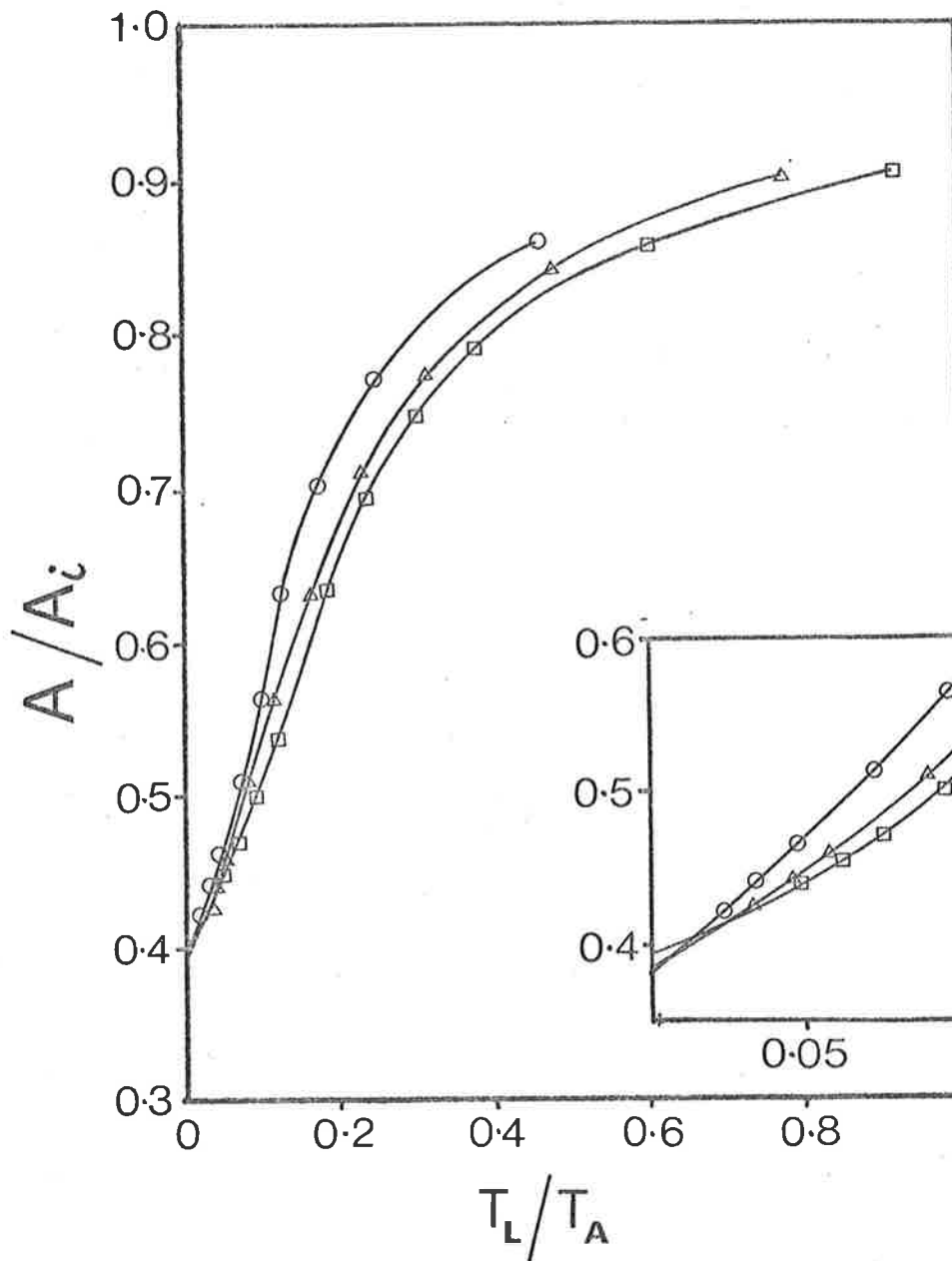


Fig. 4-6. The variation of A/A_i with T_L/T_A for 9AA and native DNA at 45°C. This plot enables the determination of the ratio of the extinction coefficients of 9AA bound to native DNA (ϵ_b) and free 9AA (ϵ_f) viz.

$$\frac{A}{A_i} = \frac{\epsilon_b}{\epsilon_f} \text{ as } \frac{T_L}{T_A} \rightarrow 0$$

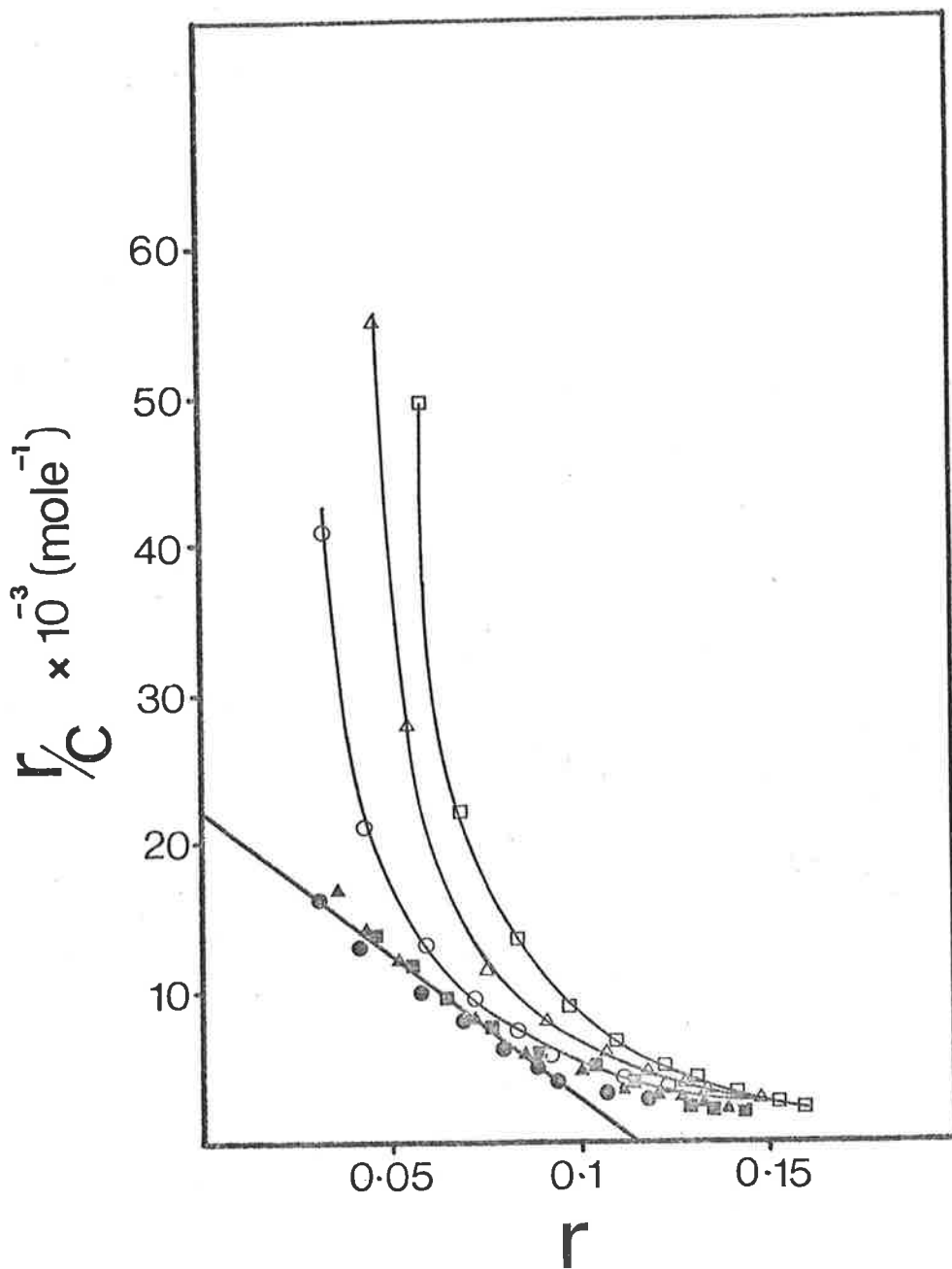


Fig. 4-7. Scatchard plots for 9AA and native DNA in 0.1M NaCl at 45°C. The results in Fig. 4-5. are replotted ($\square, \triangle, \circ$) and these results recalculated using A'_{ex} (obtained from Fig. 4-6.) are also given ($\blacksquare, \blacktriangle, \bullet$).

$$Q = \frac{\epsilon_b}{\epsilon_f} \quad \text{eqn. 4-11.}$$

It will be shown later that this value can be a diagnostic for changes in the binding site.

The plot of A/A_i versus T_L/T_A does have the disadvantage of being a non linear function and thus the extrapolation requires a small measure of subjectivity; however if measurements at sufficiently low values of T_L/T_A are obtained this extrapolation can be made with more certainty.

The fact that Q is observed to vary slightly with the initial dye concentration (Fig. 4-6.) is a consequence of the presence of 9AA dimers in the initial dye solution. The dimers do not present a problem in determining values of r in the region of interest, at low r , where complex I binding dominates as:

$$r_{\text{measured}} = \frac{A_i - A}{A_i - A'_{\text{ex}}} \cdot \frac{T_L}{T_A} \approx \frac{A_i + \delta - A}{A_i + \delta - A'_{\text{ex}}} \cdot \frac{T_L}{T_A} = r_{\text{true}} \quad \text{eqn. 4-12.}$$

where δ is the decrease in A_i due to 9AA dimer in solution.

Equation 4-12 holds providing that $\delta \ll \Delta A = A_i - A'_{\text{ex}}$. At high r values there will be a slight error resulting from this approximation. This is not of significance in any of the experiments described in this work where association constants have been evaluated from values of r below $r = 0.1$.

6. Extinction coefficient of bound 9AA (ϵ_b).

Figures 4-6, 4-8, 4-9 and 4-10 are plots of A/A_i versus T_L/T_A for four different temperatures. Each figure shows the results for three binding curves each distinguished by a different

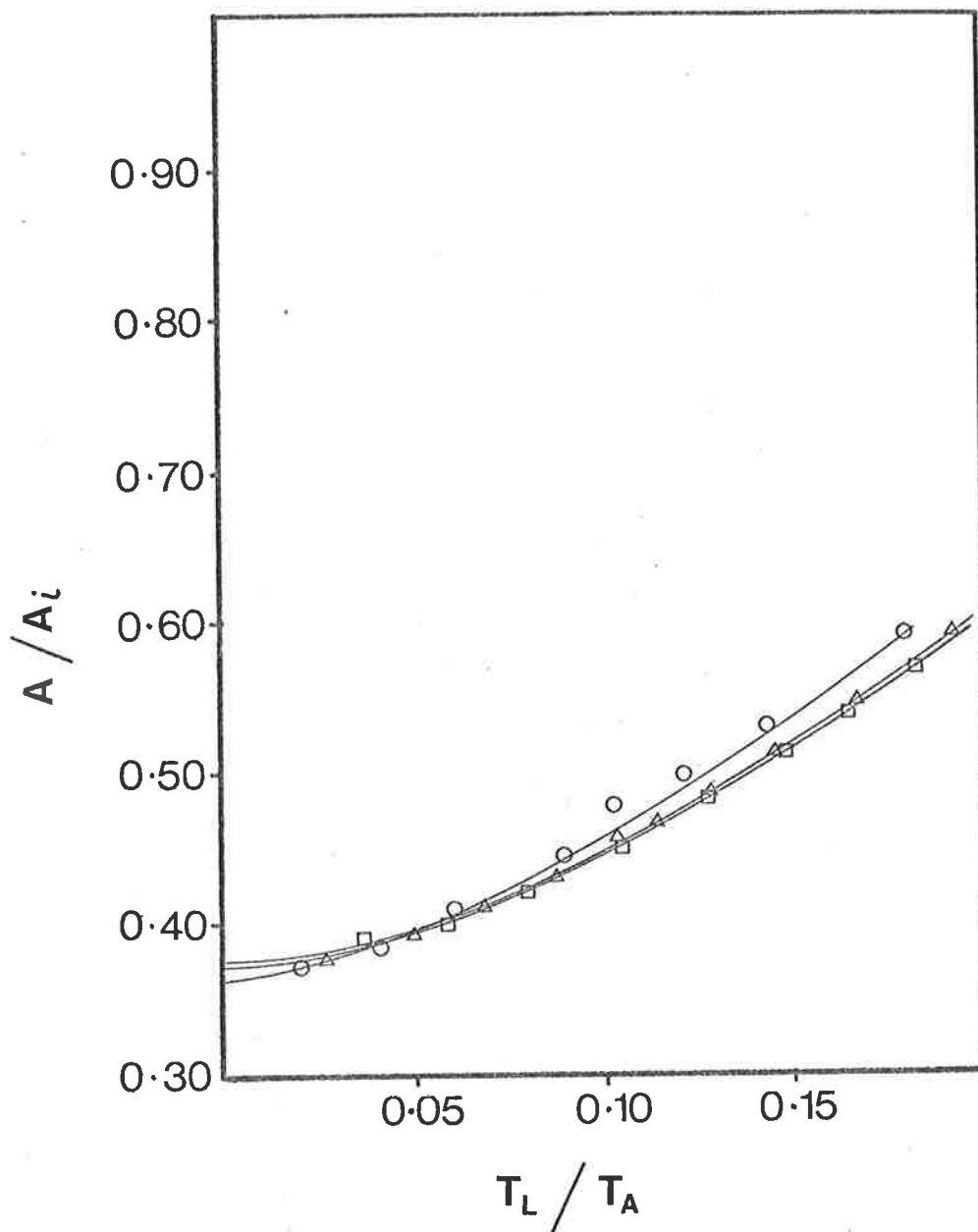


Fig. 4-8. Plot to determine the ratio of extinction coefficients of 9AA bound to native DNA (ϵ_b) and free 9AA (ϵ_f) at 22°C.

$$\frac{A}{A_i} = \frac{\epsilon_b}{\epsilon_f} \text{ as } \frac{T_L}{T_A} \rightarrow 0.$$

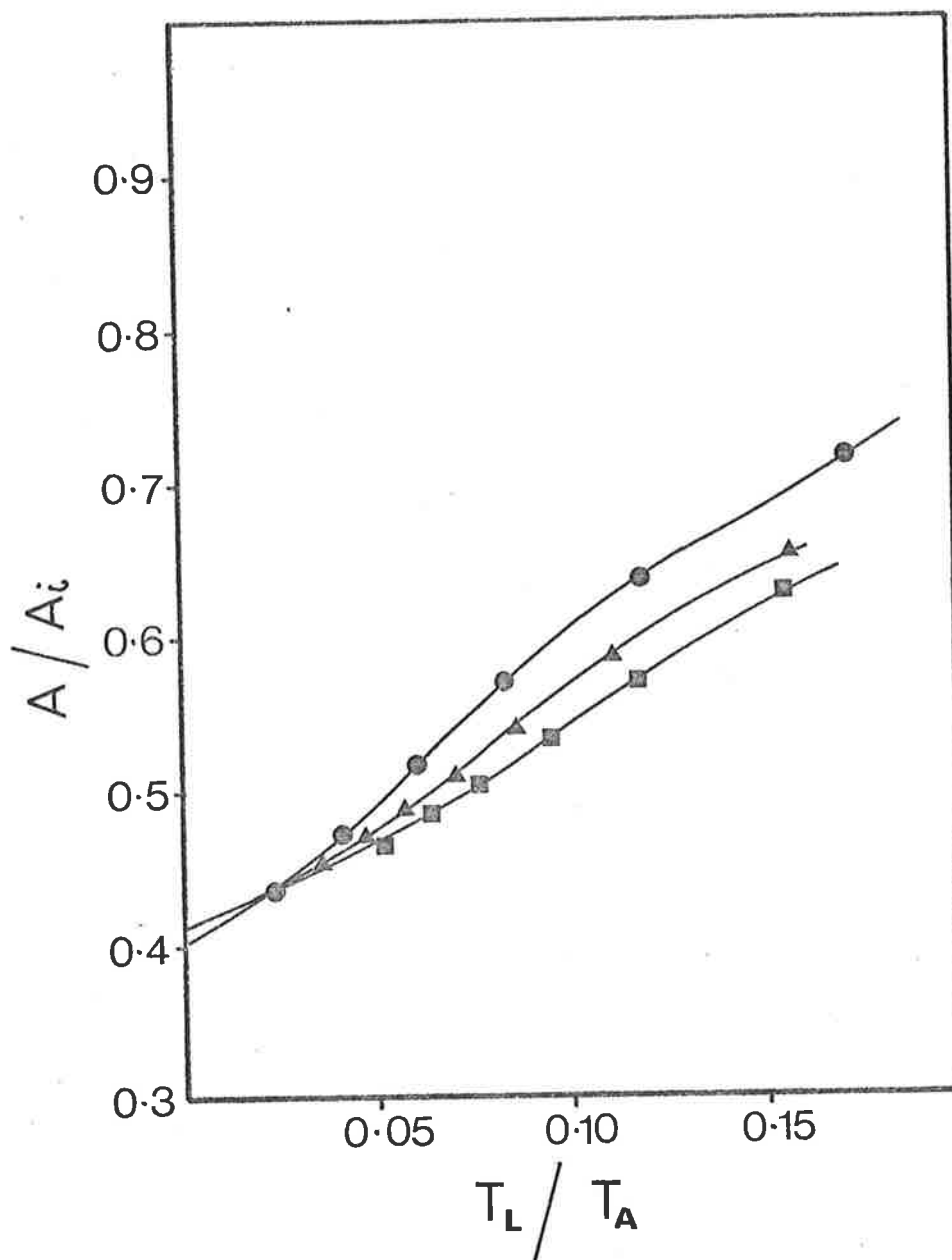


Fig. 4-9. Plot to determine the ratio of extinction coefficients of 9AA bound to native DNA (ϵ_b) and free 9AA (ϵ_f) at 55°C.

$$\frac{A}{A_i} = \frac{\epsilon_b}{\epsilon_f} \text{ as } \frac{T_L}{T_A} \rightarrow 0$$

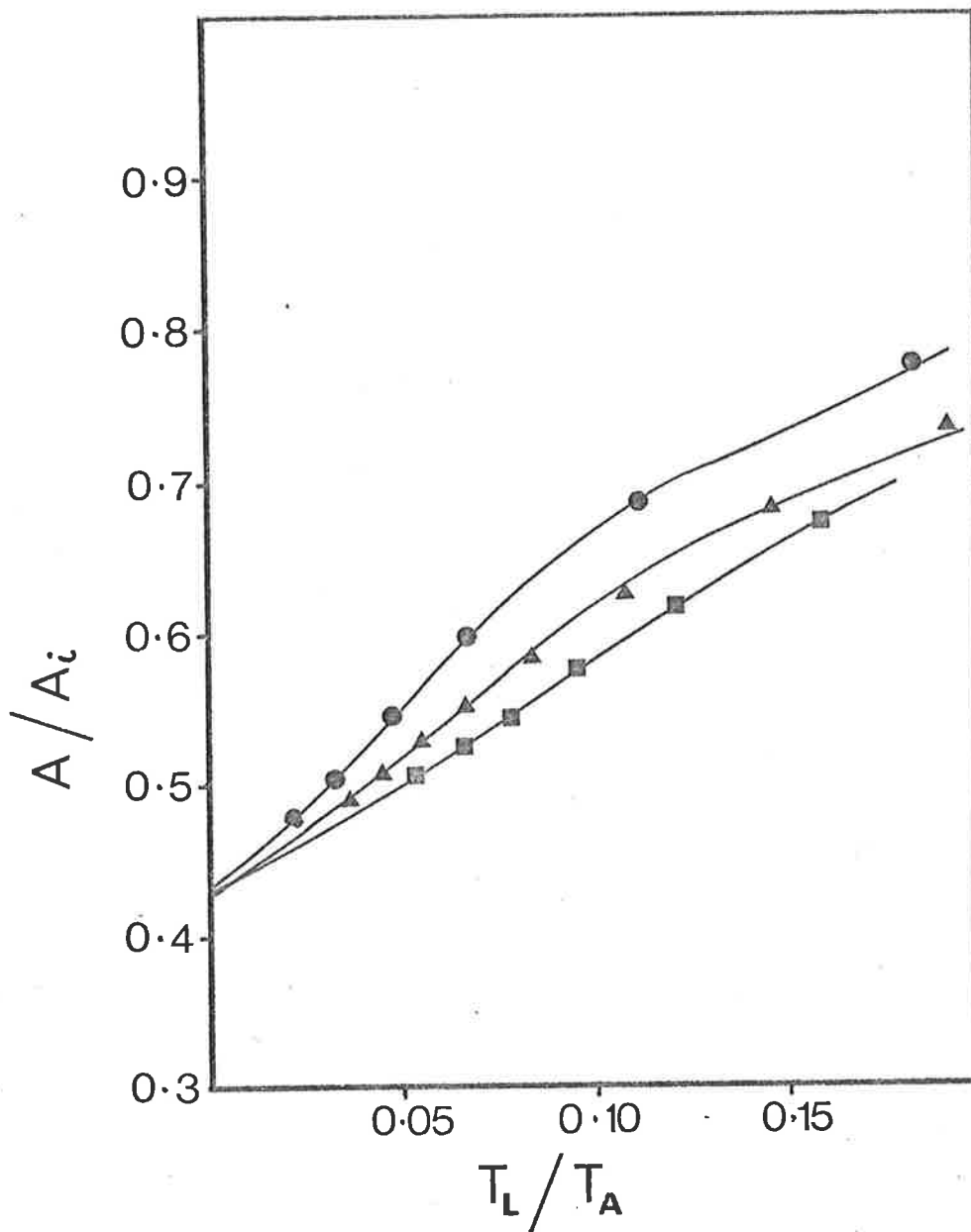


Fig. 4-10. Plot to determine the ratio of extinction coefficients of 9AA bound to native DNA (ϵ_b) and free 9AA (ϵ_f) at 65°C.

$$\frac{A}{A_i} = \frac{\epsilon_b}{\epsilon_f} \text{ as } \frac{T_L}{T_A} \rightarrow 0$$

initial concentration of 9AA. The curves have been extrapolated to the A/A_1 axis at $T_L/T_A = 0$. (The curve will be asymptotic to the axis at $A/A_1 = Q$). Table 4-2 below shows that values of Q change only slightly with temperature.

TABLE 4-2.

Variation of Q^* with temperature for 9AA and native DNA

Temp. ($^{\circ}$ C)	22	45	55	65
$\frac{\epsilon_b}{\epsilon_f} = Q$	0.37 ± 0.001	0.39 ± 0.01	0.40 ± 0.01	$0.42_5 \pm 0.01$

* as defined in the text

The slight increase in Q with temperature may be explained by a reduction in ϵ_b with increasing temperature. This may be due to a slight weakening of the interaction between the planar 9AA cation and the planar bases of the DNA. These electronic interactions give rise to the depression of the aminoacridine extinction coefficient on binding¹⁰. This weakening interaction will be a consequence of thermal energy increasing

the relative motion of the interacting species (see footnote).

In summary it may be said that the ratio of extinction coefficients of the bound and free species of 9AA is only slightly dependent on temperature through the range 22°C to 65°C. This is taken as further evidence that the complex is relatively unchanged by temperature and hence the binding site, also, is relatively unchanged by temperature.

7. Determination of the intrinsic association constant (k).

(a) Introduction

Scatchard plots for the interaction of 9AA with native DNA determined from equations 4-8., 4-9., and 4-10. are shown in Figs. 4-7., 4-11., 4-12. and 4-13. The curves are shown using the absorbance in experimental excess DNA, A_{ex} , and corrected for A'_{ex} as $T_L/T_A \rightarrow 0$. In the latter case the experimental curves at each temperature coalesce and the straight line drawn in the figures is the line of best fit determined by the Method of Least Squares through data points in the range $0 < r < 0.1$. The coalesced curves show some departure from linearity at r values greater than about $r = 0.1$. As discussed

Footnote:

It is possible that the observed increase in Q with temperature may be due to a decrease in ϵ_f , which is observed, with increasing temperature. This change, after correction for thermal expansion, is in the opposite direction to that expected for a change in ϵ_f due to a shift in the monomer-dimer equilibrium which will favour the monomer with increasing temperature.

The observed decrease in ϵ_f with increasing temperature is presumably due to a change with temperature in the distribution of 9AA molecules amongst the vibrational energy levels available to them¹¹. Such a change will not necessarily alter the ability of 9AA to bind to DNA. However the effect of this change on ϵ_b is not known and so a conclusive argument is not possible.

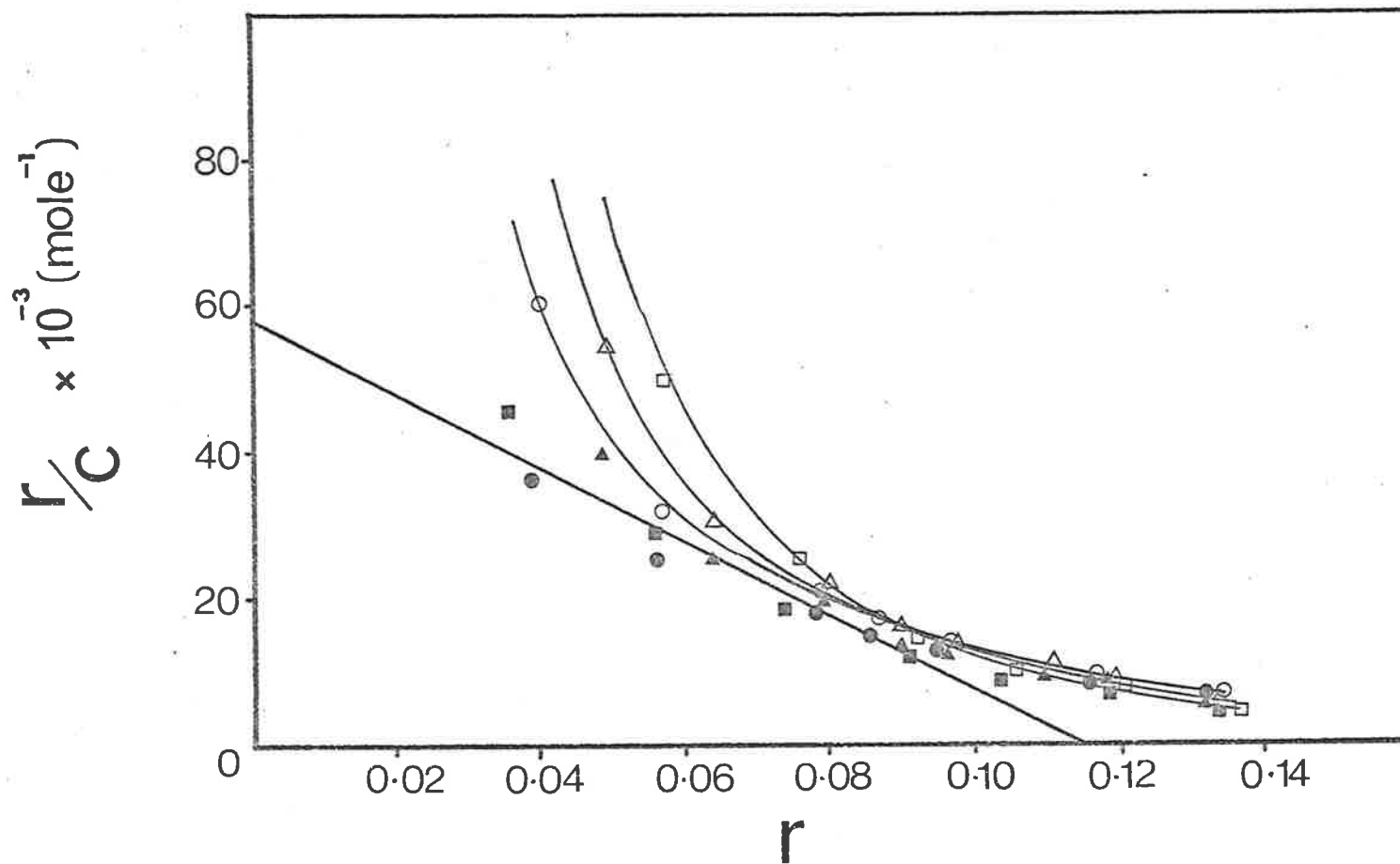


Fig. 4-11. Scatchard plots for the interaction of 9AA with native DNA in 0.1M NaCl at 22°C. Experimental values of T_A/T_L at which A'_{ex} is determined are (O) 48.6, (Δ) 38.1, (□) 27.1. Values corrected for A'_{ex} from Fig. 4-8. are shown (●, ▲, ■).

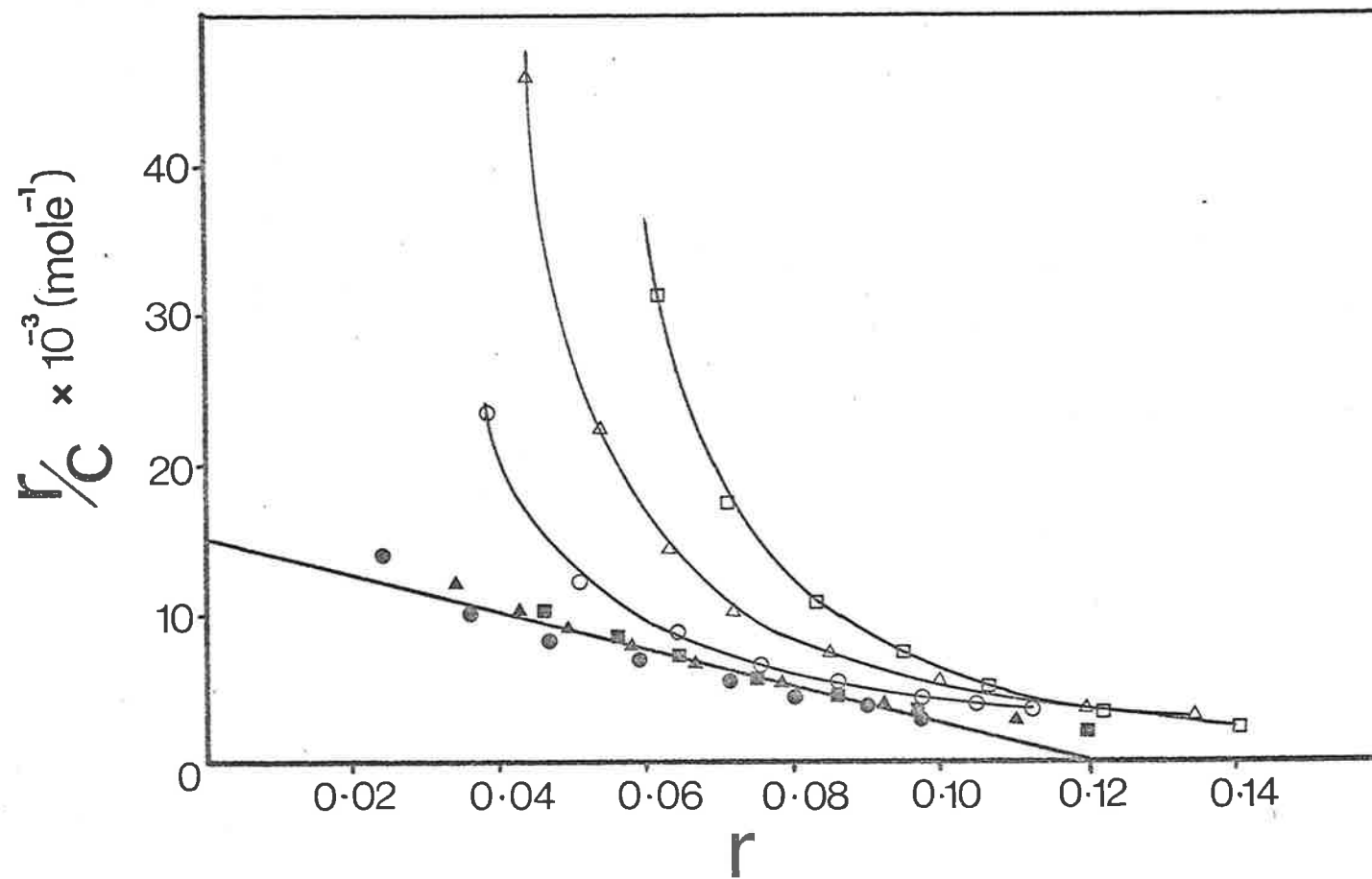


Fig. 4-12. Scatchard plots for the interaction of 9AA with native DNA in 0.1M NaCl at 55°C. Experimental values of T_A/T_L at which A_{ex} is determined are, (O) 38.7, (Δ) 27.0, (\square) 19.7. Values corrected for A'_{ex} from Fig. 4-9. are shown (\bullet , \blacktriangle , \blacksquare).

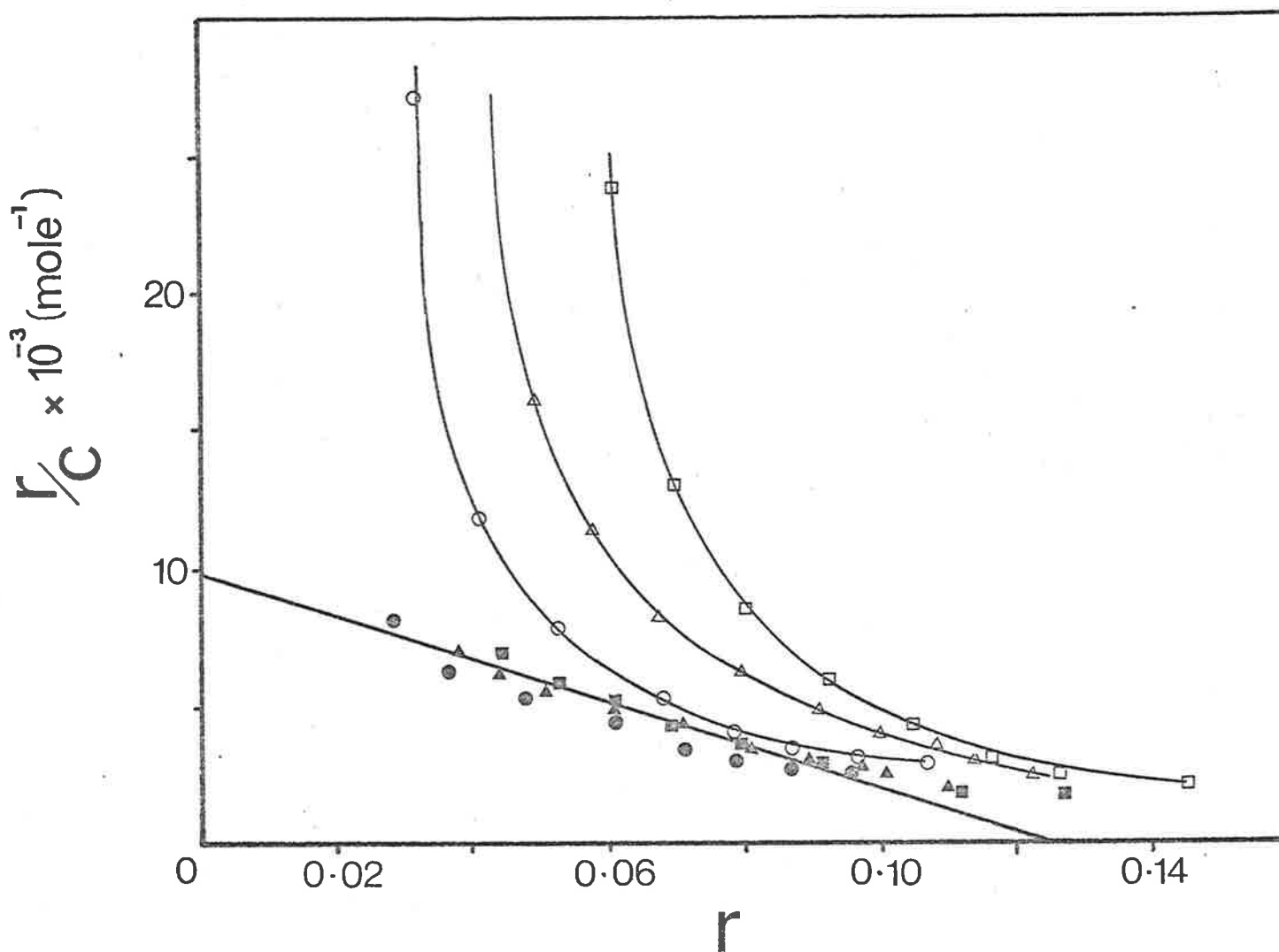


Fig. 4-13. Scatchard plots for the interaction of 9AA with native DNA in 0.1M NaCl at 65°C. Experimental values of T_A/T_L at which A_{ex} is determined are (O) 44.8, (Δ) 27.7, (\square) 19.4. Values corrected for A'_{ex} from Fig. 4-10. are shown (\bullet , \blacktriangle , \blacksquare).

in Chapter III, such departures from linearity in Scatchard plots can arise from a number of causes. In this instance the presence of the weaker complex II is not the cause as at these low r values complex II has been shown to make an immeasurably small contribution to the binding of 9AA to native DNA². Nor is it likely in ionic strength $\mu = 0.1$ that the curvature is due to an r value which has an electrostatically dependent free energy term³. The most likely cause is anti-cooperative binding.

(b) Anti-cooperative binding

Anticooperativity is manifested as a reduction in the favourable free energy change associated with binding at a binding site when a nearby site is occupied. This reduction in free energy may be due to a number of quite long range interactions between bound moieties¹⁵ and not just nearest neighbour interactions. As such, it is important to distinguish between anti-cooperative behaviour and neighbour exclusion phenomena. This distinction is not drawn in some recent texts¹². As defined by Armstrong *et al*¹³ (reviewed in Chapter III), binding of aminoacridines to DNA is such that neighbour exclusion places a limit on the extent of binding to form complex I at $r = 0.25$. In a similar way Müller and Crothers¹⁴ have proposed a limiting r value for the binding of an antibiotic to DNA. However, anti-cooperative behaviour implies that while the maximum extent of binding may be $r = 0.25$ for complex I in the binding of aminoacridines to DNA, the favourable free energy change associated with the interaction is a monotonically decreasing function with the extent of binding. This is manifest as a decreasingly (modulus) negative slope in the associated Scatchard plot (see Fig. 4-14).

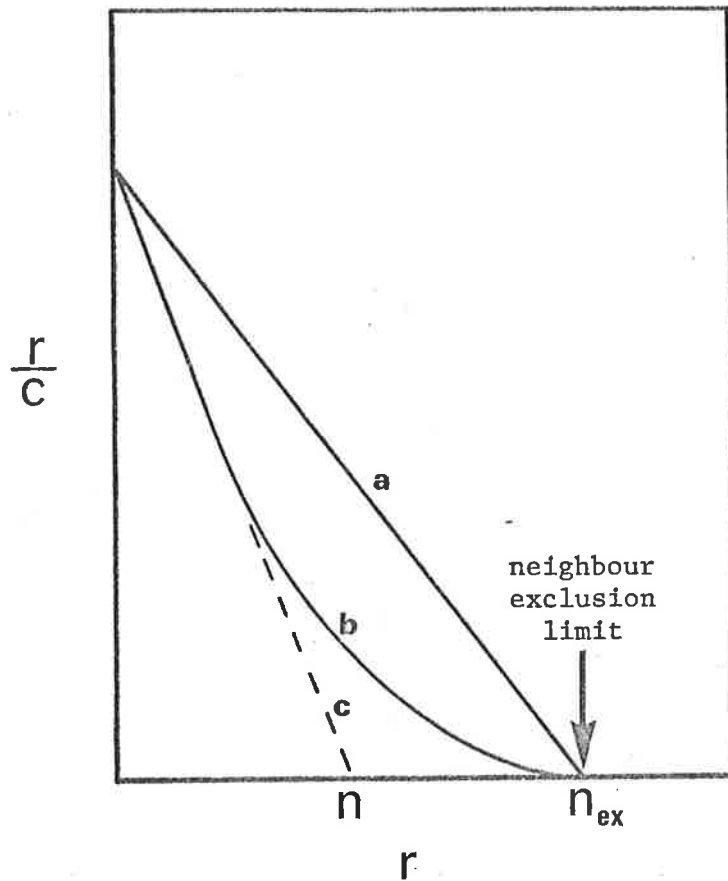


Fig. 4-14. Schematic Scatchard plots for:

- (a) one type of non-interacting binding site with neighbour exclusion limit. Slope $-k$ intercept n_{ex} .
- (b) one type of binding site, neighbour exclusion limit, anti-cooperative binding. Slope $-k(r)$ intercept n_{ex} .
- (c) isolated binding site for curve B at low r values. Slope $-k$ intercept n .

In Fig. 4-14. the Scatchard plot for ideal, non-interacting sites with a neighbour exclusion limit is shown in curve (a). Curve (a) has characteristics of slope $-k'$ and intercept on the r axis of n_{ex} . Curve (b) is a typical experimental curve of anti-cooperative binding. The limit of the extent of binding is still the same (n_{ex}) however the modulus of the favourable free energy change associated with the binding is a monotonically decreasing function of r . This is reflected in the slope, $-k(r)$, a function of r . As drawn in Fig. 4-14., with the intercept on the r/c axis the same, the relationship between the linear Scatchard plot and the anti-cooperative plot is:

$$\lim_{r \rightarrow 0} \frac{r}{c} = k' n_{ex} \quad \text{for the Scatchard plot:}$$

non-interacting sites.

and

eqns. 4-13.

$$\lim_{r \rightarrow 0} \frac{r}{c} = kn \quad \text{for the Scatchard plot}$$

anti-cooperative behaviour.

where k and n are the slope and intercept on the r axis of the straight line in Fig. 4-14., namely curve (c). At these low values of r , $\frac{\partial r/c}{\partial r}$ will be the value of the intrinsic association constant k associated with an isolated site since at low r interactions between neighbouring aminoacridines will be a minimum. Thus the values of k and n may be estimated from the linear initial portion of the Scatchard plot at low r ; though, inevitably, a degree of subjectivity is associated with estimating at what extent of binding significant curvature in the Scatchard plot occurs. In this work only experimental points below

$r = 0.1$ have been used in estimating the initial slopes of Scatchard plots for the interaction of 9AA with native DNA.

Crothers¹² has suggested that the value of n obtained from curve (c) must be associated with a potential number of binding sites thus requiring an intimate knowledge of the nature of the complex. However this has not been thought necessary in the work described here since the degree of curvature in an anti-cooperative Scatchard plot will be a very complex function of a number of intermolecular interactions¹⁵ which cannot, at this time, be unambiguously determined. Rather, the value of n obtained from curve (c) in Fig. 4-14. is an empirical number of binding sites which have no a priori association with a binding model except in so far as, at low r values, the slope of the Scatchard plot which yields the intrinsic association constant for an isolated site is applicable for n binding sites per nucleotide phosphorus. That is k and n satisfy the following experimentally observed equilibrium relationship at low r :

$$k = \frac{[\text{bound sites}]}{[\text{isolated unbound sites}] [\text{free aminoacridine}]} = \frac{rT_A}{(n-r)T_A \cdot c} \quad \text{eqn. 4-14.}$$

While the value of n so obtained cannot be associated with a model for the interaction, variations of n with temperature can be related to associated changes in the complex. This will be discussed further in Chapter V.

(c) (i) Results

As described in the previous section, equation 4-7. can be redefined as follows:



The equilibrium constant for the equation 4-15. on page 79 is then k as defined in equation 4-14. This value of k is the negative value of the slope of the initial portion of the Scatchard plot at low r , for which the intercept on the r axis is n which appears explicitly in equation 4-14. Intrinsic association constants, which are equilibrium constants, often appear in the literature as the lower case letter, k , rather than the upper case letter, K , usually associated with equilibrium constants. Both are used at various times in this work. Whenever a lower case letter k appears with a subscript or subscripts, however, it refers to a rate process.

The values of the intrinsic association constants obtained from the data presented in Figs. 4-7., 4-11., 4-12. and 4-13. are given in Table 4-3. The Standard Errors are also provided. Table 4-3 also gives the values for n associated with the Scatchard plots.

TABLE 4-3

The intrinsic association constant (k) for the interaction of 9AA with native DNA in 0.1M NaCl.

Temp. ($^{\circ}$ C)	22	45	55	65
$k(\text{moles}^{-1}) \times 10^5$	5.02 (S.E.O.46)	1.95 (S.E.O.11)	1.25 (S.E.O.08)	0.79 (S.E.O.05)
n	0.115 (S.E.O.007)	0.116 (S.E.O.004)	0.121 (S.E.O.004)	0.125 (S.E.O.004)

(c) (ii) Thermodynamic parameters

A study of the variation of equilibrium constant (intrinsic association constant) with temperature allows the evaluation of the thermodynamic parameters which govern the reaction. The thermodynamic parameters ΔG° , ΔH° and ΔS° , respectively, the total free energy change, the enthalpy change and the entropy change of reaction have previously been reported for proflavine with native DNA¹⁶ and acridine orange with native and denatured DNAs¹⁷.

The free energy change for the reaction eqn. 4-15. is evaluated from the expression:

$$\Delta G^{\circ} = -RT \ln k \quad \text{eqn. 4-16.}$$

Table 4-4 shows the values of ΔG° as a function of temperature obtained for the interaction of 9AA with native DNA in 0.1M NaCl. Table 4-4 is shown on page 82. There is a small but finite increase in ΔG° (i.e. becoming less negative) with increasing temperature indicating a slight reduction in the tendency of 9AA to bind to native DNA at higher temperatures still well below the T_m (T_m for native DNA in the presence of 9AA $> 86.2^{\circ}\text{C}$).

The Van't Hoff plot, that is the plot of $\ln k$ versus inverse temperature, $1/T$, ($^{\circ}\text{K}^{-1}$) yields the enthalpy of the reaction:

$$\frac{\partial \ln k}{\partial (1/T)} = \frac{-\Delta H^{\circ}}{R} \quad \text{eqn. 4-17.}$$

TABLE 4-4

Thermodynamic parameters for the interaction of 9AA with native DNA in 0.1M NaCl.

Temp. (°C)	22	45	55	65
ΔG° (kJ/mole)	-32.2 (SE 0.2)	-32.2 (SE 0.2)	-32.0 (SE 0.2)	-31.7 (SE 0.25)
ΔH° (kJ/mole)	-35.2 (SE 0.8)			
ΔS° J/deg /mole	-9.6 (SE 5.0)			

Thermodynamic parameters refer to equation 4-15. and hence refer to per mole of bound 9AA or per mole of binding site.

The Van't Hoff plot is shown in Fig. 4-15 and is linear within experimental error. The value of the enthalpy of reaction so obtained and the standard error arising from the experimental values is given in Table 4-4.

The entropy change associated with the reaction has generally been derived^{16,17} from the expression:

$$\Delta S^\circ = \frac{\Delta H^\circ - \Delta G^\circ}{T} \quad \text{eqn. 4-18.}$$

where ΔH° has been itself determined from equation 4-17.

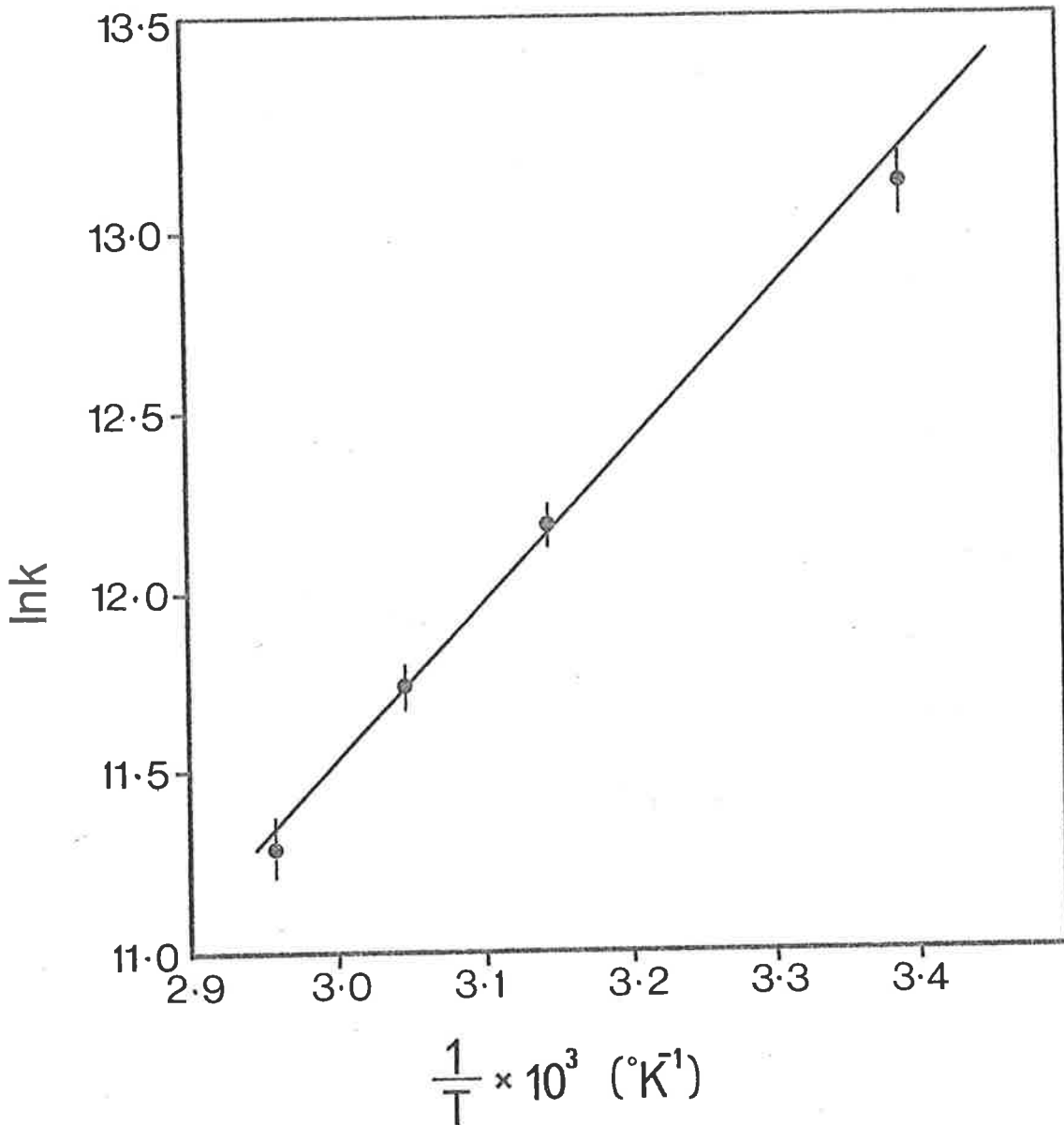


Fig. 4-15. Van't Hoff plot for the interaction of 9AA with native DNA in 0.1M NaCl. Equilibrium constants (k) determined from Scatchard plots.

However there is a tendency in doing this to quote a greater accuracy for ΔS° than is appropriate from the experimental results¹⁷. Without an independent measurement of ΔH° , and with an enthalpy of reaction which is observably independent of temperature within experiment error, the appropriate expression for the evaluation of ΔS° is not equation 4-18. but rather;

$$\frac{\partial \Delta G^\circ}{\partial T} = -\Delta S^\circ \quad \text{eqn. 4-19.}$$

The value of ΔS° calculated by equation 4-19., for data obtained in this work is given in Table 4-4.

8. Discussion

On the basis of the results obtained in this work it does not appear necessary to invoke a model for the interaction of 9AA with native DNA which requires a reversible change of state of the macromolecule at a temperature well below the melting temperature, as proposed by Chambrón et al¹⁶ for the interaction of proflavine with DNA. This is a consequence of the temperature dependence of ΔG° , as observed in this work, being a monotonic function of temperature, as has also been observed by Ichimura et al¹⁷ for the interaction of acridine orange with DNA. The reason for this disparity is not clear. The other parameter in the work of Chambrón et al¹⁶ which shows a variation markedly different from that obtained by Ichimura et al¹⁷, and also observed in this work is the variation of n with temperature. Chambrón et al¹⁶ observed a marked change in n with temperature at all ionic strengths whereas

Ichimura and co-workers¹⁷ observed no change. In this work (Table 4-3) the variation in n is very slight and in the opposite direction to that observed by Chambron *et al*¹⁶. It may be that the latter group carried out experiments with complexes which were not entirely in the region dominated by complex I. This would explain the variation in binding site number, n , but still leaves the variation in ΔG° an open question. Certainly the observations in the work described here of the internal linearity of the several spectra obtained for 9AA and native DNA each at various temperatures and the relatively temperature independent value of n does not require the proposition of heterogeneity amongst the binding sites as proposed by Chambron *et al*¹⁶.

The thermodynamic parameters given in Table 4-4. are in general agreement with the parameters obtained for other compounds in the papers previously mentioned^{16,17}. (A comparison of these results is given in the Appendix). In particular, the following characteristics are observed. The total free energy change for the reaction is large and negative, characteristic of the strong binding process associated with the formation of complex I³. Theoretical calculations have shown that complex I binding, assuming the fully intercalated model, will yield large negative values for the free energy change associated with the interaction whereas purely electrostatic, external binding is associated with significantly lower free energy changes¹⁸.

The large negative value of ΔH° ($\Delta H^{\circ} = -35$ kJ /mole) is indicative of the formation of strong bonding interactions. These presumably arise from intermolecular interactions between the planar bases of the DNA and the planar aminoacridine cation. These

interactions will be the sum of electrostatic, dipole-dipole (or monopole-monopole), dipole-induced dipole interactions and London forces¹⁸.

The entropy change (ΔS°) is found to be small and negative for the overall reaction. This is an important observation as it indicates that the reaction cannot be considered to be "entropy driven" but rather "enthalpy driven".

9. Concluding remarks

Spectra of the complex formed between 9AA and native DNA at low r values have been shown to be internally linear over a range of temperatures $22^\circ\text{C} - 65^\circ\text{C}$. The interpretation placed on this observation is that at low r values the 9AA exists in only two forms, namely, free 9AA and bound 9AA, which coexist in a single equilibrium defined by equation 4-7.

Scatchard plots of the binding show marked curvature well below the limiting level of binding associated with the formation of complex I. This curvature has been interpreted as being due to anti-cooperative effects arising from interactions between bound 9AA cations. These interactions most probably extend beyond nearest neighbour interactions. It has been shown, nonetheless, that the association constants for isolated binding sites can be obtained from the limiting slope, at low r , of the Scatchard plot. This intrinsic association constant, k , and the binding site number, n , are applicable to equations 4-14. and 4-15.

The binding site number, n , does not change significantly with temperature which may be indicative of little associated change in the binding site itself. This is entirely consistent with the extinction coefficient of the bound species ϵ_b which has also been shown to change only slightly with temperature.

The thermodynamic parameters determined for the reaction are consistent with an intercalation model in which the stability arises primarily from strong (bonding) intermolecular forces between the planar cationic dye and the planar bases of the DNA rather than from a favourable entropy of reaction.

REFERENCES

1. Drummond, D.S., Simpson-Gildemeister, V.F.W. and Peacocke, A.R.,
Biopolymers, 3, 135 (1965).
2. Sansom, L.N., Ph.D. Thesis, University of Adelaide, 1972.
3. Peacocke, A.R. and Skerrett, J.N.H., Trans. Faraday Soc., 52,
261 (1956).
4. Albert, A., "The Acridines", 2nd edition, Arnold (Publishers)
Ltd., 1966.
5. Gersch, N.F., Ph.D. Thesis, University of Adelaide, 1966.
6. Michaelis, L., Cold Spring Harbour Symp. Quant. Biol., 12,
131 (1947).
7. Brynstad, J. and Smith, P.G., J. Phys. Chem., 72, 296 (1968).
8. Kleinwachter, V. and Koudelka, J., Biochim. Biophys. Acta,
91, 539 (1964).
9. Chambron, J., Daune, M. and Sadron, C., Biochim. Biophys. Acta.
123, 319 (1966).
10. Weill, G. and Calvin, M., Biopolymers, 1, 401 (1963).
11. Kurucsev, T., personal communication.
12. See for example: Bloomfield, V.A., Crothers, D.M. and Tinoco, I.,
"Physical Chemistry of Nucleic Acids", Harper and Row
(Publishers), New York, 1974.
13. Armstrong, R.W., Kurucsev, T. and Strauss, U.P., J. Amer. Chem.
Soc., 92, 3174 (1970).
14. Müller, W. and Crothers, D.M., J. Mol. Biol., 35, 251 (1968).
15. Schellman, J.A., Israel J. Chem. 12, 219 (1974).
16. Chambron, J., Daune, M. and Sadron, C., Biochim. Biophys. Acta,
123, 306 (1966).

17. Ichimura, S. et al, Biochim. Biophys. Acta, 190, 116 (1969).
18. Gersh, N.F. and Jordan, D.O., J. Mol. Biol., 13, 138 (1965).
19. Kleinwachter, V., Balcarova, Z. and Bohacek, J., Biochim. Biophys. Acta, 174, 188 (1969).

CHAPTER V

The interaction of 9-aminoacridine with denatured DNA

<u>CONTENTS</u>	<u>Page</u>
1. Introduction	90
2. 9-aminoacridine and denatured DNA : spectra	90
3. 9-aminoacridine and denatured DNA : melting the complex	95
4. Renaturation of denatured DNA in the presence of 9-aminoacridine	96
5. Determination of the extent of binding (r) and the extinction coefficient of the bound species (ϵ_b)	98
6. Determination of the intrinsic association constant (k) and the number of binding sites (n).	101
7. Thermodynamic parameters	104
8. Concluding remarks	107
References	109

1. Introduction

It has been shown that denatured DNA interacts with aminoacridines in a manner which has some of the characteristics of the interactions of aminoacridines with native DNA¹⁻⁵. In particular, at room temperature, the interaction appears to be of a similar strength^{1,3,4} although the number of potential binding sites for strong binding is increased for some aminoacridines^{4,5}. The strong binding is, however, much more strongly temperature dependent below the T_m of the complex, than complex I for the interaction of aminoacridines with native DNA⁵.

In this Chapter the same techniques used in Chapter IV to study the interaction of 9AA with native DNA are used to study the interaction of 9AA with denatured DNA. In particular, the spectra of the complexes are studied with reference to the solution state of denatured DNA discussed in Chapter II. It is found that the system can be studied in a manner entirely analogous to that used for native DNA (Chapter IV) to obtain an intrinsic association constant for the interaction. The intrinsic association constant is found to vary markedly with temperature, as is also the number of potential binding sites. The thermodynamic parameters for the interaction are evaluated and these together with measurements are discussed in terms of an intercalation model which is applicable for 9AA bound to denatured DNA.

2. 9-aminoacridine and denatured DNA : spectra

The spectra of aminoacridines bound to denatured DNA have a number of features of the spectra of aminoacridines bound to native DNA. In particular, at low r , the interaction produces a red shift in the visible absorption maxima of the aminoacridine and a

reduction in its associated extinction coefficient. Also, a blue shift analogous to the same observation in native DNA - aminoacridine solutions is observed at high values of r . Indeed, this formation of the aggregated aminoacridine complex appears to be more favourable in denatured DNA than in native DNA^{2,6}. The similarities are so great that two binding sites for the interaction have been proposed similar to those of the native DNA system. The stronger binding is associated with interactions between the aminoacridine cation and the nucleotide bases; the weaker interaction is associated with electrostatic interactions between the cation and the negative phosphate groups of the DNA, and is restricted to solutions at low ionic strengths. These two types of binding sites are entirely analogous to the binding sites in native DNA. Two questions are immediately raised.

- (i) Since the structure of denatured DNA is disordered with respect to native DNA, of what importance is the secondary structure (i.e. the double helix) in the interaction with aminoacridines?
- (ii) As denatured DNA in neutral salt solutions has a conformation not only of some variety and complexity, but also with significant temperature dependence (as demonstrated in Chapter II), how valid is it to explain the interaction in terms of a simple equilibrium as was the case for native DNA - aminoacridine interactions (equations 4-7. and 4-15)?

In seeking an answer to the second question a study of the internal linearity of spectra can be expected to yield valuable information.

The spectra of the 9AA solutions in the presence of various concentrations of denatured DNA (prepared as described in Chapter II) at three temperatures, 25°C, 45°C and 65°C are shown in Figures 5-1., 5-2. and 5-3.

The spectra have been corrected for a small absorbance contribution from the denatured DNA. The extinction coefficient of this contribution is a linear function of wavelength, decreasing with increasing wavelength. The value of the extinction coefficient is found to be dependent on the instrument used during experimental work and it is assumed that this absorbance is a scattering phenomenon. The extinction coefficient of the denatured DNA does not appear to change in the presence of 9AA when measured at wavelengths at which 9AA is non absorbing and so it has been assumed that the contribution to observed absorbance due to denatured DNA is dependent on its concentration and the experimental configuration: corrections have been made accordingly.

It is immediately apparent in Fig. 5-1. that an isosbestic point does not occur within experimental error at 25°C. However at 45°C and 65°C apparent isosbestic points do occur (see Fig. 5-4. for enlargements of the region around the isosbestic points in Figs. 5-1. to 5-3.). If these spectra are tested for internal linearity by using equation 4-5., for the spectra appropriately numbered, the following values of β_2 are observed. (See Table 5-1.). Clearly, a comparison of the values of β_2 for native DNA (Table 4-1.) and denatured DNA (Table 5-1.) at any particular temperature shows a substantially greater degree of scatter in the latter case for what should be a single valued parameter for a single equilibrium. This is manifest as a marked increase in standard deviation for the values of β_2 at any particular temperature. The difference is most pronounced at 25°C, where there

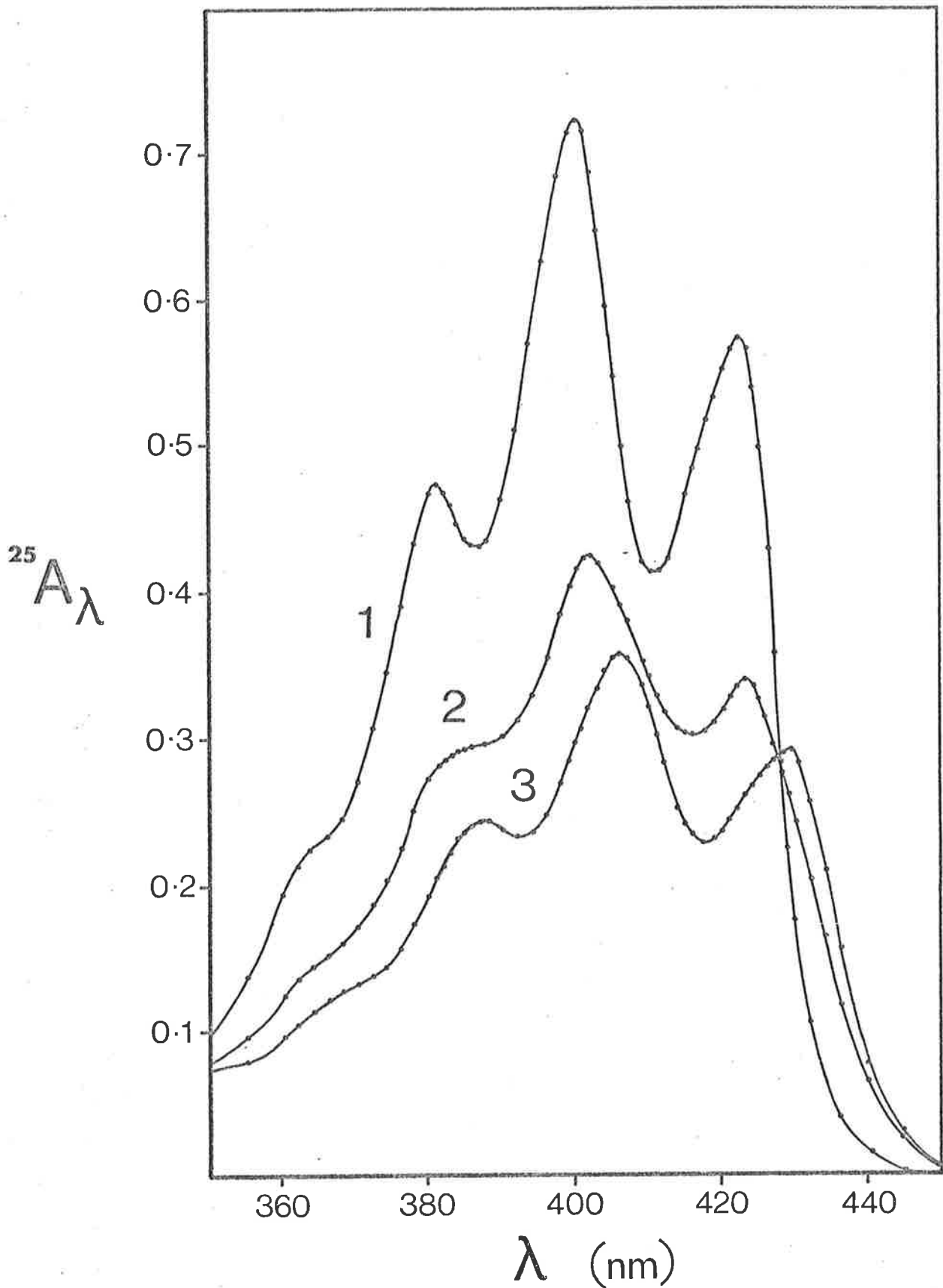


Fig. 5-1. Spectra of 9AA and denatured DNA in 0.1M NaCl at 25°C: constant 9AA concentration, 7.31×10^{-5} M; curve 1: 9AA, curve 2: 9AA and denatured DNA: $T_L/T_A = 0.252$; $r = 0.170$, curve 3: 9AA and denatured DNA: $T_L/T_A = 0.085$; $r = 0.082$.

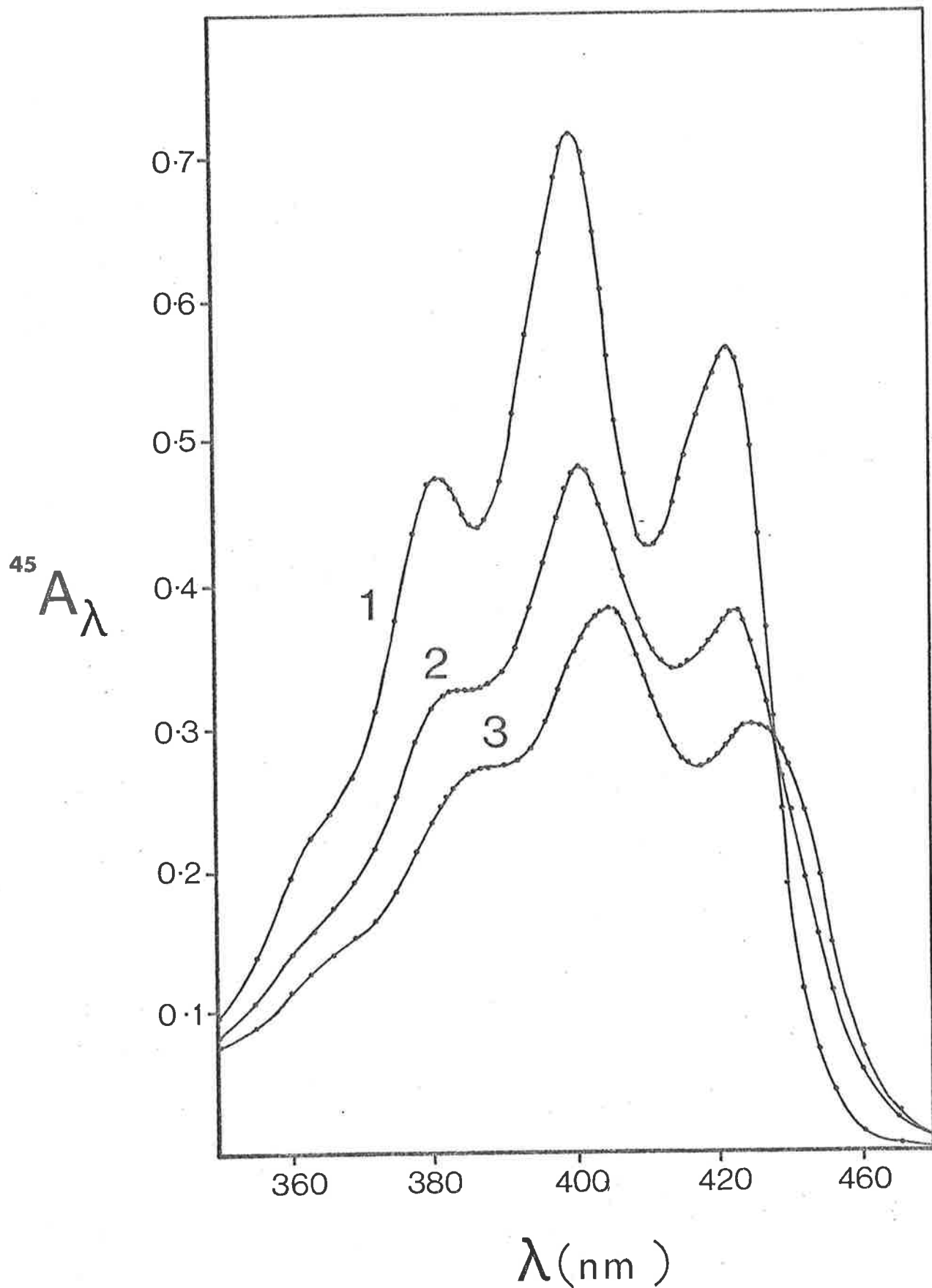


Fig. 5-2. Spectra of 9AA and denatured DNA in 0.1M NaCl at 45°C: constant 9AA concentration, 7.31×10^{-5} M; curve 1: 9AA, curve 2: 9AA and denatured DNA: $T_L/T_A = 0.252$; $r = 0.143$, curve 3: 9AA and denatured DNA: $T_L/T_A = 0.085$; $r = 0.075$.

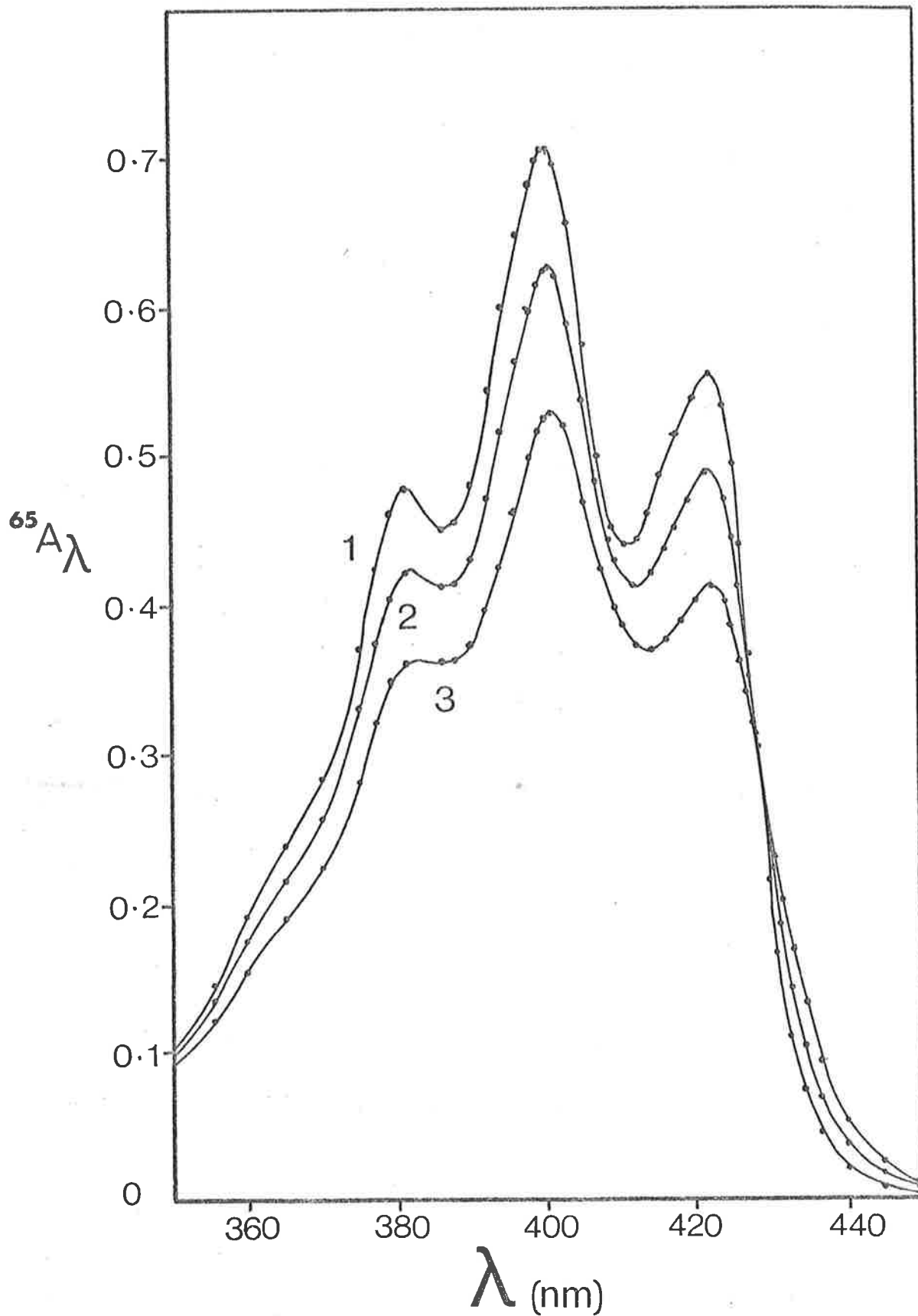


Fig. 5-3. Spectra of 9AA and denatured DNA in 0.1 M NaCl at 65°C: constant 9AA concentration, 7.31×10^{-5} M; curve 1: 9AA, curve 2: 9AA and denatured DNA: $T_L/T_A = 0.252$; $r = 0.057$, curve 3: 9AA and denatured DNA: $T_L/T_A = 0.085$; $r = 0.044$.

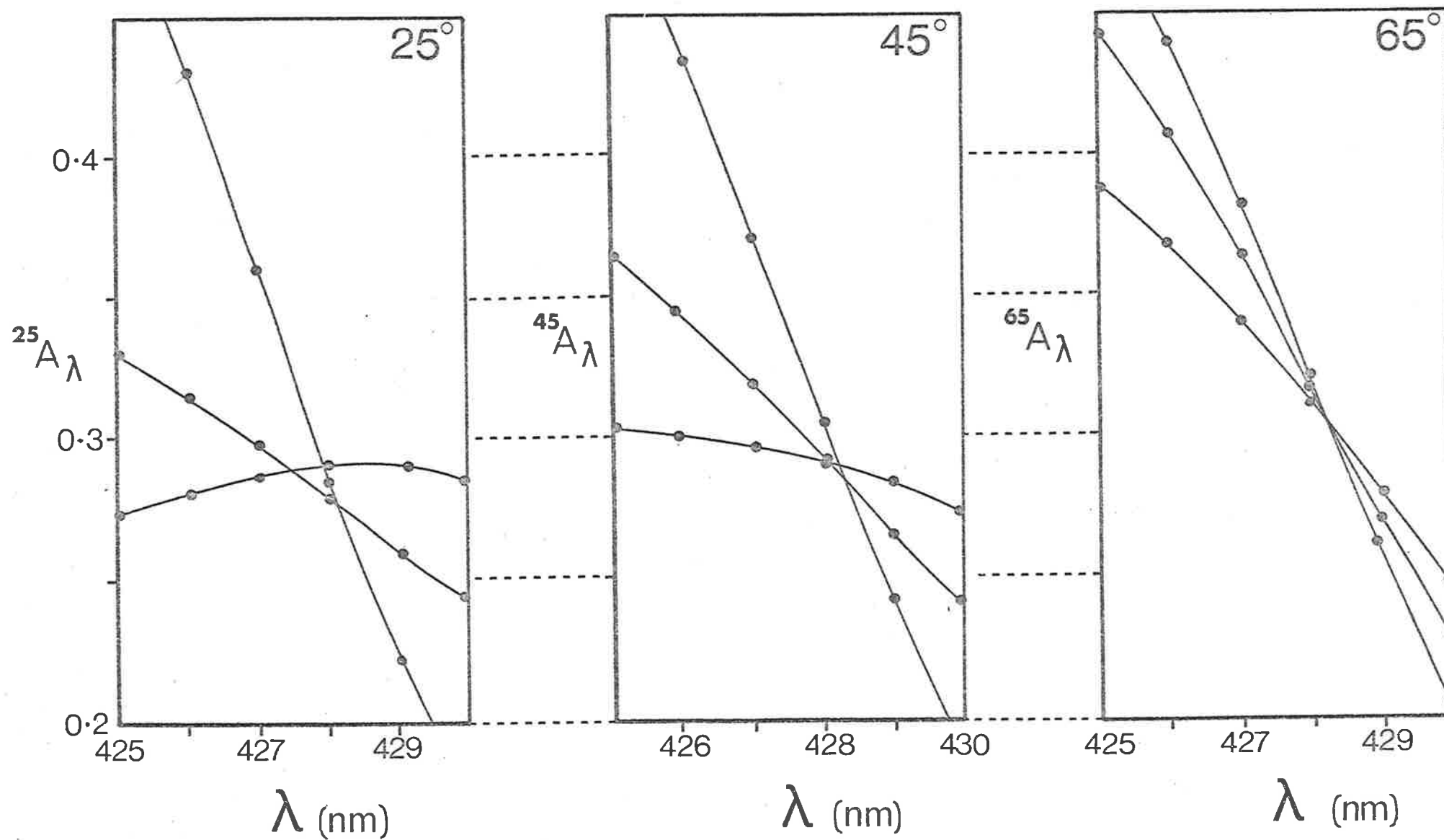


Fig. 5-4. Enlargements of the spectra shown in Figs. 5-1. to 5-3. showing the presence of isosbestic points at elevated temperatures in solutions of 9AA and denatured DNA.

TABLE 5-1.

The values of β_2^* for a set of spectra of 9AA and denatured DNA.

Temp. (°C) λ	25	45	65
380	0.715	0.661	0.470
390	0.714	0.658	0.457
400	0.721	0.659	0.459
410	0.769	0.674	0.429
420	0.728	0.660	0.453
432	0.662	0.632	0.484
average	0.718	0.657	0.459
S.D. (σ)	0.031	0.013	0.017

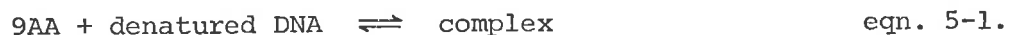
* as defined in the text

is an absence of an isosbestic point in the spectra, but is still significant at 45°C and 65°C where there is an apparent isosbestic point. Internal linearity is thus a more sensitive test for homogeneity of binding species than is the presence of an isosbestic point.

These observations are consistent with the structure of denatured DNA proposed in Chapter II. Shock cooled denatured DNA at room temperature may be considered to have three broad types of conformation:

- (i) short-range helical order,
- (ii) single strand, base-stacked regions,
- (iii) random coils.

As the temperature is increased the first of these "melts" out in what is observed as a broad cooperative transition at relatively low temperatures. All through this temperature range and at higher temperatures the single strand, base-stacked regions become progressively more disordered and finally the truly random coil structure becomes the only structure above the T_m of the native material. It can be expected (and will be demonstrated later) that aminoacridines bound to (i) and (ii) above have different extinction coefficients. The third conformation, that of the random coil, may not bind aminoacridines at all. Thus at 25°C, 9AA is distributed amongst two differing types of binding site (viz. short range, helical ordered DNA and single strand, base-stacked DNA). This heterogeneity gives rise to the lack of internal linearity observed for the spectra. As the temperature is increased, the short range helical order is lost and the heterogeneity is reduced as the principal binding site becomes the temperature dependent, single strand, base-stacked regions of the DNA. There is a consequent return to a virtual internal linearity of spectra at higher temperatures (45°C to 65°C). The foregoing argument suggests that at elevated temperatures, 45°C and above, the system of 9AA and denatured DNA at low r can be considered to be a single equilibrium of the form:



where the denatured DNA is principally the single strand, base-stacked structure. At lower temperatures equation 5-1. must be used with caution for it must be remembered that at these temperatures the denatured DNA is more heterogeneous.

3. 9-aminoacridine and denatured DNA : melting the complex.

The release of aminoacridines from complexes with DNA at elevated temperatures has been observed by Sansom⁴. The characteristic shape of the absorbance versus temperature curve is of a steady (quasi-cooperative) increase in absorbance with temperature which is complete at 70°C irrespective of the neutral salt concentration in the range: 10^{-3} M to 10^{-1} M NaCl. These results present a marked contrast to the release of aminoacridines from native DNA which has been observed to occur almost entirely coincident with the destruction of the double helical conformation of native DNA at the melting temperature of the complex^{4,7,8,9}. A careful study of the results obtained by Sansom⁴ shows that the limiting value of absorbance obtained at 70°C does not coincide with complete release of the aminoacridine from the complex. This is particularly noticeable in 0.1M NaCl neutral salt. The reason for this is apparent in Fig. 5-5, where the melting profiles of denatured DNA alone (observed at 260 nm - curve B) and denatured DNA in the presence of 9AA at low T_L/T_A are shown (observed at 260 nm and 400 nm - curves A and C, respectively). Despite the complexity of interpreting curve A, as even at this low ratio of T_L/T_A the contribution of 9AA to the absorbance in curve A is about 40%, several observations can be made.

- (1) The release of 9AA from denatured DNA is associated with a loss of structure in the denatured DNA (marked hyperchromicity between 30°C and 55°C in curve B). This hyperchromicity has already been interpreted as being principally due to loss of short range helical order. The loss of structure will also include a reduction in single strand, base-stacking.

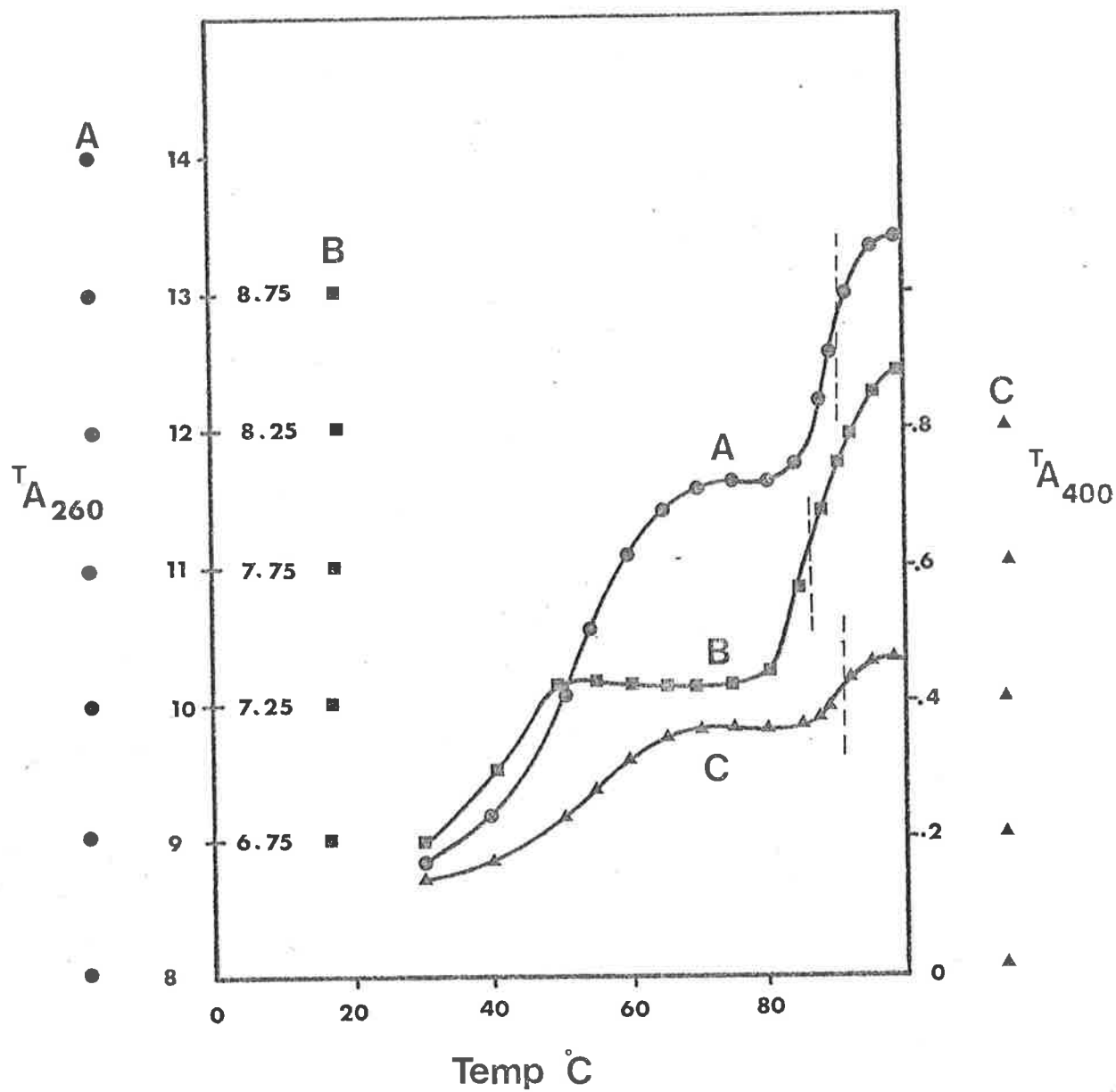


Fig. 5-5. Melting curves of 9AA and denatured DNA in 0.1M NaCl.

curve A: 9AA and denatured DNA observed at 260 nm.

curve B: denatured DNA equimolar to that in curves A and C observed at 260 nm.

curve C: 9AA and denatured DNA observed at 400 nm.

- (2) A further loss of aminoacridine (curves A and C) which occurs in the absence of a marked change in hyperchromicity of the denatured DNA (curve B, 55°C - 75°C). This is attributed to a reduction in the binding of 9AA to denatured DNA as the single strand, base-stacked regions of the macromolecule become progressively less energetically favourable as binding sites with increasing temperature. (Chapter II and reference ¹⁰). It has been suggested that this progressive loss of single strand base-stacking is not associated with a major change in hyperchromicity¹⁰. Certainly the plateau in curve B, Fig. 5-5., could be interpreted in this manner, however concurrent with this loss of single strand base-stacking is renaturation which is expected to decrease the absorbance significantly. The hypochromism associated with single strand, base-stacking is therefore still an open question in this system.
- (3) The reason for incomplete release of aminoacridine from complexes observed in reference ⁴ is due to the formation of some renatured DNA during the course of the melting curve determination. This is released at the T_m of the complex which is observed to occur at the same temperature when observed both at 400 nm where 9AA only is being monitored, curve C: and at 260 nm, where both the secondary structure of the macromolecule and the absorbance of the aminoacridine are being monitored, curve A. This supports earlier work, ^{4,7,8,9} and has been discussed in Chapter IV.

4. Renaturation of denatured DNA in the presence of 9-aminoacridine

Inhibition of extent of renaturation of denatured DNA by acridine orange has been reported⁵. In this work renaturation

in the presence of 9AA has been observed as a decrease in absorbance with time at 400 nm in solutions of denatured DNA and 9AA at elevated temperatures. The decrease in absorbance is due to the formation of double helical (renatured) DNA which binds 9AA with a lower extinction coefficient and higher association constant (see sections 5. and 6. - this Chapter) than denatured DNA at the same temperature. An extensive study is required to explore this phenomenon, however some qualitative observations have been made.

- (1) Renaturation of denatured DNA in the presence of 9AA in 0.1M NaCl is a principally second order process. Figure 5-6. is an experimental plot of absorbance (at 400 nm) versus time for a solution of 9AA and denatured DNA which has been heated rapidly to 70°C and maintained at that temperature. The infinite time value of the absorbance has been evaluated from a plot of absorbance versus $(\text{time})^{-1}$ at $(\text{time})^{-1} = 0$. The second order plot, also shown in Fig. 5-6., is seen to be linear for a substantial part of the reaction. This indicates that the rate limiting step is the migration of complementary strands of the denatured DNA.
- (2) High concentrations of 9AA appear to inhibit the rate of renaturation of denatured DNA with respect to low concentrations of 9AA. Fig. 5-7. shows the melting profiles of 3 solutions of identical concentrations of denatured DNA in the presence of differing concentrations of 9AA. The melting was carried out simultaneously for all solutions. The absorbance has been normalized to that pertaining at 98°C when the 9AA behaves as unbound aminoacridine. Clearly there appears to be, successively, less renaturation with increased

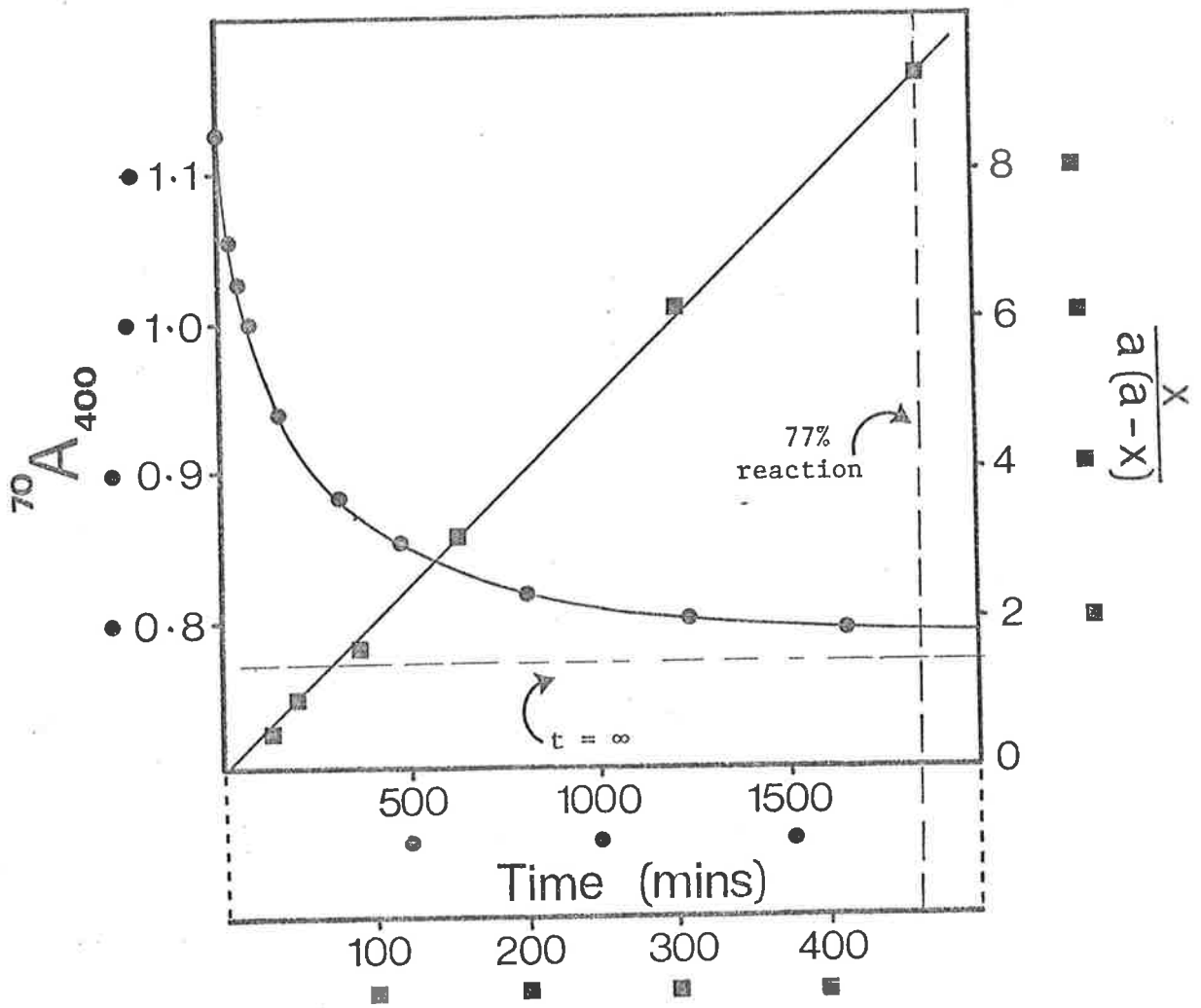


Fig. 5-6. Renaturation of denatured DNA in the presence of 9AA. Solution heated rapidly to 70°C and absorbance monitored with time at 400 nm (●). The straight line plot (■) indicates that for the first 77% of reaction, at least, renaturation follows second order kinetics (equation 2-4.).

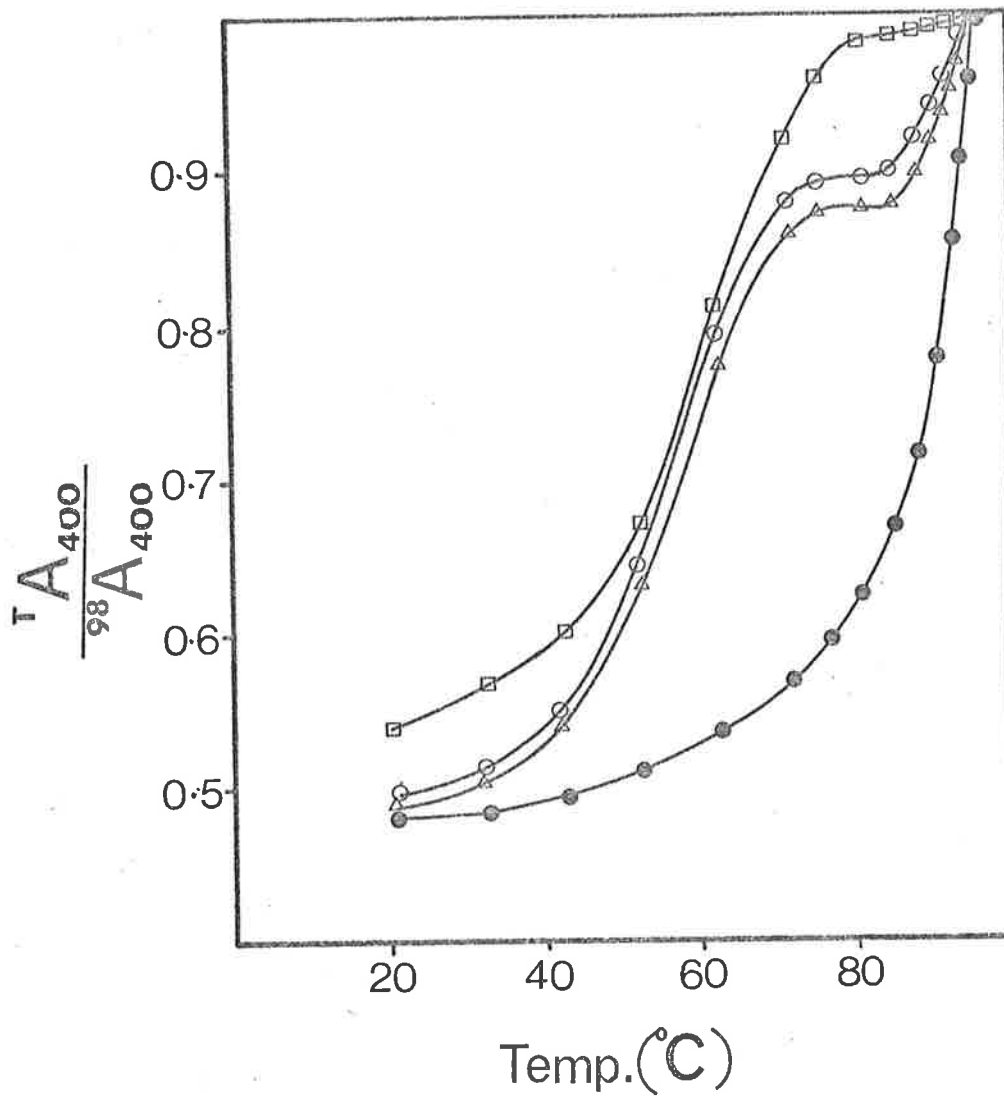


Fig. 5-7. Effect of 9AA on the extent of renaturation during melting. Simultaneously determined curves

- (□) 9AA and denatured DNA, ${}^9A_{400} = 2.000$
- (○) 9AA and denatured DNA, ${}^9A_{400} = 0.802$
- (△) 9AA and denatured DNA, ${}^9A_{400} = 0.673$

the above curves are at constant denatured DNA concentration.

For comparison a melting curve of 9AA and native DNA is shown (●).

9AA concentration. However these results are of a preliminary nature only as they do not take into account the possibility of any preferential distribution of the dye amongst available binding sites. Also these results do not give any indication of whether or not inhibition occurs with respect to the renaturation of denatured DNA alone.

These results and those of Ichimura *et al*⁵, are consistent with the latter's proposition that the inhibition of extent of renaturation, and possibly the rate of renaturation, is brought about by the stabilization, by aminoacridines, of mismatched pairs during renaturation and a reduction in the rapidity of subsequent intramolecular rearrangements necessary for further renaturation⁵.

The observations outlined in this work make a reduction in absorbance at 400 nm a good criterion for the presence of renaturation in solutions of denatured DNA and 9AA, particularly at low T_L/T_A , where absorbance at 400 nm is observably sensitive to the DNA structure (Fig. 5-7.).

5. Determination of the extent of binding (r) and the extinction coefficient of the bound species (ϵ_b).

In view of the analysis of spectra given in section 2 of this Chapter it seems appropriate to evaluate the extent of binding and the strength of binding of 9AA to denatured DNA in a manner entirely analogous to that used in Chapter IV for the interaction of 9AA with native DNA. This is so because the interaction appears, substantially, to obey a single equilibrium. The system of denatured DNA, as has been pointed out, is not as ideal as that of native DNA: at 25°C it does deviate from a single equilibrium in its interaction with 9AA. However, it is reasonable to carry out the analysis even at this temperature provided that the approximation of internal linearity is recognised and emphasis is placed on

qualitative arguments rather than quantitative ones.

Accordingly, binding curves have been measured for 9AA and denatured DNA at 22°C, 45°C, 55°C and 65°C. Plots of A/A_i versus T_L/T_A (where the variables have been defined in equation 4-8.) have been obtained from experimental data and the results of three separate binding curves, each with different initial concentrations of 9AA, at each temperature are shown in Figure 5-8. As discussed in the previous Chapter (section 5.) the value obtained by extrapolation of these curves to $T_L/T_A \rightarrow 0$ provides the ratio (Q) of the extinction coefficients of the bound and free aminoacridine species; it also provides the value of A'_{ex} which is required to calculate the value of r , the extent of binding (equations 4-10. and 4-11.).

In some of these plots considerable extrapolation to the A/A_i axis is required. The extrapolation is less ambiguous than it might appear as each set of 3 curves at a particular temperature must extrapolate to the same point (within the variation of A_i caused by dimerization - see Chapter IV section 5.). Furthermore, a measure of the accuracy of extrapolation can be gauged a posteriori by the observation of coalesced Scatchard plots (see the next section of this Chapter). Nonetheless, it is immediately apparent that the value of Q is far more temperature dependent than the same parameter in the case of 9AA and native DNA (Table 4-2). The values of Q for 9AA and denatured DNA are given in Table 5-2. on page 100. The observed variation in Q , which implies a significant variation in ϵ_b , with temperature is indicative of a binding site which changes with temperature, as the extinction coefficient of the bound aminoacridine arises from the electronic interactions between the planar aminoacridine and the planar bases of the DNA. As ϵ_b approaches unity, at higher

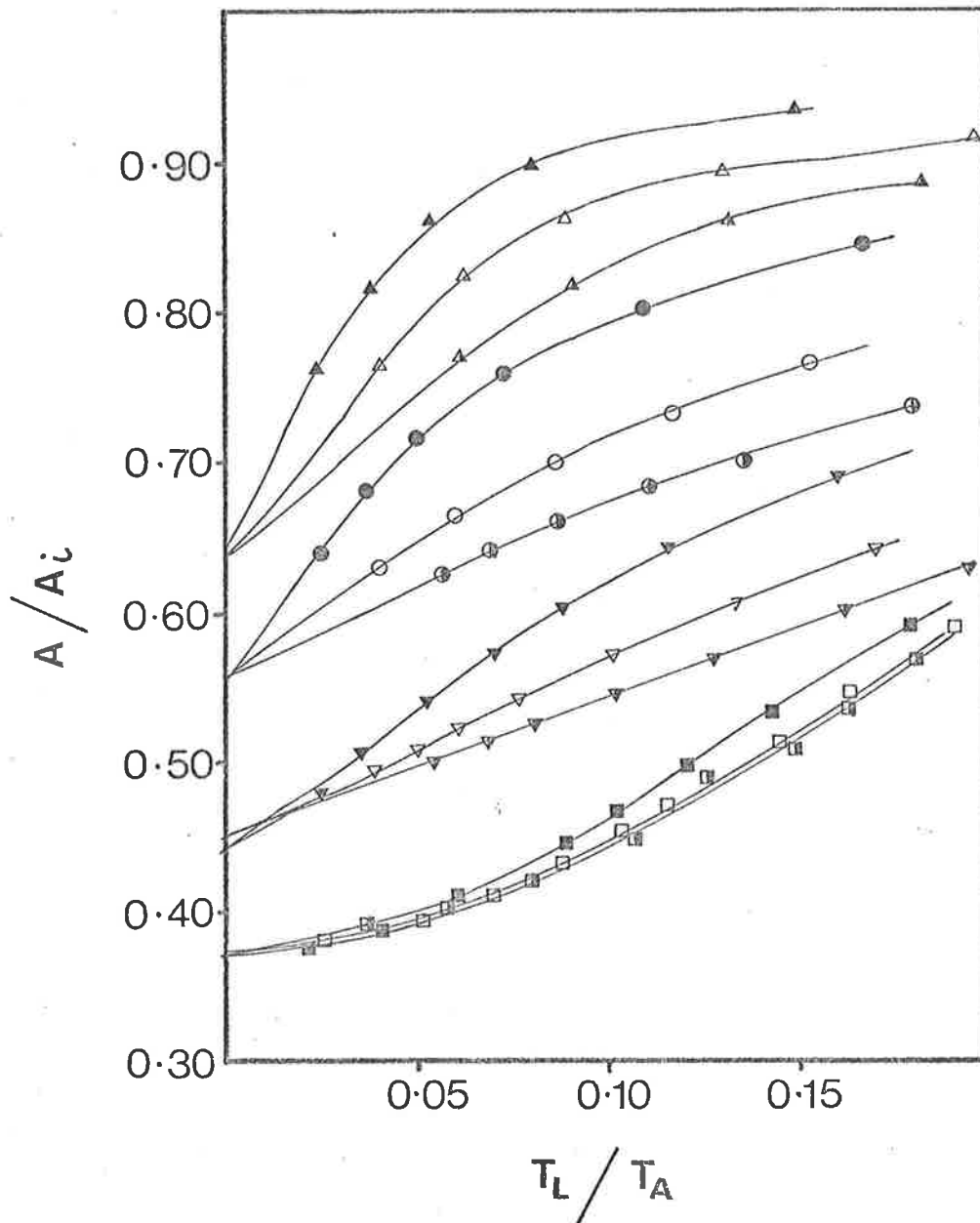


Fig. 5-8. Plots to determine the ratio of extinction coefficients of 9AA bound to denatured DNA (ϵ_b) and free 9AA (ϵ_f) at various temperatures.

$$\frac{A}{A_i} = \frac{\epsilon_b}{\epsilon_f} \text{ as } \frac{T_L}{T_A} \rightarrow 0$$

($\blacktriangle, \triangle, \blacktriangle$) at 65°C; (\bullet, \circ, \bullet) at 55°C,
 ($\blacktriangledown, \triangledown, \blacktriangledown$) at 45°C, ($\blacksquare, \square, \blacksquare$) at 22°C.

TABLE 5-2.

Variation of Q^* with temperature for 9AA and denatured DNA

Temp. ($^{\circ}$ C)	22	45	55	65
$Q = \frac{\epsilon_b}{\epsilon_f}$	0.37 ± 0.01	0.45 ± 0.01	0.56 ± 0.01	0.63 ± 0.02

* as defined in the text

temperatures, so it may be concluded that the bound 9AA is less influenced by the binding site. This proposition is in accord with the structure proposed for denatured DNA. At elevated temperatures the 9AA is bound only to single strand base-stacked regions of the macromolecule. The strength of this base-stacking is very temperature dependent and becomes weaker at higher temperatures¹⁰. It may be pictorially demonstrated as adjacent bases which are parallel to each other and which oscillate with respect to each other. The strength of the stacking is then proportional to the amount of overlap of planar surfaces that occurs per unit time. As the temperature is increased so the amplitude of the oscillation increases producing a reduction in the degree of overlap of planar surfaces. A 9AA molecule intercalated between two such bases will experience a less favourable environment as the temperature increases. This model explains why such a variation in Q does not occur in native DNA-9AA solutions. Clearly, below the T_m of the complex the bases of native DNA are constrained by the double helix and are not free to



oscillate. These proposals will be summarized with further evidence later in the Chapter.

6. Determination of the intrinsic association constant (k) and the number of binding sites (n)

With the spectrophotometric evaluation of the extent of binding, r and the consequent evaluation of the free 9AA concentration, c from equation 4-9., it is possible to produce Scatchard plots of r/c versus r for the interaction. Scatchard plots obtained in this manner for the interaction of 9AA with denatured DNA are shown in Figures 5-9 (a)., 5-10 (a)., 5-11 (a). and 5-12 (a). at temperatures 22°C , 45°C , 55°C and 65°C , respectively. In these figures only the points using the value of A'_{ex} in equation 4-8. are shown. The points determined using the value of A_{ex} calculated from the experimental excess DNA concentration show the same type of variation as that observed in Figures 4-7., 4-11., 4-12. and 4-13., but are not shown here for greater clarity in the diagrams.

Renaturation of DNA during the course of the experiment is minimal because, as described in Chapter VIII section 4., denatured DNA is added to 9AA solutions. This means that:

- (a) denatured DNA is in low concentration until the final few additions of denatured DNA which are made over a relatively short period of time.
- (b) 9AA is in excess until the final few additions of denatured DNA.

Both (a) and (b) minimize renaturation. There is no measurable decrease in absorbance of the final solution, observed at 400 nm, during equilibrium time at all the temperatures studied indicating that renaturation is slight.

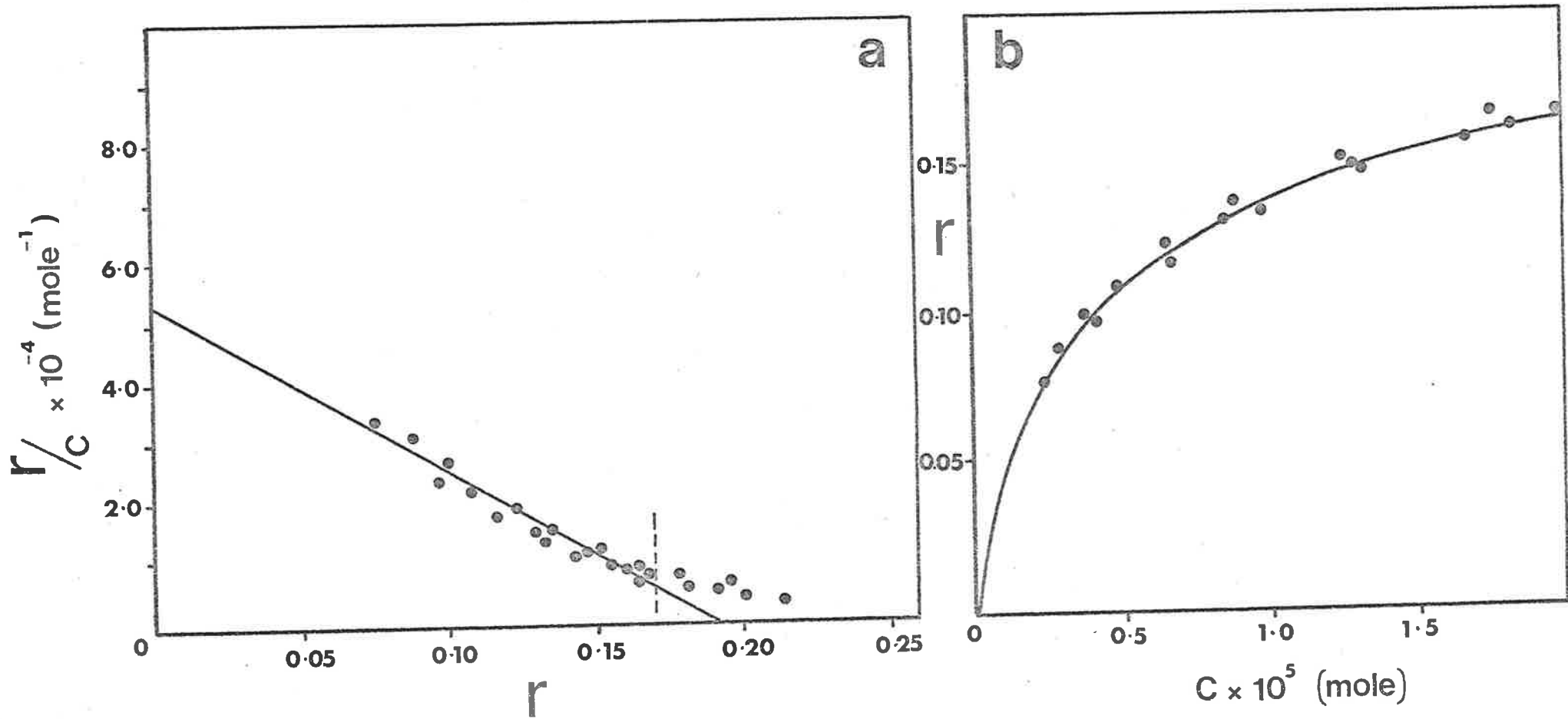


Fig. 5-9. (a) Scatchard plot for the interaction of 9AA with denatured DNA at 22°C in 0.1M NaCl.
 (b) Langmuir isotherm for the interaction.

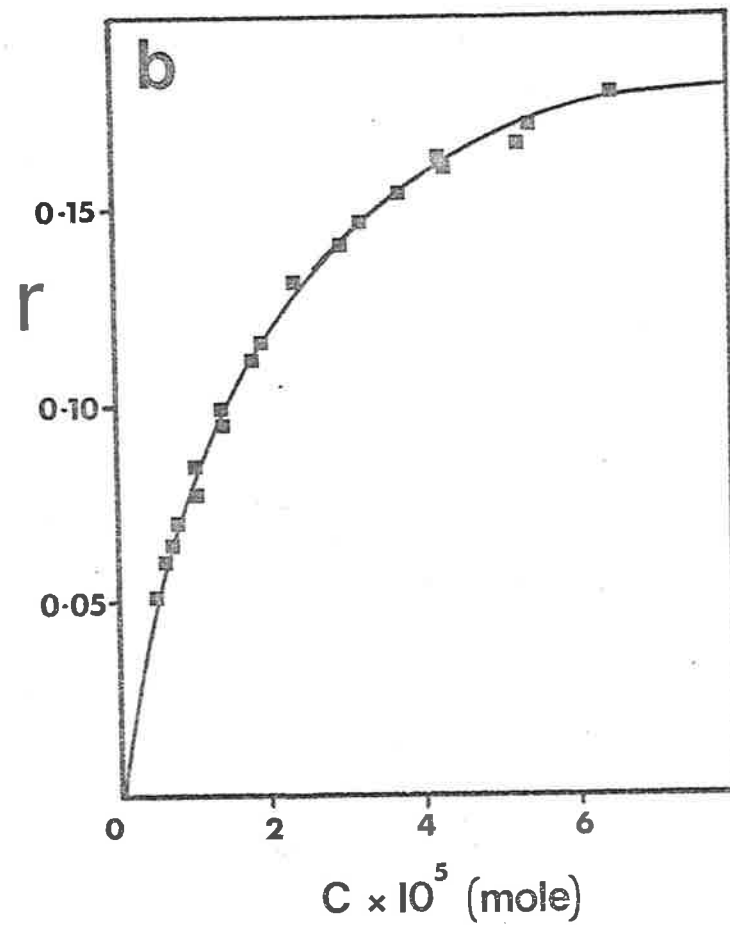
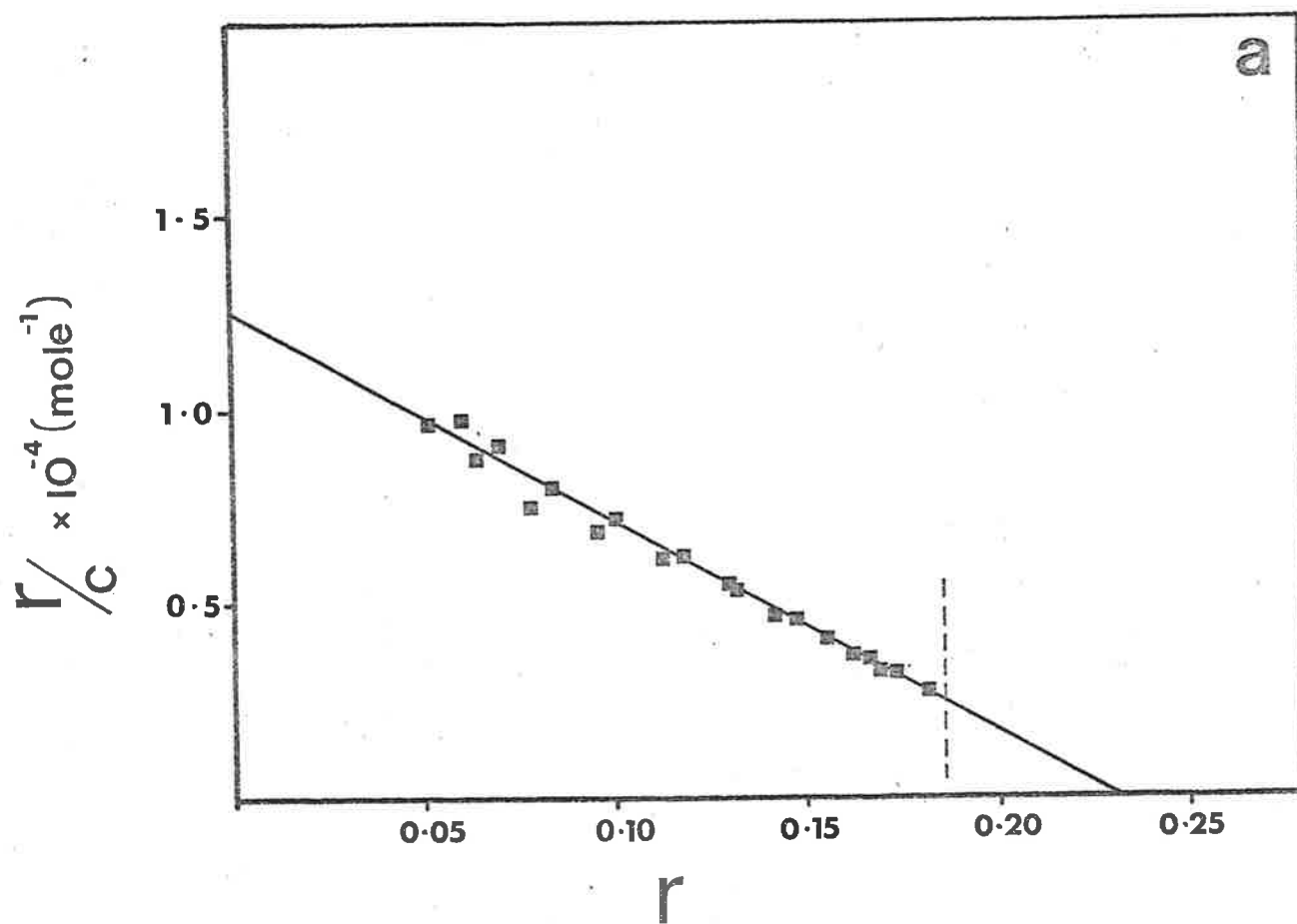


Fig. 5-10. (a) Scatchard plot for the interaction of 9AA with denatured DNA at 45°C in 0.1 M NaCl.
 (b) Langmuir isotherm for the interaction.

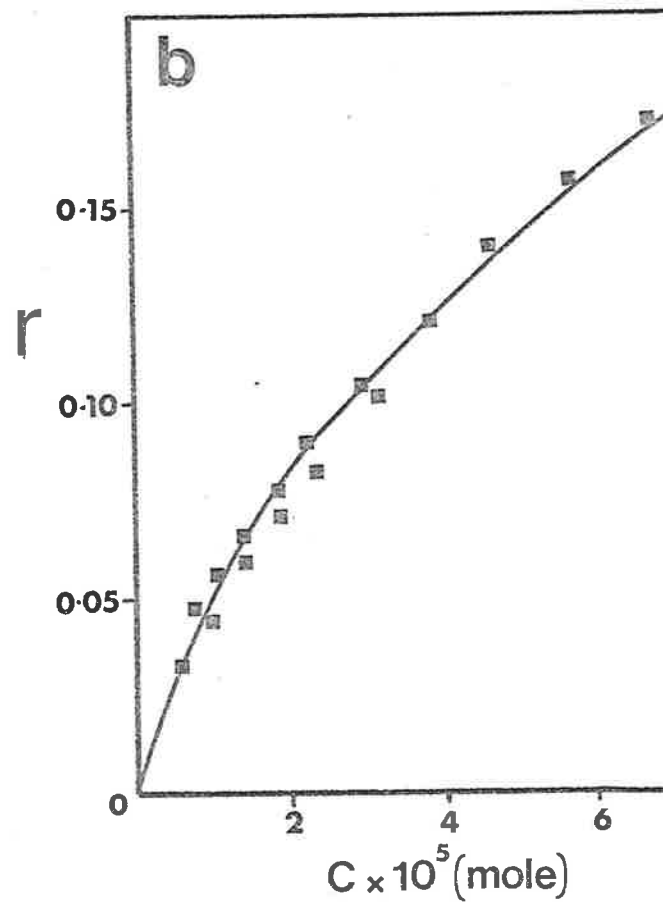
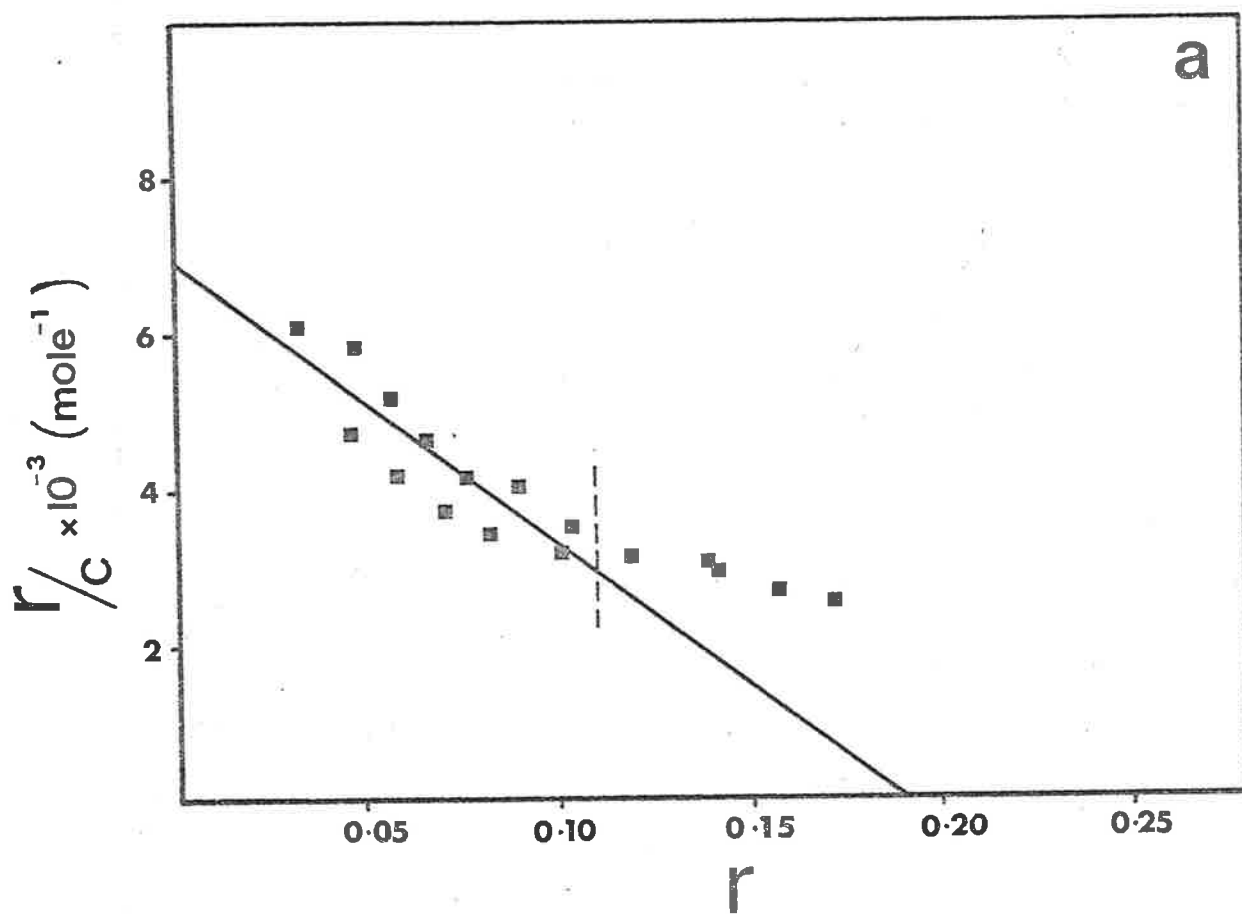


Fig. 5-11. (a) Scatchard plot for the interaction of 9AA with denatured DNA at 55°C in 0.1 M NaCl.
 (b) Langmuir isotherm for the interaction.

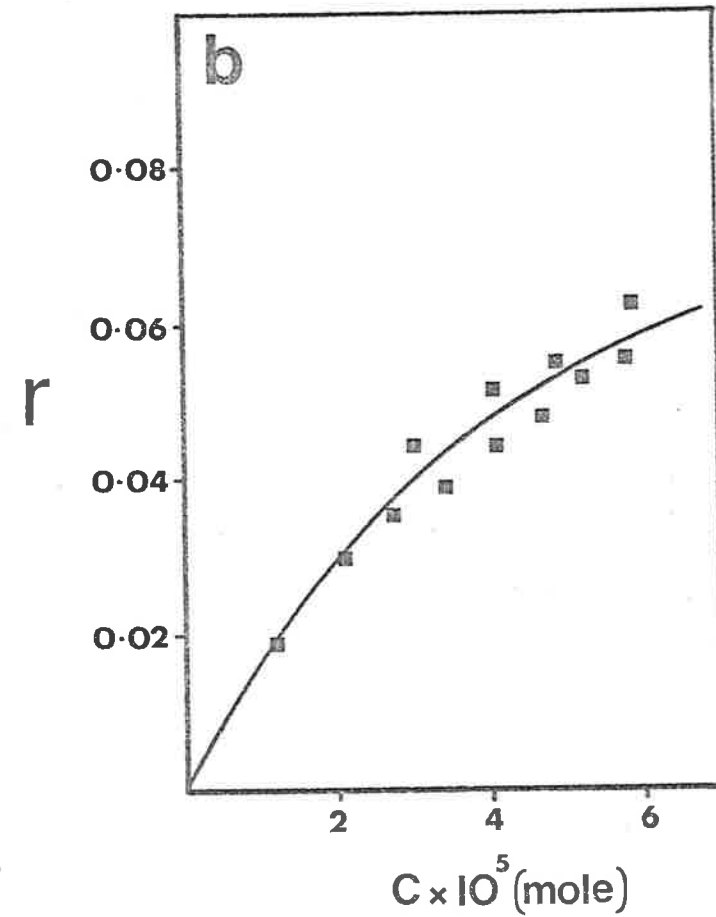
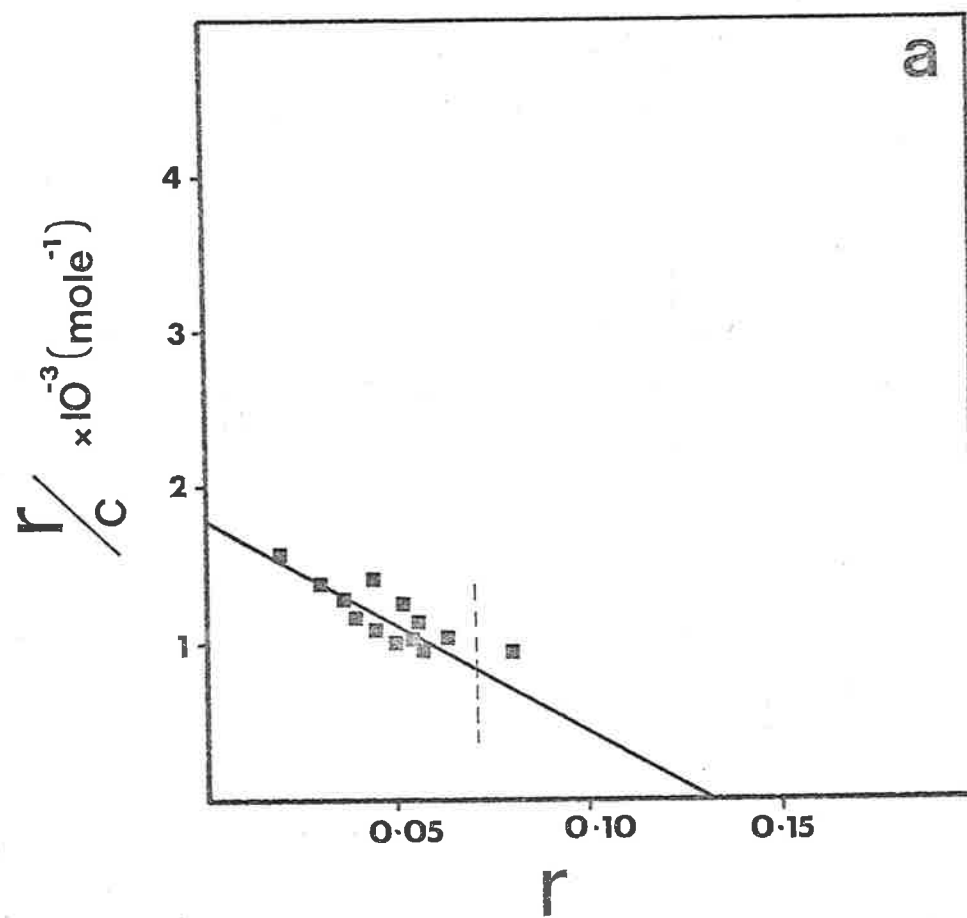


Fig. 5-12. (a) Scatchard plot for the interaction of 9AA with denatured DNA at 65°C in 0.1M NaCl.
 (b) Langmuir isotherm for the interaction.

As can be seen from the variation in n a cut-off point in r cannot sensibly be chosen for the evaluation of the intrinsic association constant, k , as it was for the case of 9AA with native DNA (all r values ≤ 0.10). In Figures 5-9 (a), to 5-12 (a), the cut-off point for the calculation of k has been chosen subjectively from the curvature of the plot. The cut-off point is marked in the figures by a short vertical line. Only points at r values less than this value have been used in the evaluation of k and hence of n , which is the limiting number of binding sites associated with the equilibrium of the form given by equation 4-14. The values of k and n for the interaction of 9AA with denatured DNA are given in Table 5-3.

TABLE 5-3

Intrinsic association constant (k) for the interaction of 9AA with denatured DNA in 0.1M NaCl

Temp. ($^{\circ}$ C)	22	45	55	65
k (moles $^{-1}$) $\times 10^{-5}$	2.80 (S.E.O.16)	0.54 (S.E.O.016)	0.36 (S.E.O.063)	0.136 (S.E.O.031)
n	0.190 (S.E.O.009)	0.231 (S.E.O.004)	0.191 (S.E.O.013)	0.133 (S.E.O.010)

In spite of the subjectivity involved in assessing the curvature of the Scatchard plots in Figs. 5-9 (a). to 5-12 (a), it is clearly apparent from the figures and from Table 5-3. that the value of n changes significantly with temperature; increasing between 22 $^{\circ}$ C and 45 $^{\circ}$ C and decreasing above this latter temperature.

This variation in n is far greater than that observed for 9AA and native DNA over the same temperature range (Table 4-3.).

Furthermore, as can be seen from a comparison between Tables 4-3. and 5-3. the association constant for the interaction of 9AA with denatured DNA also varies more markedly with temperature than the same parameter for 9AA and native DNA.

The model outlined in the previous section of this Chapter (section 5.) to explain the variation in ϵ_b , combined with the model of the structure of denatured DNA in solution can be used to explain these observations. As a corollary to the variation of ϵ_b with temperature, associated with a decrease in the interactions between the 9AA chromophore and the nucleotide (stacked) bases, it can be expected that there will be a decrease in k with temperature since both are a measure of the favourability of interaction. This change in k can be expected to be greater than that observed, over the same temperature range, for the 9AA and native DNA system for which there was only a slight variation in ϵ_b of the bound species with temperature. The change in n with temperature, however, must arise from a different cause. It is proposed that the variation in n is due to a change in proportion of denatured DNA which exists in the single strand, base-stacked form and in the random coil form. Since the random coil is favoured at higher temperatures then the observation of a reduction in n with increasing temperatures implies inter alia that the truly random coil form of denatured DNA either does not bind 9AA at all or only to a markedly lesser degree.

The apparently anomalous observation of n at 22°C being lower than n at 45°C (Table 5-3.) is also satisfactorily explained by the proposed structure of denatured DNA. It has already been observed (in Chapter II and this Chapter sections 2. and 3.) that at low temperatures a significant amount of short range helical

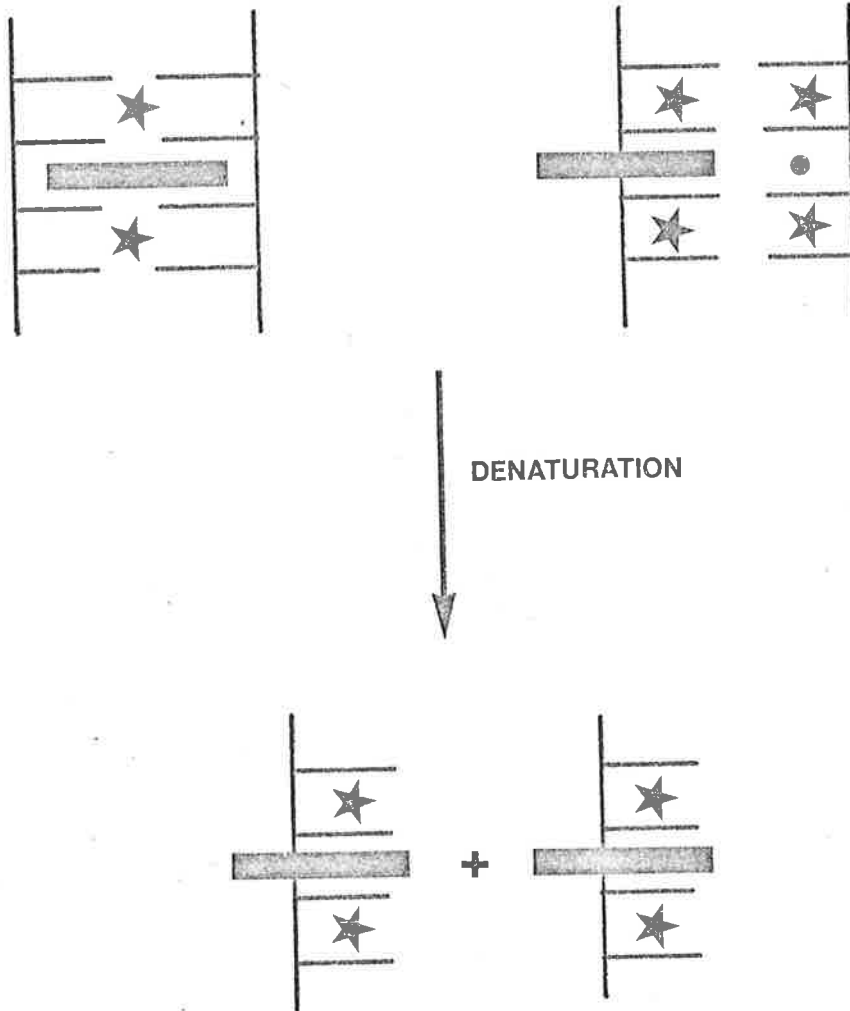
order exists in denatured DNA. In these ordered regions, which are analogous to native DNA, the presence of a bound 9AA cation in the Pritchard et al¹¹ model restricts the binding of further aminoacridines both at bases immediately adjacent to the bound site on the same strand and between the bases of the strand opposite to the bound site. This is true not only of the Pritchard et al¹¹ model but also of the Lerman model¹². This has been used to explain the limit of intercalation binding (complex I) at $r = 0.25$ ¹³. Anti-cooperativity produces a lower apparent binding limit as described in Chapter IV. However, as proposed by Ichimura et al⁵ and Sansom⁴, denatured DNA can effectively bind more aminoacridines per nucleotide phosphorous than native DNA since with strand separation the restriction of a potential binding site on the complementary strand is removed. Thus the loss of short range helical order between 22°C and 45°C introduces an increase in the number of potential binding sites in denatured DNA as the short range helical ordered structure gives way to single strand base-stacking. At higher temperatures this increase is eroded as single strand base-stacking is weakened and replaced by the random coil structure. In denatured DNA at 22°C the value of n is still greater than for native DNA at the same temperature as some of the macromolecule is certainly single stranded and is hence able to bind more aminoacridine per nucleotide phosphorous than purely native DNA. The above comments on the restriction of binding sites are schematically represented in Figure 5-13.

7. Thermodynamic parameters

The values of the thermodynamic parameters evaluated by equations 4-16., 4-17. and 4-19., from the change in the intrinsic association constant with temperature for the interaction of 9AA with

LERMAN MODEL

PRITCHARD MODEL



- ★ Restricted site
- Potential site on denaturation

Fig. 5-13. Schematic representation of the increase in the number of intercalation sites when native DNA or folded sections of denatured DNA melt to form single strand, base-stacked regions of the macromolecule.

denatured DNA are given in Table 5-4.

TABLE 5-4

Thermodynamic parameters for the interaction of 9AA with
denatured DNA in 0.1M NaCl

Temp. ($^{\circ}\text{C}$)	22	45	55	65
ΔG° (kJ/mole)	-30.8 (S.E.O.2)	-28.8 (S.E.O.1)	-28.6 (S.E.O.4)	-26.7 (S.E.O.6)
ΔH° (kJ/mole)	-56.0 (S.E.5.0)			
ΔS° (J.deg $^{-1}$ mole $^{-1}$)	-88 (S.E.17)			

While it is valid to evaluate the free energy of the interaction (ΔG°) from the intrinsic association constant as measured from the Scatchard plot, some care must be taken in discussing the values of the other thermodynamic parameters, namely the enthalpy of reaction (ΔH°) and the entropy of reaction (ΔS°). These last two quantities are calculated from the change in association constant with temperature. However, it has been inferred in previous sections of this Chapter that the binding site in denatured DNA changes with temperature, as exemplified by the significant change in the extinction coefficient of the bound 9AA (ϵ_b) with temperature. Thus ΔH° and ΔS° are derived from product and reactant states which themselves are changing with temperature. This is unlike the native

DNA-9AA system in which any change to the binding site is small, the macromolecule being constrained by its secondary structure and hence the product and reactant states not varying greatly with temperature in this latter case. Nonetheless, it seems reasonable to treat the results in a semi-quantitative manner, more particularly as the Van't Hoff plot for the interaction of 9AA with denatured DNA is substantially linear (see Figure 5-14.). This plot has been used to evaluate the ΔH° value given in Table 5-4. The observation of linearity in the Van't Hoff plot and equation 4-19. have been used to evaluate ΔS° . That the Van't Hoff plot is linear within experimental error, in view of the changing nature of the binding site and complex with temperature, is fortuitous, but does allow single valued parameters to be considered as valid descriptions of ΔH° and ΔS° of reaction over the temperature range studied.

The enthalpy of reaction is large and negative, even more so than for the interaction of 9AA with native DNA (Table 4-4.). This is indicative of the formation of strong bonding interactions, presumably composed of electrostatic, dipole-dipole, dipole-induced dipole and London forces interactions between the planar heterocyclic aminoacridine structure and the heterocyclic bases of the DNA.

The most important thermodynamic distinction between the native and denatured DNA complexes formed with 9AA lies in the significantly larger negative value of the entropy of reaction (ΔS°) for the formation of the 9AA-denatured DNA complex. This term indicates that the reaction has a component which becomes unfavourable with increased temperature, as observed. It is suggested that this arises from an ordering of the single strand, base-stacked regions of denatured DNA when 9AA is bound. That is, the binding of the 9AA cation constrains the oscillatory motion of the single strand

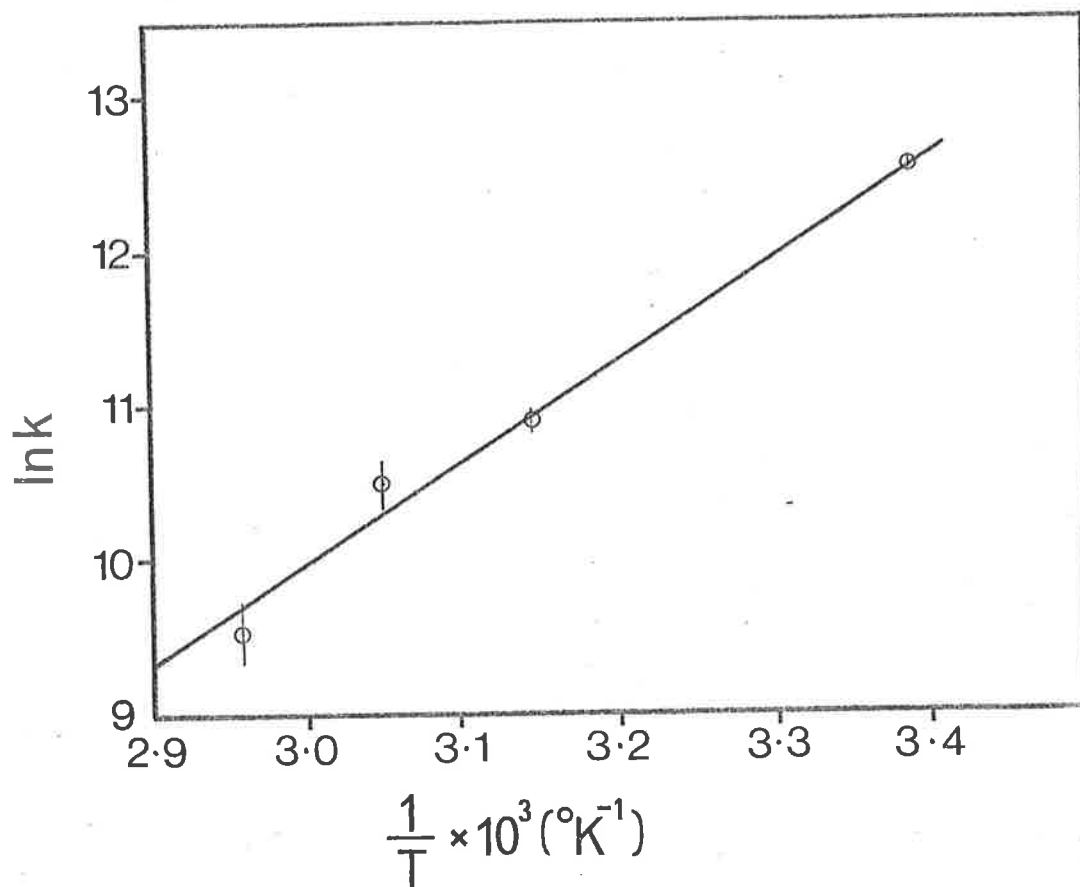


Fig. 5-14. Van't Hoff plot for the interaction of 9AA with denatured DNA in 0.1 M NaCl. Equilibrium constants (k) determined from Scatchard plots.

base-stacked regions of the denatured DNA as the bonding occurs. The results are in good agreement with those observed by Ichimura *et al*⁵ for acridine orange and denatured DNA (for a comparison see Appendix). Changes in solvation contributing to ΔS° are not considered for 9AA and denatured DNA complex formation to be very different from those for 9AA and native DNA complex formation, as both interactions require the inclusion of an aromatic moiety (9AA) into a similar hydrophobic environment (intercalation between nucleotide bases). Although the bases of denatured DNA will be more solvated than native DNA they will, similarly, be more solvated in the product state also. It is, therefore, reasonable to assign most of the entropy change difference between the interactions for native and denatured DNA with 9AA to effects at the binding site.

Concluding remarks

The techniques for determining the characteristics of the binding of 9AA to denatured DNA are the same as those described in Chapter IV of this work. Denatured DNA in 0.1M NaCl exists in a variety of conformations which are temperature dependent and which manifest themselves in heterogeneity of binding sites at room temperature. This heterogeneity has been observed as a lack of internal linearity in a set of spectra of the bound 9AA. The heterogeneity is reduced at higher temperatures and internal linearity is substantially restored. This has been interpreted as a change in the structure of denatured DNA caused by a loss of short range helical order which is present at low temperatures and its replacement by temperature dependent, single strand, base-stacking which is present throughout the temperature range studied. In the region of temperature where internal linearity of spectra is obtained the interaction of 9AA with denatured DNA can be considered as a single

equilibrium and the parameters defining the system can be measured accordingly.

Binding curves for the interaction have been obtained at a number of temperatures. The extinction coefficient of the bound species, ϵ_b , has been shown to vary greatly with temperature: a result consistent with the changing binding site associated with the temperature dependent conformation of denatured DNA. The intrinsic association constant, as expected from the above comments, is also substantially more temperature dependent than for 9AA and native DNA.

The number of binding sites varies with temperature, unlike in the interaction between 9AA and native DNA. This has been interpreted as a progressive shift with increasing temperature from single strand, base-stacked regions of the macromolecule to random coil regions. The random coil regions do not bind 9AA significantly. An apparently anomalous value of n at room temperature has been satisfactorily explained in terms of the denatured DNA structure at that temperature.

Finally, the thermodynamic parameters measured for the interaction are in agreement with the above model for the interaction. The enthalpy of reaction (ΔH°) is large and negative which demonstrates, as with native DNA, the importance of bonding interactions. The entropy term (ΔS°) is large and negative and is consistent with a model in which intercalation of the 9AA cation between adjacent bases which are in a single strand, base-stacked conformation serves to constrain the relative motion of the bases as the free energy of the system is reduced on interaction.

REFERENCES

1. Liersch, M. and Hartmann, G., *Biochem. Z.*, 343, 16 (1961).
2. Drummond, D.S., Simpson-Gildemeister, V.F.W. and Peacocke, A.R.,
Biopolymers, 3, 135 (1965).
3. Dalgleish, D.G., Fujita, H. and Peacocke, A.R., *Biopolymers*,
8, 633 (1969).
4. Sansom, L.N., Ph.D. Thesis, University of Adelaide, 1972.
5. Ichimura, S. et al, *Biochim. Biophys. Acta*, 190, 116 (1969).
6. Blake, A. and Peacocke, A.R., *Biopolymers*, 5, 383 (1967).
7. Chambron, J., Daune, M. and Sadron, C., *Biochim. Biophys. Acta*,
123, 319 (1966).
8. Kleinwachter, V., Balcarova, Z. and Bohacek, J., *Biochim. Biophys.*
Acta, 174, 188 (1969).
9. Walker, I.O., *Biochim. Biophys. Acta*, 109, 585 (1965).
10. Studier, F.W., *J. Mol. Biol.*, 41, 189 (1969).
11. Pritchard, N.J., Blake, A. and Peacocke, A.R., *Nature*, 212, 1360
(1966).
12. Lerman, L.S., *J. Mol. Biol.*, 3, 18 (1961).
13. Armstrong, R.W., Kurucsev, T. and Strauss, U.P., *J. Amer. Chem. Soc.*,
92, 3174 (1970).

CHAPTER VI

A temperature-jump study of the interaction of 9-aminoacridine
with native and denatured DNA

CONTENTS

Page

Part A - The temperature-jump technique

1.	Introduction	112
2.	The temperature-jump method	
	(a) Theoretical aspects	113
	(b) Apparatus	116
	(c) Calibration of the temperature rise	118
3.	Preparation of solutions	120
4.	Analysis of relaxation times	120
	(a) Single relaxation	121
	(b) Two discrete relaxations	122

Part B - 9-aminoacridine and native DNA

5.	A temperature-jump study of 9AA and native DNA solutions	
	(a) Preparation of solutions	125
	(b) Experimental	126
	(c) Results	126
	(d) Discussion	132

Part C - 9-aminoacridine and denatured DNA

6.	A temperature-jump study of 9AA and denatured DNA solutions	
(a)	Preparation of solutions	138
(b)	Experimental	139
(c)	Results	139
(i)	Proposed mechanism	142
(ii)	Rapid relaxation - results	147
(iii)	Rapid relaxation - discussion	149
(iv)	Slow relaxation - results	151
(v)	Slow relaxation - discussion	153

Part D - Conclusions

7.	Concluding remarks	156
	References	158

PART A - THE TEMPERATURE-JUMP TECHNIQUE1. Introduction

In Chapters IV and V equilibrium measurements of the interaction of 9AA with native and denatured DNA were made. These results, however, give no insight into the rate processes which establish the equilibria studied. The reaction between aminoacridines and DNA goes to completion very rapidly. Any study of the kinetics of the interaction, which can be expected to give valuable insight into the mechanisms involved, must therefore utilize techniques which have resolution times shorter than the processes establishing equilibrium. Over the last twenty years a number of techniques have been developed which enable studies of rapid reactions to be carried out. Two such methods, each representative of a different class of technique, have been used to study the interaction of various aminoacridines with DNA. These are the stopped flow method¹, typical of a rapid mixing technique and the temperature-jump method², typical of a perturbation technique. This latter method has been used to study the interaction of 9AA with native and denatured DNA.

Perturbation techniques are more suited to studies of the interaction of aminoacridines with DNA than are mixing techniques because it is usually possible to choose an experimental situation in which the resolution time of the apparatus is substantially shorter than the processes being observed.

There are many extensive treatments of the theoretical and practical aspects of perturbation techniques in the literature³⁻⁶. In this Chapter, therefore, only a brief résumé of the technique has been given. However, full details particular to the apparatus and systems used in the work described are provided.

2. The temperature-jump method

(a) Theoretical aspects

As the name of this perturbation method implies the technique uses a heating pulse to perturb a chemical reaction at equilibrium. A reaction at equilibrium at an initial temperature heated to a different temperature is in a metastable state and will undergo a chemical relaxation to the new equilibrium at the new temperature. If the chemical relaxation is slower than the heating pulse which caused it then the relaxation process may be followed and information gained on the rate processes which establish equilibrium. Chemical relaxations arising from small perturbations from equilibrium obey linear first order differential equations, the solutions of which are linear combinations of exponential functions. Each exponential function has an associated relaxation time, the inverse of which is related directly to the rate constants of the processes establishing the equilibrium.

The technique has wide applicability as all reactions with a non zero enthalpy of reaction will have a temperature dependent equilibrium constant. Even those reactions which do have a zero enthalpy term can usually be coupled to another temperature dependent equilibrium.

Temperature perturbations in solution can be readily achieved by Joule heating caused by the discharge of energy stored in a high voltage capacitor to earth through a small element of solution. Clearly, the solution must be electrically conducting. The temperature change of the solution, at constant pressure, can be calculated in the following way⁷. The voltage at time t across the circuit resistance, R (assuming negligible inductance) upon discharge of a capacitor of capacitance C , charged to an

initial voltage V_0 is:

$$V_t = V_0 e^{-t/RC} \quad \text{eqn. 6-1.}$$

The energy E dissipated through resistive heating in time dt is:

$$dE = \frac{V_t^2}{R} dt \quad \text{eqn. 6-2.}$$

thus the temperature rise ΔT after time t is:

$$\Delta T(t) = \int_0^t \frac{V_0^2}{c_p R} e^{-2t/RC} dt \quad \text{eqn. 6-3.}$$

for unit mass, where c_p is the heat capacity of the solution at constant pressure.

If the volume of solution heated is V and the density of solution is ρ then equation 6-3. becomes:

$$\Delta T(t) = \int_0^t \frac{V_0^2}{V \rho c_p R} e^{-2t/RC} dt \quad \text{eqn. 6-4.}$$

thus the "time constant" for the temperature rise is $\frac{RC}{2}$ and the total temperature rise, at sufficiently long times is:

$$\Delta T(\infty) = \frac{1}{2} \frac{c V_0^2}{V \rho c_p} \quad \text{eqn. 6-5.}$$

where variations in R and c_p with temperature have been neglected. It is useful in designing experiments to know the "rise time" of the heating pulse, that is the time for the heating pulse to be virtually complete. If an arbitrary level of 90% of total temperature rise is called the rise time then it can be readily shown that this is approximately equal to $1.3 RC$ for an aperiodic discharge. Alternatively, this may be verified experimentally by using an indicator equilibrium with a very short relaxation time compared to that of the discharge.

At almost all temperatures for aqueous solutions an increase in temperature will be associated with a change in volume. Changes in volume are propagated at approximately the speed of sound and in a small volume sample there can be large increases in pressure associated with a shock wave if the temperature rise is more rapid than the inertial response of the solution. Reflection of such a shock wave at the walls of a cell containing a solution causes cavitation in the solution which disrupts measurement of chemical relaxations. There is thus a lower limit to the rise time of the system that can be practically used which is set by the experimental conditions as well as the RC time of the apparatus. In general, cavitation is minimized by small temperature changes, adequate RC times of the circuitry, and by working at maximum density of solution.

Finally, it is clearly necessary in order to measure chemical relaxations to have a quantity which is accessible for measurement and which is either directly or indirectly coupled to the equilibrium of interest. In the work described in this Chapter the 9AA chromophore may be conveniently studied by spectrophotometry as the extinction coefficients of the forms of 9AA at equilibrium differ. Thus a change in absorbance of the

9AA with time is a direct measure of a concurrent shift in the equilibrium.

(b) Apparatus

The temperature-jump apparatus is described briefly here rather than in Chapter VIII (Materials and Methods) because the theory and practice of the temperature-jump technique are closely interwoven.

The temperature-jump apparatus used is similar to that described by Eigen and De Maeyer³. A block diagram of the apparatus is shown in Figure 6-1. The apparatus may be conveniently described by dividing it into three sections; the heating circuit, the detection circuit, and the sample cell.

The heating circuit

Rapid heating is achieved by the manual discharge of a high voltage, low inductance capacitance (0.1 μF) charged by a Brandenburg M50/R High Voltage Generator through a 500 $\text{M}\Omega$ resistor. The discharge occurs when a spark gap is manually closed. The current is carried by a short coaxial cable to the cell and thence through the solution to earth. The sample solution serves as the discharge resistance. Aluminium and iron shielding are used to minimize electric and magnetic interference of the spark with other electronic equipment.

The detection circuit

Changes in the absorbance of a solution are detected by an optical bench assembly consisting of a lamp, monochromator, sample cell and photomultiplier. The lamp used is a Phillips type 7023, 100W., quartz-iodide lamp securely mounted to the optical

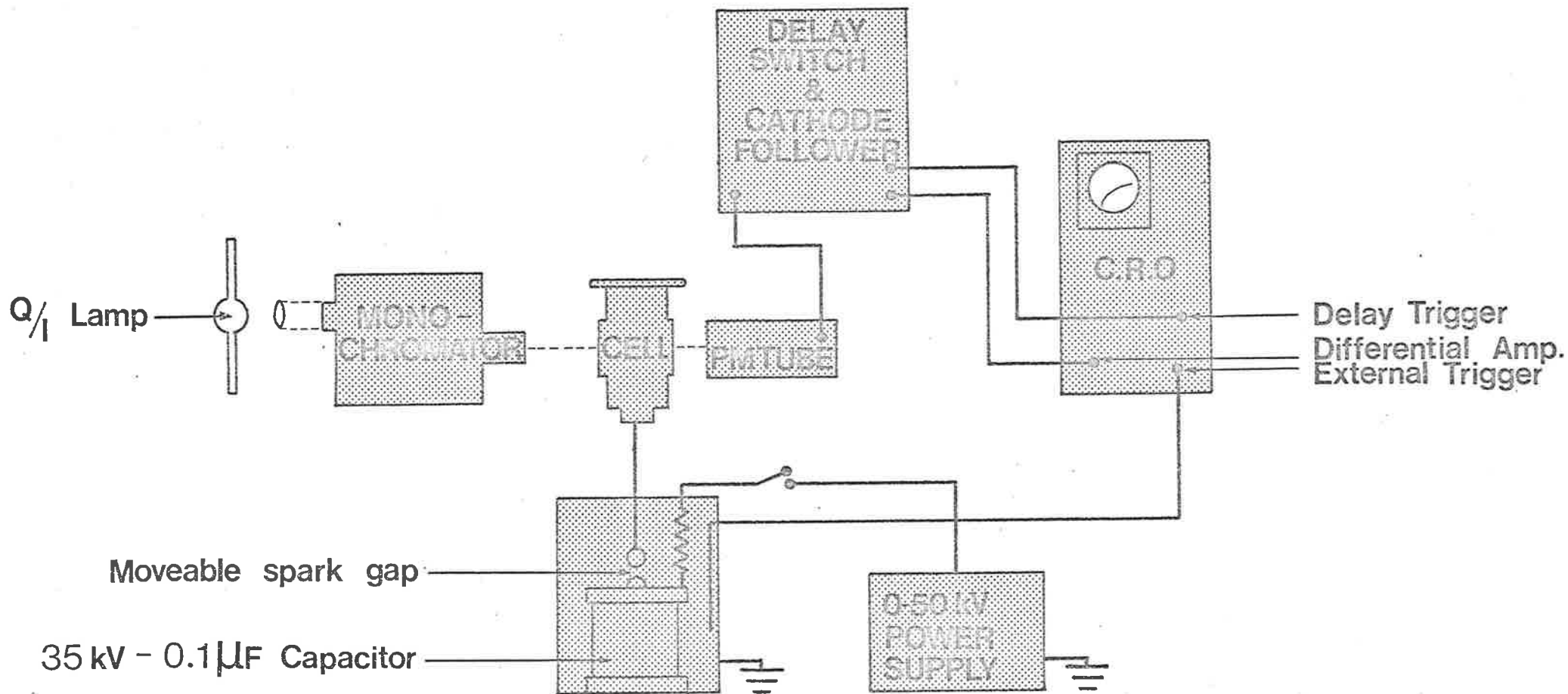


Fig. 6-1. Schematic representation of the temperature-jump apparatus.

bench with free floating leads to the power supply. Light from the lamp passes through a Bausch and Lomb High Intensity Grating Monochromator, (1350 grooves/mm) with entrance and exit slits to minimize the passage of stray light, to the sample cell. The transmitted light is detected by a photomultiplier, type EMI 6256/B, powered from a Nuclear Enterprises Ltd. type NE 5307 E.H.T. supply. Photomultiplier dynode accelerating voltages have been kept low and some photomultiplier stages have been shorted to the anode to reduce the gain while maintaining a high light intensity without saturating the photomultiplier. In this configuration the signal to noise ratio is optimized³. The output potential of the photomultiplier (the signal) is fed into a cathode follower used to improve the rise time of the connecting circuitry. The signal is then fed into a delay switching device which is capable of grounding out an initial portion of the signal to enable amplification of the final portion. This device is similar to one described elsewhere⁸. The modified or unmodified signal is then fed by coaxial cable into the high gain differential amplifier of a Tektronix Storage Oscilloscope, type 549 with a type 1A7A time base. The oscilloscope is triggered to record the signal (if necessary after a delay prescribed) by an unshielded wire antenna connecting the oscilloscope external trigger to the inside of the capacitor discharge box. The resulting oscilloscope trace is recorded on Polaroid P/N55 film mounted in a Tektronix Oscilloscope Camera type C-12.

Sample cell

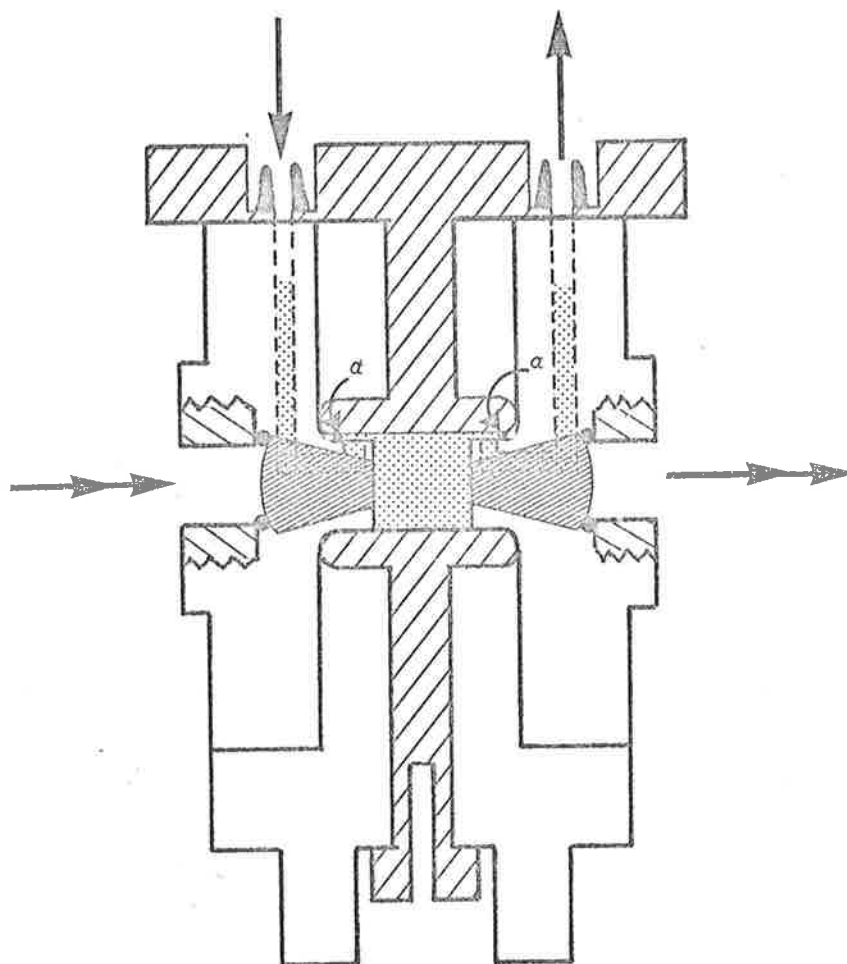
A cell for holding the sample solution has been designed for use at elevated temperatures. The cell is similar in design to those described by Blagrove⁹ with some modifications. A

schematic diagram of the cell is shown in Fig. 6-2. The body of the cell is made of polycarbonate (machining characteristics of this polymer are given in Chapter VIII section 5.) which has a higher resistance to temperature than the more commonly used perspex which has been found to craze with prolonged exposure to heat at 65°C. Polycarbonate also has a much higher heat distortion temperature (135°C) than perspex (66°C). The cell is filled through injection ports in the top of the cell. A steady flow of solution through the cell will remove small bubbles which tend to collect in the corners of the sample space and disrupt spectrophotometric measurements. The total volume of solution needed is only slightly more than 0.5 cm³. If sufficient solution is left in the injection ports no air leaks into the cell after temperature perturbations. Some previously designed cells have suffered from this disadvantage. The cell and solution are thermostated in a housing in the apparatus. It has been possible to maintain the temperature of solutions to within 0.04°C of the desired temperature by pumping water at a fast rate through the thermostating jacket from a large thermostated reservoir. As the volume of the solution in the cell is quite small, re-equilibration following a temperature perturbation is essentially complete within five minutes: the thermal sink of the cell electrodes assisting in the re-equilibration.

(c) Calibration of the temperature rise

As indicated by equation 6-5. the temperature rise of a perturbed solution is proportional to V_0^2 . This fact may be exploited to calibrate the temperature rise associated with a given perturbation for a particular cell and ionic strength of solution without explicitly determining the volume heated (V) or either

Fig. 6-2. Schematic representation of the small volume, polycarbonate, temperature-jump cell.



Polycarbonate 

Steel 

Silica 


Syringe inlet and outlet 

Light 

 Solution

 Kel F

 Rubber

 Hole drilled in body of Polycarbonate

 Nylon gaskets (dia < 0.001")

the density (ρ) or the specific heat of solution (c_p).

A solution of phenol red in tris buffer at pH 7.4 is prepared¹⁰. The variation of absorbance (ΔA) of this solution with temperature is then obtained in a spectrophotometer with a thermostated cell housing. This variation may then be directly compared with the variation in voltage output of the photomultiplier when a sample of solution is perturbed by temperature jumps obtained at differing discharge voltages. This is so because for small changes (δV) in photomultiplier output (V):

$$\Delta A = \log \frac{I_O}{I_{T_2}} - \log \frac{I_O}{I_{T_1}} = \log \frac{I_{T_1}}{I_{T_2}} \quad \text{eqn. 6-6.}$$

now, as $I \propto V$,

$$\log \frac{I_{T_1}}{I_{T_2}} = \log \frac{V_{T_2} + \delta V}{V_{T_2}} = \log \left(1 + \frac{\delta V}{V_{T_2}} \right) \approx \frac{\delta V}{2.303 V_{T_2}} \quad \text{eqn. 6-7.}$$

where I_O , I_{T_1} , and I_{T_2} refer to, respectively, incident light on the solution sample, the transmitted light at initial temperature (T_1) and the transmitted light at the final temperature (T_2). If the initial temperature is known and all temperatures reached are within the range covered by spectrophotometry, then it is possible to produce a plot of temperature rise versus V_O^2 . The capacitor is reproducibly charged for 250 seconds (that is, 5RC times of the charging circuit). For the cell shown in Fig. 6-2. the temperature rise for applied E.H.T. is shown in Fig. 6-3.

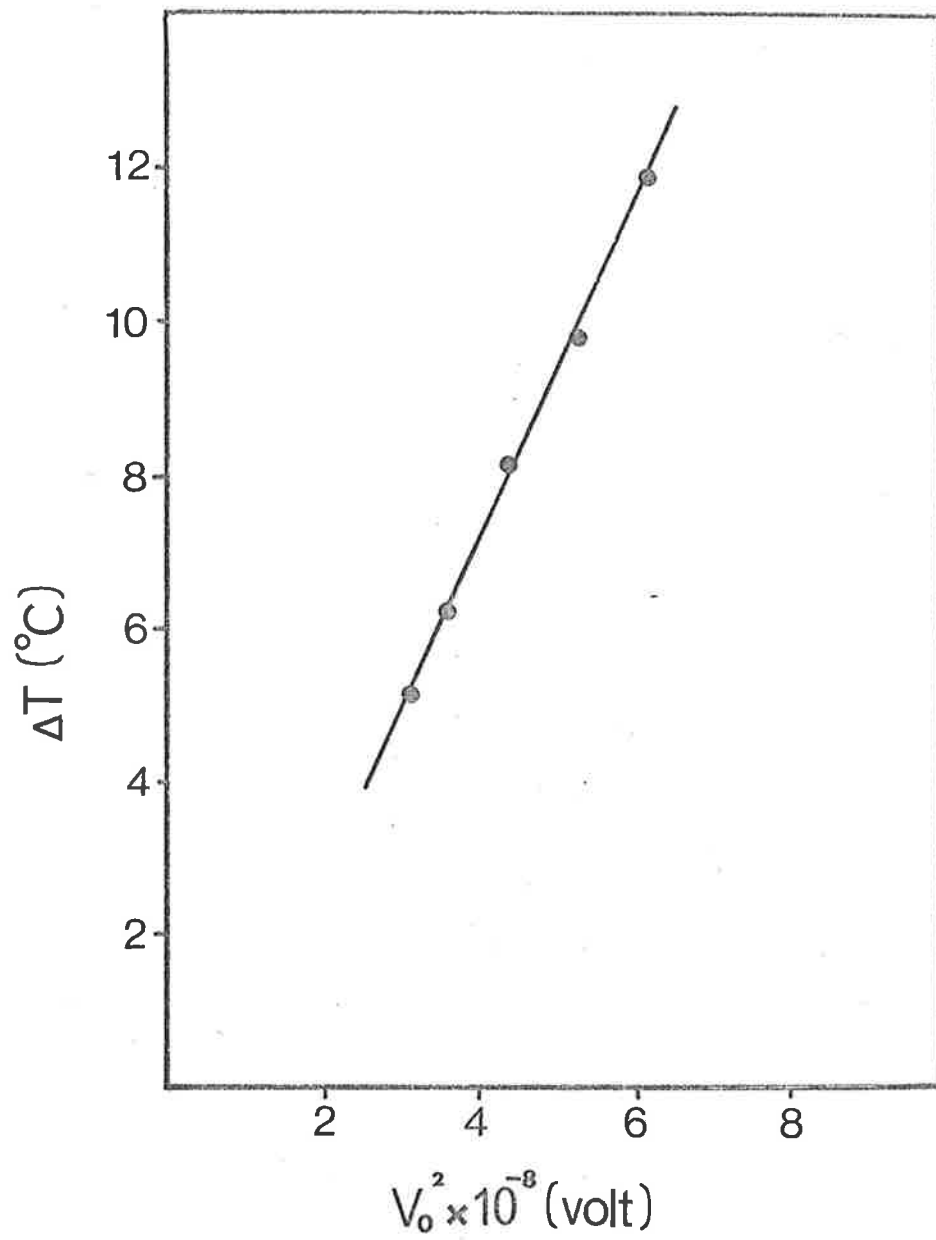


Fig. 6-3. The variation in temperature rise of solutions contained in the cell depicted in Fig. 6-2. with the second power of applied EHT.

3. Preparation of solutions

As it is necessary to study the variation of relaxation times with the concentrations of reactants at equilibrium it has been found convenient to prepare solutions of 9AA and DNA and store them frozen until required. Frozen storage of solutions has been found to have no effect on their absorbance or on their melting profiles when thawed. All solutions have been prepared by the addition, by weight, of quantities of 9AA solution, DNA solution and neutral salt as required. This is mentioned in more detail in the relevant sections for native and denatured DNA. Prior to introduction into the temperature-jump cell the solutions are thawed in an evacuated container which is also the container in which they have been stored frozen. This "freeze-pump-thawing" technique effectively degasses the solution. Solutions in the temperature-jump apparatus must be degassed otherwise perturbation induces the formation of microfine bubbles in the solution which interfere with optical measurements and can disrupt even heating of the solution by residing on electrode surfaces. Solutions are then introduced into the sample cell by syringe. The cell is mounted in the apparatus and thermostated as described in the previous section.

Repeated temperature-jump perturbations are not observed to have any measurable effect on the melting profile of 9AA-DNA solutions when compared with identical solutions which have not been perturbed.

4. Analysis of relaxations times

In the course of experiments described in this Chapter two types of chemical relaxation have been observed. There is a chemical relaxation involving only a single relaxation time and

a relaxation which can be fully described in terms of two, discrete relaxation times.

(a) Single relaxation

It has already been demonstrated in equations 6-6. and 6-7. that there is a simple relationship between the change in photomultiplier voltage and the change in absorbance of the solution which caused it. Thus the change in photomultiplier voltage may be taken as a direct measure of the change in absorbance of solution which is, in turn, a measure of the shift in equilibrium caused by the heating pulse (perturbation).

In experiments yielding a single relaxation the relaxation time (τ) may be described by the expression:

$$\Delta V_t = \Delta V_0 e^{-t/\tau} \quad \text{eqn. 6-8.}$$

where ΔV_t is the change in photomultiplier voltage from its rest position ($V_{t=0}$) at time t after the initiation of perturbation,

and ΔV_0 is the total change in photomultiplier voltage, that is, $(V_{t=0} - V_{t=\infty})$. $V_{t=\infty}$ must be assessed during the period of stable elevated temperature, up to approximately one second after the initiation of perturbation. This instability of temperature after about one second does limit the apparatus to the study of reactions which go to completion within this time.

It is usual to assess ΔV_0 directly from the photographic record and this is readily achieved if the signal is measured over a period of at least 5τ . Thus a plot of $\ln \Delta V_t$ versus t will give a straight line of slope $-(\tau)^{-1}$ and intercept ΔV_0 when $t = 0$.

An example of this plot is shown in Figure 6-4.

The slopes of plots produced in this way have been determined by a Least Squares analysis of the most linear portion of the graph. In very rapid relaxations some initial points have been discarded where the heating time of the cell, being incomplete, has reduced the observed response. Also points beyond 90% completion of the relaxation have been discarded as these are associated with an increasingly large percentage error as ΔV_t approaches the level of noise in the experimental record.

(b) Two discrete relaxations

In experiments where two discrete relaxations have been observed and the relaxation times are separated by at least an order of magnitude, a different method for evaluating the τ values has been used.

For two relaxations, the output of the photomultiplier will vary in the following way, analogous to equation 6-8.

$$\Delta V_t = \Delta V_o^f e^{-t/\tau_f} + \Delta V_o^s e^{-t/\tau_s} \quad \text{eqn. 6-9.}$$

Where the parameters have the same meaning as before and where the superscripts and subscripts f and s refer, respectively, to the faster and slower relaxations observed.

The principal difficulty arises in attempting to determine $(\Delta V_o^f + \Delta V_o^s)$ while still retaining a suitable scale for measuring the faster relaxation. A plot of $\ln V_t$ versus time can be made if the observation is continued for about $5\tau_s$ and from this plot it is possible to evaluate $(\tau_s)^{-1}$ from the limiting slope of the plot at long times, where the faster relaxation is complete. By subtraction of $\Delta V_o^s e^{-t/\tau_s}$ from ΔV_t and replotting

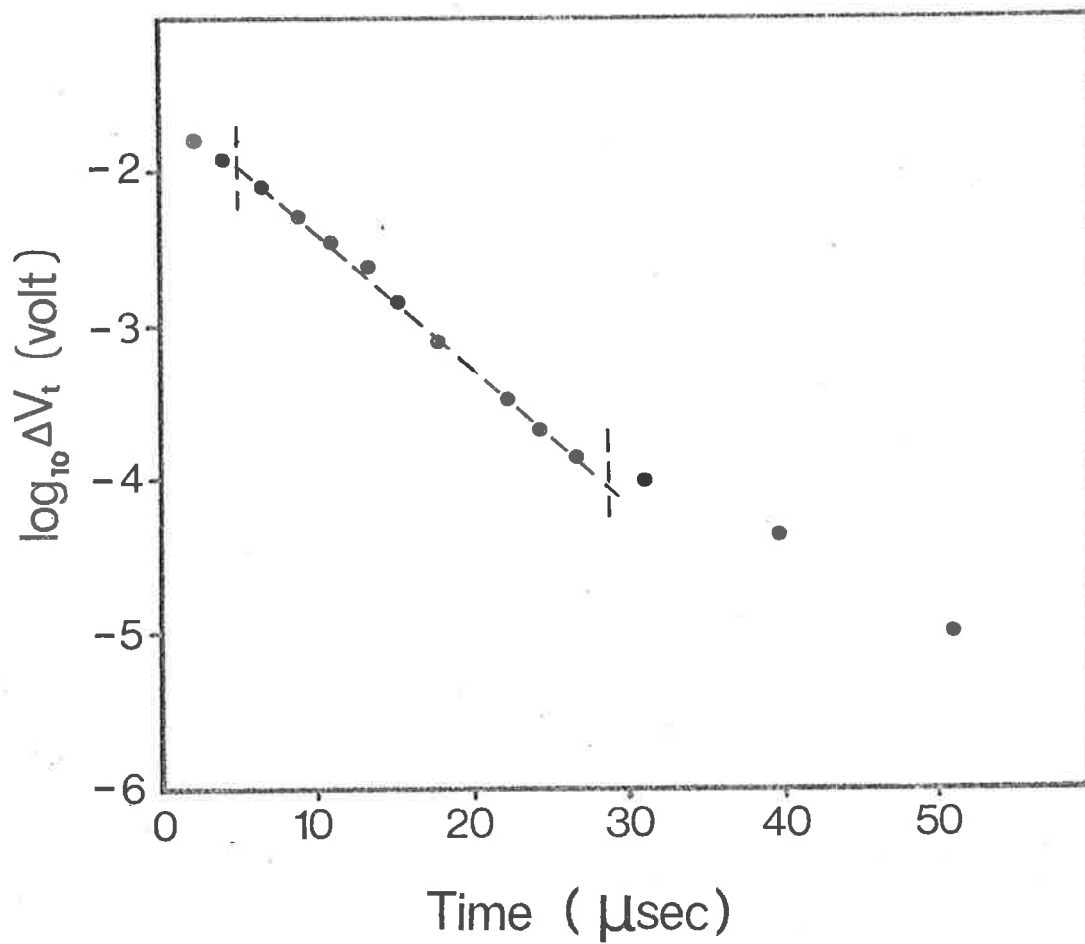


Fig. 6-4. A semi-log plot of photomultiplier voltage output versus time for a single chemical relaxation process. The slope of the linear portion of the plot is the negative of the inverse relaxation time ($-\tau^{-1}$) for the relaxation.

it is possible to evaluate the parameters ΔV_o^f and $-(\tau_f)^{-1}$. However, this method is laborious, requires some degree of subjectivity in estimating the region dominated by the slow relaxation and in general leads to large errors in the determinations of $(\tau_f)^{-1}$.^{2,11}

For this reason, in this work, a different method has been used. The parameters in equation 6-9. have been fitted to the experimental results by means of a non-linear fitting program (NONLIN)¹². A large number of experimental points is measured from each photographic record of a chemical relaxation: typically between 60 and 100. Measurement has been facilitated by using a projected image of the photograph in an OSCAR F/DCF Strip Chart and Film Digitizing System. This System is a manually operated X-Y plotter which furnishes a resistance output proportional to calibrated amplitudes. The analog information is converted to digital values and given as an automatic readout to an IBM Card Punch.

By using program NONLIN on data collected it has been possible to fit the four parameters, ΔV_o^f , τ_f , ΔV_o^s and τ_s , concurrently to the data presented from each photograph. Furthermore, by a suitable choice of time scale in the photographs of the signal arising from a perturbation, each of the relaxations can be measured in isolation if only those regions where each of the relaxations predominates is measured. In measuring the slow relaxation in isolation the grounding switch described in section 2 (b). of this Chapter has been used to "short out" the large initial relaxation and permit amplification of the slower and smaller amplitude relaxation.

The results obtained from program NONLIN provide good correlations between the τ values derived from the fitting of both relaxations simultaneously and independently to appropriate photographs.

The experimental accuracy of the fitted parameters is difficult to assess. Program NONLIN does provide a measure of the reliability of fit; but this refers only to the record of a single event (the signal) which does, itself, have errors associated with experimental variables. In these circumstances the best measure of accuracy is the reproducibility of results. For this reason in the work described measurements have usually been taken for a number of photographic records of perturbations at each experimental concentration and temperature.

PART B - 9-AMINOACRIDINE AND NATIVE DNA5. A temperature-jump study of 9AA and native DNA solutions(a) Preparation of solutions

All solutions have been made up in 0.1M NaCl. A stock solution of 9AA/native DNA has been prepared by the slow addition, with gentle stirring, of a 9AA solution of accurately known concentration to a native DNA solution of a known concentration. Rapid addition of 9AA to DNA solutions sometimes causes precipitation of a complex. All solutions have been weighed and it is therefore possible to determine the concentration of 9AA (T_L) and DNA (T_A) in the stock solution.

As discussed in Chapter IV some of the 9AA will exist in solution at equilibrium as the free cation (\bar{c}_{9AA}). With an experimentally determined Langmuir Isotherm at the appropriate temperature and a knowledge of $\frac{T_L}{T_A}$ and either T_L or T_A , it is possible to calculate the extent of binding, r , in the stock solution. The extent of binding, r , is the number of 9AA cations bound per nucleotide phosphorous. Once r is known it is possible to obtain the value of \bar{c}_{9AA} , as:

$$\bar{c}_{9AA} = T_L - rT_A \quad \text{eqn. 6-10. (}\equiv \text{eqn. 4-9.)}$$

or

$$\frac{T_L}{T_A} = \frac{\bar{c}_{9AA}}{T_A} + r \quad \text{eqn. 6-11.}$$

Thus there will be a unique value of \bar{c}_{9AA} and r on the Langmuir Isotherm at which eqn. 6-11. is satisfied for the stock solution.

If the stock solution is now diluted by a solution of 9AA at concentration \bar{c}_{9AA} present in the stock solution then r will remain constant in the diluted fraction. Langmuir Isotherms generated from the experiments described in Chapter IV have been obtained at 45°C , 55°C and 65°C and together with the known concentrations of 9AA and DNA in the stock solutions have been used to prepare, in the manner described above, a series of solutions of known concentration of DNA and 9AA which have a constant r when at the required temperature. Dilution of the stock solution of 9AA and native DNA by neutral salt alone would have produced a series of solutions of decreasing r with increasing dilution. This may have presented problems in the interpretation of results obtained from the temperature-jump experiments if the values of r for the solutions perturbed were to have fallen outside the observably linear portion of the experimentally obtained Scatchard plots.

(b) Experimental

The solutions prepared as in section 5 (a). have been degassed, introduced into the temperature-jump cell and thermostated at the required temperature, as outlined in section 3. of this Chapter. Solutions have been perturbed by a discharge which produces a 10°C temperature-jump, with final equilibrium temperatures of 45°C , 55°C and 65°C . Photographs of oscilloscope traces which record the signals of the photomultiplier responses resulting from absorbance changes on heating have been measured as described in section 4. of this Chapter.

(c) Results

The measurement of the concentration dependence of discrete relaxations may give, for simple systems, unambiguous information

on rate constants and reaction mechanisms³. The concentrations which must be known are the concentrations of reactants at equilibrium. For 9AA and native DNA these are, respectively, the free 9AA concentration (\bar{c}_{9AA}) and the number of free binding sites (\bar{c}_{DNA}). While the former of these is readily determined, as discussed in section 5 (a)., the latter needs to be discussed further.

It has been shown in Chapter IV that the binding of 9AA to native DNA is of an anti-cooperative nature. Thus, while the limit of complex I binding is not reached until an r value of $r \approx 0.25$, the free energy change associated with the binding is substantially reduced at r values well below $r = 0.25$. Those binding sites which behave as isolated sites with a free energy of binding (or intrinsic association constant) independent of r are restricted to the initial linear fraction of the Scatchard plot (see Figure 4-14.). The extrapolation of this linear portion of the Scatchard plot to the r axis gives a value of n associated with the form of binding described by the equilibrium:



where the concentrations of reactants are:

$$\text{free 9AA} = \bar{c}_{9AA}$$

$$\text{free isolated binding site} = (n - r) T_A \quad \text{eqns. 6-13.}$$

$$\text{complex I} = r T_A$$

Hence the equilibrium concentration of binding sites, \bar{c}_{DNA} , is:

$$\bar{c}_{\text{DNA}} = (n - r)T_A \quad \text{eqn. 6-14.}$$

for a solution, with extent of binding r , within the initial linear portion of the Scatchard plot, and of total DNA concentration T_A ; and where n is the limiting value of the linear portion of the Scatchard plot at the appropriate temperature (Table 4-3.).

In previous papers^{2,13,14} Crothers and co-workers have avoided defining n by nominating the number of potential binding sites per nucleotide phosphorous residue as unity. This requires that a new equilibrium constant be defined which is some (unknown) fraction of the true value. In a similar way equilibrium measurements may be redefined. This method has been adopted elsewhere^{11,15}. While this method does allow for a comparison of equilibrium and kinetic measurements it gives neither a true measure of second order rate constants¹⁴ nor, therefore, the absolute magnitude of equilibrium constants as the standard state of DNA reactant is undefined. Furthermore, thermodynamic measurements determined from the variation of equilibrium constants with temperature become open to doubt if n is a function of temperature; for it must be assumed in order to obtain thermodynamic values by this method that n is invariant with temperature.

Typical oscilloscope records of chemical relaxations following rapid temperature perturbations of 9AA/native DNA equilibria are shown in Fig. 6-5 (a), (b), and (c). On first inspection these appear to indicate a single relaxation response and this has been borne out by an analysis of the variation of the logarithm of the amplitude of the response with time as described in section 4 (a). of this Chapter. This variation is linear

Fig. 6-5. Chemical relaxations of a solution of 9AA and native DNA perturbed by a 10°C temperature rise to a final temperature of 65°C. $r = 0.066$

(a) 20 $\mu\text{sec}/\text{cm}$ (major division, horizontal axis)
100 mV/cm (major division, vertical axis)

(b) 10 $\mu\text{sec}/\text{cm}$
100 mV/cm

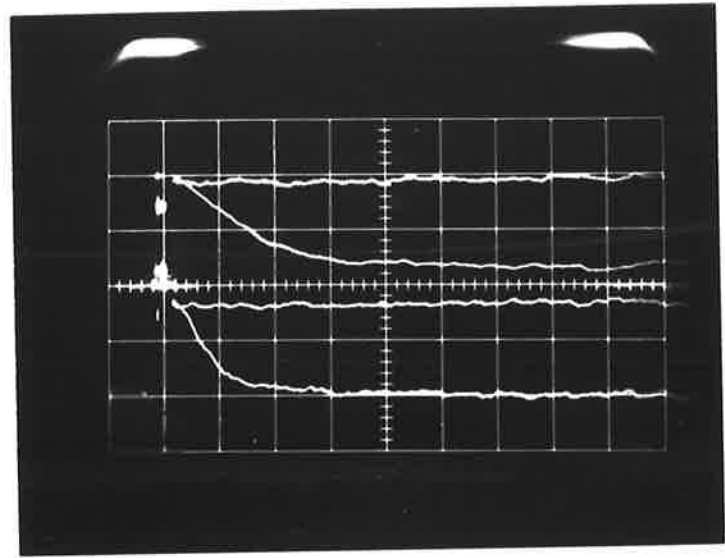
(c) 500 $\mu\text{sec}/\text{cm}$
50 mV/cm

.....

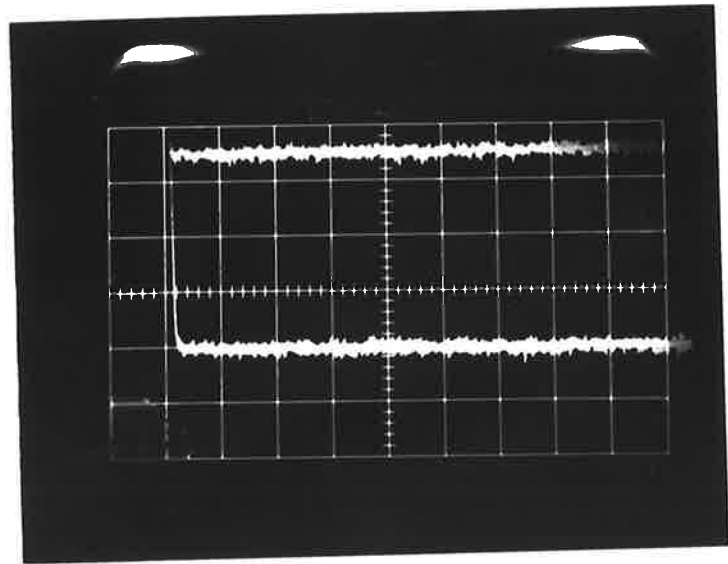
$$[\bar{c}_{\text{DNA}} + \bar{c}_{9\text{AA}}] = 1.26 \times 10^{-4} \text{ M}, \frac{1}{\tau} = 9.1 \times 10^4 \text{ sec}^{-1}$$

a

b



c

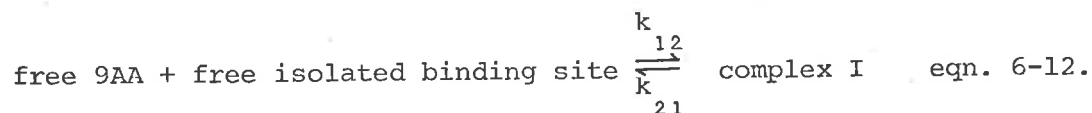


throughout the range of concentrations and temperatures studied. This implies that the relaxation process can be assigned to a single relaxation. The single relaxation has an associated relaxation time (τ). The concentration dependences of the inverse relaxation times (τ)⁻¹ with equilibrium reactant concentration ($\bar{c}_{9AA} + \bar{c}_{DNA}$) are given in Fig. 6-6. for the three temperatures studied. The extent of binding, r , is also given for each temperature; the solutions studied in any particular series of experiments being at constant r as described earlier. Scatchard plots of 9AA and native DNA at these temperatures have been given in Chapter IV and indicate that at the r values used in these temperature-jump experiments the complex is that existing in the simple equilibrium described by equation 6-12.

It has been shown³ that for a single bimolecular process at equilibrium of the type shown in equation 6-12, the relationship between the forward (k_{12}) and backward (k_{21}) rate constants and the inverse relaxation time arising from perturbations of the equilibrium may be described thus:

$$\frac{1}{\tau} = k_{21} + k_{12} (\text{equilibrium reactant concentration}) \quad \text{eqn. 6-15.}$$

Thus in Figure 6-6. the intercept at ($\bar{c}_{DNA} + \bar{c}_{9AA}$) = 0 yields a value of k_{21} and the slope is equal to k_{12} for the reaction.



The values of the kinetic parameters evaluated from data presented in Fig. 6-6. are given in Table 6-1.

Fig. 6-6. Variation of the inverse relaxation time (τ^{-1}) with the concentration of equilibrium reactant for 9AA and native DNA in 0.1 M NaCl.

(●) 45°C : $r = 0.071$, (▲) 55°C : $r = 0.070$,
(■) 65°C : $r = 0.066$.

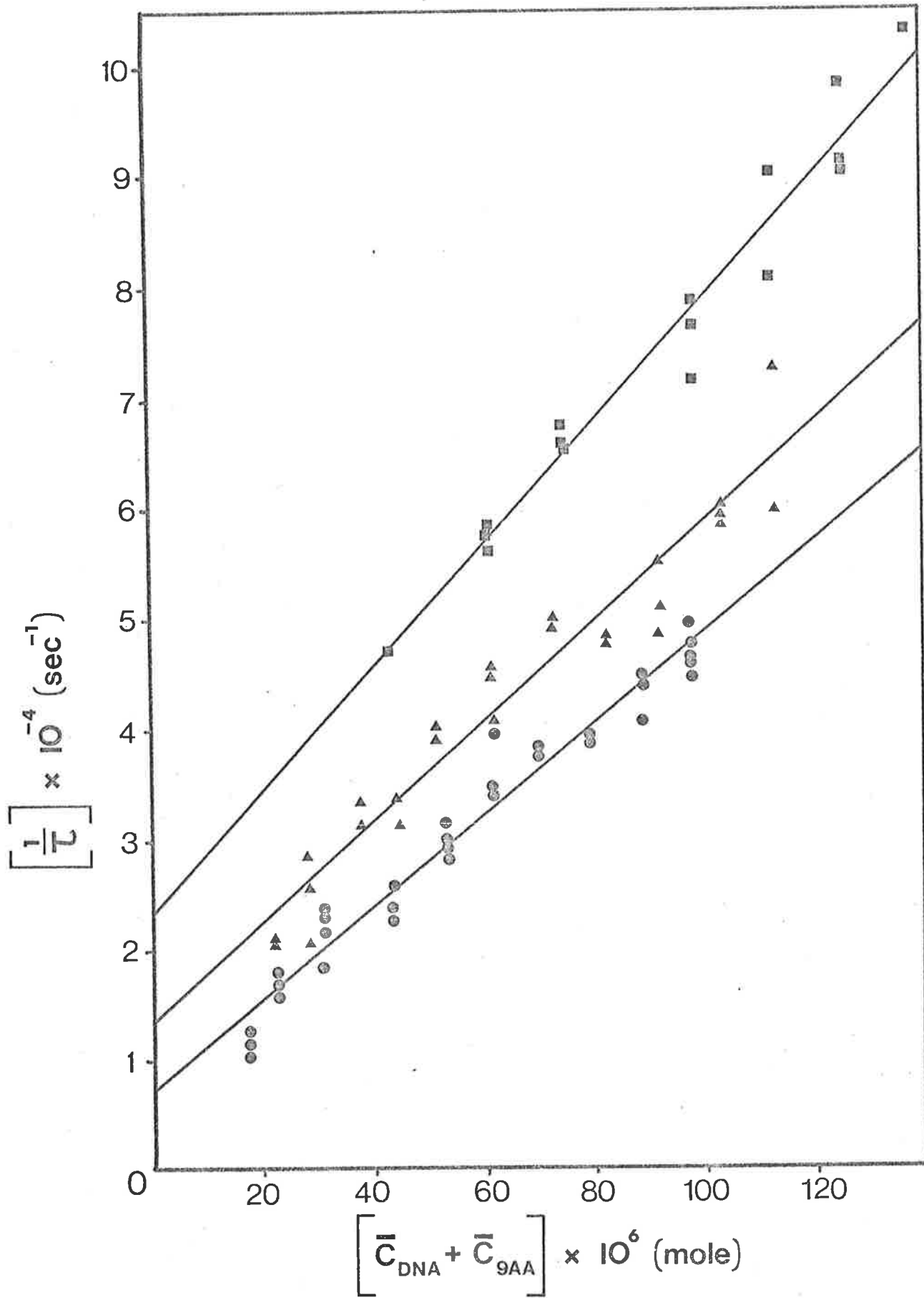


TABLE 6-1

Rate constants for the bimolecular reaction between
9AA and native DNA in 0.1M NaCl.

Temp. (°C)	k_{12} ($M^{-1}sec^{-1}$)	k_{21} (sec^{-1})	k (M^{-1})
45	$4.13(S.E.O.14) \times 10^8$	$7.13(S.E.O.9) \times 10^3$	5.79×10^4
55	$4.49(S.E.O.24) \times 10^8$	$1.34(S.E.O.17) \times 10^4$	3.35×10^4
65	$5.54(S.E.O.29) \times 10^8$	$2.34(S.E.O.28) \times 10^4$	2.37×10^4

The value of the equilibrium constant k (M^{-1}) which is equal to:

$$k = \frac{k_{12}}{k_{21}} \quad \text{eqn. 6-16.}$$

is also given in Table 6-1. The Standard Errors given in the table refer to a Least Squares analysis of the data points only: as described in section 4 (b). There will be a further contribution to errors involved arising from experimental variations. However, additional errors are not very large, at their greatest they are of the same order as those already quoted and do not significantly influence the discussion of results. Therefore, only Standard Errors arising from scatter in results will be considered.

From the variation of equilibrium constants with temperature it is possible to calculate the thermodynamic parameters which define the equilibrium, as described in Chapter IV. The Van't Hoff plot for the determination of the enthalpy of reaction (ΔH°) is shown in Fig. 6-7. The values of ΔH° , together with that of the entropy of reaction (ΔS°) calculated by using equation 4-19. are given in Table 6-2. Table 6-2. also includes the values of the same parameters for the reaction measured by equilibrium techniques (spectrophotometry) described in Chapter IV.

TABLE 6-2

Enthalpy and entropy changes for the reaction of 9AA
with native DNA in 0.1M NaCl

	Temperature-jump method	Equilibrium spectrophotometry
ΔH° (kJ/mole)	-39.7 (S.E.4.2)	-35.2 (S.E.0.8)
ΔS° (J.deg. ⁻¹ mole ⁻¹)	-33.5 (S.E.17)	- 9.6 (S.E.5.0)

A plot of the natural logarithm of a rate constant for a process as a function of inverse temperature ($^\circ\text{K}^{-1}$) yields a straight line with a slope which is equal to $E_{12}^\ddagger = 12.6$ kJ/mole and $E_{21}^\ddagger = 52.3$ kJ/mole. These results are consistent, as is expected, with the enthalpy values given in Table 6-2. as :

$$E_{12}^\ddagger - E_{21}^\ddagger = \Delta U \approx \Delta H^\circ \quad \text{eqn. 6-17.}$$

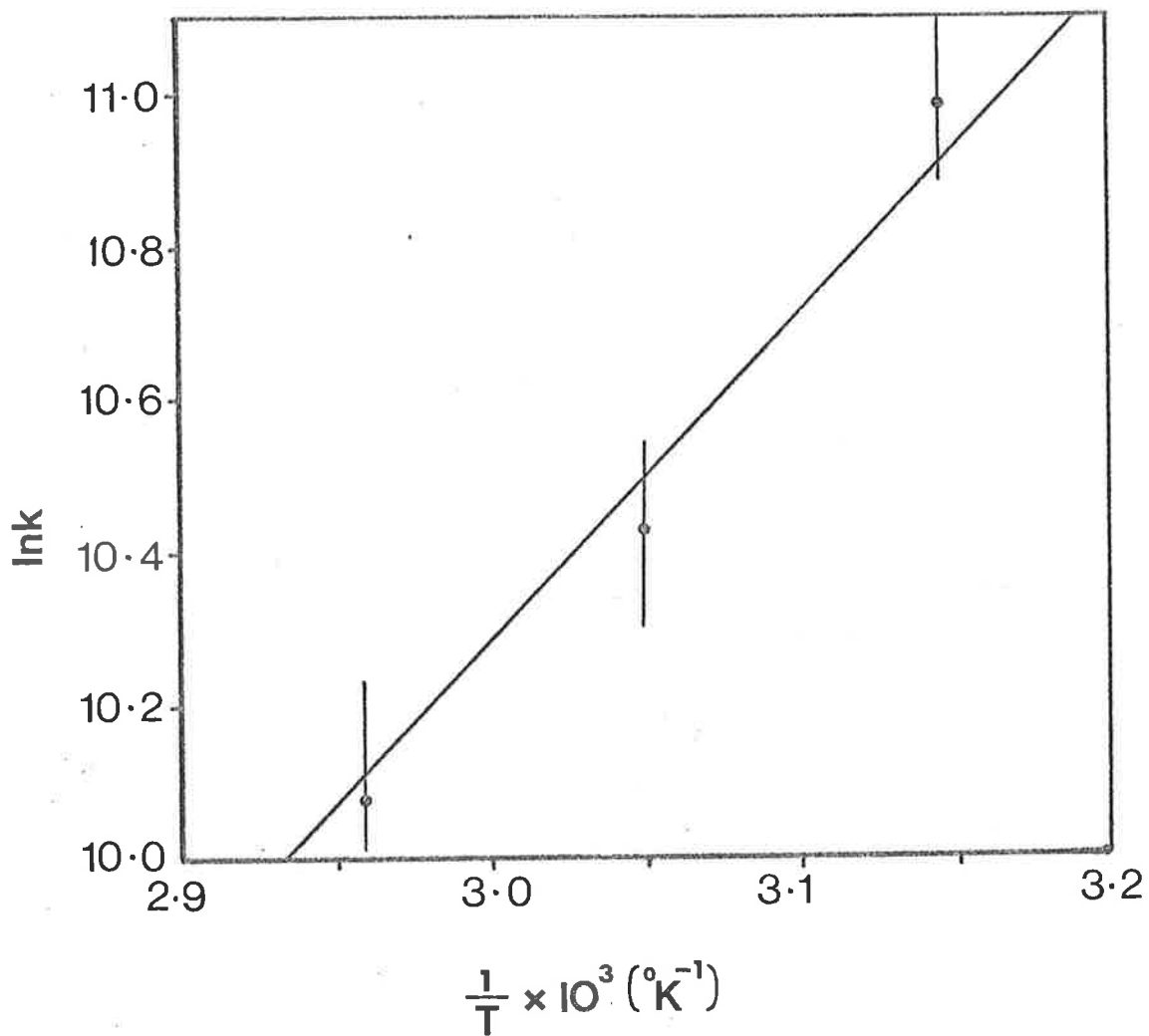
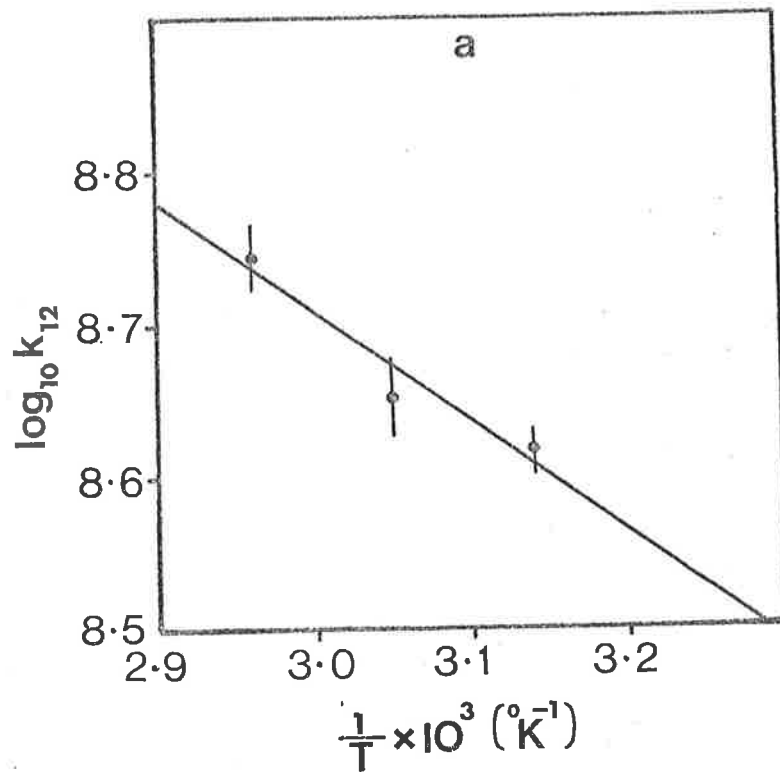
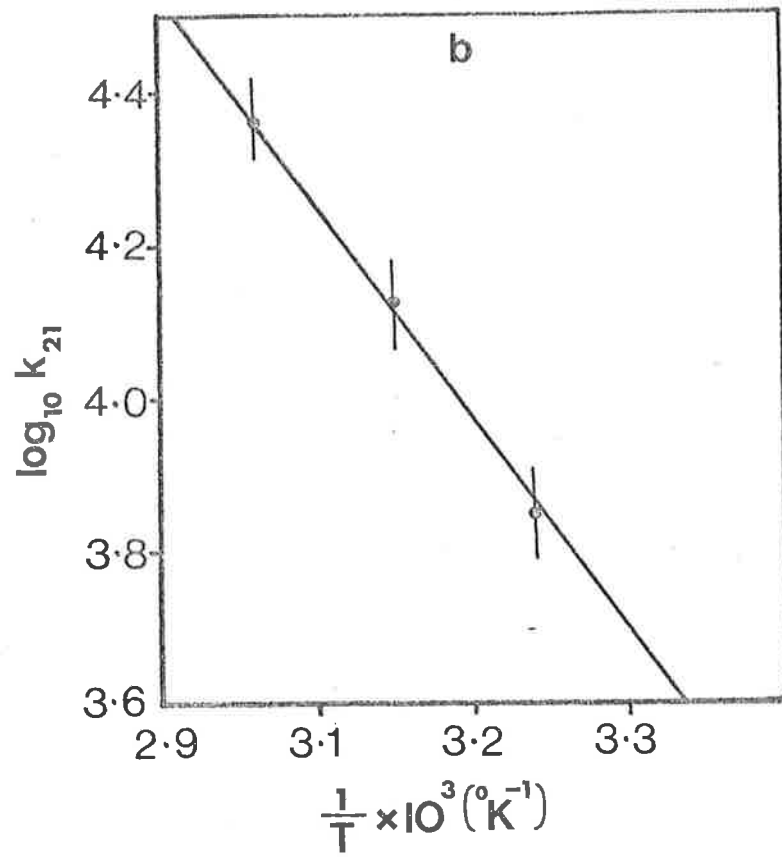


Fig. 6-7. Van't Hoff plot for the interaction of 9AA with native DNA in 0.1M NaCl. Equilibrium constants evaluated from rate constants determined by the temperature-jump method.

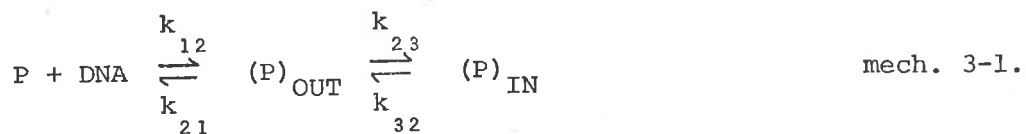
Fig. 6-8. Plots of the logarithm of the rate constants for the forward rate, k_{12} (Fig. 6-8.(a)) and for the backward rate k_{21} (Fig. 6-8.(b)) against the inverse absolute temperature to evaluate the activation energies for each of the processes: 9AA and native DNA in 0.1M NaCl.



for reactions in solution.

(d) Discussion

The observation that the chemical relaxations arising from perturbations of equilibria between 9AA and native DNA can be described by a single relaxation process is in marked contrast to previously published reports on the interaction of proflavine with calf thymus DNA² and polyA-polyU¹³ (reviewed in Chapter III). In these papers^{2,13} two discrete relaxations have been observed and an appropriate two step mechanism proposed (mech. 3-1. - reproduced below).



Mechanism 3-1. has been widely adopted as the general mechanism for intercalation.

More recently, Ramstein et al¹¹, in temperature-jump studies on the interaction of proflavine with M. lysodeikticus^{DNA}, have observed only a single rapid relaxation. Ramstein et al¹¹ have chosen to explain their observations of a single relaxation by suggesting that observed differences between equilibrium constants determined by equilibrium spectrophotometry and the temperature-jump technique are due to the presence of another, unresolvably small, relaxation corresponding to the slow step in mechanism 3-1. In this way it is possible to generate an equilibrium constant for the unresolvable slower step as Li and Crothers² have shown that the relationship between the equilibrium constants is:

$$K(\text{spectrophotometry}) = K_{12} (1 + K_{23}) \quad \text{eqn. 6-18.}$$

where the Ks are equilibrium constants such that:

$$K \equiv k \text{ (intrinsic association constant)}$$

$$K_{12} = \frac{k_{12}}{k_{21}} \quad \text{eqns. 6-19.}$$

$$K_{23} = \frac{k_{23}}{k_{32}}$$

where the rate constants refer to those in mechanism 3-1.

However, the equilibrium constant, K_{23} , generated in this way is very small, $K_{23} \approx 0.25$ in reference 11. This implies that the majority of the bound proflavine exists in what Ramstein *et al*¹¹ have called the "outside" bound species. At the r values used in these experiments¹¹ this outside bound species cannot be the electrostatically bound complex II of mechanism 3-1., as it has been well characterized that almost all the proflavine bound at low r is intercalated. Ramstein *et al*¹¹ have indicated that the "outside" bound form may be another intercalated form of the proflavine. They have further suggested that this quasi-intercalated form of proflavine may be base specific as it is apparent in *M. lysodeikticus* $\left\{ \begin{array}{l} \text{DNA} \\ \text{(GC content : 72\%)} \end{array} \right.$ but not, or to a much lesser degree, apparent in calf thymus $\left\{ \begin{array}{l} \text{DNA} \\ \text{(GC content 42\%)} \end{array} \right.$.

In the temperature-jump work described in this Chapter a single relaxation has been observed for perturbations of 9AA and *E. coli* DNA (GC content 50%); thus, although no comparative study on DNAs of lower GC content has been carried out, it seems unlikely that the interaction of 9AA with DNAs of lower GC content would

yield two detectable discrete chemical relaxations. This throws into doubt the necessity of introducing for 9AA the base specificity suggested for proflavine¹¹.

It is true that, as with the results of Ramstein *et al*¹¹, there is a discrepancy in the values of the equilibrium constants determined by spectrophotometry (Table 4-3.) and the temperature-jump technique (Table 6-1.) for the interaction of 9AA with native DNA. The former method yields a value greater by a factor of 3 at each temperature than the latter method. If the proposition of Ramstein *et al*¹¹ is invoked, that an immeasurably small amplitude relaxation occurs then the value of K_{23} obtained from equation 6-18. is, $K_{23} \approx 2$. This would imply that approximately 33% of the bound 9AA exists as an outside bound form described by mechanism 3-1. While at this time it has not been possible to definitively account for the discrepancy between equilibrium constants measured by spectrophotometry and the temperature-jump method the model of Ramstein *et al*¹¹ of another quasi-intercalated complex is unacceptable for 9AA for two reasons.

- (1) Evidence of internal linearity of spectra (Chapter IV) at the r values studied in the temperature-jump experiments indicates that there are only two spectroscopically distinct forms of 9AA in equilibria between 9AA and native DNA. These are free 9AA and bound 9AA. Furthermore, viscosity and sedimentation studies¹⁶ have shown that this bound form of 9AA is unquestionably intercalated. The presence of another bound form of 9AA constituting 33% of the total 9AA bound would be expected to remove internal linearity in the spectra.

- (2) The value of the thermodynamic parameters of the equilibrium derived from the single relaxation are in good agreement with values of the same parameters obtained from equilibrium studies (Table 6-2.). In a sequential reaction it would be expected that the enthalpy and entropy of reaction for the overall reaction (as measured by equilibrium spectrophotometry) would differ from the same parameters for the first step only, unless the values for the second step are zero within experimental error. Which, in the limit, becomes a trivial case.

There is a superficial resemblance between the first step of the Li and Crothers² two step mechanism (mech. 3-1.) - the formation of complex II - and the equilibrium proposed for the interaction between 9AA and native DNA based on the observed single relaxation. This is so especially as the rate constants for the forward reaction are approximately the same for proflavine and DNA, and 9AA and DNA (see footnote). The activation energies are also similar. However, the feature which unambiguously distinguishes the two processes is the entropy of reaction, which in the bimolecular process of mechanism 3-1. is large and negative

Footnote:

Although the values of k_{12} quoted by Li and Crothers² are approximately a factor of 30^{12} lower than those recorded in this work (Table 6-1.), the values of the rate constants are nearly the same. This is so because in the paper of Li and Crothers k_{12} is actually an apparent rate constant ($k_{12,app}$) related¹² to the true rate constant, k_{12} , by the relationship:

$$k_{12,app} [(1-r)T_A + \bar{c}_{9AA}] = k_{12} [(n-r)T_A + \bar{c}_{9AA}]$$

where $n \approx 0.12$ and r is very small. Also, the results quoted in reference 2 are at temperatures at least 20°C below those given in Table 6-1.

$(\Delta S_{12}^{\circ} \approx -77 \text{ J.deg.}^{-1}\text{mole}^{-1})^2$, a result to be expected from a purely ion pairing process; whereas the bimolecular process of equation 6-12. has an entropy of reaction which is small and negative, $\Delta S^{\circ} = -33.5 \text{ J.deg.}^{-1}\text{mole}^{-1}$; a result which is consistent, as mentioned earlier, with the overall equilibrium measurement and, incidentally, in good agreement with the overall entropy change for the two step process for proflavine and DNA² leading to intercalation ($\Delta S_{12}^{\circ} + \Delta S_{23}^{\circ} \approx -28.4 \text{ J.deg.}^{-1}\text{mole}^{-1}$).

In conclusion, therefore, it appears the intercalation of 9AA into native DNA can be explained by a single step mechanism without the necessity of postulating the presence of an intermediate. This is in contrast to the results of Li and Crothers² on interaction of proflavine with DNA which has been described in terms of a two step mechanism. The first rapid step being the formation of an outside bound, ion-pair (complex II), followed by a conformational change of the DNA concurrent with intercalation. There may be intermediates required in the interaction of 9AA with native DNA, however, these are not present in detectable quantities. The important observation is that, at the elevated temperatures studied, the intercalation process is apparently achieved by a single step bimolecular reaction which is at least as fast as that observed for the formation of the intermediate (complex II) in the two step mechanism 3-1. The thermodynamic parameters, ΔH° and ΔS° for the single step reaction measured by perturbation techniques are consistent with the same parameters determined by equilibrium spectrophotometry (Table 4-4.). These are, in turn, in agreement with previously published results for similar reactions measured by equilibrium methods^{17,18} and for the overall reaction measured by the temperature-jump technique². Thus it can be stated that

at elevated temperatures the structure of native DNA is such that a conformational change of the DNA is not a pre-requisite or concomitant requirement for the intercalation of 9AA to occur. Presumably, flexion² in the structure of DNA is sufficiently great to allow the rapid intercalation of 9AA with its well characterized spectral, thermodynamic, and structural effects, without a detectable intermediate.

PART C - 9-AMINOACRIDINE AND DENATURED DNA

6. A temperature-jump study of the interaction of 9AA with denatured DNA.

(a) Preparation of solutions

All solutions have been made up in 0.1M NaCl. A stock solution of 9AA and denatured DNA has been prepared by the slow addition, with gentle stirring, of a 9AA solution of accurately known concentration to a solution of denatured DNA of known concentration. The denatured DNA has been prepared by the method described in Chapter II. Both solution aliquots have been weighed and it is therefore possible to determine the concentrations of both 9AA (T_L) and DNA (T_A) in solution.

In this series of experiments dilution of the stock solution has been carried out by the addition of 0.1M NaCl in weighed aliquots to weighed quantities of the stock solution. In a manner analogous to that described in section 5 (a). of this Chapter it is thus possible to calculate r and \bar{c}_{9AA} unambiguously from a knowledge of T_L/T_A , T_L or T_A and the Langmuir Isotherm for 9AA and denatured DNA at the appropriate temperature (Figs. 5-10 (b)., 5-11 (b)., 5-12 (b).). Dilution with 0.1M NaCl means that the value of r differs in the various diluted fractions of the stock solution. The value of r becomes smaller with increasing dilution. The way in which r changes with dilution of the stock solution is shown in Fig. 6-9 (a).(b). and (c). Figure 6-9 (a).(b). and (c). gives the value of r as a function of the extent of dilution of the stock solutions prepared for the temperature-jump analysis of 9AA and denatured DNA solutions at temperatures 45°C, 55°C and 65°C. A comparison with the Scatchard plots at the appropriate temperature (Figs. 5-10 (a)., 5-11 (a). and 5-12 (a).) shows that all dilutions of the stock

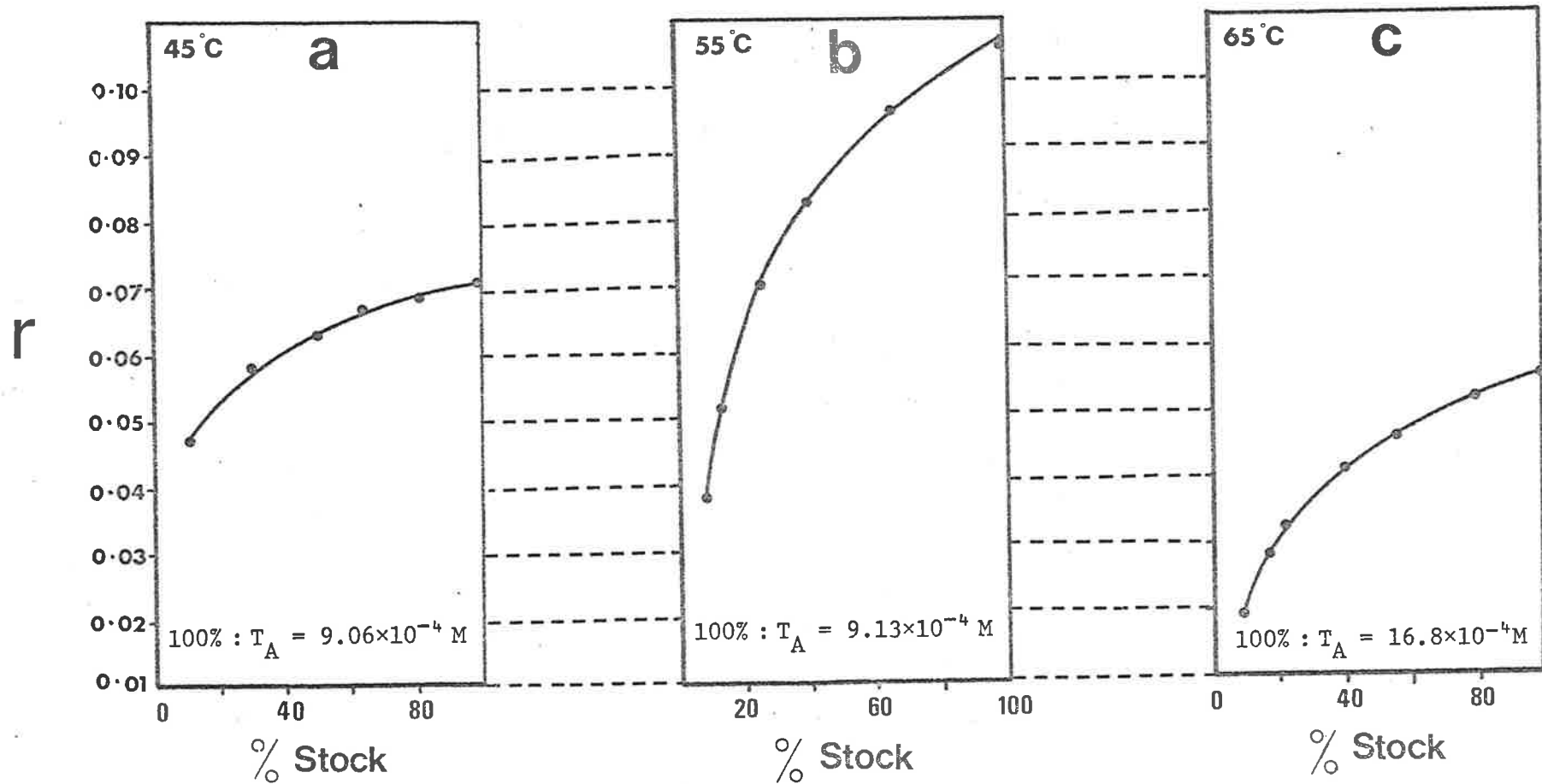


Fig. 6-9. Effect of dilution of stock solutions of 9AA and denatured DNA by neutral salt; resultant extent of binding, r , in the diluted fraction.

solutions have resultant r values in the region of the Scatchard plots which are substantially linear and which have been used to determine both the intrinsic association constant and the number of binding sites pertaining at that temperature. It is therefore assumed that for these solutions the kinetic parameters will be independent of the r value as it is implicit in the linearity of the Scatchard plot that there are no significant interactions between the bound 9AA molecules. All the binding sites are therefore considered to behave as isolated binding sites (vide: the discussion in Chapter IV on anti-cooperativity).

(b) Experimental

The experimental work was carried out as outlined in section 5 (b). of this Chapter and described earlier in this Chapter.

(c) Results

In a manner analogous to that described in section 5 (c). of this Chapter, the concentration of reactants at equilibrium has been determined in the following way. Knowledge of the extent of binding, r , calculated in section 6 (a). yields the concentration of free 9AA in solution at equilibrium from equation 4-9.

As before, the concentration of free binding sites is calculated from equation 6-14., restated below.

$$\bar{c}_{\text{DNA}} = (n - r) T_A \quad \text{eqn. 6-14.}$$

where n is considered to be the number of binding sites per DNA phosphate residue which is consistent with the equilibrium defined by equation 6-12., where the "free isolated binding site" is now the

binding site on denatured DNA, and for which the equilibrium constant is the intrinsic association constant given by the straight line portion of the Scatchard plot. The values of n are those which appear in Table 5-3.

Typical oscilloscope records of chemical relaxations following rapid temperature perturbations of 9AA/denatured DNA equilibria are shown in Fig. 6-10 (a), (b), and (c). It is immediately apparent that in contrast to chemical relaxations of 9AA with native DNA where only a single relaxation is observed, chemical relaxations of 9AA and denatured DNA involve more than one relaxation.

Program NONLIN has been used, as described in section 4 (b) of this Chapter to determine the relaxation times associated with the chemical relaxations. It has been found that the chemical relaxation can be expressed as the sum of two discrete relaxations; the more rapid of which has a relaxation time (τ_f) of the order of 50 μ sec. and the slower relaxation time (τ_s) of about 1 msec. There is no significant improvement of the fitted curve to the observed signal if a larger number of exponential terms is tried. The concentration dependences of these relaxation times are shown in Figs. 6-11. and 6-12. which show, respectively, the dependence of τ_f on the concentration of equilibrium reactant, $(\bar{c}_{DNA} + \bar{c}_{9AA})$ and the dependence of τ_s on the same concentration. It is apparent that the two relaxations observed for the interaction of 9AA with denatured DNA do not arise from a sequential reaction of the form described by mechanism 3-1. and which has been shown to be valid for the interaction of proflavine with native DNA². For, although the inverse of the rapid relaxation time $(\tau_f)^{-1}$ is linearly dependent on the concentration of equilibrium reactant, the slower relaxation is independent of

Fig. 6-10. Chemical relaxations of a solution of 9AA and denatured DNA perturbed to a final temperature of 65°C. $r = 0.046$

(a) 20 $\mu\text{sec}/\text{cm}$ (major division, horizontal axis)
 100 mV/cm (major division, vertical axis)

(b) 200 $\mu\text{sec}/\text{cm}$
 100 mV/cm

(c) Delayed trigger record; the first 200 μsec have been shorted out enabling amplification of the slower relaxation.

1.0 m sec/cm
 20 mV/cm

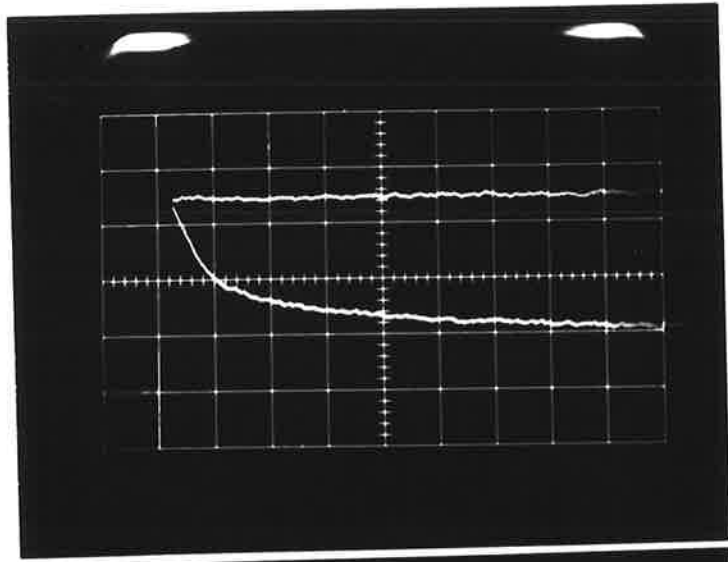
(A typical photographic record showing optical interference from a bubble in the sample space)

.....
 $[\bar{c}_{\text{DNA}} + \bar{c}_{9\text{AA}}] = 1.20 \times 10^{-4} \text{ M}$

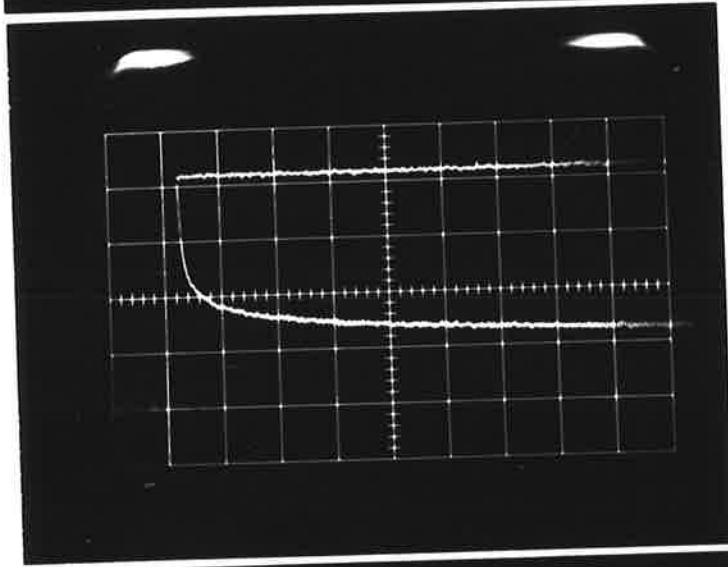
$$\frac{1}{\tau_f} = 6.0 \times 10^4 \text{ sec}^{-1}$$

$$\frac{1}{\tau_s} = 1.04 \times 10^3 \text{ sec}^{-1}$$

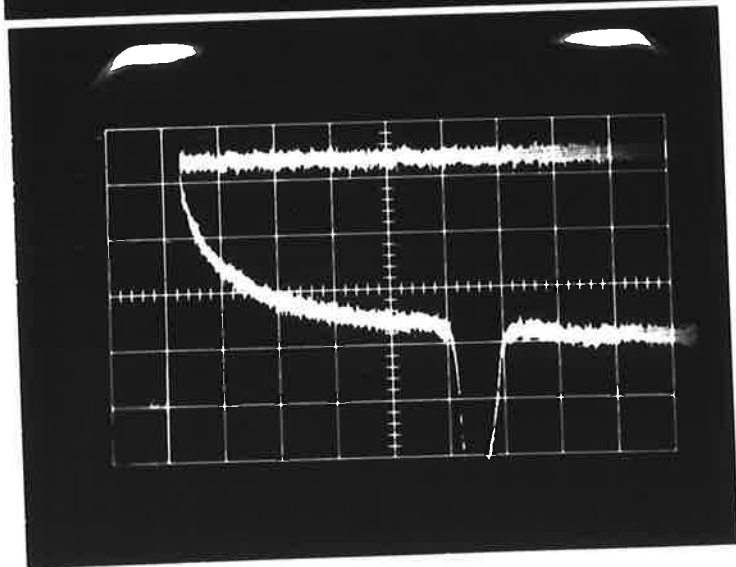
a



b



c



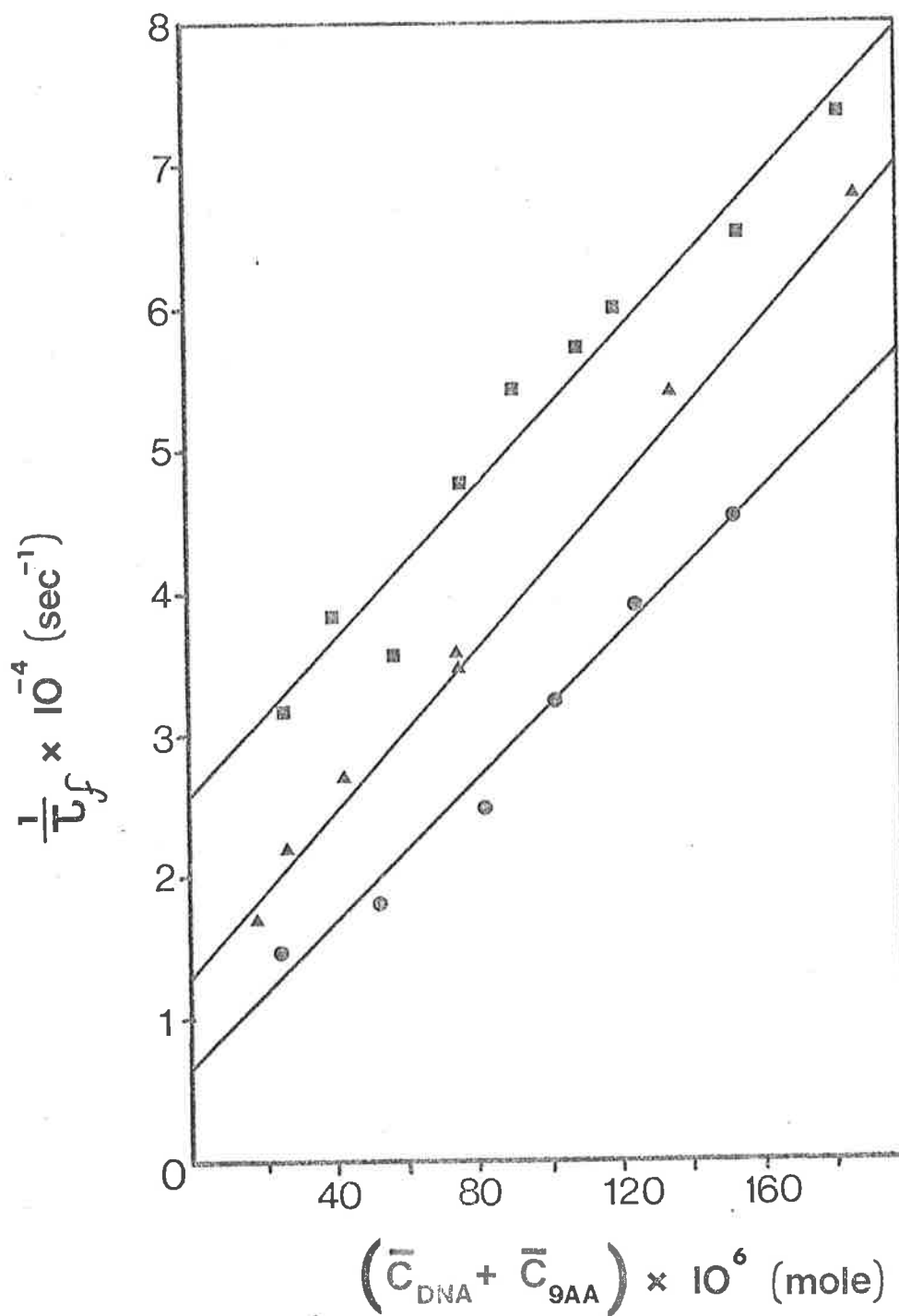


Fig. 6-11. The variation of the inverse relaxation time for the more rapid relaxation observed in perturbations of equilibria between 9AA and denatured DNA in 0.1 M NaCl on the concentration of reactant at equilibrium.

(●):45°C, (▲):55°C, (■):65°C.

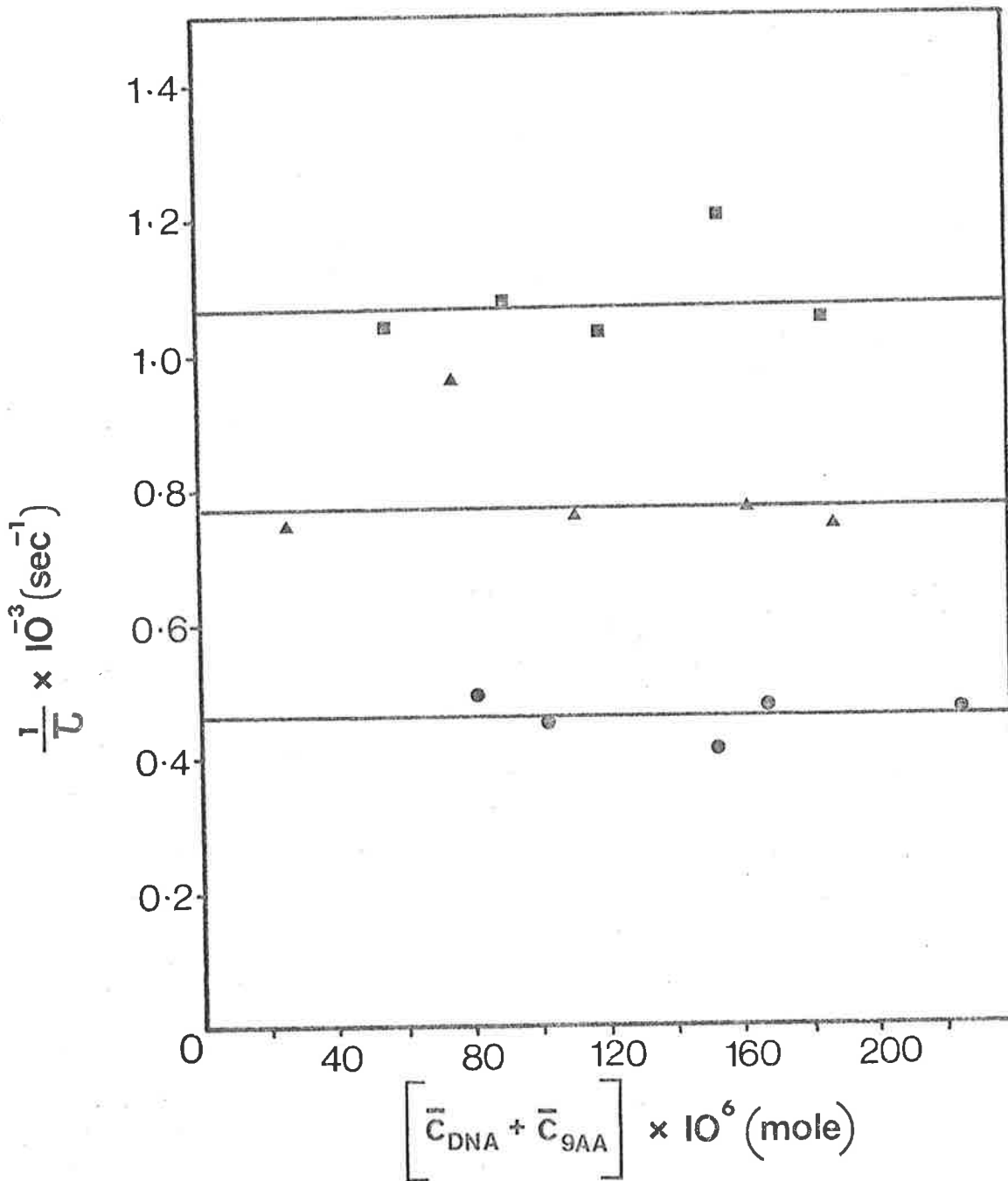


Fig. 6-12. Variation of the inverse relaxation time for the slower relaxation observed for perturbations of equilibria formed between 9AA and denatured DNA in 0.1M NaCl with the concentration of reactant at equilibrium.

(●):45°C, (▲):55°C, (■):65°C.

equilibrium reactant concentration. In a two step mechanism composed of a rapid bimolecular interaction followed by a slower molecular rearrangement, as in mechanism 3-1. the slower relaxation has an inverse relaxation time of the form:

$$\tau_s^{-1} = k_{32} + \frac{k_{23} [(\text{equilibrium reactant})]}{1/K_{12} + [(\text{equilibrium reactant})]} \quad \text{eqn. 6-20.}$$

where the rate constants and the equilibrium constant refer to those in mechanism 3-1. and have been defined previously. It is true that at high concentrations of equilibrium reactant the inverse relaxation time becomes independent of concentration, thus:

$$\tau_s^{-1} \approx k_{32} + k_{23} \text{ as } [(\text{equilibrium reactant})] \gg \frac{1}{K_{12}}$$

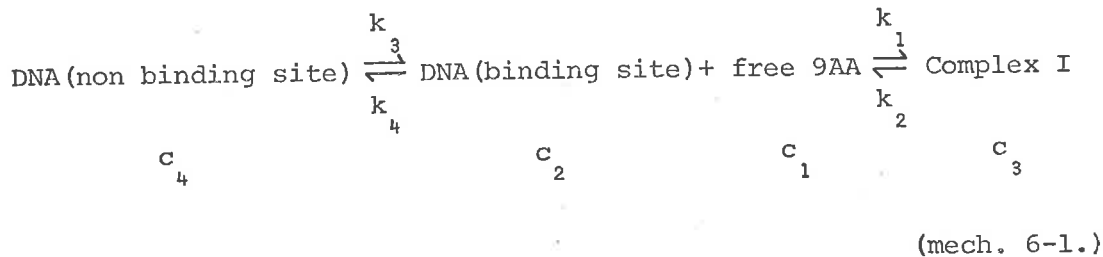
However, it can be readily shown that for appropriate values of K_{12} which may be extracted from Fig. 6-11. significant concentration dependence of the inverse slower relaxation time (τ_s^{-1}) should be observed in Fig. 6-12. This is not so and therefore mechanism 3-1 is not an appropriate reaction scheme for the equilibrium (see footnote).

Footnote:

The slow relaxation could be virtually concentration independent in mechanism 3-1. if $k_{32} \gg k_{23}$; i.e. $(\tau_s)^{-1} \approx k_{32}$. However this would require the equilibrium concentration of complex I (in mechanism 3-1.) to be very small. Temperature perturbations would then yield no measurable shift in concentration. This is certainly not the case experimentally where the slow relaxation is clearly associated with a significant change in absorbance.

(c) (i) Proposed mechanism

The following mechanism is proposed for the interaction of 9AA with denatured DNA at low r values.



For the purpose of simplifying the notation for the derivation of relaxation times to be expected from this mechanism the equilibrium species are numbered thus:

- c_1 free 9AA concentration in solution
- c_2 the concentration of isolated denatured DNA binding site - entirely equivalent to that proposed for the equilibrium process defined by equation 6-12. for denatured DNA
- c_3 the concentration of the complex existing at low r
- c_4 the concentration of DNA unavailable for binding: the nature of this species will be discussed later.

Equations describing chemical relaxations due to perturbations of equilibria described by mechanism 6-1. can be derived as follows. The rate laws for mechanism 6-1. are:

$$\frac{dc_1}{dt} = k_2 c_3 - k_1 c_2 c_1 \qquad \text{eqn. 6-21.}$$

$$\frac{dc_4}{dt} = k_4 c_2 - k_3 c_4 \qquad \text{eqn. 6-22.}$$

where the derivative is with respect to time and c_i refers to the instantaneous concentration of the i^{th} species defined earlier.

The following conservation relations apply:

$$\Delta c_1 = -\Delta c_3$$

eqns. 6-23.

$$-\Delta c_2 = \Delta c_3 + \Delta c_4$$

Now, if $c_i = \bar{c}'_i + \Delta c_i$ where:

c_i = instantaneous concentration of the i^{th} species

\bar{c}'_i = final equilibrium concentration of the i^{th} species

Δc_i = time dependent instantaneous concentration change

then for small perturbations the differential equation 6-21.

may be written:

$$\frac{d}{dt} (\bar{c}'_1 + \Delta c_1) = k_2 (\bar{c}'_3 + \Delta c_3) - k_1 (\bar{c}'_2 + \Delta c_2) (\bar{c}'_1 + \Delta c_1) \quad \text{eqn. 6-24.}$$

As \bar{c}'_1 is constant and the principle of microscopic reversibility

requires that $k_{23} \bar{c}'_3 = k_{12} \bar{c}'_2 \bar{c}'_1$:

$$\frac{d\Delta c_1}{dt} = k_2 \Delta c_3 - k_{12} \bar{c}'_2 \Delta c_1 - k_{11} \bar{c}'_1 \Delta c_2 \quad \text{eqn. 6-25.}$$

where, for small perturbations, the product $k_{11} \bar{c}'_1 \Delta c_2$ has been

neglected. Similarly equation 6-22. may be expressed:

$$\frac{d\Delta c_4}{dt} = k_4 \Delta c_2 - k_3 \Delta c_4 \quad \text{eqn. 6-26.}$$

Substitution of the conservation relations, equations 6-23, into equations 6-25. and 6-26. gives:

$$\frac{-d\Delta c_4}{dt} = \left[k_1 (\bar{c}'_1 + \bar{c}'_2) + k_2 \right] \Delta c_1 - \left[k_1 \bar{c}'_1 \right] \Delta c_4 \quad \text{eqn. 6-27.}$$

and

$$\frac{-d\Delta c_4}{dt} = -k_4 \Delta c_1 + \left[k_3 + k_4 \right] \Delta c_4 \quad \text{eqn. 6-28.}$$

The coefficients of the time dependent concentration changes may be abbreviated and the equations 6-27. and 6-28. rewritten:

$$\frac{-d\Delta c_1}{dt} = a_{11} \Delta c_1 + a_{12} \Delta c_4 \quad \text{eqn. 6-29.}$$

$$\frac{-d\Delta c_4}{dt} = a_{21} \Delta c_1 + a_{22} \Delta c_4 \quad \text{eqn. 6-30.}$$

These equations form a set of coupled, first order, linear homogeneous differential equations, the solutions to which are the sums of exponential terms, the number of terms being equal to the number of independent rate equations. Thus the solutions can be written:

$$\Delta c_1 = A_{11} e^{-\frac{t}{\tau_1}} + A_{12} e^{-\frac{t}{\tau_2}} \quad \text{eqn. 6-31.}$$

$$\Delta c_4 = A_{21} e^{-\frac{t}{\tau_1}} + A_{22} e^{-\frac{t}{\tau_2}} \quad \text{eqn. 6-32.}$$

The condition for a non trivial solution can be shown to be:

$$\begin{vmatrix} a_{11} - \frac{1}{\tau} & a_{12} \\ a_{21} & a_{22} - \frac{1}{\tau} \end{vmatrix} = 0 \quad \text{eqn. 6-33.}$$

Equation 6-33. may be expressed as:

$$\left(\frac{1}{\tau}\right)^2 - (a_{11} + a_{22}) \frac{1}{\tau} + (a_{11} a_{22} - a_{12} a_{21}) = 0 \quad \text{eqn. 6-34.}$$

this is a quadratic equation, the solutions of which are:

$$\frac{1}{\tau}_{1,2} = \frac{(a_{11} + a_{22})}{2} \left[1 \pm \left(1 - \frac{4(a_{11} a_{22} - a_{12} a_{21})}{(a_{11} + a_{22})^2} \right)^{1/2} \right] \quad \text{eqn. 6-35.}$$

It is reasonable to assume by analogy with the results obtained for the system of 9AA and native DNA that the faster relaxation is associated with the bimolecular step resulting in the formation of complex I. Then the slower relaxation may be associated with the pre-equilibrium between the binding and non binding sites. In this situation the presence of discrete relaxations indicates that $k_1, k_2 \gg k_3, k_4$ by a factor of at least 20. Hence $a_{11} \gg a_{22}$ and thus the roots of equation 6-35. simplify to:

$$\frac{1}{\tau_1} \approx a_{11}$$

eqn. 6-36.

and:

$$\frac{1}{\tau_2} \approx \frac{a_{11}}{2} \left[1 - \left(1 - \frac{4(a_{11}a_{22} - a_{12}a_{21})}{(a_{11})^2} \right)^{1/2} \right]$$

eqn. 6-37.

now for a quantity $x \ll 1$,

$$(1 - x)^{1/2} \approx (1 - \frac{x}{2})$$

eqn. 6-38.

and using this approximation in equation 6-37. the expression simplifies to:

$$\frac{1}{\tau_2} \approx a_{22} - \frac{a_{12}a_{21}}{a_{11}}$$

eqn. 6-39.

Thus the two roots of the quadratic equation, namely, equations 6-36. and 6-39., can be expressed by resubstituting the coefficients of equations 6-27. and 6-28. as:

$$\frac{1}{\tau_f} \approx k_1 (\bar{c}'_1 + \bar{c}'_2) + k_2$$

eqn. 6-40.

and:

$$\frac{1}{\tau_s} \approx k_3 + k_4 \left(1 - \frac{\bar{c}'_1}{\bar{c}'_1 + \bar{c}'_2 + K_{21}} \right)$$

eqn. 6-41.

or:

$$\frac{1}{\tau_s} \approx k_3 + k_4 \left(\frac{\bar{c}'_2 + K_{21}}{\bar{c}'_1 + \bar{c}'_2 + K_{21}} \right) \quad \text{eqn. 6-42.}$$

where:

$$K_{21} = \frac{k_2}{k_1} \quad \text{eqn. 6-43.}$$

Hence, for mechanism 6-1. two relaxations are observed, one of which is linearly dependent on the reactant concentration at equilibrium of the bimolecular step, and the second of which is described by equation 6-42. This mechanism can now be discussed as it pertains to the reaction between 9AA and denatured DNA.

(c) (ii) Rapid relaxation - results

In mechanism 6-1. the free 9AA, DNA binding site and complex I are entirely equivalent to the same species in equation 6-12. as it applies to 9AA and denatured DNA.

That is:

$$\begin{aligned} \bar{c}'_1 &= \bar{c}_{9AA} \\ \bar{c}'_2 &= \bar{c}_{DNA} = (n - r)T_A \\ \bar{c}'_3 &= rT_A \end{aligned} \quad \text{eqns. 6-44.}$$

Thus the equilibrium constant $K_{12} = \frac{k_1}{k_2}$ in mechanism 6-1. is equal to the overall equilibrium constant determined by

spectrophotometry, k (the intrinsic association constant). The rapid chemical relaxation observed is associated with this rapid bimolecular association reaction step. From Fig. 6-11. the rate constants k_1 and k_2 at the temperatures studied can be determined from the slope and intercept of the straight lines through the experimental points at each temperature. These rate constants, the equilibrium constant K_{12} and the same equilibrium constant (k) determined by equilibrium spectrophotometry (Table 5-3.) are shown in Table 6-3.

TABLE 6-3.

Rate constants and equilibrium constants determined by the temperature-jump method for the rapid relaxation (9AA and denatured DNA in 0.1M NaCl)

Temp. (°C)	k_1 ($M^{-1}sec^{-1}$)	k_2 (sec^{-1})	K_{12} (M^{-1})	k (M^{-1})
45	2.52×10^8 (S.E.O.18)	6.31×10^3 (S.E.1.8)	(perturbation) 4.0×10^4 (S.E.2.0)	(equilibrium) 5.40×10^4
55	2.85×10^8 (S.E.O.29)	1.30×10^4 (S.E.O.15)	2.2×10^4 (S.E.O.5)	3.61×10^4
65	2.72×10^8 (S.E.O.25)	2.52×10^4 (S.E.O.28)	1.10×10^4 (S.E.O.2)	1.36×10^4

The data in Table 6-3. show reasonable agreement between the results obtained by perturbation and equilibrium methods.

The Van't Hoff plot for the variation of $\ln K_{12}$ with inverse temperature is shown in Figure 6-13. The slope of the straight line gives the enthalpy of reaction for this reaction step,

ΔH_{12}° . In a manner described earlier, the entropy for the

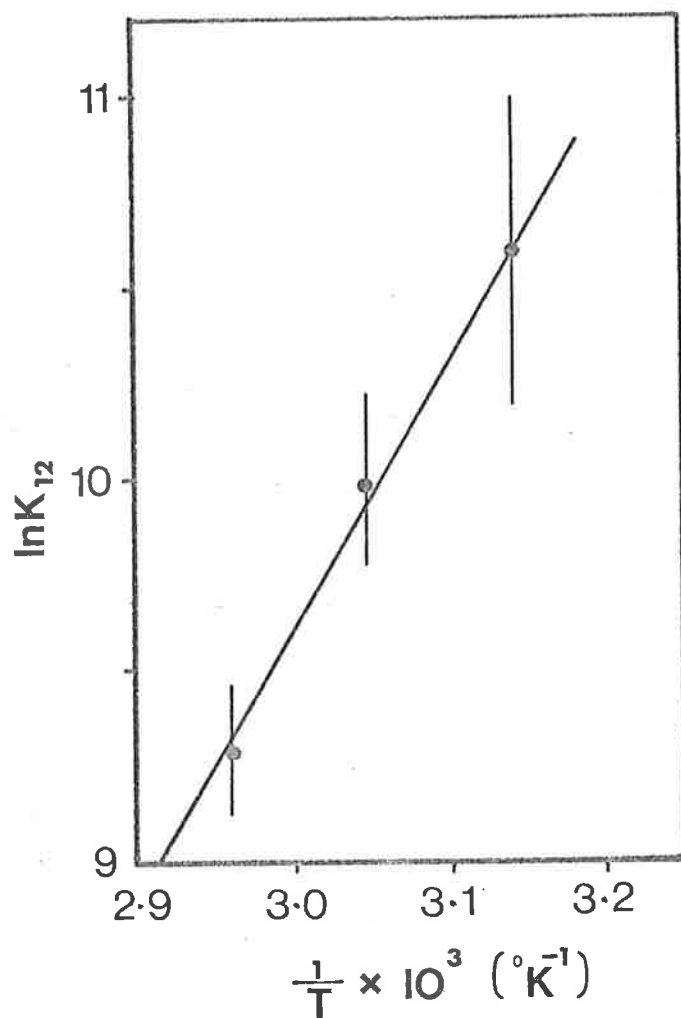


Fig. 6-13. Van't Hoff plot for the interaction of 9AA with denatured DNA in 0.1 M NaCl. Equilibrium constants evaluated from rate constants for the rapid bimolecular process determined by the temperature-jump method.

reaction step (ΔS_{12}^0) can also be calculated. A comparison of the results obtained by the temperature-jump method and those obtained by equilibrium spectrophotometry is given in Table 6-4.

TABLE 6-4.

A comparison of the enthalpy and entropy of reaction for 9AA and denatured DNA in 0.1M NaCl determined by equilibrium spectrophotometry and the temperature-jump technique.

	temperature-jump method		equilibrium spectrophotometry
ΔH_{12}^0 (kJ/mole)	-58 (S.E. 4)	ΔH^0 (kJ/mole)	-56 (S.E. 6)
ΔS_{12}^0 (J.deg. ⁻¹ mole ⁻¹)	-94 (S.E.13)	ΔS^0 (J.deg. ⁻¹ mole ⁻¹)	-88 (S.E.17)

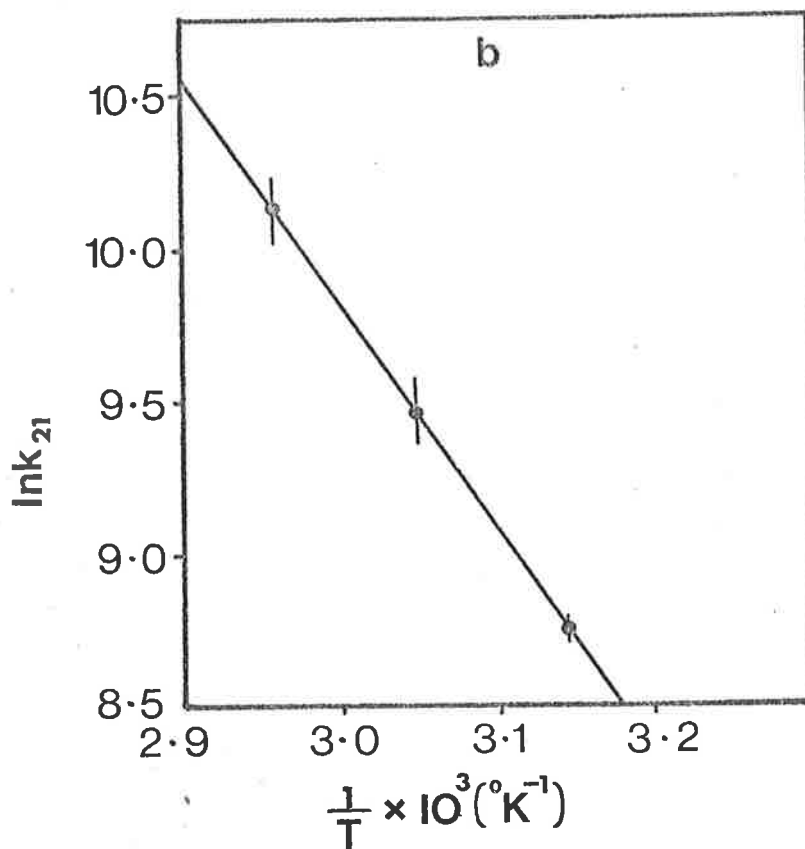
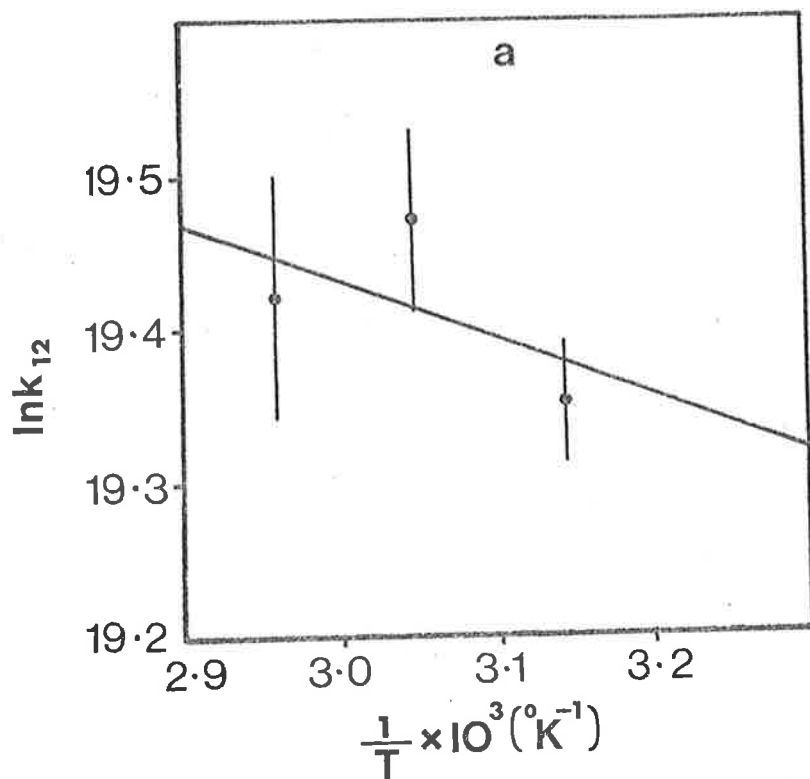
The energies of activation for the forward (k_1) and reverse (k_2) rate processes can be obtained from the plot of the logarithm of the rate constant versus the inverse temperature.

These plots are shown in Fig. 6-14. The value of the activation energy for the forward process is low ($E_{12}^\ddagger = 4$ kJ/mole), but is large for the reverse process ($E_{21}^\ddagger = 61$ kJ/mole). These are in agreement with enthalpy data as required by equation 6-17.

(c) (iii) Rapid relaxation - discussion

The interaction of 9AA with denatured DNA has been shown to yield characteristics of an intercalation process (Chapter V). The free energy of the reaction is large and negative, the spectral shifts are characteristic of the interaction and the

Fig. 6-14. Arrhenius plots for the forward (k_{12}) and backward (k_{21}) rate processes in the bimolecular association of 9AA with denatured DNA in 0.1 M NaCl. Evaluation of activation energies for the processes.



thermodynamic parameters are consistent with the proposed model.

The temperature-jump results just described (section 6 (c) (ii).) are in agreement with these observations for the mechanism of the interaction which has been proposed (mech. 6-1.). In particular, the rate constants are very similar to those observed for the interaction of 9AA with native DNA. They are characterized by a very rapid forward rate (k_1) with a slower back reaction (k_2) producing a large equilibrium constant for the reaction which is in good agreement with equilibrium measurements.

It is therefore proposed, in common with the proposition for native DNA, that the interaction between 9AA and denatured DNA produces an intercalated 9AA complex without a detectable intermediate. This intercalated 9AA moiety is presumably located between single strand, base-stacked nucleotide bases (see Chapter V).

The thermodynamic parameters for the interaction are in good agreement with the model described in Chapter V. The reaction is "enthalpy driven", that is, the formation of bonding interactions is the driving force in the reaction. These are sufficiently large to overcome the significant decrease in entropy due to the additional ordering effect of the intercalation process on the single strand, base-stacked structure of denatured DNA, and still produce a favourable free energy change for the reaction.

The energy of activation for the forward rate process (E_{12}) is significantly lower than that observed for the formation of the complex from the analogous bimolecular association of 9AA with native DNA. This may be a consequence of the relatively more

open structure of denatured DNA, unconstrained by base pairing compared with native DNA, facilitating insertion of the 9AA cation between the nucleotide bases.

(c) (iv) Slow relaxation - results

The slower relaxation arising from perturbations of equilibria defined by mechanism 6-1. has an inverse relaxation time described thus:

$$\frac{1}{\tau_s} \approx k_3 + k_4 \left(\frac{\bar{c}'_2 + K_{21}}{\bar{c}'_1 + \bar{c}'_2 + K_{21}} \right) \quad \text{eqn. 6-42.}$$

It is generally true at low r that the value of $\bar{c}'_1 = \bar{c}'_{9AA}$ is very small, as most of the 9AA exists in the bound form in view of the favourable equilibrium constant. It is certainly true that in all the solutions perturbed for which the results are shown in Figs. 6-11. and 6-12. that $\bar{c}'_1 < \bar{c}'_2$ by a factor of at least 5. Thus, for these solutions, equation 6-42. reduces to:

$$\frac{1}{\tau_s} \approx k_3 + k_4 \quad \text{eqn. 6-45.}$$

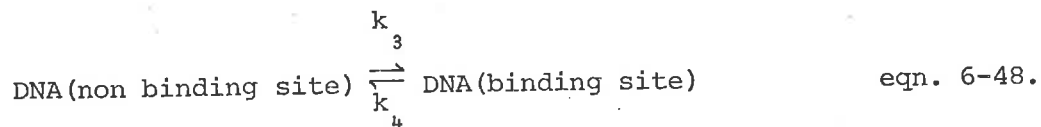
It is now necessary to try and separate these rate constants. The principle of microscopic reversibility requires that for mechanism 6-1.

$$k_3 \bar{c}'_4 = k_4 \bar{c}'_2 \quad \text{eqn. 6-46.}$$

Thus equations 6-45. and 6-46. may be expressed:

$$\left(\frac{1}{\tau_s} - k_4 \right) \bar{c}'_4 = k_4 \bar{c}'_2 \quad \text{eqn. 6-47.}$$

In equation 6-47. both k_4 and \bar{c}'_4 are unknown and so there is no unique solution to the equation. This means in physical terms that the values of k_4 (and hence k_3) will depend on the units of concentration used for DNA in the equilibrium:



If the following conservation relation is used:

$$\bar{c}'_4 + \bar{c}'_2 + \bar{c}'_3 = \text{concentration of DNA phosphate} \quad \text{eqn. 6-49.}$$

then it is possible to extract values for k_3 and k_4 in the following manner. From equations 6-44. it follows that:

$$\bar{c}'_4 = (1 - n)T_A \quad \text{eqn. 6-50.}$$

whence, substitution of equation 6-50. and equations 6-44.

into equation 6-47. gives:

$$\left(\frac{1}{T_S} - k_4\right)(1 - n) = k_4(n - r) \quad \text{eqn. 6-51.}$$

The experiments with 9AA and denatured DNA were not carried out at constant r . However, as $(n - r)$ is significantly less than $(1 - n)$, the use of a median value of r for the solutions used (from Fig. 6-9 (a). (b). and (c).) and the appropriate value of n for the temperature, does enable a good estimate of k_4 and hence k_3 to be made from equation 6-51. Table 6-5. gives the values of the rate constants calculated in this manner. The equilibrium constants and the thermodynamic parameters calculated from them, for the equilibrium described by equation 6-48., are

also given in Table 6-5.

TABLE 6-5.

Rate, equilibrium and thermodynamic data for the slow pre-equilibrium between binding and non binding sites of denatured DNA. (eqn. 6-48.)

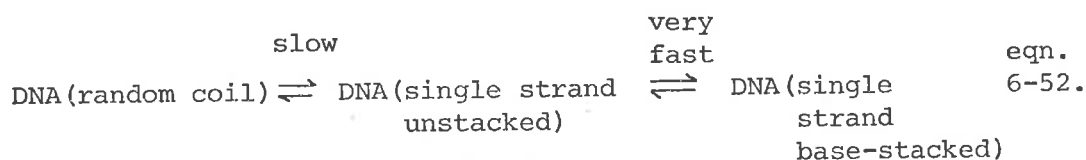
Temp (°C)	45	55	65
k_4 (sec ⁻¹)	3.7×10^2	6.7×10^2	9.6×10^2
k_3 (sec ⁻¹)	0.8×10^2	1.0×10^2	1.1×10^2
$K_{34} = \frac{k_3}{k_4}$	0.22	0.15	0.11
ΔH_{34}^0 (kJ/mole)	-31.4 (S.E. 2)		
ΔS_{34}^0 (J.deg. ⁻¹ mole ⁻¹)	-170 (S.E.65)		

(c) (v). Slow relaxation - discussion

As described by mechanism 6-1. the slower relaxation is due to a slow pre-equilibrium step influencing the concentration of potential binding sites of the denatured DNA at equilibrium. It has already been proposed that, at elevated temperatures, the binding sites on denatured DNA are considered to be in regions of the denatured DNA which exist in a single strand, base-stacked conformation. Thus the equilibrium between binding sites and non binding sites (eqn. 6-48.) may be pictorially described as the equilibrium between single strand, base-stacked regions of the macromolecule (binding sites) and unstacked regions (non binding sites). The results in Table 6-5. are as expected for this model.

The tendency to go from the unstacked conformation to the stacked conformation would be expected to decrease with increasing temperature, would be associated with the formation of bonding interactions (stacking energy; implies a negative ΔH_{34}^0), and would be associated with a significant decrease in entropy of reaction as a result of the ordering process. All these factors are observed in Table 6-5.

Some further comments need to be made about the rapidity of the relaxation. Walz¹⁹ has investigated the chemical relaxation response of single strand DNA using the temperature-jump technique, by observing absorbance changes in the UV on perturbation. A spectrum of relaxations has been observed¹⁹. One very rapid relaxation has been associated with single strand unstacking. This relaxation is at least as fast as the heating time of the cell, a few microseconds¹⁹. Thus it is necessary to modify equation 6-48. to explain why the pre-equilibrium step is so much slower when observed at 400 nm. The following modification is suggested:



Equation 6-52 would appear to satisfy all the experimental observations. The rapid UV change observed by Walz¹⁹ is due to unstacking of the bases by thermal motion in a very fast equilibrium. The slow equilibrium which becomes the rate determining step when observed at 400 nm by the release of 9AA to preserve the coupled equilibria is due to the collapse of the unstacked conformation into the random coil structure: a conformational change for which relaxation times are typically

of the order of one millisecond, as observed here. As discussed previously in Chapters II and V, changes in the slow equilibrium step in equation 6-52. are not associated with any significant change in UV absorbance, however, its influence by coupling to the very fast equilibrium may be one contributing factor to the spectrum of slower relaxations observed in the UV¹⁹.

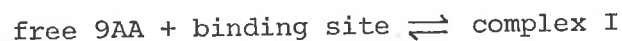
The thermodynamic parameters in Table 6-5. refer to the overall reaction, and no further breakdown of results is possible into components attributable to the coupled reactions in equations 6-52.

These results are consistent with those expected for the interaction of 9AA with denatured DNA for which the structure is such that there is a decreasing number of binding sites with increasing temperature. This change in the number of binding sites has previously been attributed to a shift in distribution of conformations of single strand, base-stacked regions of the macromolecule to random coil regions as the temperature is increased (Chapter V). The temperature-jump study provides further evidence for this change in structure and indicates, as proposed earlier, that random coil regions below the T_m do not bind 9AA significantly.

PART D - CONCLUSIONS7. Concluding remarks

The interaction of 9AA with both native and denatured DNA in 0.1M NaCl has been studied by the temperature-jump method at 45°C, 55°C and 65°C.

Chemical relaxations arising from temperature perturbations of 9AA and native DNA equilibria can be explained in terms of a single rapid relaxation process. There is a linear concentration dependence of the inverse relaxation time of this relaxation on the concentration of reactant at equilibrium. A bimolecular interaction of the form:

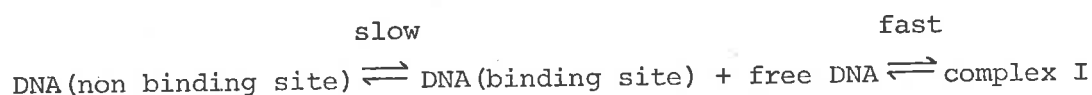


is proposed to explain the observations which have been made at low r where complex I binding (intercalation) is known to predominate.

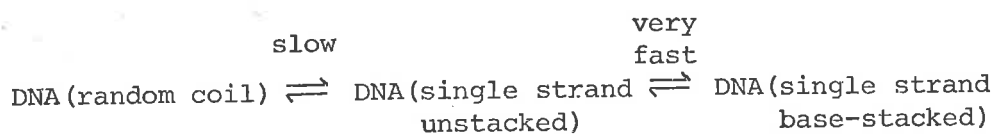
These results are in marked contrast to previous reports on temperature-jump experiments with proflavine and native DNA for which two discrete relaxations have been observed and equated with a two-step mechanism. Although there is a slight discrepancy between the equilibrium constants measured by temperature-jump methods and equilibrium spectrophotometry there is reasonable agreement with the thermodynamic parameters obtained by the two techniques. The thermodynamic parameters are also in good agreement with previously published equilibrium data on the intercalation of other aminoacridines into DNA. It is thus suggested that intercalation of 9AA between the bases of native DNA can occur, at the elevated temperatures studied, without the

formation of a detectable intermediate at rates which approach that of diffusion controlled reactions. This may indicate that DNA at these temperatures is an expanded structure with pronounced flexibility such that local distortion of the helix allows insertion of 9AA without a detectable intermediate.

Chemical relaxations of 9AA and denatured DNA are characterized by the presence of two relaxation processes. The following mechanism has been proposed:



where the binding sites are regions of the macromolecule which exist as single strand, base-stacked regions. The fast reaction step has characteristic features of an intercalation type reaction and the results are consistent with those obtained by equilibrium spectrophotometry (Chapter V). The slow reaction is probably due to a two step process:



where the DNA (non binding site) is the random coil form of the DNA and the slow process above is a conformational change of the DNA collapsing from an unstacked conformation into the random coil. The very rapid process must be invoked to explain results in the literature for an observed UV change associated with single strand unstacking. This mechanism has the advantage of explaining the strong dependence of the number of non interacting binding sites (n) on temperature, an observation made in Chapter V. The thermodynamic parameters of the overall slow reaction have been measured and are as expected for the conformational change proposed.

REFERENCES

1. Akasaka, K., Sakoda, M. and Hiromi, K.,
Biochem. Biophys. Res. Comm., 40, 1239 (1970).
2. Li, H.J. and Crothers, D.M., J. Mol. Biol., 39,
461 (1969).
3. Eigen, M. and De Maeyer, L., "Techniques of Org. Chem."
vol. 8. pt. 2., eds. Freiss, Lewis, Weisberger,
pub. Interscience, New York, 1963.
4. Czerlinski, G.H., "Chemical Relaxation" Arnold (Publishers),
London, 1966.
5. Hammes, G.C., Advances in Protein Chem., 23, 1 (1968).
6. Hammes, G.C., Tech. Chem. (N.Y.), 6, (2) 147 (1974).
7. Czerlinski, G. and Eigen, M., Deutsches Bunsenges. physik.
Chemi., 63, 652 (1959).
8. Faeder, E.J., Ph.D. Thesis, Cornell University, Ithaca,
New York, 1970.
9. Blagrove, R.J., Ph.D. Thesis, University of Adelaide, 1968.
10. Biochemists' Handbook, Ed. Long, C., Spon Ltd.,
(Publishers), London, 1961.
11. Ramstein, J., Dourlent, M. and Leng, M., Biochem. Biophys.
Res. Comm., 47, 874 (1972).
12. Program NONLIN: Technical report 7292/69/7292/005;
C.M. Metzler, Nov. 25 1969; The Upjohn Company,
Kalamazoo, Michigan 49001, U.S.A.
13. Schmechel, D.E.V. and Crothers, D.M., Biopolymers,
10, 465 (1971).

14. Muller, W., Crothers, D.M. and Waring, M.J.,
Eur. J. Biochem., 39, 223 (1973).
15. Ramstein, J. et al, Dyn. Aspects of Conf. Changes in
Biol. Macromol. Proc. Annu. Meet. Soc. Chim. Phys.,
23rd (1972). (Published 1973) 333. Sadron, C., Ed.
16. Sansom, L.N., Ph.D. Thesis, University of Adelaide, 1972.
17. Ichimura, S. et al, Biochim. Biophys. Acta, 190, 116 (1969).
18. Chambron, J., Daune, M. and Sadron, C., Biochim. Biophys.
Acta, 123, 306 (1966).
19. Walz, F., Biopolymers, 11, 2365 (1972).

CHAPTER VII

General discussion and conclusions.

At the beginning of the work described in this thesis it was intended that the major portion of the work would entail temperature-jump studies of 9AA with native and denatured DNA. As the temperature-jump method requires recording of chemical relaxations by spectrophotometric techniques it has been necessary to obtain accurate equilibrium spectrophotometric data on the interactions to prove the validity of the method and provide for a comparison of results. In carrying out these equilibrium measurements by spectrophotometry it became apparent that some safeguards are necessary to ensure that reproducible results are achieved (Chapter IV, section 5). It also became apparent that denatured DNA in the solution state is a more complex system than has been generally appreciated. Accordingly, an investigation by equilibrium spectrophotometry of the complexes formed between 9AA and both native and denatured DNA has been made.

The models for native and denatured DNA which have been formulated on the basis of observations described in this thesis and the published observations of other authors will now be discussed.

Native DNA

Native DNA in 0.1M NaCl at neutral pH and at room temperature is considered to exist in solution as a solvated double helix of the Watson-Crick type. This structure is maintained without significant modification with increasing temperature until the cooperative thermal transition occurs (at temperature T_M)

when the double helical structure is destroyed and the macromolecule collapses to the random coil.

Denatured DNA

Denatured DNA in solution may be considered to be composed of three coexisting structures within the macromolecule.

These are:

- (i) "folded" or short range helical ordered regions of the macromolecule which are progressively lost in a cooperative type transition at low temperatures.
- (ii) Single strand, base-stacked regions which exist throughout the temperature range but are themselves temperature dependent as increasing temperature will increase the thermal motion (oscillation) of the bases with respect to each other.
- (iii) Random coil conformations which become the dominant structure as the T_M of native DNA in equivalent neutral salt is approached.

It has been found that the results described in this thesis on the binding of 9AA to native and denatured DNA can be explained in terms of these models of native and denatured DNA.

General characteristics of the interaction of aminoacridines with DNA

Many aminoacridine cations are found to interact with native DNA and yield two distinct types of complexes as products of the interaction. Complex I has been widely studied. It is

found to be associated with marked changes in the structure of DNA, changes which are consistent with intercalation of the aminoacridine between the nucleotide bases of the double helix, with a consequent increase in base-pair separation. The formation of complex I also has a pronounced effect on the spectrum of the aminoacridine, producing both a decrease in extinction coefficient and a red shift in the spectrum. The formation of complex I is a favourable process with a free energy of reaction of the order of 25-40 kJ/mole. The formation of the complex stabilizes the double helix towards thermal denaturation and the thermal destruction of the complex is coincident with the loss of secondary structure of native DNA. Complex II, although it has been less widely studied, is generally considered to arise from the interaction of the aminoacridine cations with the polynucleotide phosphates. Spectral evidence suggests that it may also involve the aggregation of aminoacridines onto the "outside" of the helix. It is a significantly weaker interaction.

A number of aminoacridines that have been studied have been found to interact with denatured DNA in a manner which, at room temperature, is very similar to that of native DNA. Thus it is evident that while the cooperative loss of secondary structure of native DNA going to the random coil is associated with the loss of aminoacridines bound in complex I, the intact double helix is not a prerequisite for a strong binding interaction at room temperature. However the observation of strong binding to denatured DNA cannot be taken to indicate that the mode of binding to both native and denatured DNA is identical.

The current intercalation models for aminoacridine-native DNA complexes still leave open to question the exact location of the aminoacridine nucleus with respect to the nucleic acid bases. (Chapter III, sections 3 (b)., 5 (a).). It seems reasonable to suggest that the precise location of an intercalated aminoacridine cation will be that in which the lowest free energy state can be achieved for the bound complex as a result of molecular interactions and steric factors, assuming always that a mechanism to achieve this energy state is possible. As the nature of substituents on the acridine nucleus can vary the electron distribution significantly, then, quite apart from any steric considerations, it seems reasonable to suggest that the exact location of an intercalated aminoacridine cation will be different for each individual aminoacridine (Chapter III, section 3 (b).).

The interaction of 9AA with both native and denatured DNAs has been studied in this work at a neutral salt concentration of 0.1M NaCl. It has been shown previously¹ that the interaction of 9AA with native DNA yields a complex with all the properties of complex I described previously (intercalated 9AA). In the work which has been described here, only solutions in which the bound 9AA is believed to exist in the complex I form have been studied. Similarly, investigations have been restricted to those solutions of 9AA and denatured DNA in which the bound 9AA also exists in the strongly bound form.

The interaction of 9AA with native DNA

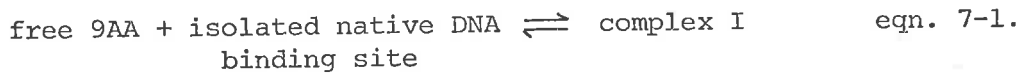
It has been demonstrated that spectra of solutions of 9AA and native DNA are internally linear for a set of spectra of solutions for which the extent of binding (r) is within the region dominated by complex I binding. This relationship provides

additional information to the observation of an isosbestic point in these spectra. The conclusion drawn is that the interaction is adequately described by a single, bimolecular reaction with only two species of 9AA present in solution, viz free 9AA and bound 9AA (Chapter IV, section 3).

The spectrophotometric determination of the extent of binding² has been used to determine Scatchard plots of the interaction. Some safeguards have to be used to ensure that the absorbance due only to the bound species can be determined. The relative invariance with temperature of the extinction coefficient of 9AA bound in complex I form to native DNA is taken as evidence of little change in the nature of the binding site with temperature (Chapter IV, section 6).

Scatchard plots of the interaction of 9AA with native DNA show marked curvature at r values below $r = 0.25$, the value considered to be the limit for complex I binding³. This curvature is not due to the presence of different types of bound 9AA but is considered to arise from interactions between bound 9AA cations. These interactions progressively reduce the favourable free energy associated with binding as the extent of binding increases. The interactions may be collectively termed anti-cooperative interactions; Schellman⁴ has pointed out that these may occur between other than only nearest neighbour bound 9AA cations (see also Chapter IV, section 7 (b).). Although it is not possible to analyse the results obtained in terms of discrete interactions giving rise to anti-cooperative binding it seems reasonable to associate the binding at low r with the binding associated with isolated sites⁵. Thus the initial (linear) portion of the Scatchard plot gives values of the intrinsic association constant (k), an equilibrium constant

(the slope of the line is $-k$) and the extrapolation of this linear portion to the r axis gives n , a number of binding sites which is associated with the following equilibrium:



where the corresponding concentrations at equilibrium are:

$$\text{free 9AA} = c = \bar{c}_{9AA}$$

$$\begin{array}{l} \text{isolated native DNA} = (n - r)T_A \\ \text{binding site} \end{array} \quad \text{eqns. 7-2.}$$

$$\text{complex I} = r T_A$$

for values of r within the linear portion of the Scatchard plot. (Chapter IV, section 7 (b).).

The values of k and n have been determined at 22°C , 45°C , 55°C and 65°C for the interaction of 9AA with native DNA. The value of n is almost invariant with temperature indicating that the structure of native DNA is not changing greatly with temperature. This result complements the observation of a relatively temperature independent extinction coefficient of bound 9AA. The temperature dependence of the intrinsic association constant (k) has been used to evaluate the thermodynamic parameters which describe the reaction, eqns. 7-1. (Chapter IV, section 7 (c) (ii).). These results indicate that the reaction is "enthalpy driven" rather than "entropy driven". Thus bonding interactions are of primary importance in the formation of complex I in native DNA. The bonding interactions will arise from interactions between the planar aminoacridine heterocyclic rings and the nucleotide bases when the aminoacridine is in the intercalated form. The results

are in general agreement with theoretical calculations which indicate that these bonding interactions which give rise to what are usually called, collectively, "stacking energies" are of major importance in intercalation type interactions⁶. (Chapter IV, section 8). The thermodynamic parameters are also in agreement with previously published data on systems of intercalated aminoacridines with DNA^{7,8}.

The interaction of 9AA with denatured DNA

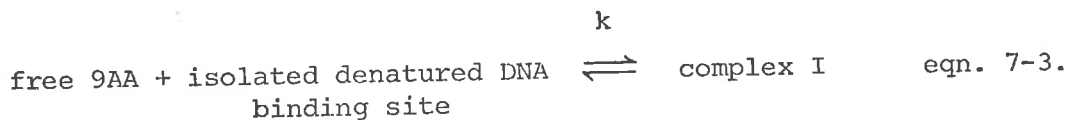
In contrast to complex I formed between 9AA and native DNA, the complex formed at low r between 9AA and denatured DNA is very temperature dependent. This dependence on temperature results from the sensitivity to temperature of the denatured DNA structure described earlier in this Chapter.

Equilibrium spectrophotometric measurements of the interaction of 9AA with denatured DNA have been carried out as described for native DNA. The values of n and k obtained are both markedly temperature dependent. The value of n is found initially to increase with temperature and then to decrease. This is consistent with a model in which 9AA may bind to both folded regions and single strand, base-stacked regions of denatured DNA, but not to random coils. The initial increase in n arises from the increase in single strand, base-stacked regions of the macromolecule as the folded regions melt and give way to two single strands each of which contains potential binding sites (Fig. 5-13.). This suggestion explains the generally higher values of n for denatured DNA than for native DNA at room temperature^{1,8}. The decrease in n at still higher temperatures is consistent with the preferred formation of random coils which are presumably non bonding structures at temperatures below the

T_M (the melting temperature of native DNA complexes in the same neutral salt) as well as above the T_M , as observed for native DNA complexes with aminoacridines.

The extinction coefficient of the bound 9AA is markedly temperature dependent as may be expected from binding to single strand, base-stacked regions which themselves are temperature dependent: the extinction coefficient of bound 9AA reflecting the extent of interaction between the 9AA ring structure and the nucleotide bases (Chapter V, section 5).

Thermodynamic parameters have been obtained for the interaction of 9AA with denatured DNA. The fact that the binding site (reactant) and the bound complex (product) are themselves changing with temperature requires that care must be taken not to attribute too much to the thermodynamic parameters which refer to the equilibrium:



However the magnitude of the values for the enthalpy and entropy of reaction are unambiguous as the Van't Hoff plot is virtually linear over the temperature range studied. In view of the changing structure of reactant and product states with temperature in the equilibrium defined by equation 7-3. the linearity of the Van't Hoff plot is fortuitous. The thermodynamic parameters indicate that the bonding interactions are of great importance, as with native DNA, and the reaction can be considered as "enthalpy driven". In 9AA-denatured DNA complex formation the entropy change is large and negative. This is taken to indicate that the binding of 9AA induces a higher degree of order in the single strand, base-stacked regions of the macromolecule. This may be

pictorially expressed as a reduction in the thermal motion (oscillation) of nucleotide bases with respect to each other when a lower free energy state is reached in the presence of an intercalated, bound 9AA cation (Chapter V, section 7).

In summary, the greater temperature dependence of the binding of 9AA to denatured DNA than native DNA is due not only to a decrease in the number of available binding sites (decreasing n) with temperature at elevated temperatures, which does not occur in native DNA, but also to a progressive change in the nature of the binding site which becomes a markedly less favourable site with increasing temperature. This latter observation also contrasts with the situation in native DNA-9AA complexes in which the binding site, constrained by the double helical structure, remains comparatively unaltered until the secondary structure of the macromolecule is lost at the T_M of the complex.

Kinetics and mechanisms of the interactions

The temperature-jump technique has been used to study the kinetics and mechanisms of the interaction of 9AA with both native and denatured DNA (Chapter VI). At temperatures 45°C, 55°C and 65°C, 9AA and native DNA equilibria exhibit a single, rapid chemical relaxation on perturbation. The concentration dependence of the relaxation time (τ) associated with this relaxation has been studied. The linear dependence of τ^{-1} on the concentration of reactant at equilibrium has led to the proposal that the interaction occurs in a single bimolecular reaction step. The rate constants for the forward and reverse processes have been measured. The forward rate process is fast, approaching a diffusion controlled rate. This suggests that intercalation of 9AA into native DNA occurs without the

necessity of an intermediate. This proposal is in marked contrast to that of Li and Crothers¹¹ based on their observations of temperature-jump perturbations of the interaction of proflavine with calf thymus DNA. In this work¹¹ two relaxations were observed and a sequential reaction was proposed. A single relaxation has also been observed by Ramstein *et al*¹² for the interaction of proflavine with *M. lysodeikticus* DNA. However, these authors¹² have chosen to explain this observation in a way which is not applicable for the interaction of 9AA with native DNA (Chapter VI, section 5 (c)). The thermodynamic parameters determined from the temperature-jump data are in agreement with equilibrium measurements.

Perturbations of equilibria formed between 9AA and denatured DNA exhibit two chemical relaxations. The more rapid of the relaxations has been associated with intercalation of the 9AA between single strand, base-stacked regions of the macromolecule. The rate constants are of the same order of magnitude as those for the intercalation process observed for 9AA and native DNA. Again, there is no observable intermediate for the reaction (Chapter VI, section 6 (c) (ii)).

The slower relaxation has been attributed to an equilibrium between binding and non binding sites on denatured DNA. These may be associated with the foreshadowed single strand, base-stacked regions and random coil regions of the macromolecule, respectively (Chapter VI, section 6 (c) (iv)). The observation of a very rapid relaxation in the UV study of temperature-jump perturbations of single strand DNA¹⁰ requires the postulation of an intermediate in the slow relaxation so that the overall reaction mechanism for 9AA and denatured DNA becomes:

REFERENCES

1. Sansom, L.N., Ph.D. Thesis, University of Adelaide, 1972.
2. Peacocke, A.R. and Skerrett, N.J.H., *Trans. Faraday Soc.*,
52, 261 (1956).
3. Armstrong, R.W., Kurucsev, T. and Strauss, U.P., *J. Amer. Chem. Soc.*, 92, 3174 (1970).
4. Schellman, J.A., *Israel J. Chem.*, 12, 219 (1974).
5. Crothers, D.M. in "The Physical Chemistry of Nucleic Acids",
Harper & Row (Publishers), New York, 1974.
6. Gersch, N.F. and Jordan, D.O., *J. Mol. Biol.*, 13, 138 (1965).
7. Chambron, J., Daune, M. and Sadron, C., *Biochim. Biophys. Acta*,
123, 306 (1966).
8. Ichimura, S. *et al*, *Biochim. Biophys. Acta*, 190, 116 (1969).
9. Studier, F.W., *J. Mol. Biol.*, 41, 189 (1969).
10. Walz, F.G., *Biopolymers*, 11, 2365 (1972).
11. Li, J.H. and Crothers, D.M., *J. Mol Biol.*, 39, 461 (1969).
12. Ramstein, J. *et al*, *Dyn. Aspects of Conf. Changes in Biol. Macromol. Proc. Annu. Meet. Soc. Chim. Phys.*
23rd (1972) (Published 1973) 333. Sadron, C. ed.
13. Kelly, G., Ph.D. Thesis, University of Adelaide, 1974.
14. Lerman, L.S., *J. Mol. Biol.*, 3, 18 (1961).
15. Pritchard, N.J., Blake, A. and Peacocke, A.R., *Nature*, 212,
1360 (1966).

CHAPTER VIII

Materials and methods

<u>CONTENTS</u>	<u>Page</u>
1. DNA	
(a) Preparation of DNA sample	173
(b) Preparation of DNA solutions	173
(c) Determination of DNA concentration	173
2. 9-aminoacridine solutions	174
3. Spectrophotometric apparatus	
(a) Melting curves	175
(b) Scatchard plots and spectra	176
4. Scatchard plot measurement technique	176
5. Construction of the polycarbonate temperature-jump cell	178
6. Cleaning of apparatus	178
References	182

1. DNA

(a) Preparation of DNA sample

The DNA sample used throughout this work has been extracted from E.coli K-12 bacteria by the method of Marmur¹ with an additional phenol extraction as recommended by Hirschman and Felsenfeld².

(b) Preparation of DNA solutions

Native DNA solutions have been prepared by the dissolution of a solid sample of DNA in 0.001M NaCl with gentle shaking at 4°C for a period of at least 48 hours. The concentration of DNA solutions prepared is usually 2 mgm/ml, however, less concentrated solutions have been prepared. After a minimum of 48 hours the neutral salt concentration is increased to 0.1M NaCl by the addition of the appropriate volume of 0.2M NaCl. After a further period of gentle shaking at 4°C (4 hours) the solution is centrifuged at 16,000 g for 30 mins at 4°C. The DNA solution is then carefully decanted.

Denatured DNA solutions have been prepared as described in Chapter II, section 3.

(c) Determination of DNA concentration

The concentration of native and denatured DNA solutions has been determined from parameters given by Hirschman and Felsenfeld² for spectra of DNA solutions. Spectra of DNA solutions have been measured at 98°C where both native and denatured DNA exist in the same random coil conformation. Where necessary DNA solutions have been diluted by weight to give absorbance readings of convenient magnitude. The absorbance values at a number of prescribed wavelengths of the DNA solution at

98°C are presented as input to program DNANAL (see Appendix). Program DNANAL computes the concentration of the DNA solution and gives an estimate of the GC content. The use of DNA spectra at 98°C in the analysis provides for consistency between the evaluation of concentrations for both native and denatured DNA solutions. While the absolute concentration of DNA may differ slightly from the value returned by program DNANAL, this difference would appear consistently and would in any case be the same for both native and denatured DNA. The parameters used in program DNANAL are the widely accepted values of Hirschman and Felsenfeld². Program DNANAL also provides for evaluation of concentrations from both spectra of native DNA alone and from hyperchromic spectra.

The concentration of stock solutions of native DNA have been periodically checked by this method.

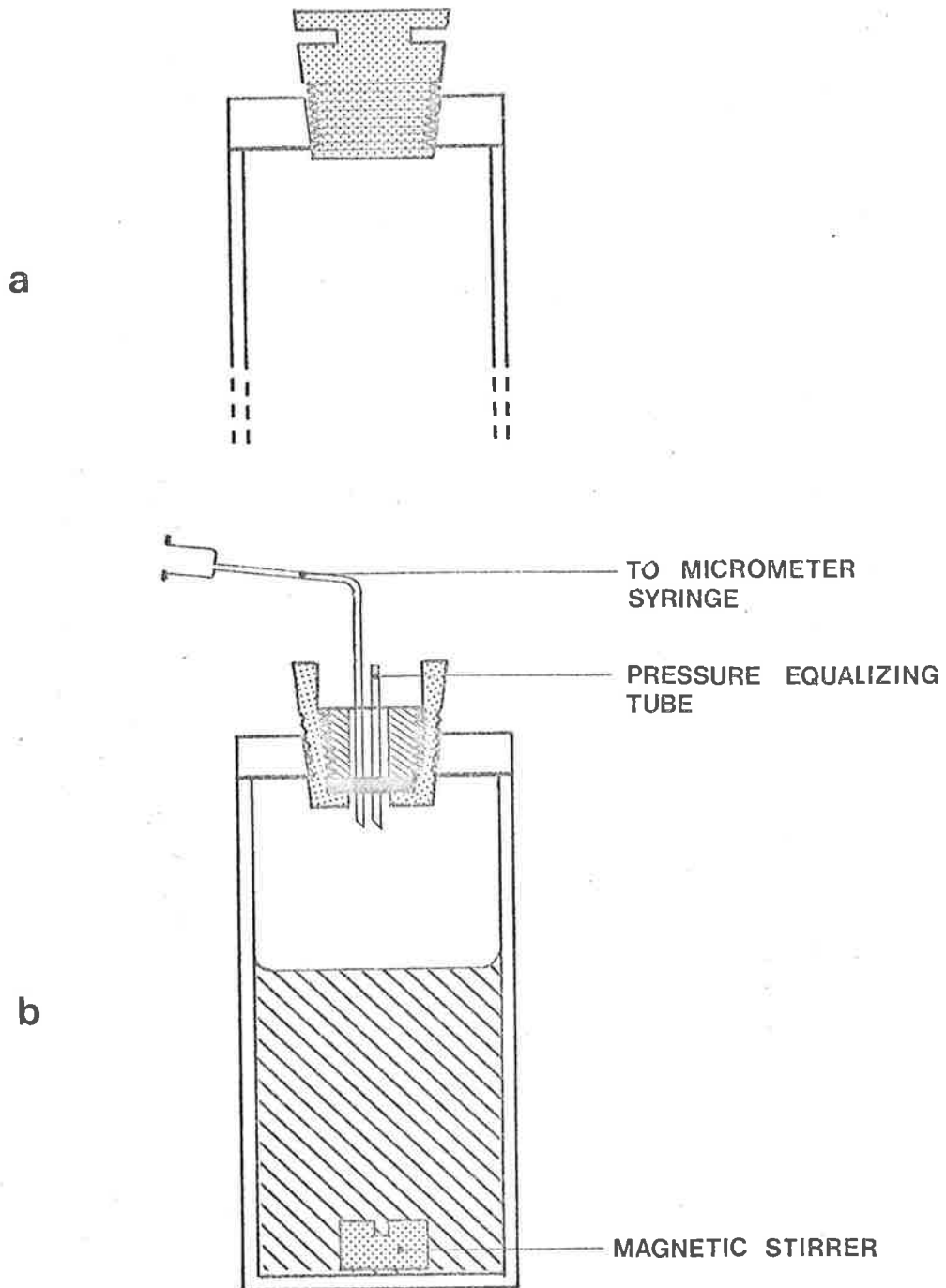
2. 9AA solutions


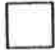



9-aminoacridine (9AA) hydrochloride (A.G. Fluka puris) has been recrystallized twice from ethanol and dried under vacuum. The hydrochloride salt has been found, by weighing of a repeatedly vacuum dried and rehydrated sample, to contain one water of crystallization. The spectral characteristics of dilute solutions of 9AA in 0.1M NaCl are:

$$\lambda_{\max} = 400 \text{ nm} \quad \text{and} \quad \epsilon_{400} = 10440 \pm 40 \text{ (molar extinction),}$$

9AA forms aggregates in solution at quite low concentrations as has been observed by significant deviations from linearity of the

Fig. 8-1. Schematic representations of cuvette stoppers designed to prevent solution loss at high temperatures.



Teflon			Silica
Nylon			Rubber ('Burna-N')
Solution			

Beer's Law plot of absorbance versus concentration of 9AA³.

Thus all 9AA solutions have been prepared by weighed dilution with neutral salt of a stock solution prepared by the dissolution of an accurately known weight of 9AA.HCl in an A-grade volumetric flask.

3. Spectrophotometric apparatus

(a) Melting curves

A Gilford Model 2000 Spectrophotometer has been used to measure the changes in absorbance of solutions with temperature. Solutions contained in silica spectrophotometer cuvettes (path lengths of 1, 2, 5 and 10 mm) are heated in an electrically heated cuvette block constructed for the purpose. Thermostating is achieved by two Solon 25W heaters mounted in the block to which the current supplied is controlled by thermistors mounted in the block. Each thermistor (10 k Ω and 100 k Ω) acts as one arm of a bridge system which alters the phase angle of voltage applied to an S.C.R. thereby providing proportional heating control⁴. Temperature control is possible to better than 0.1°C and calibration of the heating circuit has been checked periodically against calibrated thermistors.

Loss of solution by evaporation has been prevented by using spectrophotometer cuvettes into which are fitted grooved teflon stoppers (Fig. 8-1 (a).). The stoppers press seal and with heating the teflon expands and deforms to the silica surface thereby presenting an effective seal against vapour loss without undue pressure on the cuvette walls. Stoppers have been made to fit cuvettes of all path lengths used. Solutions are weighed at

the beginning and end of an experiment. If solution loss is in excess of 0.4% during the course of heating and cooling the results have been rejected. The monochromator and photomultiplier are isolated from conductive heating by thermospacers through which water at 22°C has been circulated. Absorbance measurements have been corrected for volume expansion as described in Chapter II, section 2. Solutions of 0.1M NaCl concentration have been used as references.

(b) Scatchard plots and spectra

A Gilford 220 Spectrophotometer with a Beckman DU monochromator has been used to measure absorbance changes during experiments to determine Scatchard plots and spectra of 9AA in the presence and absence of native and denatured DNA at various temperatures. As the temperatures required have never exceeded 65°C, heating the cuvettes and cuvette housing has been achieved by circulating water at the required temperature through thermospacers which abutt the cuvette housing. Only 10 mm silica cuvettes have been used in these experiments. The temperature is monitored by a platinum resistance thermometer immersed in a blank cell in the cuvette housing. The resistance thermometer produces a resistance which is displayed on a digital volt meter calibrated to read the temperature directly⁴. The absorbance is also displayed directly on the digital volt meter.

4. Scatchard plot measurement technique

The measurement of binding curves to determine Scatchard plots for the interaction of 9AA with native and denatured DNA has been carried out in the following way.

- (i) The absorbance of a known concentration and weight of 9AA in 0.1M NaCl contained in a silica spectrophotometer cuvette has been measured at 400 nm when thermostated at the required temperature.
- (ii) A weighed aliquot of a DNA solution of known concentration is added, the solution is stirred by a magnetic stirrer in situ and the absorbance is again taken when the solution is re-equilibrated to the required temperature.
- (iii) Further weighed aliquots of the DNA solution are added and the measurements of absorbance are taken with successive additions.

The absorbance reading and the weight addition which gives rise to it are given as input to program BINDING (see Appendix). As well as these measurements, the following information is also given as input: the initial weight and concentration of the 9AA solution, the concentration of the DNA solution added, the cell correction factor, the extinction coefficient of DNA at 400 nm (only a significant factor for denatured DNA: see Chapter V, section 2), and the path length of the cuvette. The program returns in the output the parameters r , c , r/c , T_L/T_A and A/A_i . The value of A/A_i as $T_L/T_A \rightarrow 0$ is then obtained graphically (Chapter IV, section 5) and fed back as input to program BINDING. The final values of r , c , and r/c are produced from which the Scatchard plot may be obtained.

To prevent solution loss at high temperatures during the course of an experiment a cuvette stopper has been designed which allows the injection of DNA solutions at room temperature from a calibrated AGLA micrometer syringe (Burroughs-Wellcome Ltd.) directly into the cuvette at the elevated temperature (Fig. 8-1.(b)).

This arrangement has proved highly successful and as many as 15 additions of DNA solution may be made to a cuvette with a total weight loss of less than 1.5% of the calibrated syringe delivery weight. This has been found to hold through the temperature range 22°C - 65°C.

5. Construction of the polycarbonate temperature-jump cell

The polycarbonate temperature-jump cell (Fig. 6-2.) has performed successfully at high temperatures. This is in marked contrast to a comparable perspex cell which, above 60°C, began to deform sufficiently to give rise to air leaks which interfered with optical measurements.

Polycarbonate ("LEXAN") mechanical grade, cast rod was used. It has been found necessary to machine this material with very sharp tools using copious quantities of water as coolant. It was necessary to strain relieve the cell several times during its manufacture. This was achieved by initially baking in an oven for 20 hours at 142°C and then for further periods of about 7 hours at 135°C during construction. When viewed under polarized light, distinct strain boundaries present after machining were found to disappear and be replaced by diffuse regions of stress following heating in the oven. Machined material which was not strain relieved was found to craze readily when machining was attempted in some other location near to a region of stress.

6. Cleaning apparatus

All glassware used throughout this work has been cleaned by one of two procedures each of which has been rigorously adhered to.

Optical glassware - cleaning

All glassware with optical surfaces has been cleaned in the following manner. The dry object has been immersed for at least 12 hours in concentrated sulphuric acid (A.R.) in which has been dissolved 2% w/w each of sodium nitrate (A.R.) and sodium perchlorate (A.R.). After repeated washing in deionized water the object has been rinsed in distilled water and leached in distilled water for a minimum period of 24 hours. After further rinsing it has been both dried and stored at 160°C until required.

Optical glassware - calibration

It has been found that storage of silica spectrophotometer cuvettes at 160°C does not impair their characteristics when returned to temperatures at which experiments have been carried out. The path lengths of cuvettes used throughout this work have been determined from the absorbance of a standard solution⁵ and the optical surfaces have been checked on a microcomparator for parallelism to 0.001 mm. These characteristics have been found to remain unchanged throughout the work. Furthermore, absorbance differences ("cell corrections") between matched pairs of cuvettes have been found to remain constant within the limits of spectrophotometric accuracy. The appropriate cell correction has been used in all absorbance measurements.

Non-optical glassware - cleaning

All non-optical glassware has been cleaned in the following manner. The object has been immersed in alkaline (10% w/v sodium hydroxide L.R) potassium permanganate (A.R.) (2% w/v) for a period of at least 24 hours. After repeated

washing with deionized water the object has been leached in a bath of acidified metabisulphite (0.1% w/v) for at least 12 hours. After further washing in deionized water the object is leached in deionized water for a further 24 hours. The object is then dried and stored at 160°C until required after washing with distilled water. In addition, flasks which are used for storage of DNA solutions are steam cleaned for 30 minutes and then dried before use.

Non-glass apparatus - cleaning

The only non-glass apparatus which has been in contact with solutions during the course of this work are, cuvette stoppers which have been made of teflon, magnetic stirrers (teflon coated), stainless steel, luer lock needles and the temperature-jump cell sample space (polycarbonate/chrome-plated steel). All teflon apparatus has been cleaned in the acid mixture and leached as described for optical glassware with additional prolonged steaming before drying. This ensures that the entire surface is wetted and rinsed. Stainless steel needles have been subjected to the same cleaning procedure. The temperature-jump cell sample space has been copiously irrigated with methanol (A.R.) and rinsed with distilled water.

Distilled water and pH of solutions

The distilled water used in cleaning and in the preparation of solutions is distilled from a well seasoned all glass apparatus. The conductivity of distilled water has been monitored continuously and has been found to be constantly lower

than 2.5×10^6 mho. cm^{-1} .

The pH of solutions has been monitored frequently during the work described here using a Metrohm pH meter employing a combined glass-calomel electrode. All pH values of stock 9AA, DNA and neutral salt solutions have been in the range pH 5.8 to pH 6.5. As the extent of binding of 9AA to DNA is independent of pH within this range⁶ buffering has been considered unnecessary.

REFERENCES

1. Marmur, J., J. Mol. Biol., 3, 208 (1961).
2. Hirschman, S. and Felsenfeld, G., J. Mol. Biol., 16, 347 (1966).
3. Boehm, G., personal communication.
4. Apparatus designed and built by K. Shepardson, Department
of Physical and Inorganic Chemistry, The University of
Adelaide.
5. Haupt, G.W., J. Opt. Soc. Amer., 42, 441 (1952).
6. Sansom, L.N., Ph.D. Thesis, University of Adelaide, 1972.

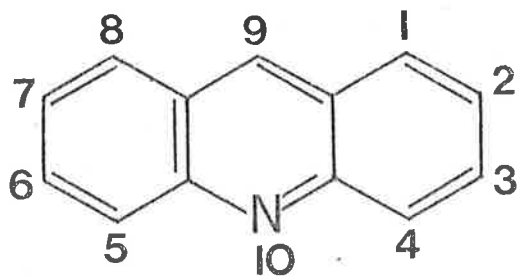
Appendix

Contents

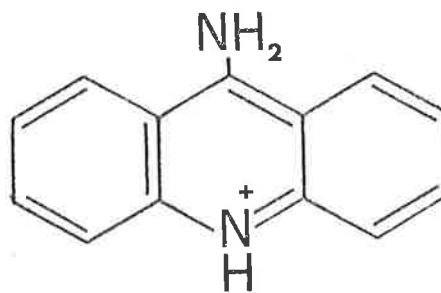
	page
Appendix I Structures of compounds mentioned in the text.	184
Appendix II A comparison of published thermodynamic data on the interaction of aminoacridines with native and denatured DNA with the results obtained in this work.	186
Appendix III Program BINDING	188
Appendix IV Program DNANAL	196

APPENDIX I

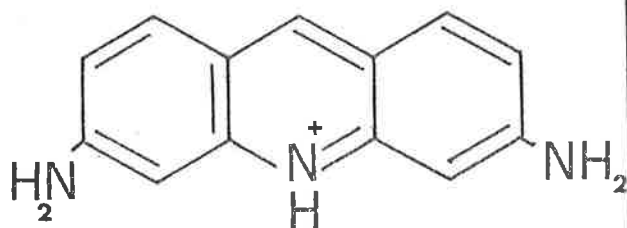
Structures of compounds mentioned in the text.



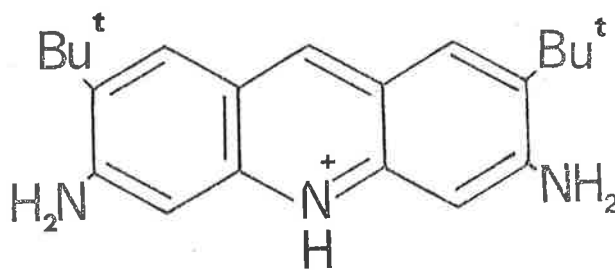
acridine



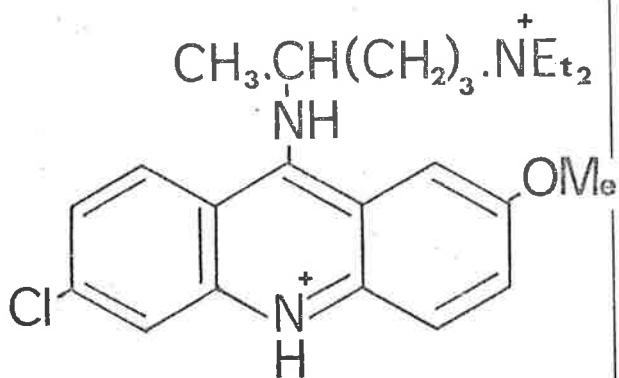
9-aminoacridine cation



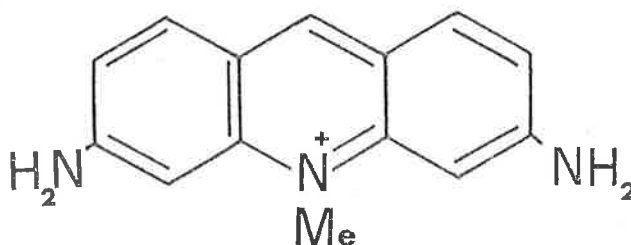
proflavine cation



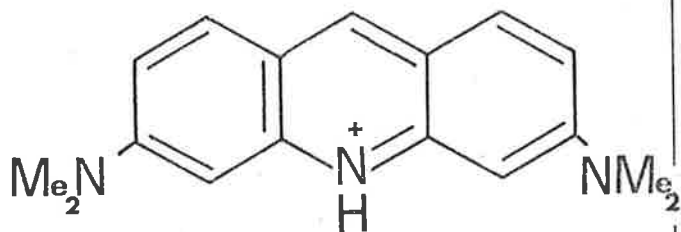
2,7-di-tert-butylproflavine cation



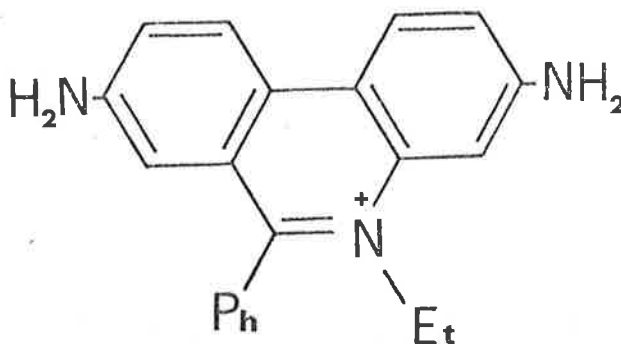
Mepacrine (quinacrine, atebrin) cation



acriflavine cation



acridine orange cation



ethidium cation

APPENDIX II

A Comparison of thermodynamic data published on the interaction of aminoacridines with native and denatured DNA with the results obtained in this work.

Native DNA

	Chambron <u>et al</u> Biochim. Biophys. Acta, <u>123</u> , 306 (1966)	Ichimura <u>et al</u> Biochim. Biophys. Acta, <u>190</u> , 116 (1969)	Li and Crothers J. Mol. Biol., <u>39</u> , 461 (1969)	This work
	$\mu = 0.1$	$\mu = 0.11$	$\mu = 0.2$	$\mu = 0.1$
	proflavine + DNA (equilibrium dialysis)	acridine orange + DNA (equilibrium dialysis)	proflavine + DNA (temperature- jump technique)	9AA + DNA (equilibrium spectro- photometry)
ΔG° (kJ/ mole)			not available (see Chapter VI, section 5(c).)	
Temp (°C)				
0	- 30.3			
20	- 30.8			- 32.2 (S.E.0.2)
22				
25		- 31.4		
30		- 31.0		
35	- 31.4			
40		- 31.0		- 32.2 (S.E.0.2)
45				
50	- 31.0	- 30.5		- 32.0 (S.E.0.2)
55				
65				- 31.7 (S.E.0.3)
70	- 30.1			
ΔH° (kJ/mole)	- 42.0 (at 70°C)	- 40.0	- 32.6	- 35.2 (S.E.0.8)
ΔS° (J.deg ⁻¹ . mole ⁻¹)	- 33.5 (at 70°C)	- 28.5	- 28.4	- 9.6 (S.E. 5.0)

Denatured DNA

	Ichimura <u>et al</u> Biochim. Biophys. Acta. <u>190</u> , 116 (1969)	This work
	$\mu = 0.11$	$\mu = 0.1$
	acridine orange + denatured DNA (equilibrium dialysis)	9AA + denatured DNA (equilibrium spectrophotometry)
ΔG° (kJ/mole) at Temp (°C)		
22		- 30.8 (S.E. 0.2)
25	- 30.5	
30	- 29.7	
40	- 28.9	
45		- 28.8 (S.E. 0.1)
50	- 27.6	
55		- 28.6 (S.E. 0.4)
65		- 26.7 (S.E. 0.6)
ΔH° kJ/mole	- 61	- 56 (S.E. 6)
ΔS° J.deg. ⁻¹ mole ⁻¹	- 102	- 88 (S.E. 17)

APPENDIX III

Program BINDING

```

PROGRAM BINDING(INPUT,TAPE1=INPUT,PJNCH,OUTPUT,TAPE2=OUTPUT)
C
C THIS PROGRAM IS APPLICABLE TO SPECTROPHOTOMETRIC TITRATION OF A MACROMOLECULE
C WITH A LIGAND.
C
C THE PROGRAM CALCULATES THE EXTENT OF BINDING (R) AND THE FREE LIGAND
C CONCENTRATION (C) FROM SPECTROPHOTOMETRIC DATA BASED ON THE METHOD OF PEACOCKE
C AND SKERRETT. ADDITIONAL SAFEGUARDS ARE USED TO PERMIT (1) THE INCLUSION OF
C ABSORBANCE DUE TO ENTIRELY BOUND LIGAND(PROVUDED AS INPUT) (2) ALLOWANCE FOR
C FINITE MACROMOLECULE ABSORBANCE AT THE WAVELENGTH OF INTEREST (3) INDICATION
C OF POINTS FOR WHICH DELTA ABSORBANCE IS EXPERIMENTALLY INSIGNIFICANT.
C THIS PROGRAM WAS WRITTEN BY G. BOEHM FROM AN ALGORITHM BY D.R. TURNER AND G.
C BOEHM. WRITTEN IN FORTRAN IV FOR USE ON A CDC 6400 COMPUTER SYSTEM.
C
C ABSORBANCE MEASUREMENTS,SOLUTION WEIGHTS AND CONCENTRATIONS ARE INPUT ON
C PUNCHED CARDS. THE OUTPUT IS AS PRINTED TABLES,LINE-PRINTER PLOTS AND PUNCHED
C CAPDS. THE PROGRAM REQUIRES ONE EXTERNAL,A LINE-PRINTER PLOTTING ROUTINE
C SUBROUTINE QIKPLT.
C
C      DIMENSION C(50),IERR(50),OD(50,3),ODD(50),R(50),RC(50),TA(50),TL(5
10),TLTA(50),TITLE(6),WT(50),SOLVENT(2),LIGAND(2),ODODI(50)
C      DATA STAR/10H*****/,BLANK/10H
C
C INDEX OF VARIABLES--- VARIABLES NOT MENTIONED IN THIS LIST ARE DEFINED AS THEY
C OCCUR. C--FREE LIGAND CONCENTRATION. IERR--ERROR FLAG FOR POINTS NOT
C EXPERIMENTALLY SIGNIFICANT. OD--ABSORBANCE AND CORRECTED ABSORBANCE
C MEASURMENTS. ODD--DELTA ABSORBANCE. R--RATIO OF BOUND LIGAND TO SITE
C CONCENTRATION. RC--R/C. TA--MACROMOLECULE CONCENTRATION. TL--LIGAND
C CONCENTRATION. TLTA--TL/TA. WT--WEIGHTS OF SOLUTION ADDITIONS. ODODI--
C ABSORBANCE/INITIAL ABSORBANCE. TITLE,SOLVENT,LIGAND--TITLE INFORMATION. STAR,
C BLANK--FLAG INFORMATION.
C
C
C INPUT,TITLE AND IDENTIFIER INFORMATION,TEST FOR END OF DATA DECK.
C

```



```

10 READ(1,2) RUNNO,DATE
   IF(EOF,1)140,20
20 READ(1,3) TEMP,DNATYPE,SOLVENT,LIGAND
   READ(1,3) TITLE
C
C READ INITIAL ABSORBANCE,FINAL ABSORBANCE,CONCENTRATION OF MACROMOLECULE STOCK,
C CONCENTRATION OF LIGAND STOCK,INITIAL LIGAND SOLUTION VOLUME,CELL CORRECTION
C FACTOR,MACROMOLECULE EXTINTION COEFFICIENT AT WAVELENGTH OF INTEREST,CELL PATH
C LENGTH.
C
   READ(1,4) ODI,ODF,CDNA,CDYE,DYEVOL,CF1,CF2,CP
   READ(1,24) LPUNCH,LPLLOT,LODCH
C
C OPTIONS   LPUNCH--0,NO PUNCH,1 PUNCH
C           LPLLOT--0,PLOTS,1 NO PLOTS
C           LODCH--0,NO ACTION,1 READ FINAL ABSORBANCE CORRECTION
C
C READ ABSORBANCES AND CORRESPONDING WEIGHT ADDITIONS -- DETERMINE NUMBER OF
C POINTS. (NOP)
C
   DO30I=1,100
   READ(1,5) OD(I,1),WT(I)
   IF(OD(I,1).EQ.0.0)40,30
30 CONTINUE
40 NOP=I-1
   ODF=OD(NOP,1)
   RCP=1./CP
   CUMWT=0.
C
C CORRECT ABSORBANCES INCLUDING CORRECTION FOR DILUTION. CALCULATE CONCENTRATION
C AT EACH POINT.
C
   DO50I=1,NOP
   OD(I,2)=(OD(I,1)+CF1)*RCP

```

```

50 CUMWT=CUMWT+WT(I)
   ODI=(ODI+CF1)*RCP
   CUMWT=0.
   TOTVOL=DYEVOL
   DO60I=1,NOP
   CUMWT=CUMWT+WT(I)
   TOTVOL=TOTVOL+WT(I)
   TL(I)=CDYE*(DYEVOL/TOTVOL)
   TA(I)=CDNA*(CUMWT/TOTVOL)
   IF(CF2.EQ.0.0) GO TO 60
   XX=TA(I)*CF2
   OD(I,2)=OD(I,2)-XX
60 OD(I,3)=OD(I,2)/(DYEVOL/TOTVOL)

```

C
C OPTION TO INSERT CORRECTED FINAL ABSORBANCE AS LAST POINT. DUMMY WEIGHT ADDED.
C

```

   IF(LODCH.EQ.0) GO TO 150
   NOP=NOP+1
   READ(1,5) OD(NOP,3)
   WT(NOP)=0.0001
   OD(NOP,1)=0.
   OD(NOP,2)=0.
150 ODF=OD(NOP,3)
   DELOD=ODI-OD(NOP,3)
   NP=NOP-1
   IP=NP

```

C
C CALCULATION OF R,C,R/C AND TL/TA.
C

```

   DO70I=1,NP
   TLTA(I)=TL(I)/TA(I)
   R(I)=((ODI-OD(I,3))/DELOD)*TLTA(I)
   C(I)=TL(I)-(R(I)*TA(I))
   UODOI(I)=OD(I,3)/ODI
70 RC(I)=R(I)/C(I)

```

```

      ODDDI(NOP)=OD(NOP,3)/ODI
C
C PRINT FIRST TABLE OF OUTPUT INFORMATION.
C
      WRITE(2,6)
      WRITE(2,7) TITLE,RUNNO,DATE
      WRITE(2,8) RUNNO,ODI,TEMP,ODF,DNATYPE,CDYE,SOLVENT,CDNA,LIGAND,DYE
      1VOL
      WRITE(2,9)
      CUMWT=0.0
      FINVERT=-1.0
C
C TEST FOR SIGNIFICANCE OF POINTS AND INSERT ERROR FLAGS AS APPROPRIATE.
C
      DO100I=1,NOP
      CUMWT=CUMWT+WT(I)
      ODD(I)=OD(I+1,3)-OD(I,3)
      WW=WT(I)/0.01
      DD=ODD(I)/WW
      TEST=ODD(I)*FINVERT
C
C EXCLUDE INSIGNIFICANT POINTS.
C
      IF(TEST.LT.0.001)80,90
80 FLAG=STAR
      IERR(I)=1
      GO TO 95
90 FLAG=BLANK
      IERR(I)=0
95 IF(I.EQ.NOP) GO TO 105
      ODD(I)=-ODD(I)
C
C PRINT FINAL TABLE OF VALUES.
C
100 WRITE(2,11) I,OD(I,1),OD(I,2),OD(I,3),WT(I),CUMWT,TLTA(I), ODDDI(I)

```

```

      1),FLAG,ODD(I),DD
105 CONTINUE
      TOTVOL=DYEVOL+CUMWT
      TLL=CDYE*(DYEVOL/TOTVOL)
      TAA=CDNA*(CUMWT/TOTVOL)
      TLTAX=TAA/TLL
      TLTA(NOP)=1./TLTAX
      WRITE(2,22) NOP,OD(NOP,1),OD(NOP,2),OD(NOP,3),WT(NOP),CUMWT,TLTA(N
10P),ODDI(NOP)
      WRITE(2,12) TLL,CF2,TAA,CF1,TLTAX,C2
      IJUMP=0
      DO110I=1,NP
      IF(IERR(I).EQ.0) GO TO 110
      IF(IJUMP.EQ.0)200,110
200 IP=I-1
      IJUMP=1
110 CONTINUE
      IF(IP.LT.3)210,220
210 IP=NP
220 CONTINUE
      WRITE(2,6)
      WRITE(2,7) TITLE,RUNNO,DATE
      WRITE(2,13)
      WRITE(2,14)
      WRITE(2,14)
      WRITE(2,15)
      WRITE(2,14)
      WRITE(2,13)
      WRITE(2,14)
      DO120I=1,IP
      WRITE(2,14)
      WRITE(2,16) RC(I),R(I),C(I),TA(I),TL(I),TLTA(I)
120 WRITE(2,14)
      WRITE(2,13)
      IDIF=NP-IP

```

```

        WRITE(2,23) IP,IDIF
C
C TEST LPLOT AND PRODUCE PLOTS IF INDICATED.
C
      IF(LPLOT.EQ.0) GO TO 130
      CALL QIKPLT(R,RC,-IP,1,16H*FREE DYE CONC*,3H*R*)
      CALL QIKPLT(C,R,-IP,1,3H*R*,5H*R/C*)
C
C TEST LPUNCH AND PRODUCE PUNCHED OUTPUT IF INDICATED.
C
130 IF(LPUNCH.EQ.0) GO TO 10
      PUNCH17
      PUNCH18,RUNNO,DATE,TITLE
      PUNCH19,IP
      PUNCH21,(R(I),I=1,IP)
      PUNCH21,(RC(I),I=1,IP)
      PUNCH17
      PUNCH19,IP
      PUNCH21,(C(I),I=1,IP)
      PUNCH21,(R(I),I=1,IP)
      NDUM=IP-1
      PUNCH17
      PUNCH19,NDUM
      PUNCH21,(TLTA(I),I=2,IP)
      PUNCH21,(ODODI(I),I=2,IP)
      GO TO 10
140 STOP
C
C FORMATING OF INPUT/OUTPUT.
C
      2 FORMAT(A5,5X,A10)
      3 FORMAT(8A10)
      4 FORMAT(8F10.0)
      5 FORMAT(2F10.0)
      6 FORMAT(*1*)

```

```

7 FORMAT(/,* SCATCHARD BINDING RESULTS .... *,6A10,* RUN NUMBER
1*,A5,* DATE *,A10,/)
8 FORMAT( /,25X,*RUN NUMBER = *,A5,25X,*OD INITIAL = *,F8.3,/,2
15X,*TEMPERATURE = *,A10,20X,*OD FINAL = *,F8.3,/,25X,*DNA TY
2PE = *,A10,20X,*CONCN OF DYE = *,E12.3,/,25X,*SOLVENT = *
3,2A10,10X,*CONCN OF DNA = *,E12.3,/,25X,*LIGAND = *,2A10,10
4X,*INITIAL VOLUME = *,F8.3)
9 FORMAT(//,* POINT NO OD OBS OD CORR 1 OD CORR 2 WT ADDE
1ED CUML WT TL/TA OD/ODI DELTA OD OD/WT E
2RR FLAG*,/)
11 FORMAT( 4X,I2,7X,F6.4,6X,F6.4,7X,F6.4,6X,F6.4,4X,F7.4,5X,F7.4,5X,F
17.4,29X,A5,/,95X,F7.4,4X,E10.3)
12 FORMAT(//,25X,*FINAL DYE CONCN = *,E10.3,15X,*E. C. DNA = *,F7.3,/,
1,25X,*FINAL DNA CONCN = *,E10.3,15X,*CELL CORR = *,F7.4,/,25X,*FIN
2AL TA/TL = *,F8.3,17X,*CELL PATH = *,F7.3)
13 FORMAT(32X,67(1H*))
14 FORMAT(32X,7(1H*,10X))
15 FORMAT(1H+,35X,*R/C*,9X,*R*,10X,*C*,10X,*TA*,9X,*TL*,7X,*TL/TA*)
16 FORMAT(1H+,33X,E9.3,3X,F7.3,3X,E9.3,2X,E9.3,2X,E9.3,2X,F9.5)
17 FORMAT (80(1H*))
18 FORMAT(A5,2X,A10,3X,6A10)
19 FORMAT(I2)
21 FORMAT(8E10.3)
22 FORMAT( 4X,I2,7X,F6.4,6X,F6.4,7X,F6.4,6X,F6.4,4X,F7.4,5X,F7.4,5X,F
17.4)
23 FORMAT(//,32X,*NUMBER OF POINTS *,I3,* / *,I2,* POINTS OMITTED*)
24 FORMAT(3I2)
END

```

APPENDIX IV

Program DNANAL

```

PROGRAM DVANAL(INPUT,TAPE1=INPUT,OUTPUT,TAPE2=OUTPUT)
C
C THIS PROGRAM AND ITS SIX SUBROUTINES PERFORM ANALYSIS OF DNA SPECTRAL DATA.
C THE METHOD USED IS THAT OF FELSENFELD AND HIRSCHMAN. ANALYSIS OF NATIVE
C DENATED AND HYPERCHROMIC SPECTRA MAY BE SELECTED. WHERE APPLICABLE ADDITIONAL
C INFORMATION IS GIVEN.
C
C SUBROUTINE INDEX
C INPUTD--READS ABSORBANCES FROM CARDS AND CORRECTS FOR SOLUTION EXPANSION
C WHERE APPLICABLE.
C NATIVE--PERFORMS 3 TERM ANALYSIS OF NATIVE DNA SPECTRUM.
C DENAT--PERFORMS 2 TERM ANALYSIS OF THE DENATURED DNA SPECTRUM.
C HYPER--PERFORMS 3 TERM ANALYSIS OF THE HYPERCHROMIC DNA SPECTRUM.
C REPORT--PRINTS OUT TITLE INFORMATION AND TABLES OF RESULTS.
C RESTACK--RESTACKS ARRAY WHERE MULTIPLE ANALYSIS OF ONE DATA SET IS TO BE
C UNDERTAKEN.
C
C INDEX OF VARIABLES. OD--ABSORBANCE DATA. ODC--CORRECTED ABSORBANCE DATA.
C DOD--DELTA ABSORBANCE FOR HYPERCHROMIC ANALYSIS. T--OUTPUT VARIABLES. TITLE--
C TITLE. IT--TEMPERATURE IF OTHER THAN ROOM TEMPERATURE. NSET--NUMBER OF DATA
C SETS. LTYPE--TYPE OF ANALYSIS REQUIRED.
C
C COMMON OD(15,2),ODC(15,2),DOD(15),T(3)
C COMMON TITLE(8),IT(2)
C
C READ NUMBER OF DATA SETS AND INITILIZE LOOP TO PROCESS THAT NUMBER OF SETS.
C
C READ(1,1) NSET
C 1 FORMAT(3I2)
C D070M=1,NSET
C
C READ TYPE REQUIRED FOR THIS SET AND ASSIGN TO APPROPRIATE CODING.
C
C READ(1,1) LTYPE,IT
C IF(LTYPE-1)10,20,30

```


C
C PROCESS NATIVE ANALYSIS AND RETURN TO NEXT DATA SET.

C
10 CALL INPUTD(12,1)
CALL NATIVE
CALL RESTACK(3)
CALL REPORT(12,5,10HNATIVE ,10H ,0)
GO TO 70

C
C PROCESS DENATURED ANALYSIS AND RETURN TO NEXT DATA SET.

C
20 CALL INPUTD(5,1)
CALL DENAT
CALL REPORT(5,0,10HDENATURED ,10H ,0)
GO TO 70

C
C PROCESS HYPERCHROMIC ANALYSIS AND THEN RESTACK DATA TO PERFORM NATIVE AND
C DENATURED ANALYSIS OF THIS DATA.

C
30 CALL INPUTD(15,2)
D040I=1,15
40 D0D(I)=0DC(I,1)-0DC(I,2)
CALL HYPER
CALL REPORT(15,17,10HHYPERCHROM,10HIC ,1)
CALL RESTACK(1)
D050I=1,12
II=I+3
50 OD(I,1)=OD(II,2)
CALL NATIVE
CALL REPORT(12,5,10HNATIVE ,10H ,0)
CALL RESTACK(2)
IC=4
D060I=1,6
II=I+IC
OD(I,1)=OD(II,1)

```
ODC(I,1)=ODC(II,1)
60 IC=IC+1
CALL DENAT
CALL REPORT(5,0,10HDENATURED ,10H ,0)
70 CONTINUE
STOP
END
```

```

      SUBROUTINE INPUTD(N,L)
C
C THIS SUBROUTINE READS IN ABSORBANCE DATA AND CORRECTS IT FOR SOLUTION
C EXPANSION IF APPLICABLE.
C
      COMMON OD(15,2),ODC(15,2),DOD(15),T(3)
      COMMON TITLE(8),IT(2)
      DIMENSION COR(5)
      DATA COR/1.001981,1.022711,1.028998,1.035904,1.041870/
      READ(1,1) TITLE
1  FORMAT(8A10)
      DO10J=1,L
10  READ(1,2) (OD(I,J),I=1,N)
2  FORMAT(8F10.0)
      IF(N.EQ.12) GO TO 30
      DO20J=1,L
      II=IT(J)
      DO20I=1,N
20  ODC(I,J)=OD(I,J)*COR(II)
30  RETURN
      END

```

SUBROUTINE NATIVE

C
C THIS SUBROUTINE PERFORMS THE 3 TERM ANALYSIS OF THE NATIVE DNA SPECTRUM. IT
C RETURNS THE OUTPUT VARIABLES TO THE CALLING ROUTINE THROUGH COMMON STORAGE.
C

```
DIMENSION S(6)
COMMON OD(15,2),ODC(15,2),DDD(15),T(3)
DATA S/9.329E-8,2.0631E-7,6.198E-8,2.792E-8,2.124E-8,8.513E-8/
U1=-2026.*OD(1,1)-1989.*OD(2,1)-1390.*OD(3,1)+43.*OD(4,1)-319.*OD(5
B5,1)-608.*OD(6,1)+2515.*OD(7,1)+871.*OD(8,1)-386.*OD(9,1)+1159.*OD(
B(10,1)+1797.*OD(11,1)+1187.*OD(12,1)
U2=-656.*OD(1,1)-1251.*OD(2,1)-1917.*OD(3,1)-2830.*OD(4,1)-1807.*0
BD(5,1)-1141.*OD(6,1)-3379.*OD(7,1)-1409.*OD(8,1)-154.*OD(9,1)-1558.
B.*OD(10,1)-2424.*OD(11,1)-2099.*OD(12,1)
U3=3952.*OD(1,1)+5031.*OD(2,1)+6338.*OD(3,1)+7480.*OD(4,1)+7616.*0
BD(5,1)+7307.*OD(6,1)+7052.*OD(7,1)+5740.*OD(8,1)+4587.*OD(9,1)+393
B8.*OD(10,1)+3164.*OD(11,1)+2188.*OD(12,1)
THETA=U1*S(1)+U2*S(2)+U3*S(3) $ T(1)=U1*S(4)+U2*S(3)+U3*S(5)
THETA=THETA/T(1) $ T(2)=(1.-THETA)*100.
B=U1*S(6)+U2*S(1)+U3*S(4) $ T(3)=(B-T(1)*THETA*THETA)/(T(1)*THETA)
RETURN $ END
```

SUBROUTINE DENAT

C
C THIS SUBROUTINE PERFORMS THE 2 TERM ANALYSIS OF THE DENATURED DNA SPECTRUM. IT
C RETURNS THE OUTPUT VARIABLES TO THE CALLING ROUTINE THROUGH COMMON STORAGE.
C

```
DIMENSION S(6)
COMMON OD(15,2),ODC(15,2),DOD(15),T(3)
DATA S/5.473E-8,1.2806E-7,3.879E-8,8.97E-9,1.55E-8,7.62E-8/
U1=-2745.*ODC(1,1)+2354.*ODC(2,1)+1090.*ODC(3,1)+3095.*ODC(4,1)+17
B05.*ODC(5,1)
U2=-1545.*ODC(1,1)-4786.*ODC(2,1)-1263.*ODC(3,1)-3849.*ODC(4,1)-44
B21.*ODC(5,1)
U3=7210.*ODC(1,1)+10154.*ODC(2,1)+9506.*ODC(3,1)+8980.*ODC(4,1)+69
B42.*ODC(5,1)
THETA=U1*S(1)+U2*S(2)+U3*S(3) $ T(1)=U1*S(4)+U2*S(3)+U3*S(5)
THETA=THETA/T(1) $ T(2)=(1.-THETA)*100.
B=U1*S(6)+U2*S(1)+U3*S(4) $ T(3)=(B-T(1)*THETA*THETA)/(T(1)*THETA)
RETURN $ END
```

SUBROUTINE HYPER

C
C THIS SUBROUTINE PERFORMS THE 3 TERM ANALYSIS OF THE HYPERCHROMIC DNA SPECTRUM.
C IT RETURNS THE OUTPUT VARIABLES TO THE CALLING ROUTINE THROUGH COMMON STORAGE.
C

```
DIMENSION S(6)
COMMON DD(15,2),ODC(15,2),DDD(15),T(3)
DATA S/8.55E-8,6.643E-8,2.534E-8,5.311E-8,2.535E-8,2.969E-7/
U1=-542.*DDD(1)-180.*DDD(2)+494.*DDD(3)-257.*DDD(4)-1501.*DDD(5)-9
841.*DDD(6)+102.*DDD(7)-541.*DDD(8)+319.*DDD(9)-731.*DDD(10)-595.*D
800(11)-203.*DDD(12)-160.*DDD(13)+1045.*DDD(14)-149.*DDD(15)
U2=188.*DDD(1)-837.*DDD(2)-1758.*DDD(3)-1179.*DDD(4)+277.*DDD(5)+2
841.*DDD(6)-58.*DDD(7)+1403.*DDD(8)+1069.*DDD(9)+1468.*DDD(10)-34.*
800(11)-1600.*DDD(12)-2261.*DDD(13)-2991.*DDD(14)-989.*DDD(15)
U3=1753.*DDD(1)+1690.*DDD(2)+2068.*DDD(3)+2214.*DDD(4)+2060.*DDD(5
8)+2173.*DDD(6)+2287.*DDD(7)+1983.*DDD(8)+2055.*DDD(9)+2169.*DDD(10
8)+2754.*DDD(11)+3104.*DDD(12)+2884.*DDD(13)+2341.*DDD(14)+1123.*DD
8D(15)
THETA=U1*S(1)+U2*S(2)+U3*S(3) $ T(1)=U1*S(4)+U2*S(3)+U3*S(5)
THETA=THETA/T(1) $ T(2)=(1.-THETA)*100.
B=U1*S(6)+U2*S(1)+U3*S(4) $ T(3)=(B-T(1)*THETA*THETA)/(T(1)*THETA)
RETURN $ END
```

SUBROUTINE REPORT(N,IB,STITLE1,STITLE2,IH)

C THIS SUBROUTINE PRINTS THE INFORMATION TO BE OUTPUT. IT FORMATS AND PRINTS THE
 C TITLE INFORMATION, A TABLE OF ABSORBANCE AND CORRECTED ABSORBANCE VALUES AND
 C THE PREDETERMINED WAVELENGTHS AT WHICH THEY WERE RECORDED AND THE CALCULATED
 C CONCENTRATION PERCENT GC AND DELTA FACTOR FOR THE ANALYSIS.

```

COMMON OD(15,2),ODC(15,2),DOD(15),T(3)
COMMON TITLE(8),IT(2)
INTEGER W(32)
DATA W/240,250,260,270,280,235,240,245,250,255,260,265,270,275,280
1,285,290,220,225,230,235,240,245,250,255,260,265,270,275,280,285,2
290/
WRITE(2,2) STITLE1,STITLE2,TITLE(1),TITLE(2)
WRITE(2,3) (TITLE(I),I=3,8)
IF(IH.EQ.1)10,20
10 WRITE(2,4) $ WRITE(2,11) $ WRITE(2,12) $ WRITE(2,12) $ WRITE(2,13)
WRITE(2,12) $ WRITE(2,11)
D01I=1,N
L=I+IB
WRITE(2,12) $ WRITE(2,12) $ WRITE(2,14) W(L),OD(I,1),ODC(I,1),DOD(
1I)
1 CONTINUE
WRITE(2,12) $ WRITE(2,11) $ WRITE(2,9) (T(I),I=1,3)
RETURN
20 WRITE(2,4) $ WRITE(2,5) $ WRITE(2,6) $ WRITE(2,6) $ WRITE(2,7)
WRITE(2,6) $ WRITE(2,5)
D033I=1,N
L=I+IB
WRITE(2,6) $ WRITE(2,6) $ WRITE(2,8) W(L),OD(I,1),ODC(I,1)
33 CONTINUE
WRITE(2,6) $ WRITE(2,5) $ WRITE(2,9) (T(I),I=1,3)
RETURN
2 FORMAT(1H1,/, 2X,*DNA SPECTRAL ANALYSIS ..... *,2A10,10X,*DNA TYP
1E *,A10,35X,*DATE *,A10)
  
```

```
3 FORMAT(/,35X,6A10)
4 FORMAT(//58X,*INPUT DATA*,//)
5 FORMAT(47X,34(1H*))
6 FORMAT(47X,4(1H*,10X))
7 FORMAT(1H+,47X,*WAVELENGTH*,1X,*OD(EXPMTL)*,1X,*OD CORRECT*)
8 FORMAT(1H+,51X,I3,7X,F5.3,5X,F5.3)
9 FORMAT(///,47X,*CONCENTRATION OF DNA = *,E12.4,*MOLES PHOSPHOROUS/
10CDM*,//,47X,*MOLES PERCENT GC          = *,F5.1,//,47X,*DELTA FACTOR
11      2          = *,F8.3)
11 FORMAT(42X,45(1H*))
12 FORMAT(42X,5(1H*,10X))
13 FORMAT(1H+,42X,*WAVELENGTH*,1X,*OD(EXPMTL)*,1X,*OD CORRECT*,1X,* D
14      1ELTA OD *)
14 FORMAT(1H+,46X,I3,7X,F5.3,5X,F5.3,5X,F5.3)
      END
```


SUBROUTINE RESTACK(L)

C
C THIS SUBROUTINE RESTACKS THE ABSORBANCE ARRAYS FOR MULTIPLE ANALYSIS OF THE
C HYPERCHROMIC DATA SET. THESE ARRAYS ARE HELD IN COMMON STORAGE.
C

```
COMMON OD(15,2),ODC(15,2),DOD(15),T(3)
GOTO(1,2,3),L
1 D010I=1,15
  DOD(I)=OD(I,1)
  ODC(I,2)=ODC(I,1)
10 ODC(I,1)=0.
  RETURN
2 D020I=1,15
  ODC(I,1)=ODC(I,2)
20 OD(I,1)=DOD(I)
  RETURN
3 D030I=1,15
30 ODC(I,1)=0.
  RETURN
END
```